GARMENT MODELLING AND VISUALISATION

Bernhard Spanlang

A dissertation submitted in partial fulfillment

of the requirements for the degree of

Doctor in Engineering

of the

University of London.

Department of Computer Science

University College London

September 23, 2005

ProQuest LLC
789 East Eisenhower Parkway
P.O. Box 1346
Ann Arbor, MI 48106-1346

Declaration

I declare that I am the sole author of this thesis, and that the work presented is my own, except where otherwise acknowledged.

Abstract

This thesis describes methods for modelling and visualising fabrics and garments on human body shapes by means of computer systems. The focus is on automatic real-time simulation but, at the same time, realistic appearance of garments is important. Very high physical accuracy in the simulation of mechanical properties of cloth is relaxed, however.

We first introduce an image-based collision detection (IBCD) mechanism which harnesses the rasterisation, depth buffer and interpolation units of existing graphics hardware for robust and efficient collision detection and response between body-scan and garment surfaces. We introduce directional velocity modification (DVM), a numerical method to overcome a phenomenon called super-elasticity of conventional mass spring particle systems (MSPS). A reverse engineering technique is presented that enables us to extract assembly information and data for realistic visualisation from photographs of real garments. The images used in this technique are acquired in a set-up that includes a high resolution digital imaging device. Body landmark data is used automatically to pre-position garment panels around a body-scan before virtual sewing.

We show that DVM generates visually pleasing garments on static and animated body-scans. The efficiency of the IBCD is demonstrated by a comparison with a traditional geometry based method. A system that exploits the developed techniques was created for Bodymetrics Ltd., at their request. This system is integrated with a 3D whole body scanner for fully automatic virtual try-on of clothes in a department store. The system presents a world first installation and was reported in several newspapers and fashion magazines. While it demonstrates the efficiency and robustness of the developed methods, clothes shoppers can benefit in that the system gives quicker fit-feedback than a traditional mirror in a changing room and can display their dressed body from any angle and distance. In collaboration with a garment designer we also tested the system in a design scenario.

In an evaluation of the commercial potential of the developed methods the major players in markets closely related to virtual try-on technology are identified and market entry strategies are discussed.

Acknowledgements

I would like to thank Bernard Francis Buxton for guiding me through this work and for all his patience and support.

Thanks to Mel Slater who believed in me more than I did and Mel offered me the opportunity to start this work.

Thanks to Tzvetomir Ivanov Vassilev for his patience, long and fruitful collaboration with me and for his friendship.

Thanks to Céline Loscos for encouraging me to carry on with this work and for her invaluable friendship.

Thanks to Yiorgos Lambros Chrysanthou and Franco Tecchia for technical discussions and for their invaluable friendship.

Thanks to Jonathan Walters from Bodymetrics for his countless practical ideas and all his cheerful support.

Thanks to Kelvin David Lawrance, Suran Asitha Goonatilake and Andrew Crawford from Bodymetrics Ltd. for their collaboration.

Thanks to Philip Colin Treleaven for his support at UCL and at Bodymetrics Ltd.

Thanks to João Fradinho Oliveira and Dongliang Zhang for their collaboration to build the automatic body-scan animation system.

Thanks to Greg Ward for his explanations on the RADIANCE rendering system.

Thanks to Anki Lindblom for her collaboration and for designing the jacket in the augmented reality garment design scenario.

Thanks to Brian Allbriton, Anthony Sibthorpe, Steven Seget, Annie Ting Ngai Lai for their collaboration on the evaluation of the commercial potential of virtual clothing during the New Technology Ventures course led by Keith Willey at London Business School.

Thanks to Clare Elaine Hammond and Sieglinde Spanlang for their support and for proofreading.

Thanks to Peter Mayer for the many discussions about mathematics and physics, and for his close friendship and support.

Thanks to my parents Adolf and Hannelore Spanlang for their constant support.

I would also like to thank my landlady Irene Neumark, my grandmother Pauline Feischl, my dear friend Raffael Mair and my grandmother Maria Hofer for their support. Their death[1] during the second half of this work showed me new perspectives on life.

[1]Deceased †15.4.2003, †31.10.2003, †22.2.2004, †24.10.2004 respectively.

Contents

1 Introduction **20**

1.1 Applications 21

1.1.1 Internet Clothes Shopping 21

1.1.2 Fashion Design 22

1.1.3 Games Industry 22

1.1.4 Film Industry 23

1.1.5 Virtual Environments 23

1.1.6 Textile Engineering 23

1.2 Problems 23

1.2.1 Numerical Cloth Simulation 24

1.2.2 Collision Detection and Response 24

1.2.3 Modelling of Garments 25

1.2.4 Visualisation 25

1.3 Hypothesis 26

1.4 Contributions 27

1.4.1 Core Contributions 27

1.4.1.1 Image-Based Collision Detection for Cloth Simulation 27

1.4.1.2 Method to Compensate for Super-Elasticity Effects 28

1.4.2 Industrial Contributions 28

1.4.2.1 Reverse Engineering Approach for a Realistic Garment Description 28

1.4.2.2 Installation of a Fully Automatic Virtual Try-On System . . . 28

1.4.2.3 Augmented Reality System for Clothing 29

1.4.3 Complementary Contributions 29

1.4.3.1 Automatic Animation System for Body-Scans 29

1.4.3.2 Volume Preservation for Body Tissue Simulation 29

1.4.3.3 Simulation Data Visualisation for Fit Feedback 29
1.5 Structure 30

2 Background and Related Work **31**
2.1 Drape Behaviour 31
2.1.1 Mechanical Properties of Fabric 31
2.1.1.1 Elasticity Theory 32
2.1.2 Measurement of Mechanical Fabric Properties 33
2.1.3 Computer Cloth Models 34
2.1.3.1 Continuum Mechanics Models 34
2.1.4 Mass Spring Particle Systems 36
2.1.4.1 Topologies 36
2.1.4.2 Integration Methods 37
2.1.5 Collision Detection 43
2.1.5.1 Bounding Volume Hierarchies 44
2.1.5.2 Voxel Based Approaches 44
2.1.5.3 Curvature Culling 44
2.1.6 Collision Response 45
2.2 Realistic Visualisation 46
2.2.1 Surface Representation 47
2.2.2 Reflectance Measurements 47
2.2.2.1 Homogeneous Surfaces 47
2.2.2.2 Heterogeneous Surfaces 48
2.2.2.3 Virtual Reflectometers 49
2.2.3 Reflectance Models and Fitting 49
2.2.3.1 Perfect Diffuse 50
2.2.3.2 Perfect Specular 50
2.2.3.3 Specular-Diffuse 50
2.2.3.4 Off-Specular 50
2.2.3.5 Anisotropic 50
2.2.3.6 Grazing Angle 50
2.2.3.7 Empirical Models 50
2.2.3.8 Theoretical Models 51
2.2.4 Fabric Rendering 51

2.3 Summary 53

3 Our Cloth Model **55**

3.1 Cloth Model and Super-Elasticity 55

3.1.1 Velocity Modification 56

3.1.2 Directional Velocity Modification 57

3.1.3 Discussion 58

3.2 Image Based Collision Detection 59

3.2.1 Depth Maps 60

3.2.2 Normal Maps 61

3.2.3 Velocity Maps 63

3.2.4 Testing for Collisions 63

3.2.5 Quantisation Error Estimation 64

3.2.6 Layers of Depth Maps 65

3.2.7 Cloth-Cloth Collision Detection 66

3.3 Collision Response 66

3.3.1 Collision Tolerance 68

3.4 Fabric Property Mapping 68

3.4.1 Mass 69

3.4.2 Tension Force 69

3.4.3 Shear Force 69

3.4.4 Bending Moment 70

3.4.5 Discussion 71

3.5 Our Work Extended by Others 71

3.6 Summary 72

4 Garment Description **73**

4.1 Garment Exchange Format 73

4.1.1 General Garment and Environment Information 74

4.1.1.1 Mesh Resolution 74

4.1.1.2 Damping 75

4.1.1.3 Gravity 75

4.1.1.4 Collision Tolerance 75

4.1.1.5 Garment Type 75

4.1.1.6 Scale Ratio 75

4.1.1.7 Y-offset 75
4.1.2 Garment Panels 75
4.1.2.1 Panel Type 76
4.1.2.2 Cutting Pattern 76
4.1.2.3 Fabric Drape Properties 76
4.1.2.4 Fabric Reflectance 76
4.1.2.5 Darts 77
4.1.2.6 Fabric Thickness 77
4.1.3 Seams 77
4.1.3.1 Edge-Edge Seams 78
4.1.3.2 Smooth Edge-Edge Seams 78
4.1.3.3 Edge-Face Seams 78
4.1.3.4 Pressings 78
4.1.3.5 Point Seams 78
4.1.4 Garment Accessories 78
4.2 Garment Editing in a GUI 79
4.2.1 Plug-in Functions 79
4.2.2 Commonly used Illustrator Functions 80
4.3 Garment Reverse Engineering 80
4.3.1 Garment Disassembly 81
4.3.2 Lighting 82
4.3.3 Image Acquisition 82
4.3.4 Geometrical Image Calibration 83
4.3.5 Colour Calibration 83
4.3.6 Marking-up Images 84
4.3.7 Border Colours 85
4.4 Garment Simulation 85
4.4.1 Garment Meshing 86
4.4.1.1 Non-Uniform Meshing 86
4.4.1.2 Uniform Meshing 87
4.4.2 Automatic Garment Pre-Positioning 88
4.4.2.1 Automatic Body Landmark Extraction 88
4.4.2.2 Pre-Positioning of Garments 89
4.4.3 Garment Seaming 90

4.4.3.1 Edge-Edge Seams 91
4.4.3.2 Edge-Face Seams 92
4.4.3.3 Seaming process 93
4.4.3.4 Pre-Simulated Garments 94
4.5 Summary 94

5 Visualisation **96**
5.1 Surface Representation 96
5.1.1 Quadrilateral and Triangular Meshes 97
5.1.2 Fabric Thickness 99
5.2 Texture and Transparency Mapping 99
5.3 Modes of Real-Time Visualisation 100
5.3.1 False Colour Visualisation of Simulation Data 100
5.4 Global Illumination and Realistic Augmented Reality 103
5.4.1 Natural Illumination 103
5.4.2 Global Illumination of Virtual Garments 103
5.4.3 Diffuse Inter-reflections on Curved Surfaces 104
5.5 Visualisation on an Internet Interface 105
5.5.1 Data Flow 107
5.5.2 Exploitation of Parallel Processor Architecture 107
5.5.3 File Caching 107
5.5.4 Installation and Versioning over the Internet 108
5.5.5 User Interface 108
5.6 Summary 108

6 Body Modelling **109**
6.1 Real-Time Volume Preservation 109
6.1.1 Background 109
6.1.2 Support Springs with Explicit Volume Computation 111
6.1.3 Support Springs with Implicit Volume Computation 112
6.1.4 Volume preservation test 113
6.1.5 Results 113
6.2 Automatic Animation of Body-Scans 115
6.2.1 Background 115
6.2.2 Layered Human Model 116

6.2.3 Building the Skeleton 116
6.2.4 Mapping 118
6.2.5 Vertex Blending 119
6.2.6 Motion Capture Data 119
6.2.7 Results 119
6.3 Summary 120

7 Evaluation **123**
7.1 Cloth Model 123
7.1.1 Directional Velocity Modification 123
7.1.2 Fabric Property Mapping 124
7.1.3 The Influence of Cloth-Mesh Resolution on Performance 126
7.1.4 IBCD versus Traditional Collision Detection 126
7.1.5 Dynamic Body IBCD 127
7.1.6 Influence of Collision-Buffer Resolution on Performance 129
7.1.7 Influence of Body-Mesh Resolution on Performance 131
7.2 Virtual Try-On Installation at Selfridges 132
7.2.1 Implementation 133
7.2.2 User Interface and Customer Discretion 134
7.2.3 Results 135
7.2.3.1 System Reliability 135
7.2.3.2 Customer Feedback 135
7.2.3.3 Other Visitors 136
7.2.3.4 Internet Access 136
7.2.3.5 Visual Quality 136
7.3 Augmented Reality For Garment Design 137
7.3.1 Merging the Real and Virtual 138
7.3.2 Masking the Rendering for Photo Composition 139
7.3.3 Synthesis of Occluded Background 140
7.3.4 Results 140
7.3.5 Future Work 142
7.4 Summary 142

8 Commercial Potential of Virtual Clothing **144**
8.1 Strengths, Weaknesses 145

8.1.1 Advantages 145
8.1.2 Disadvantages 145
8.1.3 Uncertainties 146
8.2 Choosing a Target Market 146
8.3 Commercial Value 146
8.4 The Virtual Clothing Value Chain 148
8.5 Value Curves in Apparel Retailing 149
8.6 Demand Chain Analysis 150
8.7 Competing Innovations/Major Players 151
8.8 Challenges on the Route to Commercialisation 152
8.8.1 Coordinating Access to Complementary Technologies 153
8.8.2 Communicating the Value of Virtual Clothing to Resistant Customers . 155
8.9 Capturing Value through IPR Protection and Licensing 155
8.9.1 Licensing Contracts 155
8.10 How to Exploit the Technology? 156
8.10.1 Is the Timing Right? 156
8.10.2 Market Entry Scenario 157
8.10.2.1 Virtual Clothing in a Department Store 157
8.10.2.2 Virtual Clothing in CAD/CAM Systems 158
8.10.2.3 E-Commerce via Garment Retailers 158
8.10.2.4 E-Commerce the Made-to-Measure Way 159
8.10.2.5 From the Garment Designer Directly to the Customer 159
8.10.3 Positioning of Virtual Clothing 159
8.10.4 Bridging the Gap 161
8.10.5 Scaling 162
8.11 Financing and Partners 162
8.11.1 GAP Inc. 162
8.11.2 A Potential Financing Scenario 163
8.12 Conclusions 167

9 Conclusions and Future Work **169**

9.1 Our Hypothesis 169
9.1.1 Existing Cloth Modelling and Simulation Techniques 169
9.1.2 Existing Visualisation Techniques 170

9.1.3 Enable us to Build . . . 170
9.1.4 Fully Automatic . . . 170
9.1.5 Apparatus for Virtual Try-On . . . 170
9.1.6 Realistic Images of Clothes . . . 171
9.1.7 On Scanned People . . . 171
9.1.8 In an On-Line Manner . . . 171
9.2 Contributions . . . 171
9.2.1 Image-Based Collision Detection for Cloth Simulation . . . 171
9.2.2 Method to Compensate for Super-Elasticity Effects . . . 172
9.2.3 Reverse Engineering Approach for a Realistic Garment Description . . 172
9.2.4 Installation of a Fully Automatic Virtual Try-On System . . . 172
9.2.5 Commercialisation . . . 173
9.3 Future Work . . . 173
9.3.1 Dynamic Simulation and Garment Fit Feedback . . . 173
9.3.2 Visualisation . . . 174
9.3.3 Evaluation of Realism . . . 174
9.3.4 User Interface . . . 174
9.4 Summary . . . 175

A Pilot User Study **176**
A.1 Background . . . 176
A.2 Factors . . . 177
A.3 Image Generation . . . 178
A.4 Experimental Design . . . 178
A.4.1 Experimental Process . . . 179
A.4.2 Data Collection and Analysis . . . 179
A.5 Results . . . 180
A.6 Conclusions . . . 180

B Newspaper and Magazine Articles **185**

C The Major Players **189**
C.1 My Virtual Model . . . 189
C.2 Browzwear . . . 189
C.3 OptiTex . . . 189

C.4 Digital Fashion 190
C.5 Havok 190
C.6 SyFlex 190
C.7 PAD System 191
C.8 Gerber Technology 191
C.9 Lectra 191

D Gap Inc. **192**

E Publications, Marketing, Presentations and Patents **194**
E.1 Papers 194
E.2 Patents 196
E.3 Talks and Marketing 196

Bibliography **199**

List of Figures

2.1 Spring topology in Provot's model. 37

3.1 Velocity modification for over-elongated springs. 56
3.2 Static velocity modification in dynamic scene. 57
3.3 Directional Velocity Modification. 58
3.4 Placement of orthogonal cameras for IBCD. 61
3.5 Depth buffers computed for the front and for the back of a body-scan generated by orthographic projection. Dark areas represent pixels close to the camera while bright areas are pixels further away from the camera. 61
3.6 Normal buffer of the front and back of a body-scan. 62
3.7 Velocity buffer of the front and back of an animated body-scan. 63
3.8 Two depth map layers for resolving the overlapping of the body by the right arm. 66
3.9 Collision response using velocity manipulation. 67
3.10 Collision response using force manipulation. 67
3.11 Illustration of shear coefficient mapping. 70
3.12 Illustration of bend coefficient mapping. 70

4.1 Photography rig with a camera mounted on a tripod on the ceiling. Soft-lighting is achieved by reflecting light from polystyrene boards as described in the text. 82
4.2 Left: Photograph of disassembled jeans with MacBeth colour checker on the right of the image, directly after capture. Right: Image after MacBeth colour calibration, lens distortion correction and rectification. 84
4.3 Corner-points and distances used for non-uniform meshing. 86
4.4 Example of the front panel of a shirt meshed non-uniformly. 87
4.5 Example of a front shirt panel meshed uniformly. 88
4.6 Underarm segmentation using re-entrant point tolerance criteria. Black points illustrate the right part of a horizontal body slice at a height around the armpit. . 90

4.7 Pre-positioned garment panels; Left: A shirt; Right: A pair of trousers. Landmark description as also indicated in the text. 90
4.8 Different seaming types. 91
4.9 Left: point-point seams; Right: point-edge seams. 92
4.10 Edge-edge seam position interpolation. 92
4.11 Edge-face seams. 93
4.12 Edge-face seam position interpolation. 93

5.1 Using vertex normals to triangulate a QuadMesh. 98
5.2 Rendering comparison between standard QuadMesh triangulation, left, and QuadMesh triangulation that takes the surface normal into consideration, right. 98
5.3 Garment panel texture information is given by two UV coordinates. 99
5.4 A woman's top in different real-time rendering modes from left to right: default, wire-frame on top of default, only wire-frame, and without the client's body-scan. 101
5.5 Jeans with waist size from left to right: 25, 27, 29 and 31. The first row shows a false colour visualisation of the stretch spring elongations of a customer in jeans. The second row shows the same jeans in realistic real-time visualisation mode. Rows three and four show the same data as rows one and two but viewed from the back of the customer's scan. 102
5.6 A HDR light probe of a target location shown at increasing f-stops from left to right. We use this light-probe for natural illumination of virtual garments. . . . 104
5.7 Diffuse inter-reflections sample the hemisphere of solid angles above a surface and therefore create rendering artefacts with interpolated normals. On the bottom right, this is illustrated. Sample rays of the hemisphere start below the surface because of the interpolated normal. 105
5.8 Data flow between the internal processes of the ActiveX Internet control for garment visualisation. 106

6.1 Results from the volume preservation test. 113
6.2 Left: Deformed ellipsoid; Right: Hemisphere on a table. 114
6.3 Brassiere on a virtual body; Left: No deformation; Right: Breast deformation. . 114
6.4 From left to right: Surface landmarks and proximity spheres; Extracted skeleton; Two additional body-scans with extracted skeleton which illustrate the method is generic. 117
6.5 Left: Surface separation planes; Right: Grown surface regions. 118

6.6 Several motions applied to a model (walking, sneaking, running and drinking). 120
6.7 The same motion data applied to different models. 121
6.8 Snap-shots from an automatic animation of a body-scan dressed in trousers and shirt. 122

7.1 Tablecloth draping over a moving sphere; Left: No super-elasticity correction; Right: Super-elasticity corrected by directional velocity modification. 124
7.2 From left to right: Shirt simulated with 20×20, 30×30 and 50×50 vertices. 126
7.3 The simulation time increases linearly with the number of garment vertices simulated. 127
7.4 Two frames of a walking female model in a dress with sleeves. 129
7.5 Multi-layer collision buffers. From left to right: Initial pose; Collision problems with the right arm; Problem fixed by using multiple collision layers. 130
7.6 Left: By reducing the resolution of the collision buffer we can achieve higher frame rates in an animation sequence; Right: The percentage of time spent on creating the collision buffers. The remaining time is spent on character animation and cloth simulation. 130
7.7 Shirt simulated at different collision buffer resolutions. From left to right: 50×50; 100×100; 400×400. 131
7.8 The performance of the collision detection is independent of the mesh resolution of a body-scan. The average time per frame (TPF) in a simulation of a pair of trousers with 2355 polygons is constant. Buffer creation time (BCT) which has to be performed only once in the static case, however, increases linearly with the number of polygons. 132
7.9 From left to right: original body-scan surface reconstructed from a point cloud by $[TC]^2$ software; arms were lifted and most holes patched; head, hands and feet removed; extracted landmarks which are used for pre-positioning of garments are shown. 134
7.10 Customer in "default wear". 136
7.11 Left: Front view of a customer in jeans that fit well; Right: Back view of the same customer in the same pair of jeans. 137
7.12 Jeans that do not fit well; Left: a customer with jeans too tight; Right: a customer with very baggy jeans. 138
7.13 Side-view of six customers dressed in a default shirt and the same pair of jeans. 139

7.14 3D scan superimposed on the photograph to approximate camera. 139
7.15 From left to right: Scan in jacket the appearance of which has been produced by use of a background light-probe; Automatically generated mask image of the jacket; Extracted illuminated jacket. 140
7.16 Left: Client in the real jacket toile; Right: The illuminated and simulated jacket composited with a photograph of the client. 141

8.1 Outline of the commercial evaluation. 145
8.2 Value Chain of Virtual Clothing. 148
8.3 Generic demand chain analysis of Virtual Clothing. There is a fall-off from one stage to the next. 151
8.4 Timeline of known and predicted introduction of key technologies that are related to Virtual Clothing. 157
8.5 Virtual Clothing in a Department Store. 158
8.6 Virtual Clothing for E-Commerce. 158
8.7 Virtual Clothing for Made-to-Measure inspection. 159
8.8 Virtual Clothing to Inspect e-Commerce Designer Clothing. 160
8.9 Key findings in the commercial evaluation. 161
8.10 Partnership with a major online retailer. 162
8.11 Business Models for Virtual Clothing. 163

A.1 Cloth simulation factor levels varied by changing the mesh resolution of the mass spring particle system from left to right: Low, Medium and High. 178
A.2 Introduction to our Web-based user-study. 182
A.3 Pre-Questionnaire of our Web-based user-study. 182
A.4 Instructions for our Web based user-study. 183
A.5 Start-page of our Web-based user study. 183
A.6 Last countdown digit (from three to one) of our Web-based user study. 184
A.7 A pair of jeans in our Web-tachistoscope. 184

B.1 The Evening Standard 14th May 2003. 185
B.2 Elle May 2003. 186
B.3 Sunday Times Style May 2003. 187
B.4 Glamour October 2004. 188

D.1 Locations of stores of GAP Inc., a possible partner to introduce virtual clothing. 192

List of Tables

5.1 Inventor's mesh representations. 97

6.1 Performance of the MSPS approach for volume preservation. 114

7.1 Comparison of different fabric types mapped onto our cloth model. From left to right: Description of the fabric type; Photograph of the real fabric draped over a round table; Simulated counterpart draped over a virtual round table. 125

7.2 Performance comparison between IBCD and OBCD for a shirt with 1800 vertices. 128

7.3 Performance comparison between IBCD and OBCD with a dress for 3840 vertices. 128

7.4 Frames per second in an animation. 128

8.1 Tabular representation of the estimated value curve for Virtual Clothing in eCommerce. 149

8.2 Comparison of the major players in the Virtual Clothing markets. 152

8.3 Cash-flow projections for GAP Inc. 165

8.4 Cash-flow projections for BodyMetrics Ltd. 166

D.1 Number of stores of Gap Inc. 193

Chapter 1

Introduction

This thesis describes methods for modelling and visualising garments on human body shapes by means of computer systems. The focus is on automatic real-time simulation but, at the same time, realistic appearance of garments is important. Very high physical accuracy in the simulation of mechanical properties of cloth is relaxed, however (see Section 3.4). Deficiencies of existing approaches in cloth modelling and visualisation such as slow speed, unrealistic appearance and low complexity of simulated garments are described, tackled and, to some extent, overcome. 3D scanning technology is employed to gather shape and size information of people. Emphasis is put on automatically dressing human body models obtained from 3D scans. Body landmark information automatically extracted from the shape data by the 3D scanner system is used to correctly position garments around the body. We describe an application that exploits the developed techniques, which is integrated with a 3D whole body scanner for fully automatic virtual try-on of clothes. At the time of writing, the system has been installed and running for over 18 months in a department store. It is publicly accessible and scanned customers can also access their body-shapes remotely from a database and try-on clothes over a secure link on the Internet. The described system is a world first installation and was reported in several newspapers and fashion magazines such as Elle, The Economist, The Evening Standard and The Times[1]. Clothes shoppers can benefit from this system in that it can give quicker fit-feedback than a traditional mirror in a changing room and can display their body from any angle and distance. Since the garments are physically simulated, additional information about how well the garment fits is quantifiable and can be visualised by mapping stress and strain values to colour representations.

While garment designers may directly use the system for design and simulation of new garments on a virtual dress stand or a scanned client, the games and entertainment industries and virtual environment developers may benefit from the algorithms and methods developed for the

[1]Examples of such reports are given in Appendix B.

system in the field of real-time cloth modelling. A major automobile company has shown interest in the techniques for simulation of the cloth that covers car seats. A medical company identified the possibility of using our system for the simulation of bandages. A more detailed description of possible applications is given below. The main motivation of the methods and system developed and described was that of virtual clothes try-on in a store or for e-commerce on the Internet.

1.1 Applications

We touched briefly on a number of applications in the introduction. In this section, we give a more detailed summary of possible applications for cloth modelling and simulation.

1.1.1 Internet Clothes Shopping

E-commerce over the Internet is increasing in popularity. Dykema et al [DDJ99, DCBY99] report that online apparel sales exceeded $1 billion in 1999 and are expected to go beyond $22 billion in 2004. Some sites that offer 2D image mix and match for virtual clothes try-on already exist [MyV90, Ima99]. In such systems a customer can choose a photograph of a person with a similar body shape to their own or the customer may enter some size information. Morphing techniques are then employed to create images that depict the photograph of the mannequin that represents the customer in the chosen garment. While such images appear fairly realistic they cannot give realistic feedback about the fit of the garment. Since 3D scanning technology produced by companies such as: Cyberware [Cyb82], Hamamatsu [Ham53], TC^2 [TC2], Vitronic [Vit97], Wicks and Wilson [Wic73] and others has become available in the last few years possibilities for virtual clothes "try-on" on the Internet have emerged. Such scanning systems can acquire full human body shapes to millimetre precision. The idea then is that customers have a virtual representation of themselves. Size and landmark information can be automatically extracted from the measured 3D human shape data either by means of software supplied with the scanner system (e.g. $[TC]^2$, Hamamatsu, Vitronic) or by the application of computer vision techniques [DDBT98]. Customers can browse garments in an online catalogue to dress their virtual selves. To overcome the limitations of 3D displays not being able to give haptic feedback, which might be important for customers buying garments, the visual effects have to be very convincing in order to allow a customer to make decisions based only on images or videos. A virtual try-on system can give fit feedback through either a near photo-realistic visualisation of the attired garment or through fitting visualisation such as fabric stress and strain colour mappings. Once chosen, the desired garment of the right size can be sent to the

customer from the retailer's stocks. In the case of custom clothing, the exact sizing information of the 3D scan can be used automatically to grade the cutting patterns of a design to the correct size for manufacture and delivery of made to measure clothing.

1.1.2 Fashion Design

In garment design it is still the practice that after designers draw their creations on paper or on a CAD system. They realise a piece of garment, a so called toile, by cutting and sewing the individual panels often made of cheap fabric. The designer can then see how it looks and behaves in reality. Designers examine their prototype on a dress stand and tweak some areas which are then incorporated in their original drawings. This cycle of drawing, cutting, sewing and examining continues until the designer is satisfied or abandons the idea. A simulation with good physical approximation of the garment's behaviour would make it possible to shorten the design cycle and a designer could switch back and forth between 2D drawing and realistic 3D drape simulation of a virtual toile on a virtual dress stand or a 3D scan of a client. The virtual toile could be simulated with the properties of the usually expensive fabric of the final garment. This is particularly interesting for use over the Internet, where designers could collaborate in a shared virtual environment for garment design. Such a tool could open new possibilities in clothing design. New interface paradigms could be created that enable garment design directly in 3D on the shape of a virtual mannequin.

1.1.3 Games Industry

While physical simulation in general is becoming a growing field in the games industry in order to give environments a more natural atmosphere, cloth simulation is only just emerging. In older games some simple flags waving in the wind or t-shirts moving in a slightly distracting sinusoidal pattern can be found [NG96]. Owing to the high processing costs of draping cloth, game designers often choose tight fitting and stretchy clothes or armour for their characters that can simply be painted on the skin of the character by using texture maps. Often clothes are modelled directly on the character and, when animated, they move with the skeletal structure of the character but do not show any drape behaviour. Owing to the ever falling costs of computer memory and the increasing availability of modelling tools that include cloth simulation, more recent games show more realistically behaving clothes in real-time [Jam01, JF03]. This is possible because typically the motions and exact shapes of the characters are known and the main simulation calculations can be carried out in a pre-processing phase. This may be somewhat memory intensive but can give good visual results.

1.1.4 Film Industry

In the film industry visual quality and realistic behaviour is much more important. Very convincing garment simulations were presented in a few of the recent purely computer generated movies such as "Shrek" by DreamWorks, "Final Fantasy The Spirits Within" by SquareSoft, "Monsters Inc." by Pixar, etc. Very interesting effects have been shown in recent films that composite computer imagery with video footage such as the Star Wars episode "Attack of the Clones" and in "The Matrix Reloaded". In these movies, computer simulated characters and real actors interact. While seamlessly compositing virtual characters into scenes with real actors by taking many of the visibility, blending and light interactions into account is very challenging, it has been successfully demonstrated in many movies. In "Attack of the Clones" and "The Matrix Reloaded" photo-realistic virtual characters wear loose fitting clothes that react realistically when the character is close to a real actor. The computational cost and manual labour of skilled artists required to achieve such results by traditional ways and means is immense and the pure processing time of short sequences can be weeks or even months. In this context, cloth simulation can be regarded as a tool to assist animation artists that is less labour intensive and, therefore, less costly.

1.1.5 Virtual Environments

Owing to the ubiquity of textiles and clothing in our everyday life, accurate cloth simulation will contribute to the believability of virtual environments that aim to portray reality. Thus, for example, interactive architectural walkthroughs may benefit from the dynamic simulation of curtains, furniture, table cloth, etc. and garments on virtual actors.

1.1.6 Textile Engineering

Textile engineers are interested in cloth modelling and visualisation mainly to predict the behaviour of real cloth fabric. In this case, the simulation of fabric has to be very accurate and simulation speed is only of secondary interest. Such predictions may be used to solve the control problem in the context of computer aided manufacturing (CAM). Owing to the real-time constraints of the main application of this thesis, solutions to the requirements of highly accurate fabric simulation are not addressed.

1.2 Problems

The problem of garment simulation on human body shapes can be broken down into four subproblems: numerical cloth simulation, collision detection and response, modelling of garments, and visualisation. Here we give a rough idea of the problems and we go into more detail in

Chapter 2.

1.2.1 Numerical Cloth Simulation

Cloth can be seen as a complex mechanical system made of fibres. The often thin materials can stretch, fold and create complex flexible forms. There are two main approaches to modelling cloth on computer systems, Finite Element Methods (FEM) and Mass Spring Particle Systems (MSPS). While FEMs can be very accurate in describing the drape behaviour of the real cloth's fabric properties, they are prohibitively slow[2]. MSPSs are also capable of modelling cloth drape behaviour to a good degree of accuracy, but they offer possibilities for a trade-off between realism and speed. For very efficient models the drape behaviour can suffer in realism in two ways. Firstly, cloth damping effects may be too high which makes the cloth appear clumsy. This is often owing to use of simulation time steps that are too large or the cloth mesh resolution may be too low. Secondly, cloth may appear too stretchy caused by the ideal linear way springs are typically modelled. Numerical stability of the cloth model is another major problem. Generally, high stiffness of springs results in stability problems which can be addressed in various ways. More details on the background of modelling cloth and its problems can be found in Chapter 2.

1.2.2 Collision Detection and Response

Owing to its flexibility and deformability there are many ways cloth can touch or interfere with rigid objects and with itself. In cloth simulation, such interferences have to be identified and a response has to be found that is physically plausible. This is known as the problem of *collision detection and response*. In terms of performance, *collision detection* becomes the main bottleneck in cloth simulation, especially when dealing with a large number of polygons, as is the case with accurate object shape representations, such as those acquired by 3D scanning of the whole human body. Traditional approaches make 3D geometrical comparisons between the polygons that represent the cloth and those of the body model. Uniform and hierarchical space partitioning methods are commonly used to increase efficiency by reducing the number of potential collision tests. However, hierarchical methods become very slow with large meshes and uniform space partitioning can become very memory intensive. Both strategies require a lot of computer power for the construction of the data structures. More details on the background of collision detection and response can also be found in Chapter 2.

[2]Eischen et al [EDC96] report simulation times in the order of days for simulation of a simple piece of table cloth.

1.2.3 Modelling of Garments

A good cloth model by itself is not sufficient to represent a virtual garment realistically. The cloth model has to be extended so that it can describe cutting patterns, seaming information, fabric drape properties, fabric colours, texture and, in many cases, rigid objects added to describe buttons, etc. Surprisingly, at the time of writing there is no computer readable format that allows the description of all this information in a standard way. This would be beneficial for the fully automatic manufacturing of garments as well as for assembling virtual garments. In many cases some garment assembling information is still passed on by communication between people. Even if such an electronic garment description standard were to exist it would be difficult to obtain the description of a garment one can buy in a shop. In the case of virtual garment simulation in order to dress 3D body scans automatically, additional information is required. For example, it has to be specified where a particular garment is placed on the body. Thus, it has to be specified that a shirt goes on the torso with the front side on the front of the body and that the sleeves cover the arms, etc. Details are given in Chapter 4.

1.2.4 Visualisation

For cloth visualisation the relevant results of an MSPS garment simulation are the positions of the particles which describe the garment at every simulation step. Typically, for visualisation, the particle positions are connected and a triangular mesh is constructed in order to visualise the surface of the cloth. There are several ways to visualise the surface. One is that a customer may want to get a near photo-realistic image of the garment. Another way is that the customer may want to see a representation of the stresses and strains to which the internal structure of the fabric is exposed. Because the micro and meso-structure of the interwoven fibres of fabric create a complicated and inhomogeneous reflectance behaviour and the deformable nature of cloth often creates situations where light is inter-reflected between creases and folds, realistic visualisation of a whole garment is very difficult. Trade-offs between realism, speed and memory requirements have to be made. More details on the background of realistic fabric visualisation can be found in Chapter 2.

Existing visualisation systems for browsing 3D graphics on the Internet do not allow the exploitation of the whole system's performance for external processes such as cloth simulation. Therefore, when used for electronic commerce, the development of a specialised visualisation system that is integrated with existing Internet technology is required for Virtual Clothing. Details of such a visualisation system are given in Chapter 5.

1.3 Hypothesis

Our Hypothesis is:

"Existing cloth modelling and visualisation techniques can be extended and developed in order to enable us to build an apparatus for fully automatic virtual try-on that creates realistic images of clothes on scanned people in an on-line manner."

In order to clarify what we mean by this hypothesis we define the individual terms used in more detail.

By *"existing cloth modelling and simulation techniques"* we mean modelling techniques that have been developed over the last twenty years as described in more detail in Chapter 2.

By *"existing visualisation techniques"* we mean visualisation techniques generally used in computer graphics but also those techniques that were particularly created for rendering garments. More details on the background of visualisation of garments can be found in Chapter 2.

By *"extended and developed"* we mean that we identified the drawbacks of existing systems and developed methods to overcome some of the drawbacks.

By *"enable us to build"* we mean that the cloth modelling and visualisation techniques to be described in this thesis may be utilised with other essential pieces of technology, such as a 3D whole human body scanner, to develop the virtual try-on apparatus.

By *"fully automatic"* we mean that in the process between scanning a customer and visualising one or more garments on the customer's scan there is no manual intervention. The automatic extraction of landmarks and construction of body surfaces of the scanning system may not work with very abnormal body shapes and at present, the system has only been extensively tested with female bodies, but within such limitations, it should normally work and, should the system fail to work, it should degrade gracefully.

By *"apparatus for virtual try-on"* we mean a system that allows people to try clothes on a virtual representation of their body shapes, acquired by a 3D scanner, either in a department store or over the Internet on a personal computer.

By *"realistic images of clothes"* we mean that the appearance of the clothes on the computer display describes what we would expect to see if the scanned person were to try-on the real counterpart of the garment. In Appendix A we describe a pilot user study to evaluate the visual quality of the appearance of the garments that we simulate in our system. It

should be clear that the simulation will always be an approximation of the real garment and thus will never appear completely identical to it. Ultimately, the degree of realism required is that which is satisfying to shoppers. If this can be achieved in a cost-effective way, the system will have a chance of being a commercial success, if not it will fail.

By *"scanned people"* we mean the body model acquired via a 3D scanning system. As mentioned before our system requires landmark information that is expected to be extracted by the scanning system. The system will only work and is only expected to work with normal bodies. Thus it may not work if a person has a limb missing.

By *"in an on-line manner"* we mean that a person who has been scanned can view the available garments on their shape representation within seconds. For example, the time to extract body landmarks and shape and to convert the data for visualisation should take less time than the customer does getting dressed again after scanning.

1.4 Contributions

In this section the core contributions are listed. Industrial contributions that were made as technical solutions to requirements of the sponsoring company are listed in sub-section 1.4.2. In addition, complementary contributions that are not directly linked with the hypothesis, but were identified as interesting in the context of it, are given. A list of publications that originated from this work is given in Appendix E. Some of the work presented here was carried out in collaboration with others. Reference to such collaboration is given where appropriate. Prof. Tzvetomir Ivanov Vassilev of the University of Rousse contributed in particular on the super-elasticity handling of the mass spring system when he was a visiting Research Fellow in the Department of Computer Science at UCL and subsequently in collaboration with us, for example, in work for Bodymetrics Ltd.

1.4.1 Core Contributions

The core contributions have been to the solution of problems in cloth and garment modelling and to development and implementation of the aforementioned clothing application, as follows.

1.4.1.1 Image-Based Collision Detection for Cloth Simulation

The main contribution of this work is in cloth-body collision detection. A novel image-based collision detection (IBCD) approach is described that harnesses the graphics hardware's rasterisation, z-buffer and interpolation units to generate a representation of the body scan for very fast collision detection and response. It uses standard hardware that is available in almost any

accelerated graphics card. This approach is particularly well suited for the detection of collisions on very large polygonal meshes as is the case with data from accurate 3D body scans. The IBCD is scalable, meaning that a query for a collision is independent of the number of polygons from which the body mesh is constructed. Another advantage of this approach is that it is independent of the representation of the object. The object may be represented as a NURBS surface or as a quad-mesh. As long as the graphics hardware can render the surface our IBCD is expected to work in a robust way. The IBCD approach is described in detail in Chapter 3.

1.4.1.2 Method to Compensate for Super-Elasticity Effects

If cloth is modelled with a MSPS it may appear unrealistically stretchy. This effect is called super-elasticity and is caused by the idealised linear model of Hookean springs. An adaptation of a MSPS was developed that we call *directional velocity modification* (DVM). This approach overcomes the super-elasticity phenomenon in a very efficient way. The approach is appropriate for static bodies and has been extended to work with animated characters. The approach is described in detail in Chapter 3.

1.4.2 Industrial Contributions

Some of the work described in this thesis covers technical solutions for requirements suggested by Bodymetrics Ltd. as part of the development of its products and services. The author recognises that such products and services are the property of Bodymetrics Ltd.

1.4.2.1 Reverse Engineering Approach for a Realistic Garment Description

In order to visualise clothing very realistically a technique for reverse engineering existing garments was developed. It allows us to obtain sufficient information virtually to reconstruct the garment with very good visual quality. We are using high resolution digital imaging devices to acquire fabric colour and texture from the disassembled flat pieces of garments. This technique is used in a semi-automatic way to acquire cutting pattern and seaming information from the photographs. This is of particular relevance for e-commerce, games and the film industry, where the simulation of existing garments is of interest. Reverse engineering of existing garments is only of minor interest for garment design. This approach is described in detail in Chapter 4.

1.4.2.2 Installation of a Fully Automatic Virtual Try-On System

A fully automatic system for dressing people represented by 3D scanning data is described with a demonstration of a world first installation of such a system in a London department store. The customer's body shape and size information is stored in a central database and can be accessed over the Internet for Virtual Clothing try-on. Details can be found in Chapter 7.

1.4.2.3 Augmented Reality System for Clothing

As described earlier in the visualisation part of the problems section, realistic visualisation of garments is very difficult owing to the complicated interaction of light with fabrics. In this study, we employed the Monte Carlo path tracing of the RADIANCE rendering system [War94], in combination with an illumination acquisition technique, seamlessly to merge a computer generated image of the garment with a photograph of a person in an augmented reality sense. More details can be found in Chapter 5 on visualisation and in Chapter 7 on evaluation.

1.4.3 Complementary Contributions

The core and industrial contributions which are central to our hypothesis, are listed above. A number of additional complementary contributions were also made in the context of this work, including the following:

1.4.3.1 Automatic Animation System for Body-Scans

In collaboration with Dr. Dongliang Zhang, a visiting Research Fellow from the Hong Kong University of Science and Technology, and João Fradinho Oliveira, a PhD student at UCL, we built a system that automatically applies motion capture data to human body scans. The major contribution of this work was the use of automatically extracted body landmarks for the creation of a body skeleton for animation. In addition, in this work a surface growing technique was developed in order to segment the body scan into the required body parts. For more details see Chapter 6.

1.4.3.2 Volume Preservation for Body Tissue Simulation

The body influences clothing, for example the drape, but clothing, if very tight, may also deform the body, in particular, soft body tissue. In Chapter 6 we present a modified MSPS which, in real-time, approximately preserves the volume of body tissue under deformation. This is important since the body is largely filled with water which is very incompressible. As an example, we show the cloth-body interactions of a bra. For more details see Chapter 6.

1.4.3.3 Simulation Data Visualisation for Fit Feedback

Realistic visualisation of a garment is the most intuitive way to give feedback about its fit. Another way is to visualise the stresses and strains to which the material is exposed when the customer is dressed in a garment. We experimented with a colour mapping of the spring elongations and of the forces of the MSPS. In this way it is possible to identify the areas where the garment fits very tightly or rather loosely. More details can be found in Chapter 5.

1.5 Structure

The main body of this dissertation is structured as follows. First, in Chapter 2 we discuss related work. This starts with a short review of cloth simulation techniques. We then give an overview of collision detection and response techniques. Finally, visualisation techniques, with a focus on garment rendering, are reviewed. In Chapter 3, we describe our cloth model and the methods we use for collision detection and response. The focus here is on the IBCD. Along with the IBCD, we introduce our directional velocity modification technique to overcome super-elasticity and discuss the collision response method used in our model. Chapter 4 is on the description of garments. We introduce a garment description format and define a meshing procedure to generate cloth models from the garment description. We briefly discuss an implementation that can be used to load cutting patterns into a CAD program for editing, reading from and writing to our garment description format. Our semi-automatic reverse engineering approach for the acquisition of realistic garment description from photographs of real garments is also detailed in this chapter. Chapter 5 deals with the visualisation of garments. We describe how our cloth model is visualised in real-time using existing rendering techniques. We introduce a stress-strain colour mapping technique to give garment fit feedback. The integration of the cloth modelling system with the RADIANCE global illumination system for realistic light simulation is then outlined. Chapter 6 describes complementary methods developed that are related to body modelling. They are of particular relevance in combination with cloth modelling. An adapted MSPS for volume preservation of soft tissue for garment-body interaction is described. Following that a system for the automatic animation of body scans is detailed. Chapter 7 is the evaluation chapter. We evaluate the performance of our IBCD by comparing it to a traditional object space approach. We describe the installation of our system in a department store and discuss the customer acceptance of the system. Results of a collaboration with a designer, in which we tested our system in an augmented reality context with natural global illumination for compositing photographs with virtual garments, are also given in Chapter 7. In Chapter 8, we evaluate the industrial relevance of the methods and system developed by identifying the main competitors in the market and by proposing a market entry strategy for Virtual Clothing. We discuss our main hypothesis, we summarise our contributions, and finally we propose possible future work and draw conclusions in Chapter 9.

Chapter 2

Background and Related Work

This chapter explains terms often used in the field and gives an overview of work related to cloth simulation and visualisation. The chapter is split into two main parts. In the first section we review work on the problem of simulating the drape behaviour of cloth fabric. The focus is on numerical simulation, integration, collision detection and response. The second section concentrates on devices and methods to simulate the interaction of light and fabric which is important for the realistic visualisation of cloth and garments. A detailed survey that summarises work related to fabric drape simulation up to the year 1996 can be found in the paper by Ng and Grimsdale [NG96]. Two books [HB00, VMT00a] on cloth simulation also discuss aspects of cloth visualisation and give good surveys on cloth modelling approaches. This chapter is intended to give sufficient background for the reader to understand the chapters following. The goal is to focus on the detail of the methods we developed and extended for this thesis and closely related topics. Less attention is given to more distant topics.

2.1 Drape Behaviour

First we will discuss mechanical drape properties of cloth fabrics. We then introduce existing evaluation tests to gather drape properties from real fabrics. Accuracy and stability of computer models numerically to simulate the drape behaviour of cloth is the focus of the section immediately following. Finally, techniques for efficient collision detection and response are summarised.

2.1.1 Mechanical Properties of Fabric

The mechanical behaviour of cloth is inherently dependent on the material and structure of the fibres of which it is made. Common fibre materials are wool, cotton, synthetics, etc. and they differ in thickness and internal fibre or yarn structure. The structure of fabrics is inherent to the process of manufacturing. Fibre structures are tight or loose. *Woven*, *knitted* and *non-woven*

structures are the main types distinguished. Woven structures are made of orthogonally aligned and interlaced thread patterns created by a device called a loom, where *warp* and *weft* directions are distinguished. On a loom the *warp* threads are spaced equally and held under tension and the *weft* threads or *fillings* are interlaced into the warp threads. Warp and weft directions usually exhibit different elastic properties and are therefore responsible for the anisotropic behaviour of woven cloth. Knitted fabrics are hand made or by knitting machines and they consist of interlaced curls in successive rows. They are loose and elastic and used for woollens and underwear. Non structured fabrics are fabrics with no particular pattern structure.

2.1.1.1 Elasticity Theory

The physical properties are often categorised in four groups [MH93]. *Elasticity* describes internal forces caused by geometrical deformation. *Viscosity* describes internal forces caused by the speed of deformation. *Plasticity* describes the deformation history. *Resilience* defines the deformation limit where the structure will break. *Viscosity, plasticity* and *resilience* are often ignored in cloth simulation because they contribute only marginally to the appearance of cloth. Elasticity is further categorised into *metric elasticity* and *curvature elasticity.*

Metric elasticity describes deformations within the surface plane of the cloth while curvature elasticity describes deformations orthogonal to the surface plane. Metric elasticity is described by stress strain relations with three parameters: *Young's modulus*, the *Poisson coefficient* and the *Rigidity modulus*. *Young's modulus* E describes reactions along the deformation direction which are described by Hook's law. The *Poisson coefficient* v describes reactions orthogonal to the deformation direction described by Poisson's law. The *Rigidity Modulus* G describes oblique reactions described by a simple shear law. The stress strain relations in the one dimensional case are given by

$$\epsilon = \tfrac{1}{E}\sigma, \quad \epsilon = \tfrac{v}{E}\sigma, \; and \quad \epsilon = \tfrac{1}{G}\sigma, \tag{2.1}$$

where σ and ϵ denote stress and strain respectively along the deformation direction. For the two dimensional case of cloth the stress strain relation is given by

$$\begin{bmatrix} \sigma_{pp} \\ \sigma_{tt} \\ \sigma_{pt} \end{bmatrix} = \frac{1}{1 - v_p v_t} \begin{bmatrix} E_p & v_t E_p & 0 \\ v_p E_t & E_t & 0 \\ 0 & 0 & G(1 - v_p v_t) \end{bmatrix} \begin{bmatrix} \epsilon_{pp} \\ \epsilon_{tt} \\ \epsilon_{pt} \end{bmatrix} \tag{2.2}$$

where p denotes the fabric warp direction and t is the fabric weft direction. Owing to energetic constraints the above matrix is symmetric and therefore $\mathbf{E}_p v_t = \mathbf{E}_t v_p$. If the material were isotropic then we would have that the *Young's modulus* $\mathbf{E} = \mathbf{E}_p = \mathbf{E}_t$, the *Poisson coefficient*

$v = v_t = v_p$, and the *Rigidity coefficient* $G = \frac{E}{1+v}$. For *Curvature Elasticity* a similar formulation can be obtained. The *Poisson coefficient* for bending is 0, so the curvature strain τ and stress γ relations with flexion modulus B and flexion rigidity K are given by

$$\begin{bmatrix} \tau_{pp} \\ \tau_{tt} \\ \tau_{pt} \end{bmatrix} = \begin{bmatrix} B_p & 0 & 0 \\ 0 & B_t & 0 \\ 0 & 0 & K \end{bmatrix} \begin{bmatrix} \gamma_{pp} \\ \gamma_{tt} \\ \gamma_{pt} \end{bmatrix}. \tag{2.3}$$

More details on physical properties of textiles can be found in [MH93].

2.1.2 Measurement of Mechanical Fabric Properties

Several methods to empirically measure the properties of fabric have been proposed. The one most commonly used in the textile industries and also in computer graphics is the Kawabata Evaluation System (KES) [Kaw80], a fabric testing device and standard for measuring the properties of fabric and its drape. Five experiments are carried out on a fabric the result of which are fifteen curves and twenty-one parameters that describe the fabric. Among the twenty-one parameters are those that describe the linear elasticity. Only the Poisson coefficients are not measured. The five experiment are as follows.

- A *Tensile Test* in which the cloth sample is extended at a constant speed. The traction is reversed with the same speed after the deformation limit is reached. Rest elongation, maximum elongation, elongation ratio, traction energy, recovery energy, resilience and linearity are computed.

- A *Shearing Test* which is like the tensile test but movement is performed transversally. Shearing stiffness and the amount of hysteresis are computed.

- A *Bending Test* in which a long fabric rectangle ($1\ cm \times 20\ cm$) is fixed on one of the long edges. The other long edge is rotated and the distance between the two lines of attachment is adjusted to preserve the curvature as being a cylindrical section. Flexion stiffness at 1 cm curvature radius and its hysteresis are computed.

- A *Compression Test* in which the sample is compressed between a flat surface and a cylinder. Rest thickness, compressed thickness, compression energy, recovery energy, compressibility ratio, resilience and linearity are computed.

- A *Friction Test* in which roughness, friction and its variation are computed from the resistance of rods pulled over the fabric.

For warp and weft properties only the first three tests are widely used in the textile industry. In most computer graphics cloth simulations only stretch, shear and bending measurements are taken into account. Most non-linearities and hysteresis effects are commonly ignored and the Kawabata measurements are approximated with piecewise polynomial functions. The draping, buckling and wrinkling behaviour of fabric is a complex combination of the parameters measured with systems like the KES. The *Drapemeter* is an example of a fabric test that has been used for the validation of simulation models [CCOS91]. In the *Drapemeter* a cloth disc of given diameter is draped over a cylinder with a smaller diameter. The number and depth of wrinkles around the edge and the ratio of the projected cloth area after and before draping is measured and used for validation. More recently, Jojic et al [JH97] have used range data of cloth draped over a simple object to estimate simulation parameters. They use a MSPS for simulation and optimise the parameters according to mean square error measures between simulation results and range data. For minimisation they employ Powell's direction set technique. Bhat et al [BTH+03] report a system that allows us to acquire simulation parameters from video sequences of real cloth. Structured light techniques are used to simplify the identification of the shape of the cloth in each video frame. They develop a metric to compare cloths that involves computation of mean square errors of angular maps for fold comparison. In order to find simulation parameters they employ a simulated annealing optimisation technique as described in [PTVF92].

2.1.3 Computer Cloth Models

Mathematical models to describe cloth are complex systems of partial differential equations that are derived from the mechanical laws and material behaviour. Only elementary analytical solutions are available which are not practical for modelling complex cloth. This is why some computer graphics researchers created simple geometrical models [Wei86, HM90, NG96] to approximate at least some of the appearance of cloth. Numerical simulations are the only possibility to model cloth with some physical accuracy on a computer. Two types of discretisation can be identified: *Continuum Mechanics* models and *Particle Systems.*

2.1.3.1 Continuum Mechanics Models

Continuum mechanics models describe the material surfaces by quantities varying continuously in space and time. In such models mechanical laws that describe fabrics are represented by systems of partial differential equations. Numerical simulation requires the discretisation of the volume containing the surface. They provide the most accurate models of the material properties and are capable of reproducing the non-linearities of visco-elastic models. However,

they are computationally expensive and cannot deal with frequent collisions. Two examples are *Lagrange Equation Models* and *Finite Element Methods.*

Lagrange Equation Models

Terzopoulos et al [TPBF87] initially used the Lagrange Equation models for the simulation of visco-elastic deformable surfaces. Their goal was to create familiar deformations for animation production and not physical accuracy. Their models can be used for simulation of rubber and plastic but are not well suited for accurate simulation of cloth material. In these models the material properties such as metric elasticity and curvature elasticity are expressed in *differential geometry* terms by the *metric tensor* of the first fundamental form and the *curvature tensor* of the second fundamental form to derive internal surface energies. Their system is discretised by a *finite differences* approach and the resulting linear system is solved by use of the Gauss-Seidel method. In [TF88] Terzopoulos and Fleischer extended the model for the simulation of cloth, such as surfaces with collision constraints, flag animations and cloth tearing. Lafleur et al [LMTT91] and Carigan et al [CYTT92] developed the model for simulating garments on virtual actors. In [AK90] Aono and Ko describe a more specialised model. Instead of differential geometry metrics, Aono and Ko made a more detailed stress-strain analysis of a linear isotropic elastic body. D'Alemberts principle is applied, which assumes that the sheet is in equilibrium at every instance when in motion. The fundamental equations of motion are derived from a modified version for wave propagation within an elastic continuum.

Finite Element Methods

Instead of discretising the mechanical equations of the surface on a grid using finite differences, Finite Element Methods (FEM) discretise the mechanical energies. A sparse linear system matrix is built from the surface elements which can be solved by the conjugate gradient method [She94]. FEM was used for cloth simulation by Gan et al [GLS95] and Collier et al [CCOS91]. Eischen et al [EDC96] in addition approximate Kawabata plots (See Section 2.1.2) with fifth order polynomials on a rectangular cloth surface. The accuracy of their approach is demonstrated by comparing the bending and buckling properties with those inferred from real fabrics. Recently, in [EKS03] Etzmuß et al showed a FEM for interactive cloth simulation. They accelerated their simulations by dropping the non-linearities of the elasticity model. Non-linearities are dropped from Green's stress tensor which yields Cauchy's stress tensor. Their model is independent of the mesh topology and they show simulations for garments on virtual actors. Cloth properties are mapped

from a KES. Their system is solved by a conjugate gradient method. Simulation times are dependent on the stiffness of the material and their results are similar to those achieved with mass spring particle systems.

2.1.4 Mass Spring Particle Systems

Particle Systems discretise the surfaces with a set of "particles" (point masses) that interact via the forces they excert on each other to approximate the material behaviour. Breen et al [BHW94] first employed particle systems to describe textile behaviour from the KES. They approximate the measured shearing and bending forces with first and second order polynomials. Eberhardt et al [EWS96] improved Breen's model by adding simulation of the hysteresis effects obtained directly from Kawabata fabric tests.

2.1.4.1 Topologies

Since most of the following work is based on Provot's model [Pro95], we discuss it in more detail. Provot uses a topology as depicted in Figure 2.1 where stretch springs connect neighbouring particles horizontally and vertically, shearing springs connect diagonally and bending springs connect every other mass point horizontally and vertically. This is different to the model used by Volino et al [VCT95] who model bending properties by employing angular constraints between the surface normals of triangles. Provot uses linear (Hookean) springs and applies explicit Euler integration to solve the system (see below). Owing to use of the linear spring model, super-elongation effects appeared. This means that cloth unnaturally stretches under its own weight and behaves more like rubber than cloth. This could be overcome by modelling very stiff springs but, as mentioned below, stiff springs cause stability problems in the explicit Euler integration step. Instead, Provot accounts for super-elongation in a post correction step by constraining particle positions according to a spring length threshold. Since most cloth does not stretch much, the threshold is usually chosen to be close to the natural spring length. However, this repositioning strategy can lead to over-elongation of other springs. Provot observed that several iterations of the post correction steps are needed to reduce the number of over-elongated springs. The convergence behaviour of this correction strategy is unclear. However, the particularly well-developed aspect of Provot's model is that all internal forces are modelled by Hookean springs which makes the system very easy to implement and very efficient to process. Provot's model consists of a mesh of $M \times N$ mass points connected with mass-less springs. There are three different types of springs:

- Springs linking vertices $[i, j]$ with $[i + 1, j]$, and $[i, j]$ with $[i, j + 1]$ called "stretch springs";

- Springs linking vertices $[i, j]$ with $[i+1, j+1]$, and $[i+1, j]$ with $[i, j+1]$ called "shear springs";
- Springs linking vertices $[i, j]$ with $[i+2, j]$, and $[i, j]$ with $[i, j+2]$ called "bending springs".

As the names indicate, the first type of spring implements resistance to stretching, the second - to shearing and the third - to bending.

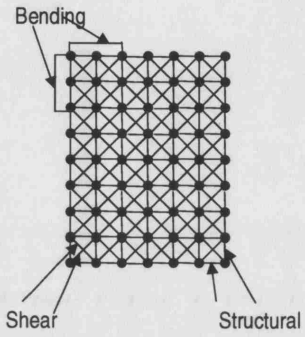

Figure 2.1: Spring topology in Provot's model.

The force acting on a particle ij can be divided in two categories, *Internal* and *External* forces. The **internal forces** arise from the springs. The internal force applied at vertex ij is a result of the stiffness of all springs linking ij to its neighbours:

$$\mathbf{f}_{ij}^{int} = -\sum_{k,l} k_{ijkl} \left((\mathbf{x}_{kl} - \mathbf{x}_{ij}) - l_{ijkl}^{0} \frac{\mathbf{x}_{kl} - \mathbf{x}_{ij}}{|\mathbf{x}_{kl} - \mathbf{x}_{ij}|} \right) \tag{2.4}$$

where k_{ijkl} is the stiffness of the spring linking ij and kl, l_{ijkl}^{0} is the rest length of the spring and $\mathbf{x}$ is the position of a vertex. Viscous damping may be regarded as an internal force as well and can be described as $\mathbf{f}_{ij}^{vd} = -C_{vd}(\mathbf{v}_i - \mathbf{v}_j)$, where C_{vd} is a damping coefficient and $\mathbf{v}$ denotes the vertex's velocity.

External forces can differ in nature depending on what type of simulation is to be made. A common force is $\mathbf{f}_{ij}^{gr} = m_{ij}\mathbf{g}$, where $\mathbf{g}$ is the acceleration owing to gravity. All the above formulations make it possible to compute the force $\mathbf{f}_{ij}(t_0)$ applied to vertex ij at any time t_0.

2.1.4.2 Integration Methods

The goal of integration methods in cloth simulation is to compute the positions of particles from the forces exerted on them. Let $\mathbf{x}_{ij}(t)$, $\mathbf{v}_{ij}(t)$, $\mathbf{a}_{ij}(t)$, where $i = 1...M$ and $j = 1...N$, be correspondingly the positions, velocities, and accelerations of the mass points at time t_0. The particle system is governed by Newton's law:

$$\mathbf{f}_{ij} = m_{ij}\mathbf{a}_{ij} \tag{2.5}$$

where m_{ij} is the mass of particle ij and $\mathbf{f}_{ij}$ is the sum of all forces applied at vertex ij. Newtonian dynamics can be integrated over time by a *forward Euler* integration method:

$$\begin{aligned}
\mathbf{a}_{ij}(t_0 + \Delta t) &= \tfrac{\mathbf{f}_{ij}(t_0)}{m_{ij}}, \\
\mathbf{v}_{ij}(t_0 + \Delta t) &= \mathbf{v}_{ij}(t) + \Delta t\mathbf{a}_{ij}(t_0 + \Delta t), \\
\mathbf{x}_{ij}(t_0 + \Delta t) &= \mathbf{x}_{ij}(t) + \Delta t\mathbf{v}_{ij}(t_0 + \Delta t)
\end{aligned} \tag{2.6}$$

where Δt is the chosen simulation time step.

For periodic systems Euler's method is guaranteed to be stable if the time steps are less than the natural period of the system, $T_0 \approx \pi\sqrt{\frac{m}{K}}$. This criterion is more generally known as the Courant condition [ZT91] and shows that the time step has to be smaller the stiffer the springs. In fact, the time step is dependent on the stiffest spring and the lightest mass-point in the system. For improved accuracy several integrations can be carried out per time step. Such strategies are known as Mid-Point or second order Runge-Kutta for two integrations and higher order Runge-Kutta [PTVF92] methods for four and more integrations per time step.

Jakobsen [Jak01] and Melis [Mel02] used the Verlet integration scheme for cloth simulation. Verlet integration originates from research on molecular dynamics [Ver67]. In the basic Verlet scheme, a particle's position at time t, $\mathbf{x}(t) = f(t)$, where $f(t)$ is a function of the particle's position at time t that is approximated by a third-order Taylor series expansion:

$$f(t) \approx f(t_0) + (t - t_0)f'(t_0) + \frac{1}{2!}(t - t_0)^2 f''(t_0) + \frac{1}{3!}(t - t_0)^3 f'''(t_0). \tag{2.7}$$

Thus on substituting $f'(t)$ by velocity $\mathbf{v}(t)$ and $f''(t)$ by acceleration $\mathbf{a}(t)$ we obtain:

$$\mathbf{x}(t_0 + \Delta t) = \mathbf{x}(t_0) + \Delta t\mathbf{v}(t_0) + \frac{1}{2}\Delta t^2\mathbf{a}(t_0) + \frac{1}{6}\Delta t^3\frac{d\mathbf{a}(t_0)}{dt}. \tag{2.8}$$

Similarly for $\mathbf{x}(t_0 - \Delta t)$ we have:

$$\mathbf{x}(t_0 - \Delta t) = \mathbf{x}(t_0) - \Delta t\mathbf{v}(t_0) + \frac{1}{2}\Delta t^2\mathbf{a}(t_0) - \frac{1}{6}\Delta t^3\frac{d\mathbf{a}(t_0)}{dt}. \tag{2.9}$$

Addition of Equation 2.8 and Equation 2.9 gives

$$\mathbf{x}(t_0 + \Delta t) + \mathbf{x}(t_0 - \Delta t) = 2\mathbf{x}(t_0) + \Delta t^2\mathbf{a}(t_0). \tag{2.10}$$

By rearranging, the final update of the Verlet method is written as:

$$\mathbf{x}(t_0 + \Delta t) = 2\mathbf{x}(t_0) - \mathbf{x}(t_0 - \Delta t) + \Delta t^2\mathbf{a}(t_0). \tag{2.11}$$

The velocity is thus approximated by the difference between the previous and the current particle's position $\frac{1}{\Delta t}(\mathbf{x}(t_0) - \mathbf{x}(t_0 - \Delta t))$. The Verlet scheme is numerically more stable because it only uses particle positions and no higher order differentiation. Errors caused by numerical differentiation are therefore avoided which leads to a more stable numerical integration scheme.

Baraff and Witkin [BW98] reintroduced implicit integration which was already used by Terzopoulus et al [TPBF87] for stable prediction of the next system state. Implicit integration is also often called *backward Euler* integration. If we define the diagonal mass matrix $\mathbf{M} \in \mathbf{R}^{3n \times 3n}$, where n is the number of nodes, by diag(M)= $(m_1, m_1, m_1, m_2, m_2, m_2, ..., m_n, m_n, m_n)$ and position and velocity state vectors $\mathbf{x}$ and $\mathbf{v}$ respectively, the acceleration $\mathbf{a}$ of the whole system can be written as

$$\mathbf{a} = \mathbf{M}^{-1}\mathbf{f}(\mathbf{x}, \mathbf{v}). \tag{2.12}$$

To compute the new state and velocity using an implicit technique, Equation 2.12 is transformed into a first-order differential equation by defining the system's velocity as $\mathbf{v} = \dot{\mathbf{x}}$, so that:

$$\frac{d}{dt}\begin{pmatrix} \mathbf{x} \\ \mathbf{v} \end{pmatrix} = \begin{pmatrix} \mathbf{v} \\ \mathbf{M}^{-1}\mathbf{f}(\mathbf{x}, \mathbf{v}) \end{pmatrix}. \tag{2.13}$$

$\mathbf{x}_0 = \mathbf{x}(t_0)$, $\mathbf{v}_0 = \mathbf{v}(t_0)$, $\Delta\mathbf{x} = \mathbf{x}(t_0 + \Delta t) - \mathbf{x}(t_0)$ and $\Delta\mathbf{v} = \mathbf{v}(t_0 + \Delta t) - \mathbf{v}(t_0)$ are then defined to simplify the notation. The explicit *forward Euler* method can then approximate $\Delta\mathbf{x}$ and $\Delta\mathbf{v}$ as

$$\begin{pmatrix} \Delta\mathbf{x} \\ \Delta\mathbf{v} \end{pmatrix} = \Delta t \begin{pmatrix} \mathbf{v}_0 \\ \mathbf{M}^{-1}\mathbf{f}_0 \end{pmatrix}, \tag{2.14}$$

where the force $\mathbf{f}_0 = \mathbf{f}(\mathbf{x}_0, \mathbf{v}_0)$. As previously discussed the step size Δt is dependent on the natural period of the system. In the implicit *backward Euler* method, $\Delta\mathbf{x}$ and $\Delta\mathbf{v}$ are approximated by

$$\begin{pmatrix} \Delta\mathbf{x} \\ \Delta\mathbf{v} \end{pmatrix} = \Delta t \begin{pmatrix} \mathbf{v}_0 + \Delta\mathbf{v} \\ \mathbf{M}^{-1}\mathbf{f}(\mathbf{x}_0 + \Delta\mathbf{x}, \mathbf{v}_0 + \Delta\mathbf{v}) \end{pmatrix}. \tag{2.15}$$

The forward method is based on the conditions at t_0 only, while the backward method's step is written in terms of the condition at the end of the step itself. The method is called "backward" Euler because it is equivalent to starting from the output state $(\mathbf{x}_0 + \Delta\mathbf{x}, \mathbf{v}_0 + \Delta\mathbf{v})$ and using a *forward Euler* step to run the system backwards in time. *Forward Euler* integration takes no notice of wildly changing derivatives, and therefore is required to step forward with small Δt. *Backward Euler* forces the derivative to point back to where it came from at $\mathbf{x}_0, \mathbf{v}_0$ and therefore adds an extra layer of consistency. The forward method requires only an evaluation of

the function $\mathbf{f}$ but the backward method requires us to solve for values $\Delta\mathbf{x}$ and $\Delta\mathbf{v}$ that satisfy Equation 2.15. This equation is non-linear and can be approximated by a first-order Taylor series expansion of $\mathbf{f}$:

$$\mathbf{f}(\mathbf{x}_0 + \Delta\mathbf{x}, \mathbf{v}_0 + \Delta\mathbf{v}) \approx \mathbf{f}_0 + \frac{\partial \mathbf{f}}{\partial \mathbf{x}}\Delta\mathbf{x} + \frac{\partial \mathbf{f}}{\partial \mathbf{v}}\Delta\mathbf{v}. \tag{2.16}$$

The derivative $\partial\mathbf{f}/\partial\mathbf{x}$ is evaluated for $(\mathbf{x}_0, \mathbf{v}_0)$ and similarly for $\partial\mathbf{f}/\partial\mathbf{v}$. Substitution of Equation 2.15 yields the linear system

$$\begin{pmatrix} \Delta\mathbf{x} \\ \Delta\mathbf{v} \end{pmatrix} = \Delta t \begin{pmatrix} \mathbf{v}_0 + \Delta\mathbf{v} \\ \mathbf{M}^{-1}(\mathbf{f}_0 + \frac{\partial \mathbf{f}}{\partial \mathbf{x}}\Delta\mathbf{x} + \frac{\partial \mathbf{f}}{\partial \mathbf{v}}\Delta\mathbf{v}) \end{pmatrix}. \tag{2.17}$$

If we take the bottom row of Equation 2.17 and substitute $\Delta\mathbf{x} = \Delta t(\mathbf{v}_0 + \Delta\mathbf{v})$ from the top row, it yields:

$$\Delta\mathbf{v} = \Delta t\mathbf{M}^{-1}\left(\mathbf{f}_0 + \frac{\partial \mathbf{f}}{\partial \mathbf{x}}\Delta t(\mathbf{v}_0 + \Delta\mathbf{v}) + \frac{\partial \mathbf{f}}{\partial \mathbf{v}}\Delta\mathbf{v}\right). \tag{2.18}$$

If we let $\mathbf{I}$ denote the identity matrix, and regroup the terms, we obtain:

$$\left(\mathbf{I} - \Delta t\mathbf{M}^{-1}\frac{\partial \mathbf{f}}{\partial \mathbf{v}} - \Delta t^2\mathbf{M}^{-1}\frac{\partial \mathbf{f}}{\partial \mathbf{x}}\right)\Delta\mathbf{v} = \Delta t\mathbf{M}^{-1}\left(\mathbf{f}_0 + \Delta t\frac{\partial \mathbf{f}}{\partial \mathbf{x}}\mathbf{v}_0\right) \tag{2.19}$$

which is solved for $\Delta\mathbf{v}$. Given $\Delta\mathbf{v}$ we can compute $\Delta\mathbf{x} = \Delta t(\mathbf{v}_0 + \Delta\mathbf{v})$.

Instead of using energy functions to map material properties onto the system, Baraff and Witkin introduce vector conditions $\mathbf{C}(\mathbf{x})$ to model resistance to stretch, shear and bend. To enforce constraints on particles' velocities and directions they introduce the idea of inverse masses. Suppose, for example, we want to keep particle i's velocity from changing. If we set the inverse mass $1/m_i$ to zero the particle acquires an infinite mass, making it ignore all forces exerted on it. In order, for example, to constrain a particle in the z direction instead of using a scalar mass they use an inverse mass matrix to compute a particle's acceleration which in this case would be of the form

$$\mathbf{a}_i = \begin{pmatrix} \frac{1}{m_i} & 0 & 0 \\ 0 & \frac{1}{m_i} & 0 \\ 0 & 0 & 0 \end{pmatrix}\mathbf{f}_i. \tag{2.20}$$

In order to constrain an arbitrary direction defined by a unit vector $\mathbf{p}$ the inverse mass matrix is computed as $\frac{1}{m_i}(\mathbf{I} - \mathbf{p}\mathbf{p}^T)$. Given two constraint directions $\mathbf{p}$ and $\mathbf{q}$ an inverse mass matrix $\frac{1}{m_i}(\mathbf{I} - \mathbf{p}\mathbf{p}^T - \mathbf{q}\mathbf{q}^T)$ is used. Baraff and Witkin replace the inverse mass matrix $\mathbf{M}^{-1}$ in Equation 2.19 by a constrained inverse mass matrix $\mathbf{W}$ constructed as above. They further alter the equation for the velocity of particle i by adding a term $\mathbf{z}_i$.

$$\left(\mathbf{I} - \Delta t\mathbf{W}\frac{\partial \mathbf{f}}{\partial \mathbf{v}} - \Delta t^2\mathbf{W}\frac{\partial \mathbf{f}}{\partial \mathbf{x}}\right)\Delta\mathbf{v} = \Delta t\mathbf{W}\left(\mathbf{f}_0 + \Delta t\frac{\partial \mathbf{f}}{\partial \mathbf{x}}\mathbf{v}_0\right) + \mathbf{z}. \tag{2.21}$$

$\mathbf{z}$ can be used, for example, for collision response. Unfortunately, the constraint inverse mass matrix $\mathbf{W}$ may contain singularities and is not positive definite symmetric as required by a conjugate gradient solver [She94]. Baraff and Witkin therefore modify the conjugate gradient solver by introducing a filter function that generates a positive definite symmetric matrix taking into consideration the constraints represented by $\mathbf{W}$ and addition of the $\mathbf{z}$. Owing to the increased stability of the implicit integration method they can simulate stiffer materials and can make larger simulation time steps than when an explicit method is used. Also, the time to solve the system is independent of the stiffness of the system which is not the case in the explicit form. However, solving the matrix that describes the system state requires far more computation than explicit integration. A description of the method accessible to programmers can be found in [Mac00].

Desbrun et al [MDDB00] employed Provot's model but they use an implicit integration scheme. Their goal was interactive real-time simulation of cloth. They only solve the linear part of the system described by Baraff and Witkin [BW98] and correct for non-linearities in a post correction step similar to that of Provot [Pro95]. They precompute the inverse of the system matrix to solve the linear part which does not change during simulation under the assumption of constant time steps and equal masses of all particles. Equation 2.19 is written as

$$\Delta\mathbf{v} = \frac{\Delta t}{m}\mathbf{X}\left(\mathbf{f}_0 + \Delta t\frac{\partial \mathbf{f}}{\partial \mathbf{x}}\mathbf{v}_0\right), \tag{2.22}$$

with

$$\mathbf{X} = \left(\mathbf{I} - \frac{\Delta t}{m}\frac{\partial \mathbf{f}}{\partial \mathbf{v}} - \frac{\Delta t^2}{m}\frac{\partial \mathbf{f}}{\partial \mathbf{x}}\right)^{-1}. \tag{2.23}$$

Desbrun et al approximate $\partial\mathbf{f}/\partial\mathbf{x}$ with a constant matrix $\mathbf{H}$, which they note is the negative of the Hessian matrix of the system. The non-linear term including $\partial\mathbf{f}/\partial\mathbf{x}$ is dropped. A change in velocity is then computed as:

$$\Delta\mathbf{v} = \frac{\Delta t}{m}\mathbf{X}(\mathbf{f}_0 + \Delta t\mathbf{H}\mathbf{v}_0), \tag{2.24}$$

with

$$\mathbf{X} = (\mathbf{I} - \frac{\Delta t^2}{m}\mathbf{H})^{-1}. \tag{2.25}$$

By precomputing the matrix $\mathbf{H}$, a velocity update becomes a simple matrix multiplication as in Equation 2.24. Matrix $\mathbf{H}$ is computed as:

$$\begin{cases} \mathbf{H}_{ij} = k_{ij} & if\ i \neq j, \\ \mathbf{H}_{ii} = \sum_{i \neq j} k_{ij} & Otherwise. \end{cases} \tag{2.26}$$

Implicit integration may be also regarded as a form of convolution filter on the particles' force field as noted by Kass in [Kas95]. At one extreme, with small time steps the convolution

distributes the forces only to nearby particle neighbours resulting in a flexible cloth model. At the other extreme, if Δt or the spring stiffness is very large the cloth behaves like a rigid sheet and therefore the convolution smoothes over all particles creating a uniform force. While the system matrix is sparse, its inverse often is not and its size grows quadratically with the number of particles. Desbrun et al [MDDB00] categorise their method as a predictor-corrector scheme. To account for non-linear rotations they introduce forces based on preservation of angular momentum. The method is very fast for small particle systems but becomes prohibitively slow and memory intensive for systems with more than 1000 degrees of freedom.

Kang et al [KCP+00] build on the idea of Desbrun but note that velocity updates are only dependent on the particle's neighbouring velocity. They thus arrive at an iterative scheme similar to Jacobi iterations [PTVF92]. To enforce interactivity they take the solution of the matrix at a fixed time step, even if it has not completely converged. This allows them to solve the system at rates similar to explicit integration but with the increased stability of implicit integration. However, the accuracy of the simulation of material properties is completely ignored.

Etzmuß et al [EEH00] exploit the fact that the stiffest springs are tension springs and therefore apply a different integration scheme depending on the stiffness of the springs. An implicit conjugate graduate solver is used for stiff tension springs and an explicit Newton solver for the remaining, less stiff spring types. They categorise their approach as an implicit explicit (IMEX) integration.

Recently, Choi and Ko [CK02] examined the buckling behaviour of cloth in more detail. They exploit new results from research on material mechanics and apply them to Provot's model. Semi-implicit integration [VMT00b] is used to solve the system. They take a closer look at damping forces and distinguish three types: artificial damping forces which stem from implicit integration, fictitious damping which is added to increase stability, and material intrinsic damping. They identify that numerical instabilities in previous systems are also caused by the incorrect treatment of buckling which often occurs in animations where large compression forces appear. They account for this problem by adding a bending energy in the form of a circular arc with curvature corresponding to the spring compression. This buckling response is exerted immediately a compression happens and therefore instabilities are avoided.

Boxerman and Ascher [BA04] use Choi and Ko's model but for integration they employ an adaptive IMEX scheme. Their adaptive scheme improves the sparsity of the system matrix and therefore increases the performance of the solver. They claim performance improvements over a purely implicit scheme of over 100%. However, their paper only shows simple simulations of a table cloth and it is unclear how their methods will behave on larger systems as required for

Virtual Clothing.

In [VMT01] Volino et al show experimental comparisons between implicit and explicit integration schemes. They find that implicit Euler gives quicker and more stable results than explicit integration. However, they also observe that the implicit integration adds artificial damping behaviour and creates unrealistic animations. For example, folds do not appear where they should and cloth behaves clumsily. Their conclusion is that explicit integration still has some benefits over implicit solutions especially if low damping materials are involved. For very stiff materials, stable explicit integration requires very many small time steps which may be more computationally intensive than solving the system of an implicit scheme. As we shall discuss in the concluding section of this chapter we introduce an improvement of Provot's cloth model in Chapter 3 which enables us to efficiently simulate fairly stiff materials with an explicit scheme.

2.1.5 Collision Detection

Collision detection problems have been extensively studied in computational geometry, computer graphics and robotics. A survey on collision detection techniques between rigid objects can be found in [LG98]. A survey on collision detection for deformable objects is given in [TKZ+04]. Different strategies exist to detect collisions between different surface representations. However, since most cloth surface representations are triangular or quadrilateral meshes, we only discuss the corresponding strategies here. Collision detection proves to be a bottleneck of dynamic simulation algorithms especially if the deformable surfaces are highly discretised owing to the number of potential colliding particles. This is also the case in cloth simulation. Most of the existing algorithms for detecting collisions are based on geometrical interference tests. The basic problem of collision detection in dynamic simulation is to find if, in a simulation time interval Δt, one or more collisions between triangles have occurred. For triangular meshes two types of collisions can be identified: *point-triangle* collisions, and *edge-edge* collisions. Moore and Wilhelms [MW88] developed a fifth order polynomial to detect point-triangle collisions. Owing to its computational complexity it has not been used much. Provot [Pro97] derived a cubic polynomial to compute point-face and edge-edge collisions. While a single collision check can be computed very efficiently, the number of possible collisions between n triangles is $O(n^2)$ since potentially every triangle point can collide with another face or an edge with an edge. To increase performance, space partitioning techniques such as Volume Hierarchy trees or Voxel Hash tables have been commonly used. In general there are three approaches to spatial subdivision: Bounding Volume Hierarchies, Voxel Based Techniques and, in particular for deformable surfaces, Curvature Culling methods.

2.1.5.1 Bounding Volume Hierarchies

Bounding volume hierarchies divide the space into volumes that contain the geometrical objects. Bounding spheres, axis-aligned bounding boxes (AABB) [VMT94, Pro97], object-oriented bounding boxes (OOBB) and k-Dop volumes [MKE03, VMT00b] are the most common techniques used. They are increasingly tight to the circumscribed object in the order in which they were mentioned above. For deformable surfaces, the individual surfaces are further subdivided to improve the performance of self-collision tests. This is typically achieved in a pre-processing step in which the divided sub-volumes are organised in a tree structure and the final triangles are stored in the leaves of the tree. Tree data structures reduce the complexity of a collision query from $O(n)$ to $O(\log n)$. However, with deformable surfaces the number of overlapping volumes can become very high. This is when curvature culling techniques, as mentioned below, become very useful. An oct-tree structure was used by Yang et al [YMT93].

2.1.5.2 Voxel Based Approaches

By partitioning the space around the cloth into uniformly sized cells (Voxels), the complexity of a collision query can be reduced further from $O(\log n)$ in the case of bounding volume hierarchies to $O(1)$. This is possible because the Voxel positions are known and can be directly indexed. However, it is not generally possible to uniformly subdivide the space so that every Voxel contains just one or two triangles. Therefore, triangles in the individual Voxels are usually put in some spatial data structure such as bounding volume hierarchies as described above. Bigliani et al [BE00] and Zhang et al [ZY00] exploit such techniques for collision detection in cloth simulation. In order to reduce memory requirements, both approaches utilise *Hash tables* for storing the Voxel data. To overcome problems with triangles close to Voxel borders for which collisions may not be correctly detected, such triangles are registered in all the neighbouring cells. Zhang et al [ZY00] avoid checking for edge-edge collisions by inserting a thin area around static objects similar to that used by Liu et al [LKC96].

2.1.5.3 Curvature Culling

Additional culling of possible interactions can be achieved by taking the surface curvature into account. The basic idea is that particles close to each other on a low curvature surface are unlikely to collide. To estimate the local curvature the surface normal is considered. In the case of bounding volumes the average normal of the triangles contained in the volume is taken. Only overlapping volumes with a large difference in surface normal have to be tested for collision. Surface curvature culling was introduced by Volino et al [VMT94] and further refined by Provot [Pro97]. Mezger et al [MKE03] use Provot's [Pro97] curvature culling technique in conjunction

with k-Dop volume hierarchies. Mezger et al's focus is on optimal tree traversal of bounding volumes.

As we shall discuss in the concluding section of this chapter we introduce image based collision detection for cloth body interference tests in Chapter 3.

2.1.6 Collision Response

Collision response describes mechanisms that simulate a natural reaction to a detected collision. The methods to be applied depend on the mechanical system model used for the cloth behaviour. The penalty method is usually used to simulate an appropriate response. It is equivalent to adding a strong damping spring to the system at the points of contact. Moore and Wilhelms [MW88] used this method to simulate the response between colliding objects.

Terzopoulos et al [TPBF87] and Lafleur et al [LMTT91] used a slight variant of Moore's technique in cloth animation by creating a thin, repulsive force field around objects. When an object is close to a surface, the auxiliary force is activated by the repulsive field to move the vertices involved away in the next simulation step. Repulsive force fields guarantee penetration free simulation but do not create very realistic looking collision responses.

Carignan et al [CYTT92] employed the law of conservation of momentum for solving collisions. This method generated more natural behaviour but allowed penetration in certain cases.

Liu et al [LKC96], whose cloth model is based on [TPBF87] with a regular grid, set up constraints such that the colliding grid points slide along the colliding triangles. If the current time step causes penetration of objects, the grid points are repositioned along the surface. They provide the expressions for the constrained iteration steps of the Gauss-Seidel integration method for the case of collisions with rigid objects and self-collisions.

Provot [Pro97] and Eberhardt et al [EWS96] exploit Coulomb's friction laws to directly modify particle velocities in proportion to the impact force to avoid penetrations.

Volino [VMT95] report a probabilistic approach for collision response to overcome problems of cloth self-intersections that are the result of earlier improper collision response. They add attractive and repulsive forces depending on the surface orientation. Surface orientation is determined from local geometry and history of vertex/face and edge/edge pairs. While they show impressive results their approach does not guarantee intersection free surfaces.

Baraff and Witkin [BW98] modify their conjugate gradient solver to constrain particles in the direction of collision to avoid penetration. Constraints are imposed on a particle's velocity and direction by means of the inverse masses as described above.

Etzmuß et al [EEHS00] adaptively insert additional vertices, which they call virtual particles, into the mesh by applying a constrained Delauny triangulation to avoid penetration of rigid objects in the environment. A similar approach was described by Hutchinson et al [HPH96].

Bridson et al [BFA02] recently demonstrated new developments in collision response to guarantee penetration free results. They use adaptive time stepping to compute the exact time of a particle collision. They treat situations where a collision response causes a new collision and iterate until no collision is detected. Provot's [Pro97] idea of *zones of impact* to handle multiple collisions is reformulated. *Zones of impact* describe particles that collide more than once per time step. These particles are merged and no movement among particles within the zone is permitted during a simulation step. In a post process, Bridson et al [BFA02] increase the mesh resolution again performing collision detection and response for the newly inserted particles.

Even though Bridson et al presented methods that guarantee intersection free collision response, Baraff et al [BWK03] found problems that frequently occur in production animation. The geometry of animated characters often self-intersect (e.g., shoulders, elbows, knees,..) and thereby creates unsolvable situations for the cloth collision detection. Similar problems were addressed earlier by Volino et al[VMT95]. Baraff et al [BWK03] introduce a method for resolving situations where the cloth surface is forced to penetrate the body of an animated character. As opposed to other collision response techniques that rely on the collision history to resolve collisions. Their method uses the global geometry of the garment to carry out intersection analysis which make sure that the garment never penetrates the body. As we shall discuss in the concluding section of this chapter we describe in Chapter 3 an adaptation of the method developed by Eberhardt et al [EWS96] which enables our model to respond efficiently to collisions detected by our image based approach.

2.2 Realistic Visualisation

The goal of realistic visualisation in general is to create images that appear natural and physically plausible. To this end, many models have been built that approximate the behaviour of light and material reflectance. Models are either a complete mathematical representation of the phenomenon to be approximated, or empirical data acquired by means of measuring devices is used. Realistic visualisation is the main topic of many computer graphics books and we do not attempt to cover all topics in this area here. Instead, we focus on work related to the visualisation of fabrics. We start with a discussion of the representations used for cloth surfaces, measurement and modelling of reflectance is the next topic and finally we briefly discuss

relevant rendering techniques.

2.2.1 Surface Representation

The most common representation for visualisation of cloth are triangular meshes. Triangular meshes are supported by most graphics hardware for efficient rendering. Since cloth is highly deformable and can bend almost arbitrarily, triangular meshes should have high resolution to be able to represent high curvature surfaces accurately. However, fine triangulation results in longer rendering times and bigger memory requirements. Deformation of a polygonal mesh can easily be achieved by changing the vertex positions according to the underlying cloth simulation. However, computation of curvature on a triangular mesh can only be approximated from the vertex normals. Surfaces may also be represented as curved surfaces such as NURBS. In this case a lower number of control points is required to animate the surface than for a triangular mesh and curvature is directly described in the surface representation. However, sharp and irregular details cannot be represented and for rendering by graphics hardware or most ray tracers, curved surfaces are converted to polygonal meshes. A trade-off between standard polygonal meshes and curved surfaces are progressive meshes. Progressive meshes are represented by algorithms that hierarchically add more triangles to surface areas with high curvature.

2.2.2 Reflectance Measurements

Nicodemus et al [NRH+77] defines reflection and reflectance as follows:
"*Reflection* is the process by which electromagnetic flux (power), incident on a stationary surface or medium, leaves that surface or medium from the incident side without change in frequency; *reflectance* is the fraction of the incident flux that is reflected."

2.2.2.1 Homogeneous Surfaces

A range of devices have been developed for reflectance measurements. Typically the sample of interest is assumed to have a homogeneous surface so that a single bidirectional reflectance distribution function (BRDF) is sufficient.

BRDF measurements were initially carried out by use of so-called gonio-reflectometers designed by Murray-Coleman and Smith [MCS90]. This instrument is composed of a mechanical goniometer system with four degrees of freedom. A light source and a photometer are mounted on the goniometer and can be moved automatically and individually around the hemisphere surrounding the sample. For every combination of light and photometer orientation the amount of light reflected from the sample that reaches the photometer is measured. The resulting data represents the sampled BRDF of the material under observation.

Since changing the positions of the photometer takes time, high-quality measurements can take several days or even weeks. The goal of later developments was thus to decrease the number of moveable parts of the device. Ward et al [War92] present an image based approach to measuring the BRDF. Instead of a photometer they use a semi-transparent hemispherical mirror around the sample. A CCD camera is placed next to the sample in the centre of the hemisphere to capture all light reflected from the sample material. The direction of the incident light is changed by moving the light source around behind the semi-transparent mirror. A single image of the hemispherical mirror can therefore capture all the samples that a gonio-reflectometer would capture by moving the photometer around to sample the hemisphere. The BRDF measurements are often fitted to Ward's model which is described below.

Karner et al [KMG96] also exploit an image based approach. They use a reference material (a near perfect Lambertian surface), a CCD web camera for reflectance measurements and a near uniform light source. To ensure the same lighting conditions for both reference and sample, an image is taken of the reference and the sample side by side on a flat surface. Location and orientation of the camera are computed from reference points on the image. The light location source is assumed to be known. From a single image they can compute a large number of incident and exitant samples to approximate the material sample BRDF. Measurements are also fitted to Ward's model. However, the quality of the measurements is not evaluated in the paper by Karner et al [KMG96].

Marschner et al [MWL+99] take a similar approach but wrap the sample material around a curved surface (a sphere or cylinder) in order to obtain more information about the reflectance behaviour at grazing angles. This is probably better suited for measuring the BRDF of paints than that of textiles. The surface geometry of the object the material is wrapped around, light and camera position are known and, from a single image of the object with the material wrapped around it, the BRDF can be approximated.

2.2.2.2 Heterogeneous Surfaces

In their pioneering work Dana et al [DvGNK99] demonstrate how to retrieve not only the BRDF but the bidirectional texture function (BTF). A planar surface sample is lit by a directional light source and photographed from different directions. The pixels of the resulting images are a function of viewing and illumination direction. The BTF is a 6 dimensional reflectance field $L = L(x, y, \theta_i, \phi_i, \theta_o, \phi_o)$ where (x, y) represents the sample point and (θ_i, ϕ_i) and (θ_o, ϕ_o) denote incoming and outgoing radiance directions.

Liu et al [LYS01] show how to use such data from a sparse set of images acquired from different viewing and lighting directions to generate bump maps from BTFs. Furthermore, Liu

et al [LYS01] show how to apply a completely synthesised version of the BTF to a surface of arbitrary geometry.

Lensch et al [LKG+01] recover a spatially varying BRDF directly on 3D objects. A 3D model is retrieved from a structured light scanner and a computer tomography scanner whilst lighting position is computed from environment maps of metal gazing balls by applying triangulation. In a manner similar to that of Marschner [MWL+99] (see above) they recover surface reflection properties from 20-25 high dynamic range (HDR) images. Spatially varying BRDFs dependent on the eigenvalues of the BRDF's covariance matrix are identified in a clustering process.

2.2.2.3 Virtual Reflectometers

Virtual reflectometers are used to obtain the BRDF of a material with known approximate micro-structure geometry. Reflectance measurements are carried out virtually in a similar way to that of real reflectometer devices. Light interactions are simulated by distributed ray tracing techniques and the surface of the micro-geometry is modelled by means of perfect diffuse, perfect specular, specular-diffuse or transparent materials (see Section 2.2.3) . In [WAT92] Westin et al describe such a virtual reflectometer. They assign a simple reflectance model to the micro-structure and they fit the sampled data to a spherical-harmonics representation, which includes anisotropy. They observe that the resultant BRDF is dependent on the distance at which the measurements are made from the micro-structure. They propose to use different representations for reflectance dependent on the scale at which the reflectance is required. Geometry, texture, bump maps and BRDFs are applied dependent on the scale of the observation. Westin et al. demonstrate renderings of brushed aluminium, satin and velvet produced by BRDFs extracted by a virtual gonio-reflectometer.

Gondek et al [GMN94] also acquire BRDFs from virtual gonio-reflectometers and store the result in a specially designed data structure representing a geodesic sphere. By taking the wavelength dependency of the BRDFs into account they manage to produce BRDFs and pictures of thin films and pearlescent paints.

2.2.3 Reflectance Models and Fitting

Since direct data storage of reflectance measurements is usually too memory-intensive, noisy and does not allow us to describe arbitrary materials, mathematical models of reflectance behaviour have been proposed. From observations of reflectance behaviour, several reflectance phenomena that can be represented by different attributes of such models have been identified as follows:

2.2.3.1 Perfect Diffuse

A perfect diffuse or as it is also called a **Lambertian** surface scatters incoming light equally in every direction. This can be described by a constant reflectance coefficient, often referred to as the **albedo**.

2.2.3.2 Perfect Specular

Perfect specular surfaces reflect light only in a single direction. This can be modelled as a Dirac delta function where the reflectance is zero except at a particular angle in the plane of incidence where it is of a high value such that the integral of the reflectance is finite and depending on the reflectivity, often close to one.

2.2.3.3 Specular-Diffuse

This type of reflectance is between specular and diffuse. This reflectance is dependent on direction and has its maximum reflectivity in the mirror direction.

2.2.3.4 Off-Specular

Like specular diffuse this type is between perfect specular and perfect diffuse but the maximum reflectance is not in the mirror direction.

2.2.3.5 Anisotropic

With anisotropic materials the reflectance changes if the surface is rotated around its normal. More intuitively, the specular area of an anisotropic material is not circular but elliptic. This is often described as the kind of effect obtained when aluminium is brushed in one direction.

2.2.3.6 Grazing Angle

This reflectance effect often occurs with coated surfaces such as varnished wood. Here, the amount of specular reflection grows at grazing angles. Only a few reflectance descriptions permit modelling of this effect [Sch94].

Two types of models can be distinguished: empirical and theoretical.

2.2.3.7 Empirical Models

Empirical models do not attempt to be physically accurate. The main goal is simply to obtain good visual results efficiently.

Gouraud shading [Gou71] is probably the simplest shading. Lambertian reflectance is only computed at the vertices of surface polygons and is linearly interpolated over the surface. Phong's model [BT75] adds a specular component which is dependent on the angle between the reflectance vector and the view vector. Blinn's model [Bli77] improves Phong's model by making the specular component dependent on the angle between the "half-vector" and the

surface normal. Strauss' model [Str90] is supposed to provide intuitive parameters that the user may change. It takes five parameters: colour, smoothness (diffuse-specular), metallness (dielectric-metal), transparency, and the index of refraction.

2.2.3.8 Theoretical Models

Cook and Torrance [CT81] introduced the first theoretical model into computer graphics. It was based on a model from optics by Torrance and Sparrow [TS67] that was itself based on so-called micro-facet theory. In such a model, the surface is composed of small, V-shaped, perfectly specular planar elements. The distribution of the facets describes the surface roughness which causes incoming light to be shadowed by some facets and reflected light masked by others.

The most complete theoretical model was introduced by He et al [HTSG91] and is often referred to as the HTSG model. This model accounts for polarisation, diffraction, conductivity and a smaller effective roughness for grazing rays. Owing to its complexity and computational expense, this model is not commonly in use.

Ward [War92] introduced the first anisotropic model which is based on a Gaussian slope model. Intuitively, the model simulates surfaces by means of scratches in a particular direction which result in the anisotropic reflectance behaviour.

Lewis [Lew93] and Lafortune et al [LFTG97] modified Phong's model to make it physically plausible by accounting for Helmholtz reciprocity and energy conservation.

Some new ideas in micro-facet modelling were recently introduced by Ashikhmin et al [APS00]. Instead of modelling a facet distribution function, the micro-facet orientations are taken directly from a height map that can easily be edited in a paint program making it possible for users to define reflectance patterns. Successfully modelled and rendered images of satin and velvet micro-structures were given in [APS00].

2.2.4 Fabric Rendering

In Yasuda et al [YYiT92], an anisotropic reflectance model for woven materials is introduced that accounts for textile micro-structure and weaving style. This model is based on the micro-facet theory. Detailed observations were made as to how fibres and yarns reflect light if they are interwoven. The influence of different weaving patterns was considered and the behaviour of light scattered through several layers of woven structures examined. Yasuda et al call these "internal reflection". These observations are then modelled with different facet distribution functions. The parameters for the distribution functions are from measurements of real fabrics. They model visually appealing BRDFs of acetate, silk, cotton and polyester fabrics but do not attempt to model the inhomogeneous reflectance behaviour of most fabrics.

Daubert et al [DLHS01] have presented an efficient technique for modelling and rendering clothes. Their approach is well suited for coarsely woven and knitted fabrics where thread shadowing significantly contributes to the BRDF. They employ a virtual ray tracing reflectometer to generate a BTF from micro-structure of modelled, knitted fabrics. Individual BRDFs of the BTF are sampled and fitted to Lafortune's model [LFTG97] by means of a Levenberg-Marquardt optimisation method. Sixty-four incident angles are sampled per BRDF. The BRDFs are then stored in the graphics hardware texture memory for efficient rendering. They show images of a torso dressed in a jumper rendered according to their approach. The image quality appears slightly better than that achieved by simple texture mapping but probably owing to memory requirements their patterns are very repetitive.

Gröller et al [GRS95] use volume rendering techniques for knit-wear. They describe a method to construct 3D textures of thread slices. Individual thread slices are described by a square grid of cells, in which each cell describes a fibre density according to some probability distributions used to model the thread. To construct a whole thread, the slices are rotated along a skeleton curve that describes a loop of the knitting. For rendering transparency, the densities in the slices are represented by alpha values in an RGBA (Red, Green, Blue and Alpha) texture. Ray casting techniques are used for rendering. They produce very realistic images of knitted fabrics and compare them favourably to photographs of real knitted fabrics. However, their approach only works for small, flat pieces of fabric.

Xu et al [XCL+01] describe a way for rendering knit-wear by introducing a graphics primitive they coin the "Lumislice". A Lumislice describes a cross-section slice of yarn that is divided into Voxels. Each of these Voxels has an associated four-dimensional array that contains its opacity and its reflectance function. Yarns are generated by rotating a Lumislice along the path of a yarn. The approach is similar to that of Gröller et al but they introduce soft shadows and demonstrate renderings of knit-wear micro-structure on curved surfaces. They employ graphics hardware for their very impressive renderings but report rendering times of 30 minutes for a knitted sweater.

Adabala et al [AFMT03] derive weave pattern geometries from an industrial weave standard [NKB+]. Weaving grammar and the colour of thread patterns are stored in texture maps as described in [Gla03]. These maps are MIP-mapped for close and distant views. From the weaving patterns they obtain a micro-facet BRDF model for light interactions with threads. The front and back sides of fabrics are rendered with complementary weave patterns. Distant views are represented by a Cook-Torrance model. Fabric transparency is modelled from the gap size in weave patterns and the angle between surface normal and viewing direction. Image compar-

ison between small rectangular pieces of real, woven fabric and their renderings are impressive, although the images of virtual actors in woven clothes appear very obviously computer generated. Rendering is carried out by a ray tracer and they report rendering times of two minutes on a 2Ghz Pentium. Adabala et al [AMT03] later modify their work for real-time rendering. They drop directional dependencies for transparency and do not take into account global illumination effects. Kautz et al's [KM99] multi-texturing approach for BRDF rendering is employed and the BRDF of the pattern is averaged over the whole garment. Again, the homogeneity of weave patterns makes the images appear unrealistic and hardly distinguishable from the often-used repetitively-tiled texture patterns.

Sattler et al [SSK03] present a real-time method for BTF rendering of arbitrary materials including in particular cloth fabrics. They acquire 256×256 pixel images by taking photographs of a sample material from different directions similar to the method used by Dana et al [DvGNK99]. They apply a principal component analysis (PCA) texture-compression as described by Nishino et al [NSI99] to be able to fit the massive BTF data into large graphics memory. In addition, they introduce an efficient shadow mapping technique for low resolution meshes as often used to represent garments. By pre-computing visibility per vertex they also approximate self shadowing effects for static clothes. They show images of a jumper illuminated by an environment map. The image quality is impressive but again owing to large memory requirements of the BTF's even after compression (260 MB for a 256×256 pixels sample) the garment surface appears repetitive. They report average rendering times of two frames per second for static meshes. Visibility pre-computation for shadow rendering takes about four seconds for a mesh with 900 vertices on a 1.5Ghz Athlon processor. Pre-computation has to be carried out each time the mesh changes. As we shall discuss in the next section we introduce a reverse engineering approach in Chapter 4 which enables us to acquire diffuse textures of a whole garment and therefore we avoid the problem of repetitive appearance.

2.3 Summary

In this chapter we gave an overview of work related to cloth modelling and visualisation. We first discussed the physical modelling of cloth material. We concentrated on the description of mass spring particle systems and integration methods for animating cloth. Many advances have been made in improving the stability of cloth simulation systems. The techniques allow us to simulate larger time steps but at the cost of a single time step requiring much more processing power than, for example, for the older, simpler methods. In addition, the gain in stability results in cloth that behaves in a clumsy manner. Techniques to overcome the problem of processing

requirements have been tackled but they remove the possibility of simulating different fabrics and they do not work for large systems. A comparison of integration methods concludes that for large systems with many potential collisions the simplest explicit Euler method with small time steps is often still the best choice in order to achieve realistic drape behaviour with little processing requirement. As mentioned earlier, we describe in Chapter 3 an improvement of Provot's model which uses an explicit integration scheme by introducing a correction step which we call Directional Velocity Modification (DVM) that enables us to simulate fairly stiff fabric. After integration methods, the main collision detection techniques are discussed. It is noted that the main problem with hierarchical collision detection methods is that their performance is dependent on the complexity of the model (the number of triangles). High memory requirements are the main drawback of uniform spatial partitioning approaches. We discussed curvature culling, a collision detection optimisation technique specially developed for cloth surfaces. A short overview of collision response and avoidance techniques for cloth simulation was then given. As mentioned earlier, we describe in Chapter 3 an adaptation of Eberhardt et al's method [EWS96] for collision response that manipulates a colliding particle's velocity based on the body surface normal and velocity information gathered in our image based collision detection approach. In the section on realistic visualisation, we first discussed surface representations, and then summarised work on reflectance modelling. In particular, we surveyed research in the area of fabric reflectance acquisition and rendering. Recent research in reflectance modelling, especially for spatially varying reflectance functions, has shown impressive results for pieces of fabric. Renderings of such fabric samples on garments, however, still look unrealistic owing to the repetitiveness of the texture even when used in combination with shadowing and self-shadowing methods on garments. Rendering times of such representations in software are often slow and, if carried out with the latest graphics hardware, performance still lies below that required for on-line feedback in a virtual try-on system. We introduce in Chapter 4 a reverse engineering approach which enables us to acquire realistic diffuse textures from digital images of a whole real garment and therefore we avoid the problem of the repetitive appearance observed in other approaches.

In the next chapter we thus describe improvements on Provot's MSPS for simulating fairly stiff cloth materials. We introduce our image space based collision detection method that can significantly improve the performance of a cloth model by harnessing state of the art graphics hardware. In Chapter 4, along with our garment description format we describe our reverse engineering approach for garments. The problem of repetitive appearance of textures in garment visualisation while the BRDF is approximated by a Lambertian reflectance.

Chapter 3

Our Cloth Model

In this chapter we describe our cloth model. The description of the cloth model is split into three parts, the mass spring particle system (MSPS), image based collision detection (IBCD), and collision response. First, we will describe a modification of a linear MSPS to compensate for a phenomenon called super-elasticity. The use of graphics hardware for collision detection and response will be the subject of the next section. Following that, we will describe our collision response method. How we map measured properties of real fabrics to our cloth model will then be discussed. A short description of publications that have cited our work will be given and, finally, conclusions will be drawn. Results and performance evaluation of our techniques will be given in Chapter 7.

3.1 Cloth Model and Super-Elasticity

We model our cloth by using a MSPS with the same spring topology as in Provot [Pro95] that we described in Chapter 2. As Provot did, we employ a simple Euler scheme for integration. However, we modified the way Provot compensates for super-elasticity. Super-elasticity is a phenomenon that is caused by the way the springs are modelled in a Hookean MSPS. Springs are modelled linearly and therefore resist stretching with the same constant value regardless of a spring's relative extension. Resistance to stretching of real cloth, however, grows quickly after a certain threshold. Super-elasticity could be overcome by introducing stiffer springs. This would, however, decrease the natural period of the system and would force us to simulate with smaller time steps or implicit integration and therefore the performance would decrease. Provot [Pro95] proposed to compensate for super-elasticity by applying a position modification. His algorithm checks the length of the springs after each iteration, and modifies the positions of the ends of a spring if it exceeds its natural length by more than a certain value (10% for example). This modification will decrease the length of some springs but it might over-elongate others. The convergence properties of this technique are therefore not clear. It proved to work

for locally distributed deformations but no tests were conducted for global elongation.

3.1.1 Velocity Modification

The main problem of Provot's position modification approach is that first it allows the springs to over-elongate and then tries to adjust their length by modifying positions. This of course is not always possible because of the many links between the mass points. Our idea was to find a constraint that does not permit any over-elongation of springs.

Our algorithm [VSC01] works as follows. After each iteration it checks each spring to see whether the spring exceeds its natural length by a pre-defined threshold. If this is the case, the velocities are modified, so that further elongation is not allowed. The threshold value usually varies from 1% to 15% depending on the type of cloth we want to simulate.

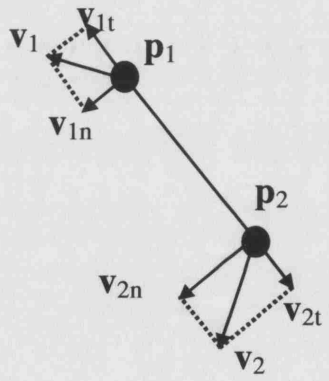

Figure 3.1: Velocity modification for over-elongated springs.

Let $\mathbf{p}_1$ and $\mathbf{p}_2$ be the positions of the end points of a spring that has been found to be over-elongated, and $\mathbf{v}_1$ and $\mathbf{v}_2$ be their corresponding velocities (see Figure 3.1). The velocities $\mathbf{v}_1$ and $\mathbf{v}_2$ are split into two components $\mathbf{v}_{1t}$ and $\mathbf{v}_{2t}$, along the line connecting $\mathbf{p}_1$ and $\mathbf{p}_2$, and $\mathbf{v}_{1n}$ and $\mathbf{v}_{2n}$, perpendicular to this line. Obviously the components causing the spring to stretch are $\mathbf{v}_{1t}$ and $\mathbf{v}_{2t}$, so they have to be modified. In general $\mathbf{v}_{1n}$ and $\mathbf{v}_{2n}$ could also cause elongation, but their contribution within one time step is negligible. There are many possible modifications, two examples are:

- Set both $\mathbf{v}_{1t}$ and $\mathbf{v}_{2t}$ to their average, i.e.

$$\mathbf{v}_{1t} = \mathbf{v}_{2t} = \frac{1}{2}(\mathbf{v}_{1t} + \mathbf{v}_{2t}). \tag{3.1}$$

- Set one of them equal to the other. But how can we decide which one to change at the current simulation step?

Our experiments showed that Equation 3.1 is good enough[1] for the static case, i.e. if cloth collides with objects that do not move. If we want to implement a system for dressing static human bodies, Equation 3.1 will be the obvious solution, because it produces good results and requires little computation.

3.1.2 Directional Velocity Modification

For the dynamics, however, the way of modifying the velocities proved to have an enormous influence on the cloth behaviour. For example, Equation 3.1 gives satisfactory results for relatively low rates of cloth deformation and relatively slow moving objects. In faster changing scenes, for example when the body is walking, it becomes "clumsy" and cannot give a proper response. This is illustrated in Figure 3.2 where a sphere is moved upwards while a piece of cloth is draped over it. The cloth model does not react quickly enough and the sphere penetrates through the cloth.

Figure 3.2: Static velocity modification in dynamic scene.

After conducting numerous tests we came up with the following solution. We introduce a vector called a "directional vector", which is computed as:

$$\mathbf{v}_{dir} = \mathbf{v}_{grav} + \mathbf{v}_{object}, \tag{3.2}$$

where $\mathbf{v}_{object}$ is the velocity of the object with which the cloth is colliding, and $\mathbf{v}_{grav}$ is a component called "gravitational velocity" computed as $\mathbf{v}_{grav} = -g\Delta t$.

[1] By good enough we mean that the simulation of cloth did not penetrate the surface of a the static object and visually pleasing results were produced.

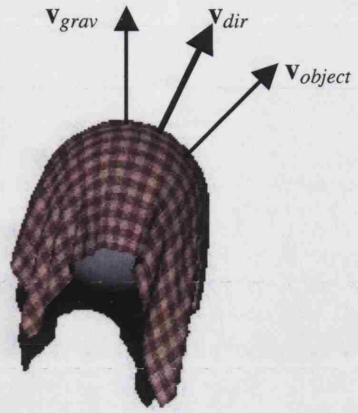

Figure 3.3: Directional Velocity Modification.

The directional vector gives us the direction, in which higher spring deformation rates are most likely to appear at the current step of the simulation, and in which the cloth should resist modification. The components of the directional vector are the sources which will cause the most rapid cloth deformation. In our case there are two such sources, gravity and the velocity of the moving object, but in other environments there might be other sources which have to be taken into account, such as wind, etc. Once the directional vector has been determined, the velocities are modified in the following way. Let $\mathbf{p}_{12} = \mathbf{p}_2 - \mathbf{p}_1$ be the spring directional vector and α be the angle between $\mathbf{p}_{12}$ and $\mathbf{v}_{dir}$. The cosine of α can be easily computed as a scalar product of the two vectors.

- If the spring is approximately perpendicular to the directional vector $\mathbf{v}_{dir}(|\cos\alpha| < 0.3)$ then modify both velocities using Equation 3.1;
- If not, set the velocity of the rear point, where rear is defined relative to the directional vector as below, equal to that of the front one, so that it can "catch up" with the changing scene. If $\cos\alpha > 0$ the rear point is $\mathbf{p}_1$ otherwise it is $\mathbf{p}_2$.

If this is applied to all springs, the stretching components of the velocities are removed and in this way further stretching of the cloth is not allowed. In addition, the "clumsiness" of the model is eliminated and it can react adequately to moving objects. Our results show that this approach works well for all types of deformation: local or global, static or dynamic.

3.1.3 Discussion

While directional velocity modification does not over-elongate springs by modifying positions, as in Provot's approach, in a MSPS with many springs the technique may still change velocities

of particles that are connected to more than one spring. This may lead to small elongations over a spring's threshold in one time step. This problem has been tackled by Dochev and Vassilev in [DV03] by sorting the order in which velocity modification is applied. This sorting procedure, however, is time consuming and the visual differences between cloth with the vertices simulated in the special sorted order and cloth without such special strategies on the order of simulation are small. Super-elasticity can also be overcome by introducing stiffer spring constants. Stiff springs, however, can only be simulated with reasonable time steps by employing implicit integration. Implicit integration, on the other hand, introduces artificial damping forces that can make the cloth appear clumsy. In addition, implicit integration requires large computational power for each time step. Our results show that directional velocity modification allows us to create relatively stiff cloth that appears visually pleasing using explicit integration. Verlet integration was considered for further improvements in stability. However, since Verlet integration does not require any velocities for an update it cannot be applied directly with our velocity modification method. A thorough mathematical investigation of the properties of the directional velocity modification is beyond the scope of this thesis and has yet to be carried out.

3.2 Image Based Collision Detection

Collision detection and response prove to be the bottleneck of dynamic simulation algorithms that use highly discretised surfaces. If good performance is a goal an efficient collision detection algorithm is essential. As detailed in Chapter 2, existing algorithms for detecting collisions between cloth and other objects in the scene are based on geometrical object-space (OS) interference tests. Some apply a prohibitive energy field around the colliding objects but most of them use geometric calculations to detect penetration between cloth and object together with culling techniques such as bounding volume hierarchies and Voxel subdivisions in order to reduce the number of collision tests. Recently, different techniques were developed, based on image-space (IS) tests [SF91, RMS92, MOK95, BWS99]. These algorithms use the graphics hardware to render the scene and then perform checks for interference between objects based on the depth map of the image. In this way the 3D problem is reduced to 2.5D. Such approaches use the graphics hardware for rasterisation of the object and to generate a depth map. As a result of using the graphics hardware, image based collision detection (IBCD) approaches are very efficient and, in addition, compared to full 3D Voxel approaches or volume hierarchies, memory requirements are reduced drastically. IBCD has been used to detect rigid object interference [SF91, BWS99], in CAD/CAM systems [RMS92], in dental practice [BWS99], but never for cloth-body collision detection and response.

Collision detection can require more then 50% of the computation time in cloth simulation and thus is the key for a fast technique. At each simulation step, a check for collision with the body model has to be performed in principle, for each vertex of the garment in an implementation without spatial partitioning. Body models acquired by 3D scanning devices are typically represented by a large number of polygons to closely approximate the real body shape. In addition, realistic representations of garments also require high resolution meshes. Without culling, every vertex has to be tested against every other vertex which leads to a complexity of $O(n)$ for a collision test with n being the number of polygons. Furthermore, vertex face collisions have to be tested. By using bounding volume hierarchies the complexity of a collision test is reduced to $O(\log n)$. In our system we implemented an IBCD approach [VSC01]. This technique makes it possible to find a collision only by comparing the depth value of a cloth vertex with the corresponding depth information of the body stored in depth maps. Thus a collision test can be performed with a complexity of $O(1)$. Vertex face tests are not required since the graphics hardware renders the faces in the depth buffer. If a collision between the body and a cloth vertex occurs, the response of that collision has to be calculated. We use the graphics hardware to generate the information required for collision response. Normal and velocity vectors of the body surface are encoded in colour channels and intermediate areas on the body surface are interpolated by the graphics hardware as described below. This can be done by encoding vector co-ordinates (x, y, z) as colour values (R, G, B). Depth, normal and velocity maps are created by using two orthogonal projections: one onto the front and one onto the back of the body's axis-aligned bounding box (AABB).

3.2.1 Depth Maps

To create depth maps we place two orthogonal cameras one at the centre of the front face and one similarly at the back of the body's AABB. The view volume is adjusted to create accurate depth values by placing the virtual camera's far clipping plane to the depth of the AABB and the near clipping plane to the near face of the AABB. Both cameras point at the centre of the AABB. This is illustrated in Figure 3.4. If body animation is required the maps have to be generated at each animation step, although, if the body movements are known, they can be pre-computed. When initialising the simulation we execute two off-screen renderings to retrieve the depth values, one for the front and one for the back. The z-buffer of the graphics hardware is moved to main memory by using OpenGL's *glReadPixels* function. The z-buffer contains floating-point values in the range $[0.0, 1.0]$. A value of 0.0 represents a point at the near clipping plane while a 1.0 represents a point at the far clipping plane. Example depth maps

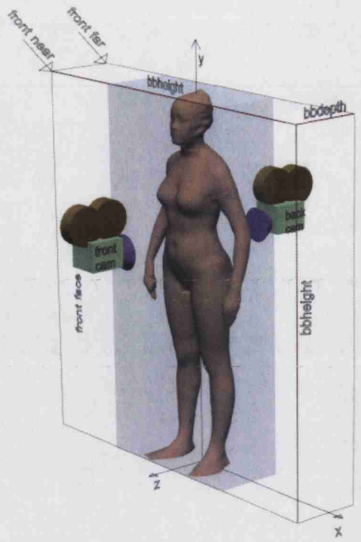

Figure 3.4: Placement of orthogonal cameras for IBCD.

are illustrated in Figure 3.5 where dark areas describe pixels near to the observing camera and bright areas describe pixels further away.

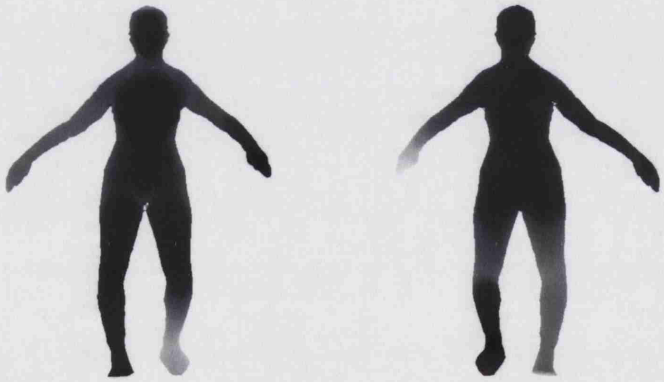

Figure 3.5: Depth buffers computed for the front and for the back of a body-scan generated by orthographic projection. Dark areas represent pixels close to the camera while bright areas are pixels further away from the camera.

3.2.2 Normal Maps

At the same time as we generate the depth maps we ask the graphics hardware to create normal maps. This is done by replacing the (R, G, B) colour value of each vertex of the 3D model with the coordinates (nx, ny, nz) of the corresponding normal vector $\mathbf{n}$. Hence, after rendering, the frame-buffer contains the normal of the surface at each pixel represented as colour values. Since OpenGL's colour fields are in a range $[0.0, 1.0]$ and normal values are $[-1.0, 1.0]$ we convert all normals to fit into the colour fields by using

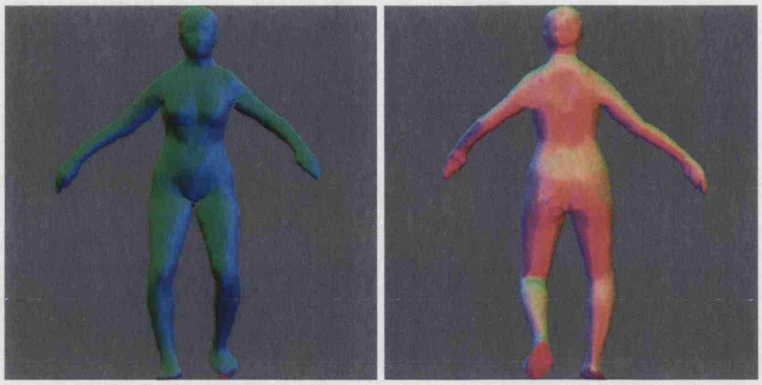

Figure 3.6: Normal buffer of the front and back of a body-scan.

$$\begin{pmatrix} R \\ G \\ B \end{pmatrix} = \frac{1}{2}\left(\mathbf{n} + \begin{pmatrix} 1 \\ 1 \\ 1 \end{pmatrix}\right). \tag{3.3}$$

We enable Gouraud shading so that the graphics hardware can interpolate between the normals for all intermediate points on the body surface. On state of the art graphics hardware this process employs a bilinear interpolation between the vertices of the triangles that describe the surface. All light shading options are disabled to make sure that the colour values we get in the frame-buffer are the same as those on the mesh. We use off-screen rendering to generate the images for collision detection and response. Again OpenGL's *glReadPixels* function is employed to transfer the frame-buffer of the graphics hardware to main memory. The result is a smooth normal map of the body surface rendered from the front and from the back. Example normal maps computed on the front and the back of a body are depicted in Figure 3.6. Depending on the architecture of the graphics system, the read-back process of the frame-buffers can be a time consuming operation and is therefore highly dependent on the buffer resolution. Thus the goal is to create buffers at low resolution, but sufficient to represent the body to a good degree of accuracy. Considerations about buffer resolution are discussed in Section 3.2.5. After read-back the colour values of all pixels are converted back to normal values by using

$$\mathbf{n} = 2\begin{pmatrix} R \\ G \\ B \end{pmatrix} - \begin{pmatrix} 1 \\ 1 \\ 1 \end{pmatrix}. \tag{3.4}$$

Figure 3.7: Velocity buffer of the front and back of an animated body-scan.

3.2.3 Velocity Maps

As in the rendering of the normal maps, we replace the (R, G, B) value of each vertex of the body model with the coordinates (vx, vy, vz) of its velocity $\mathbf{v}$. Since the velocity coordinate values range may be delimited as $[-maxv, +maxv]$ where $maxv$ is the largest absolute value that appears in any of the velocity vectors of an animated body, they are converted to fit into the colour fields by using

$$\begin{pmatrix} R \\ G \\ B \end{pmatrix} = \frac{1}{2maxv} \left(\mathbf{v} + \begin{pmatrix} maxv \\ maxv \\ maxv \end{pmatrix} \right). \tag{3.5}$$

Again the Gouraud shading option is enabled to allow the graphics hardware to interpolate the velocities for all intermediate points on the surface. The conversion back from colour space (R, G, B) to velocity space is computed by using

$$\mathbf{v} = maxv \left(2 \begin{pmatrix} R \\ G \\ B \end{pmatrix} - \begin{pmatrix} 1 \\ 1 \\ 1 \end{pmatrix} \right). \tag{3.6}$$

Example velocity maps computed on the front and back of a body are depicted in Figure 3.7.

3.2.4 Testing for Collisions

After retrieving depth, normal and velocity maps, testing for and responding to collisions can be performed efficiently. If we want to know whether a point (x, y, z) on the cloth surface collides with the body, the point's (x, y) values need to be converted from world coordinates to image coordinates (U, V) by using

$$V = \frac{y * mapsize}{bboxheight}, \tag{3.7}$$

$$U_{back} = (1 - \frac{x + \frac{bboxheight}{2}}{bboxheight}) * mapsize \tag{3.8}$$

and

$$U_{front} = (\frac{x + \frac{bboxheight}{2}}{bboxheight}) * mapsize. \tag{3.9}$$

Here *mapsize* denotes the resolution of the buffer in both dimensions. All three coordinates in Equations (3.7, 3.8 and 3.9) are obtained from calculations that involve *bboxheight*, the height of the body's AABB. This is because of the way we use left and right camera clipping planes (along the x axis - see Figure 3.4). We set them to $-\frac{bboxheight}{2}$ and $\frac{bboxheight}{2}$ respectively, which results in a square view-port and prevents non-uniform scaling of the model in our implementation. Performance could be improved by only reading the area of the front and back face of the AABB[2] into main memory. The calculation of the map coordinates is simpler than in perspective projection because we use orthogonal projection and the cameras are placed in the centre of the AABB's front and back faces.

For collision detection the z value of a particle's coordinate is used to decide which map to check for collision. If the z value is smaller than the z value of the centre of the AABB the back-map is used, otherwise the front-map is taken. The corresponding z value of the depth map is compared with the z value of the pixel's coordinates by using, for the back and front projections respectively:

$$back : z < depthmap(U_{back}, V) \quad front : z > depthmap(U_{front}, V). \tag{3.10}$$

If a collision occurred (i.e. either of the conditions above is true), we retrieve the normal and velocity vectors from the colour maps indexed by the same coordinates (U, V) used for the collision check. These vectors are required to compute a collision response described in Section 3.3 of this chapter.

3.2.5 Quantisation Error Estimation

Given the fact that most modern workstations use a 24 bit z-buffer and that $bboxdepth < 100cm$ for an average person, then the quantisation error in z may be estimated as

$$\Delta z = \frac{bboxdepth}{2^{24}} < \frac{100}{2^{24}} < 6 * 10^{-6} cm. \tag{3.11}$$

[2]In general the area of the front and back face of the AABB of a human shape will be rectangular and therefore smaller than the area described by the squared height *bboxheight*.

This is more than enough in our case, bearing in mind that the discretisation errors of the 3D scanner are in the millimetre range. The errors in x and y are equal and can be estimated as

$$\Delta x = \Delta y = \frac{bboxheight}{mapsize} = \frac{160\ to\ 180}{mapsize} cm, \tag{3.12}$$

where we consider the average person to be 160 to 180 cm tall. This means that we have control over the error in the x and y directions by varying the resolution of the maps. However, a bigger map size also means a bigger overhead, as buffer read-back times will be higher. A reasonable trade-off is $\Delta x = \Delta y = 0.5cm$, so a $mapsize = 320$ to 360 pixels is required. A Δx and Δy of $0.5cm$ also roughly correspond to the minimum scanner resolution required for clothing retail applications.

3.2.6 Layers of Depth Maps

The algorithm described above works well for body data from a 3D scanner since typical 3D scanners (especially in the case of structured light scanners) also take images from the front and the back of a body and therefore the body-data does not contain any overlapping segments. Collision detection on data of a body in a more complex pose as in walking sequences requires a more complex algorithm. For cases where there are overlaps that cannot be handled by the basic IBCD we introduced layers of depth maps [DVS04]. For this approach the body geometry has to be segmented - in our case into a torso and limbs. The approach is not general and was specially designed for collision detection between clothes and walking humans. Accordingly, some simplifications were made. Self-overlapping body parts and cross-overlapping of two parts (arms for example) are ignored. Likewise, we assume the torso is not overlapping the legs and vice versa. At each animation step we determine the presence of overlapping areas that require layers of depth maps. This task is carried out by simplified geometric computations involving the AABBs of the limbs and of the torso. The drawback of this simplification is that in some cases an overlap is identified where there is no real overlapping. Additional considerations related to specifics of the human body were made. For example, in a typical female body the width of the hip is equal to or greater than that of the shoulders. Thus, if we had used one AABB for the entire torso and simple AABB tests, the results of a test for overlap of either arm with the torso would have been always positive regardless of the real situation. If there is no overlap, the basic technique is used, otherwise layers of depth maps are generated. If more than one overlap is detected an analysis is carried out, with the aim of reducing the number of necessary depth maps. As an example, if both arms overlap the torso but not each other, then two depth maps are sufficient - one for the torso and the legs and one for the arms. Figure 3.8

shows two front depth map layers generated as a result of the overlapping of the torso by the right arm.

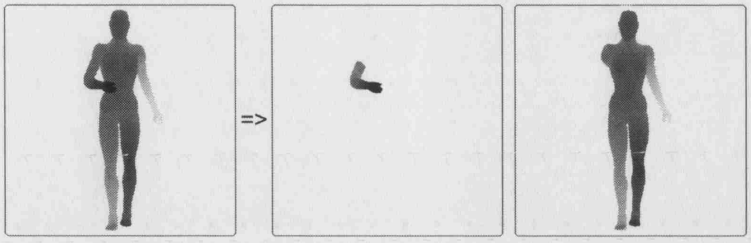

Figure 3.8: Two depth map layers for resolving the overlapping of the body by the right arm.

3.2.7 Cloth-Cloth Collision Detection

In principle it would be possible to use our IBCD technique also to test for cloth-cloth collisions. However, this would require creation of depth, normal and velocity maps at each iteration of the cloth simulation. Since read-back times from the graphics hardware to main memory can still be in the range of a few milliseconds on modern graphics hardware, simulation times would probably be slow. In addition, cloth self-collisions on garments worn by a person are very unlikely[3]. We decided to implement an approach that employs a bounding volume hierarchy for cloth-cloth collision tests. Only cloth-cloth collisions between different garment panels are tested in this approach, which proved to be sufficient for most cases while good performance can be maintained.

3.3 Collision Response

After a collision has been detected, the algorithm has to compute a response to bring the system into a collision free state in a way that appears natural for cloth. Our approach does not introduce additional penalty, gravitational or spring forces; it just manipulates the velocities, as proposed by Eberhardt et al [EWS96], which proved to be very efficient[4]. However, for the dynamic case, when the body is animated, we had to introduce some modifications. Let $\mathbf{v}$ be the velocity of the point $\mathbf{p}$ colliding with the object $\mathbf{s}$ and let $\mathbf{v}_{object}$ be the velocity of this object as shown in Figure 3.9. The surface normal at the point of collision is denoted by $\mathbf{n}$. First, the relative

[3]The likelihood of cloth self-collisions depends on the bending properties of the fabric. In the experiments we carried out with a number of garments composed of different fabrics, self-collisions only occurred rarely. Therefore, for performance reasons, we chose to enable collision tests only between different garment panels.

[4]Eberhardt et al [EWS96] report simulation times in the order of minutes which represents a drastic speed-up to the work by Breen et al [BHW94] who report simulation times in the order of weeks. Both simulate a simple rectangular piece of cloth.

velocity between the cloth and the object have to be computed: $\mathbf{v}_{rel} = \mathbf{v} - \mathbf{v}_{object}$. If $\mathbf{v}_t$ and $\mathbf{v}_n$ are the tangential and normal components of the relative velocity $\mathbf{v}_{rel}$, then the resulting velocity can be computed as:

$$\mathbf{v}_{res} = C_{fric}\mathbf{v}_t - C_{refl}\mathbf{v}_n + \mathbf{v}_{object}. \tag{3.13}$$

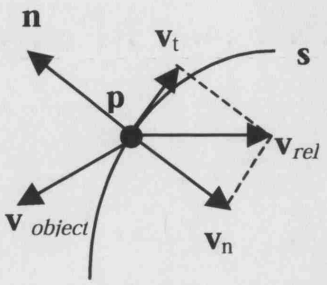

Figure 3.9: Collision response using velocity manipulation.

A similar approach can be implemented to detect and find the responses not only to collisions between the vertex and the object, but between the face of a surface patch and the object. For each quadrangle on the cloth we compute its midpoint and velocity as an average of the four adjacent vertices. Then we check for a collision of this point with the body and, if so, compute its response using Equation 3.13, and apply the same resultant velocity to the surrounding four vertices. If there is more than one response for a vertex, then an average velocity is calculated for this vertex. Our tests showed that the velocity collision response did not always produce satisfactory results. For example, when heavy cloth was simulated there were penetrations in the shoulder areas. In order to make the collision response smoother, an additional reaction force was introduced for each colliding point on the cloth (see Figure 3.10).

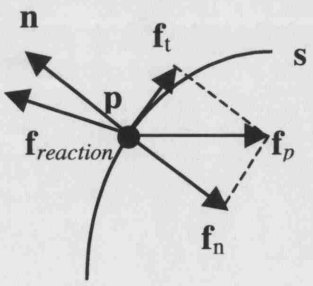

Figure 3.10: Collision response using force manipulation.

Let $\mathbf{f}_p$ be the force acting on the cloth vertex $\mathbf{p}$. If there is a collision between $\mathbf{p}$ and an object in the scene $\mathbf{s}$, then $\mathbf{f}_p$ is split in its two components: normal ($\mathbf{f}_n$) and tangential ($\mathbf{f}_t$). The

object reaction force is then computed according to

$$\mathbf{f}_{reaction} = -C_{fric}\mathbf{f}_t - \mathbf{f}_n, \tag{3.14}$$

where C_{fric} is due to the friction and is dependent on the properties of the materials involved.

3.3.1 Collision Tolerance

In a single simulation step, cloth particles with high velocity may penetrate the body before a collision can be detected and therefore make it impossible to identify where the collision actually happened. To account for this problem, geometrical approaches are usually used to compute the exact position of the collision by using the particle's position before the simulation step and after the simulation step. Such a computation may be computationally demanding and results of various research [BWK03] show that cloth-body penetrations are still possible. Since our goal is near real-time simulation, geometrical computations of the exact position of a collision would be computationally too expensive. Instead, we create a collision tolerance layer to avoid penetrations. Before we generate depth and normal maps, we grow the body surface by moving each vertex position along the corresponding normal by a tolerance factor f according to

$$\mathbf{x}_i' = \mathbf{x}_i + f * \mathbf{n}_i, \tag{3.15}$$

where $\mathbf{x}_i'$ is the new vertex position, $\mathbf{x}_i$ denotes the original position of vertex i and $\mathbf{n}_i$ denotes the normal of vertex i with $i \in 1..N$, where N is the number of body vertices. By adjusting f appropriately we can usually generate penetration free surfaces. However, cloth may appear to hover over the body surface if it is examined from nearby. For cases where penetrations still appear we introduced an additional step that is carried out at the end of a simulation. In this step all vertices are tested for surface penetration. If penetration is found the vertex is moved to the body surface.

3.4 Fabric Property Mapping

In order to simulate different types of fabric with our cloth model, corresponding measurements of real fabrics have to be mapped onto the MSPS. The masses m_{ij} of each mass point and the spring constants k_{ijkl} have to be set to values that approximate the behaviour of the real cloth. In our system, measurement values from a Kawabata Evaluation System (KES)[5] are mapped onto the parameters of the MSPS. Comparisons of real and simulated fabrics are given

[5]Thanks to Sergei Grishanov and Ray J. Harwood from De Montfort University for carrying out the KES tests. Further details on the KES are given in Chapter 2.

in Chapter 7, Section 7.1.2. The stretch, shear and bend data was fit to powers and polynomials. The ultimated goal was to approximate these properties by means of simple linear functions and to project the linear coefficients onto the springs in Provot's model. The mapping was published by Vassilev in [Vas01] but no derivations of the mapping functions were given and the formulae contained some errors. According to Vassilev [Vas04], we describe the mappings in more detail here. The mapping is a very rough approximation which was adjusted by visually comparing a 50×50 cm sample of the real cloth draped over a round table with the simulated cloth draped over a virtual round table. The results showed that for the six different fabric samples real and virtual fabrics have visually similar behaviour. Mass, resistance to stretching, shearing and bending were mapped as follows.

3.4.1 Mass

The mass of the cloth was given in grams per square metre. The mass for each mass point in the MSPS can easily be computed from this since we know the number of points per square metre in our model.

3.4.2 Tension Force

This force T represents resistance to stretching and was fit to a power law

$$T = ae^b, [g/cm], \tag{3.16}$$

where e is the relative deformation and a and b are coefficients. Equation 3.16 is valid in $[0, maxe]$, where $maxe$ is the maximum deformation. This means that the cloth can stretch to a certain limit above which further stretching must be blocked in our system. This is achieved by setting the stretch threshold of the directional velocity modification method as described above. In our model we approximate the non-linear T by means of line segments, one for [0,maxe/2] and one for [maxe/2,maxe].

3.4.3 Shear Force

Shear force data $S(d)$ was fit to a third order polynomial

$$S(d) = c_1 d + c_2 d^2 + c_3 d^3, [g/cm], \tag{3.17}$$

where d is the shear angle in radians, and c_1, c_2 and c_3 are coefficients. Equation 3.17 is valid in $[0, maxd]$ and for many fabrics is close to a straight line. Figure 3.11 illustrates the mapping between forces from the KES shear polynomial to a spring constant k_{shear}. The trigonometry can be complicated but the basic idea is that the unit square is distorted by external forces, which cause an internal force F_s that tries to restore the original rest state. F_s

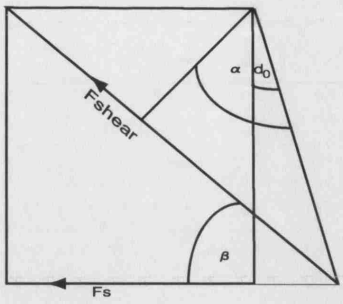

Figure 3.11: Illustration of shear coefficient mapping.

is computed by evaluating polynomial 3.17 for a shear angle d_0. d_0 has to be in the range $[0..maxd]$ and we set it to $0.7 * maxd$[6], therefore F_s=$S(0.7 * maxd)$. Now the goal is to project F_s onto the diagonal, because shear springs are diagonal in Provot's model. Since d_0 usually has a very small value we approximate the projection of F_s onto the distorted diagonal by using the angle of the original diagonal of the unit square, $\pi/4$. Therefore, the projected force $F_{shear} = F_s cos(\pi/4) = F_s\sqrt{2}/2$. The spring constant is then approximated by $k_{shear} = F_{shear}/(\Delta l/l_{new})$, where l_{new} is the length of the distorted diagonal and Δl denotes the difference between the original diagonal and l_{new}, i.e.: $\Delta l = l_{new} - \sqrt{2}$. We approximate l_{new} by $l_{new} = 2\sin(\alpha) = 2\sin(\pi/4 + d_0/2)$.

3.4.4 Bending Moment

Data for resistance to bending $M(\kappa)$ was fitted to a third order polynomial,

$$M(\kappa) = b_1\kappa + b_2\kappa^2 + b_3\kappa^3, [g/cm], \tag{3.18}$$

where κ is the bending curvature in cm^{-1} and $M(\kappa)$ describes the bending moment.

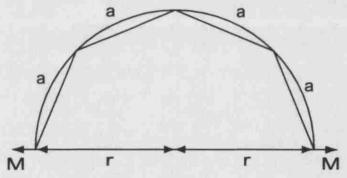

Figure 3.12: Illustration of bend coefficient mapping.

Provot's model was modified slightly in order to allow us to model cloth with higher bending coefficients. In Provot's model, bending springs connect every other mass point horizontally and vertically. So there is one mass point between the bending spring. To model higher bending

[6]We chose 0.7 because it gives a good approximation of the slope of the curves in the range [0..maxd]. To be more precise the value could be approximated, for example, by linear regression.

coefficients we connect every n^{th} particle instead. We assume that the cloth was bent as illustrated in Figure 3.12 in which, for example, $n = 4$, and a denotes the length of one spring, r denotes the radius of the semi-circle and thus $r * \pi$ describes the length of the unbent cloth and $2r$ describes the projected length of the bent cloth and M is the moment that resists bending. The curvature $\kappa = 1/r$ is approximated by $\pi/(n * a)$ since $r * \pi \approx n * a$. The moments M are assumed to be applied perpendicular to the cloth surface at the two end points as illustrated. M is computed by inserting κ in Equation 3.18. $M = F_{bend} * L$ where L is the distance on which the force is applied. Following Vassilev, L is approximated by $n * a/2$. F_{bend} is then approximated by $2M/(n*a)$. Finally, $k_{bend} = F_{bend}/(\Delta l/l)$ with $\Delta l = \pi * r - 2r$ and $l = \pi * r$ so that $\Delta l/l = (\pi - 2)/\pi$.

3.4.5 Discussion

In Provot's model the different springs used to model stretch, shear and bend are not completely independent. For example, the bending springs and shearing springs also influence the stretching behaviour of the material. This has not directly been considered in our mapping approach. We map different coefficients in the warp and weft direction for bending and stretching springs according to the KES measurements. Shear coefficients are assumed to be isotropic since there is no obvious way to map different shear coefficients in warp and weft directions onto Provot's model. The same shear coefficients are used for both diagonal springs in a quadrangle. By linear interpolation of the warp and weft components of the bend and stretch coefficients according to a defined rotation angle, the orientation of the fabric in the garment panel, the so called grain line, may be approximated.

3.5 Our Work Extended by Others

Our IBCD technique for deformable surfaces was pioneering work that has been continued and improved by work of other researchers in this field.

Heidelberger et al [HTG04] describe an IBCD approach that employs layered depth images (LDI) [SGHS98]. LDIs are used to overcome the limitation of our initial approach that can only deal with convex objects. Heidelberger et al create LDIs by use of a depth peeling approach that employs the stencil buffer tests [SAFe02] of recent OpenGL extensions. Owing to the read-back delay from graphics hardware to main memory their results show that graphics hardware performs faster than software rendering approaches only for models represented by a large number of triangles ($> 500k$). No information for collision response is generated in their approach.

Baciu and Wong [BW02] describe a hybrid method which employs both hierarchical bounding volumes and IBCD for cloth-cloth collision. They create a tree structure for curvature culling as described in Provot [Pro97]. In their implementation the performance of the collision detection is dependent on the number of triangles in the scene. They perform separate tests on object space collision detection and image space collision detection. Their results show that cloth-cloth collision detection is dependent on the number of triangles in the model for both object space and image space collision detection.

Our work is also mentioned in [PW03, CMT02, MKE03, FGL03, GBC04, GRLM03, FSG03, FGLW03, GFL03, WWY03, Kno03].

3.6 Summary

In this chapter we described our cloth model. We started with a description of the directional velocity modification method which allows us to simulate stiff springs by using explicit integration without the drawback of the super-elasticity phenomenon. A mathematical evaluation of the stability properties of this approach remains to be carried out. However, our simulation results (see Chapter 7) show that the approach works well for local, global, static and dynamic deformations. A novel IBCD approach was then introduced. This is the first time IBCD was used for cloth-body collision detection. The number of publications that cite this approach indicates the advantages over traditional geometric approaches. Since graphics hardware is used for rasterisation and for generation of the depth, normal and velocity maps required, the approach is particularly well suited for models with large polygon counts. However, the main drawback of the approach is that it cannot handle non-convex objects and that the cloth self collision test may be slow. We extended our initial method to work with overlapping limbs specifically for the case of walking humans by introducing "layered" depth maps. More general IBCD approaches that may handle non convex objects as well as self-collisions were considered by other researchers. Such approaches create layered depth images. The performance improvements of more general IBCD techniques over geometric approaches are unclear. Our collision response is an adaptation of previous work in the field. However, we use our IBCD to create normal and velocity information for collision response. Finally, we describe how fabric properties acquired by measurements on real fabrics are mapped to our MSPS. The mapping is a very rough approximation and is not physically accurate. However, as we shall see in Chapter 7, Section 7.1.2, images of simulated cloth draped over a round table with properties of the real fabric mapped in this way to our model compare favourably to the measured real cloth draped over a real round table.

Chapter 4

Garment Description

A cloth model, as described in the previous chapter, is not sufficient to virtually dress a body. Garments are complex systems consisting of cloth panels usually assembled by joining panel borders in a seaming process. In this chapter we describe a file format we developed to describe garments. The format allows us electronically to transfer a description that is sufficient for virtual assembly of fairly complex garments. The implementation of a plug-in to a commonly used graphics design application that allows us to edit and mark-up our garment description by means of a graphical user interface is then discussed. A reverse engineering technique that enables us to acquire information on existing garments using digital imaging for near photo-realistic visualisation is introduced. We also describe the meshing techniques our simulation employs to create 2D patterns from the contour description of garment panels. Automatic pre-positioning of garment panels around the body by using body-landmark information for virtual sewing is then discussed. Following that, we give details about the seaming process for joining garment panels and finally conclusions are drawn.

4.1 Garment Exchange Format

While standards to describe garments exist [fTM01, Ass92], they are vulnerable to misinterpretation by different CAD systems. Furthermore, these standards are not commonly used by designers and, most importantly, they do not provide sufficient information for virtual garment simulation. These standards are based on the AutoCad DXF file format. It is surprising that no standard description for cutting, sewing and assembling of garments exists. Such a standard would be very useful for the automatic manufacturing of garments[1]. In spite of this deficiency, information about garment assembly for real garments is still often exchanged between people.

[1]Automatic sewing of garments is still an unresolved engineering problem. Current machines manage to automatically sew simple garment panels which are sewn entirely onto another panel, such as pockets, etc. The bulk of the sewing process is still manual[Bou04].

Some proprietary formats for the exchange of information between CAD systems and cutting and sewing machines may exist but they are not open standards. A description of the techniques and terminology of pattern cutting and sewing may be found, for example, in a book by Shoben et al [SW91]. They describe terms such as darts, pressings, hems, seam allowances etc. in depth for garment designers. To meet the requirements of our simulation, we have developed a simple garment exchange format described in standard text. The format describes the set of panels comprising the garment. Garment panels are described by their cutting pattern, fabric properties, fabric reflectance, thickness and darts. How the garment panels are joined is described in the seaming section of our format. In addition, garment accessories can be specified to describe rigid objects such as buttons, cuff links, etc.

Our garment exchange format was developed at the same time as our garment simulation code. If a new garment could not be described by the format, we extended it to allow us to describe what was not possible beforehand. Extensions were made with a minimal change of existing simulation code in mind. For this reason some descriptions may not appear completely logical or consistent. However, our current garment exchange format allows us to describe fairly complex garments. It is now clearer what the requirements for a garment description for virtual garment simulation are and the existing format could be analysed, extended and used as the basis for a more structured version.

4.1.1 General Garment and Environment Information

This section of our garment exchange format describes properties of the simulation for the whole garment and not just for individual panels or seams. These are: the mesh resolution, damping, gravity, collision tolerance, garment type, scale ratio and Y-offset (described below). For clarity and flexibility, the environmental properties should probably be described in a separate file. They are in the garment description in our format because our initial simulation could only handle a single garment of a single type and not multiple layers of cloth. Therefore, it made sense to describe environment properties with the garment. The main components of our garment description are described below.

4.1.1.1 Mesh Resolution

The mesh resolution component describes the resolution of the 2D garment panel meshes in each of the directions of the two Cartesian axes and is described by two float values. In the current implementation, the same resolution is used for every garment panel. Whilst it might be better to use different resolutions for the individual panels where behaviour is required at different levels of detail for different degrees of realism, if the resolutions of two neighbouring

panels were very different it might cause problems in the seaming process.

4.1.1.2 Damping

The damping force component describes the damping constants of the springs used in the mass spring particle system simulation and the air resistance. In the file they are described by two float values, one for each property, thereby allowing the user independently to vary the air resistance if they so wish. Fabric damping is defined as a global parameter because we do not have any way to measure this coefficient and therefore we assume it to be identical for all garment panels. An estimation of the air resistance of fabric from video sequences of cloth exposed to wind was addressed in [BTH+03].

4.1.1.3 Gravity

The gravity component defines the gravitational constant of the environment and is described by a float. The gravity constant is usually set to 9.81 ms^{-2}, its value in s.i. units.

4.1.1.4 Collision Tolerance

The collision tolerance component defines the tolerance between body and cloth as described in Section 3.3.1. Collision tolerance is defined by a float.

4.1.1.5 Garment Type

The garment type component is used to classify the garment. At the moment we have five classifications: bra, shirt, dress, skirt, and trousers. Garment type is described by an integer value 0,..,4 respectively for the aforementioned categories. This classification is used for pre-positioning the garment on the body-scan as well as in the seaming process described in more detail below.

4.1.1.6 Scale Ratio

The scale ratio component describes a uniform scaling value for the individual panels to be applied in both Cartesian dimensions. This is useful for converting the size units, for example, from inches to millimetres. Scale ratio is described by a single float.

4.1.1.7 Y-offset

The Y-offset allows us to adjust the height level of the position of a garment during the pre-positioning process. Y-offset is described by a single float.

4.1.2 Garment Panels

Garment panels describe the cut fabric pieces from which a garment is made. They are described by the panel type, cutting contour, fabric properties, fabric reflectance, fabric thickness and darts.

4.1.2.1 Panel Type

The panel type is used to signify what the panel represents. At the moment our description has seven types: Front, Back, Sleeve, Bra Stripe, Collar, Cuffs, Under Sleeve. The panel type is described by an integer value, i.e. 0-6 of the above.

4.1.2.2 Cutting Pattern

Cutting patterns are described by a sequence of 2D coordinates that, when connected by straight lines, form the outline of the individual garment panels. Files exported from CAD systems usually contain a seaming allowance for the manufacture of real garments. Since we are directly joining garment panels at the edges as described in Section 4.4.3, such allowances are not taken into consideration and have to be removed from the pattern before it is converted to our format. Cutting patterns from CAD systems are often defined by spline curves which we approximate to the required precision by sequences of straight line segments.

4.1.2.3 Fabric Drape Properties

Fabric drape properties describe the weight of the fabric and the characteristics of the fabric's resistance to stretch, shear, and bend forces. In our garment description, stretch, shear, and bend are described by the polynomial and power law coefficients that were fitted to the KES data as described in Section 3.4. The coefficients are four floats for the two power law stretch coefficients in the warp and weft directions, one float for the elastic threshold, one float for the shear coefficient since it is independent of the spring length and the same in warp and weft, six floats for the three coefficients of the bending polynomials in the warp and weft directions, one float for the fabric weight and one float for the grain line orientation. The mapping from the polynomial and power law coefficients to the simpler linear spring coefficients is carried out in the simulation. The mapping of fabric properties onto our mass spring particle system (MSPS) is described in Section 3.4.

4.1.2.4 Fabric Reflectance

Fabric texture is described by photographs which are accessed via a Uniform Resource Locator (URL). Their texture position is defined by uv texture coordinates of the bounding rectangle of the garment panel. The images are treated as diffuse textures but our description also accounts for transparency. Transparency can be defined by an additional, optional URL to a grey scale texture image, where the grey values represent the alpha values which are merged in the simulation to form an RGBA image. Transparency textures use the same texture coordinates as the diffuse textures. To achieve small file size and low transmission times over the Internet, textures are usually described by JPEG images, but many other bitmap formats can be read. The diffuse

and transparency textures must have the same resolution.

More complex inhomogeneous reflectance could be added by using additional texture maps such as gloss maps [Bli78a] to include specular effects or bump maps [Bli78b] to describe small surface orientation perturbations. A homogeneous reflectance description of a garment panel defines the overall properties of a garment in the usual way that Inventor or VRML [Wer93] specify materials (e.g. via their ambient, diffuse, specular, emissive, shininess, and transparency properties).

4.1.2.5 Darts

Darts are actually seams so they could also be described in the seam section, below. However, a dart is a special form of a seam both sides of which are always on the same garment panel. Darts define neighbouring edges on the same panel which have to be joined. Often, they are used to make the cloth fit better to the 3D shape of the body. They are a form of suppression [SW91] and could also be used to describe pleats. Darts are described by an integer for the number of darts and three integers for each dart. The three integers describing the dart are indices to points on the *cutting pattern* of the garment panel which represent the start, middle and end point of the dart.

4.1.2.6 Fabric Thickness

Fabric thickness is defined for each panel by a displacement factor. In the simulation this value is used to create a second fabric surface, a polygon layer which is displaced along the normal of the first original garment panel according to the given value, from which the thickness of a fabric may be visualised. It is important to note that only the mechanical properties of the original panel are simulated. Were this not the case a simulation of the full 3D properties of the fabric would be required, as addressed in [BFA02].

4.1.3 Seams

Seam information allows us to describe where (usually) different panels should be joined. Our format allows the definition of different types of seams. Usually, seams are along the edges of two garment panels. Sometimes, however, seams are required to describe joints on the surface of a panel with another panel's edge. Such seams are described by Edge-Face seams. We also use the seam description to define pressings (e.g. ironed creases along trousers legs) [SW91]. An illustration of the different types of seams is given in Figure 4.8.

4.1.3.1 Edge-Edge Seams

This type of seaming lines denotes a pair of garment panel edges that have to be joined together. Usually, seaming pairs are on different garment panels. They are described by a unique panel number (an integer), a side number[2], and a start and end index (two integers) referring to the relevant vertices of the panel contour for both edges of the seam.

4.1.3.2 Smooth Edge-Edge Seams

This type of seam is described in a similar manner to that used for Edge-Edge seams above. The only difference is in the way these seams are treated in the simulation. In the simulation, the surface normals of the seam vertices, once joined, are averaged in order to make the seam invisible.

4.1.3.3 Edge-Face Seams

The seaming information of pockets and garment panels that are not sewn on the edge of a panel but within the panel is defined by means of edge face seams. In edge face seams the first edge is defined by panel number, side number, start and end point index. The second edge on the face is described by its initial uv coordinates and an angle to describe the seam orientation.

4.1.3.4 Pressings

Pressing seams are used to simulate creases pressed into the garment. We describe them like Edge-Edge seams but in the simulation they are treated differently. Because the two edges are guaranteed to be the same length, pressings can be simulated by point-point seams as illustrated on the left of Figure 4.9.

4.1.3.5 Point Seams

Point seams are used to simulate fastenings. They are defined by an integer for the panel ID, two floats giving the uv coordinate of the fastening, another integer for the second panel ID to which the fastening is made, and two floats for another uv coordinate pair that defines the fastening position on the second panel.

4.1.4 Garment Accessories

Often garments have rigid objects attached. The positions of such objects are dependent on the fabric's drape. In the current implementation the weight of such objects does not influence the fabric's drape. Examples of such objects are buttons or cuff links. They are defined by a URL to their geometry, the panel ID and uv coordinates for the position of the attachment on that

[2]Side number describes the side of the undistorted rectangle used in the non-uniform meshing procedure, described in Section 4.4.1.

garment panel.

4.2 Garment Editing in a GUI

There are many CAD tools (e.g. AutoCAD, MicroStation, etc.) for general vector-based editing available on the market that would be suitable for garment editing. Companies [Sys, Lec, Ger, Opt87] in the textile industry have created their own specialised CAD systems that provide facilities and editing tools targeted at the garment designer. Such tools provide a user interface that is intuitive for garment designers. They offer grading functionality to generate different sizes of garments of the same style, nesting tools that automatically minimise the wastage when arranging cutting patterns on real fabrics with a given dimension, etc. However, such tools use undocumented proprietary file formats and to our knowledge do not provide all the information required to assemble a garment from the cutting patterns. Most of the tools available have functionality to export cutting pattern information into the AutoCAD DXF format. To avoid writing yet another garment design tool we decided to integrate the required functionality into Adobe Illustrator, an illustration tool commonly used by designers that can load and export DXF files.

4.2.1 Plug-in Functions

We developed a plug-in by using Adobe Illustrator's freely available software development kit (SDK) [FHI+00] in conjunction with Microsoft Visual Studio 6.0. Adobe's plug-in SDK is bundled with documentation and example source code for different types of plug-ins. The plug-in we developed provides the following functionality to the user.

- Read garment in our file format.
- Convert "paths" (Illustrator uses "paths" to describe lines and contours) into garment patterns.
- A form to assign pattern properties: fabric properties, collision properties, pattern type, pattern offset, pattern texture, and pattern thickness.
- A form to define garment properties: garment type, horizontal and vertical mesh resolution, working directory, collision tolerance, scale ratio (mm/unit), environment properties (air damping, spring damping, gravity), button URL, etc.
- A function to visualise the texture of each garment panel.
- A corner tool to define the four corner-points of garment panels. More details will be given in Section 4.4.1.

- A seaming tool to mark-up garment panels with seaming information and to define the type of seam.
- A dart tool to define darts on a garment panel.
- A point seam tool to define fastenings, usually between different garment panels.
- Export to a file in our garment exchange format.
- Read and write only the seaming information of a garment, which can be useful if different sizes of garments are available. The seaming information marked up on one garment can then be directly loaded for a garment in a different size.

4.2.2 Commonly used Illustrator Functions

There are many functions of Illustrator that are useful for garment editing. The ones commonly used for garment editing are:

- Import and export functions to different file formats, in particular DXF.
- General editing functions such as moving, rotating, scaling of individual or groups of garment panel contour points.
- Conversion of spline contours to line segments.

4.3 Garment Reverse Engineering

In general, it is difficult to acquire cutting patterns or assembly information of garments that are sold in a shop. Garment designers are understandably reluctant to give away information on their latest designs. In order to simulate and visualise such garments we decided to develop a reverse engineering approach. As shown in Chapter 2, Section 2.2.2 on reflectance measurements there are techniques available to measure the reflectance of fabrics. The visualisation results of such measurements are impressive but the realism suffers from the repetitiveness of the appearance owing to the high memory capacity and processing power required to visualise high quality reflectance models. Human perception is very sensitive to the occurrence of repetitive patterns but less sensitive to small changes in reflectance [Sch04]. Thus, in our approach, we relax the precise measurement of reflectance and instead we approximate it by diffuse textures. However, we acquire images of all panels from which the garment is made, not only to extract colour and reflectance information, but also to acquire cutting pattern contour and seaming information in a semi-automatic process. In order to acquire realistic shape information from which size measurements can be extracted, it is necessary to flatten the individual garment panels. Having

the panels flat is also a requirement for colour acquisition since folds may cause unwanted self shadowing effects that make it difficult or impossible to extract the required colour information. In most cases, flat panels can only be achieved by disassembling the garment. Ideally, we would use a flatbed scanner to acquire images of the flat garment pieces. Flatbed scanners provide uniform lighting and often offer facilities for calibration of the colour acquisition process. Furthermore, sizes can easily be extracted from such scanned images since there is a direct pixel size correspondence. However, most flatbed scanners are designed to acquire images of the size of an A4 page. Some larger scanners exist but in order to acquire images of a garment panel we would need a scanner of the size of around 2×2 metres. We know of no such device and, even if one were to exist, it would probably be prohibitively expensive. Instead, we chose to use a high resolution digital camera to acquire images of garment panels. Digital cameras are very popular nowadays, they are constantly increasing in resolution, they are commonly available and their prices usually decrease. In order to use a digital camera to acquire colour information usable for reflectance representation as texture mapping, the garment in question has to be lit by a constant uniform light source (See Section 4.3.2). Extracting size information of the garment panels in the image can only be achieved if the images are calibrated and rectified (See Section 4.3.4 and Section 4.3.5).

4.3.1 Garment Disassembly

To extract a good contour approximation of the cutting patterns of a garment it is, as noted above, often necessary to disassemble the garment. We achieve this by manually cutting with scissors along the seams. It is not always required to cut all seams. The goal is to cut those seams that allow us to lay the resulting panel flat. Cutting the right seams depends on the type of garment. The person who does the disassembling will acquire the skills required to find the right seams for cutting after repeating the process on a few garments. Expertise in sewing and garment manufacturing may be of advantage to the person who carries out this task. The panels are further ironed before image acquisition to make sure they are as flat as possible and thereby provide a good description of the cutting patterns. If required, remaining seams can be separated in an image processing application after image acquisition. We have disassembled different types of garments, such as shirts, trousers, and bras. Depending on the skill of the person that disassembles the garment and the complexity of the garment, the process usually takes between five to ten minutes.

4.3.2 Lighting

In order to extract texture and colour information it is important that the material is lit as uniformly as possible. The type of equipment used by researchers in optical physics to provide uniform lighting for very accurate light measurements is too expensive for our application. Photographers usually use diffusers such as soft boxes or umbrella reflectors to achieve similar, but less accurate results. This would have been sufficient for our purposes but even such equipment is relatively expensive. Instead, we decided to use polystyrene boards for reflecting light to create a soft, diffuse and uniform illumination[3]. Eight strong builders' lights (500 W) were used as sources. Our photography rig with diffusers and light sources is depicted in Figure 4.1.

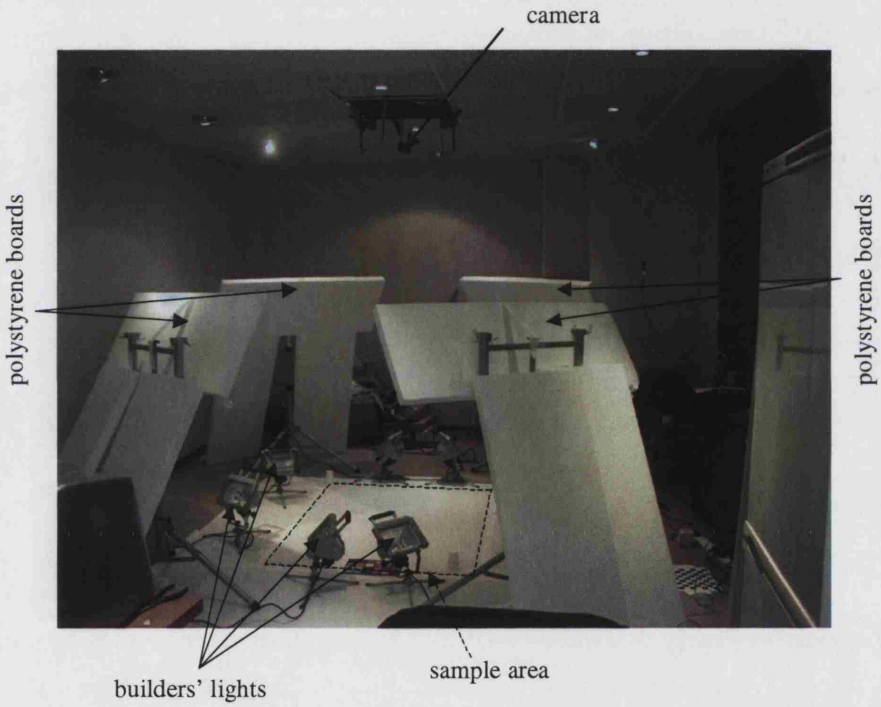

Figure 4.1: Photography rig with a camera mounted on a tripod on the ceiling. Soft-lighting is achieved by reflecting light from polystyrene boards as described in the text.

4.3.3 Image Acquisition

To acquire the images we used an Olympus C4040Z camera with 4.1 mega-pixels. The camera was mounted on a tripod on the ceiling as depicted in Figure 4.1. The camera was powered by an AC adaptor to make sure that batteries do not need to be changed during the acquisition of different garments. The camera was connected to a PC via a universal serial bus (USB). We used software (Cam2Com) [Men02] remotely to control zoom, white balancing, flash, shutter

[3]Thanks to Cliff J. Haynes from the Slade School of Fine Art for discussions about this set-up.

speed, aperture and resolution of the camera. Since camera position and orientation were fixed it was possible to use the same parameters for calibrating and rectifying the images of different garments. Whenever possible we put all panels of a garment into the rig, so that a single image could be used to describe a whole garment. The images were downloaded to the PC with the same software used for remotely controlling the camera and calibrated as described below.

4.3.4 Geometrical Image Calibration

In order to approximate the sizes of garment panels from an image, the image has to be calibrated and rectified. There are many approaches available for camera calibration [Zha00]. However, in our case the problem is simplified since the image is of a planar surface with known measurements. There are two factors that influence the distortion of an image: the perspective projection that changes with the position and orientation of the camera and the lens distortion. We compensate for lens distortion by using a tool (CAMEDIA Master) that accompanies our camera. The method probably uses known lens parameters of the camera to correct for distortion of the image. To account for distortions that stem from perspective projection we use an affine transformation. This is sufficiently accurate for our application and it is not necessary to use a homography[4]. The parameters of the transformation are found by placing the markers of the corner-points in the image onto the nearest corner-points of a rectangle circumscribing the distorted rectangle in the image as indicated in Figure 4.2. The transformation is achieved by using the *free transformation* tool in Adobe Photoshop. This employs an image transformation of the kind described by Heckbert in [Hec86]. Since the camera's position and orientation is fixed we could apply the same transformation to all garment images.

4.3.5 Colour Calibration

We approximated the spatially varying fabric reflectance by taking photographs of a sample of the fabric in diffuse light as described above. This approach has proven to work well for diffuse fabrics but we expect to encounter problems caused by reflections if we would measure more shiny materials such as velvet, etc. We achieve colour and light calibration by inserting a MacBeth colour checker in the image with the fabric. The image is balanced afterwards so that the known values of the MacBeth chart best match those of the image in a least squares sense. This is achieved with a RADIANCE tool called macbethcal [LS98] that was specifically designed for this purpose. In order to use macbethcal the positions of the four corner-points of the Mac-

[4]We carried out measurements to evaluate the size difference of real and virtual garment panels. The errors found were one to two millimetres on real garment panels with a size of one metre. This represents a relative error of 0.1% to 0.2%.

Beth colour checker in the image have to be identified. MacBeth calibration is not completely accurate and errors may occur [LS98]. Better results for measuring surface chromacity can be achieved by using spectrophotometers. Such devices are, however, much more expensive and are not required for our purposes. An example of a photograph of a disassembled pair of jeans directly downloaded from the camera is depicted on the left of Figure 4.2. The same photograph after it was colour calibrated and rectified is shown on the right of Figure 4.2.

Figure 4.2: Left: Photograph of disassembled jeans with MacBeth colour checker on the right of the image, directly after capture. Right: Image after MacBeth colour calibration, lens distortion correction and rectification.

4.3.6 Marking-up Images

Once the image is rectified and colour-balanced it can be used to extract the information required to describe the garment. This process is semi-automatic. We first compute the pixel/mm ratio. All the individual panels in the image are roughly cut and pasted into a new image. The new image should have a resolution that is well suited for hardware texture rendering, with the number of pixels in both dimensions equal to a power of two. In our case we chose 2048×2048, which is a high texture resolution for good quality rendering. In the new image, the panels are rotated so that their orientation is roughly that required for virtual seaming. This is a standard procedure that can be carried out, for example, in Adobe Photoshop or any other image editing tool. After re-orienting all panels appropriately the new image is saved in a JPEG file. The JPEG file is loaded into Adobe Illustrator in order to define the cutting patterns. The patterns are defined manually. We have tested automatic contour finding and following methods but none of the results were satisfactory. The goal of manual extraction is to describe the borders as poly-lines approximating as closely as possible the borders visible in the image while, at

the same time, the number of cutting-pattern points should be kept low in order to lead to a simple description. Since the image is also used as a texture map it is important that none of the background is marked to be within a panel cutting-pattern. Cutting patterns are associated with the texture image and texture position. Seaming information is defined manually on the panel contours as required. Fabric properties are specified by choosing from a database[5]. The size ratio is specified to correctly scale the garment in the simulation. The garment type is defined to allow automatic pre-positioning of the garment around the body in the simulation. The whole marking-up process is dependent on the complexity of the garment and the skills of the editor but usually takes between thirty minutes and an hour.

4.3.7 Border Colours

It is not always possible exactly to match the boundary contour of the garment panels with the pixels of the texture. In some cases, the background on which the garment panel was laid may be visible in the image. Since the background should be easily distinguishable from the garment panel to help contour extraction any occurrence of the background on the texture can be very distracting in the visualisation. To tackle this problem we developed a technique to fill the background with a colour close to that of the pixels of the panel colour. Since the background was chosen to be of uniform colour, filling it with a different colour is trivial. However, pixels in the border area between garment panel and background often have different colours since they are either mixed pixels or background in shade of the supposedly flat garment panel. We used the bucket fill tool of Photoshop which implements a region growing technique to identify such pixels as follows. First the image is copied. The garment panels and the background are filled with a single colour. We assume that the garment panels have sufficiently similar or uniform colouring within them, to be uniformly filled by the region grower. The remaining pixels in the image that are different from the fill-colour are those that are in border areas that cause the problem. We replace all these pixels in the original image with a colour close to that of the garment panel. This technique works well for garments with fairly uniform colouring but needs to be further developed for garments with very inhomogeneous colours.

4.4 Garment Simulation

In this section, we address the functionality and methods required to turn the garment description into a form that is suitable for garment simulation on a body. The required methods are: garment meshing, automatic garment pre-position around the body, and garment seaming.

[5]At the moment, our fabric database contains six fabric types tested by means of a KES as described in Section 3.4.

4.4.1 Garment Meshing

The meshing process creates a mass spring particle system (MSPS) for each garment panel described. It uses resolution, scale ratio, drape properties and cutting pattern information from the garment exchange format. Two types of meshing were implemented: non-uniform and uniform meshing.

4.4.1.1 Non-Uniform Meshing

When this meshing strategy is used the panel cutting pattern is assumed to be a distortion of a rectangular mesh. The four corner-points on the contour that most closely describe a rectangle are used for the meshing as for example corner-points p_0, p_1, p_2, p_3 depicted in Figure 4.3.

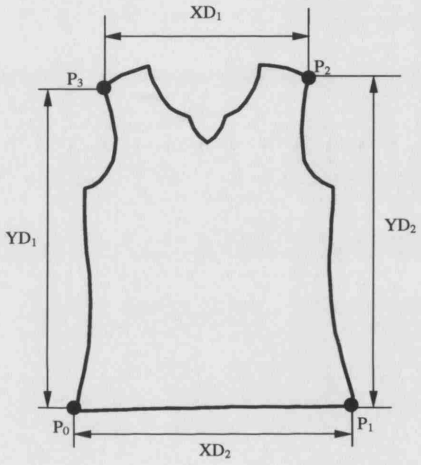

Figure 4.3: Corner-points and distances used for non-uniform meshing.

First the edges of the panels are meshed by iterating along the cutting pattern points and creating points with equal distances. The step size for horizontal mesh points is then computed as $\Delta X = P_{i,nv-1,x} - P_{i,0,x}$ where nv is the number of rows of horizontal points, $P_{i,0,x}$ is the x coordinate of the point furthest left, and $P_{i,nv-1,x}$ is the point with x coordinate furthest right. The x coordinates of the individual mesh vertices are then computed from

$$P_{i,j,x} = P_{i,j-1,x} + (P_{0,j,x} - P_{0,j-1,x})\frac{\Delta X}{XD_1}(1 - \frac{i}{nu-1}) + (P_{nu-1,j,x} - P_{nu-1,j-1,x})\frac{\Delta X}{XD_2}(\frac{i}{nu-1}),$$

where the index i runs from 0 to $nu-1$, the number of columns of vertical points, and the index j runs between 0 and $nv-1$. Similarly, the vertical step size is $\Delta Y = P_{0,j,y} - P_{nu-1,j,y}$ and the y coordinates are given by

$$P_{i,j,y} = P_{i-1,j,y} + (P_{i,0,y} - P_{i-1,0,y})\frac{\Delta Y}{YD_1}(1 - \frac{j}{nv-1}) + (P_{i,nv-1,y} - P_{i-1,nv-1,y})\frac{\Delta Y}{YD_2}(\frac{j}{nv-1}).$$

An example of the front panel of a shirt meshed in this way with a resolution of 20×20 is depicted in Figure 4.4. The advantage of this meshing strategy is that it is directly compatible with Provot's model and bending and shearing springs can be easily inserted. The disadvantage

of this approach, however, is that if the pattern is not close to a rectangle the distances between mesh points may vary substantially. In other words, the resolution of the mesh would vary depending on the shape of the pattern. This may cause undesirable fabric drape behaviour in some regions of a garment. In addition, sharp edges along the cutting pattern contour cannot be described well. However, such limitations are not severe since most real cloth fabric cutters have similar limitations[Bou04] and therefore patterns likely to cause severe problems are rare. In addition, workarounds for the mentioned problems exist. For example, by splitting a panel that is not close to a rectangle into two or more panels and by adding seaming information, sharp corners in the original pattern can be better described and the mesh resolution can be kept more uniform.

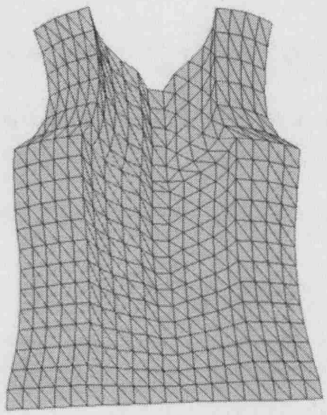

Figure 4.4: Example of the front panel of a shirt meshed non-uniformly.

However, because manual editing, to avoid the shortcomings of the non-uniform meshing, may be time consuming, we experimented with a uniform meshing strategy as described next.

4.4.1.2 Uniform Meshing

The basic idea of the construction of a uniform mesh is much simpler. The bounding rectangle around a cutting pattern contour is computed and vertices are uniformly inserted if the point is within the contour. With this meshing strategy the limitations of the non-uniform meshing are overcome. Sharp corners can be described and the resolution is by definition uniform. However, this meshing strategy creates some new problems. As can be seen in Figure 4.5 where a uniform mesh with a resolution of 20×20 is depicted, uniform meshing is only possible within the garment panel but not at the edges. Additional points at the border of the cutting pattern contour are inserted to describe the shape as well as possible. By inserting these additional points the length of springs at the edge of the cutting pattern contour can be significantly shorter than the lengths of springs in the interior of the panel. This causes problems with the stability of the

simulation. In addition, for points close to the borders it is not always possible to insert shearing and bending springs since the required neighbouring mass points may not exist. As we have not yet overcome these problems to a satisfactory extent we use the non-uniform meshing described above. Triangular meshing would solve the encountered problems but neither Provot's cloth model nor our fabric property mapping can be used on a triangular mesh.

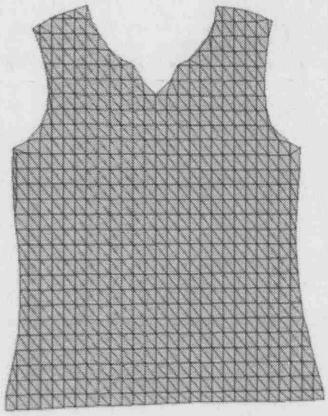

Figure 4.5: Example of a front shirt panel meshed uniformly.

4.4.2 Automatic Garment Pre-Positioning

In order to simulate garments on a body it is necessary to dress the body with the garment. This could possibly be achieved by seaming the garment panels first and then by creating an animation sequence for the body to get dressed. This, however, may be a very complex and time consuming task for a computer. Instead, we decided to seam the garment directly around the body. The seaming process is described in more detail below. Since our goal is a completely automatic process the garment panels are pre-positioned around the body by using landmark points on the body-scan. Landmark data is automatically extracted from the body geometry by software integrated in the scanning system. Methods for automatic landmark extraction have been described by Dekker et al [DDBT98] and a brief description of this technique is given below. Similar methods for garment pre-positioning have been described by Fuhrmann et al [FGLW03, GFL03].

4.4.2.1 Automatic Body Landmark Extraction

The goal of automatic landmark extraction is computationally to find feature points on a human body. Machine learning techniques such as genetic algorithms, support vector machines, neural networks, etc. have been used to achieve this goal with some success. In order to get an idea how such algorithms work we briefly describe a more intuitive approach discussed in [DDBT98, BDDV00]. The method described assumes that the body data is represented by

a set of horizontal slices. Such a representation is obtained directly by some laser scanners but if the data is not in this form it can be easily converted by intersecting the body-scan mesh with horizontal planes. Once the data is in the required "slice" form, and provided it is of sufficiently high resolution, the landmark detection and segmentation process is used to divide the body scan into six groups of slices corresponding to the head, torso, arms and legs. At a high level, primary landmarks are detected such as the top of the head, torso, neck, left and right armpits, crotch, and the ends of the arms and legs. Primary landmarks are detected by algorithms such as that designed to locate the armpits from a re-entrant surface condition as illustrated in Figure 4.6. The centroid of each horizontal data slice is calculated, and the vertices binned into sectors of angular width β, which is related to the number of samples in the slice. The arms can be segmented from the torso by detecting the transition slice that indicates the branching point at the armpits. Sector bins will typically contain only a few vertices, but at the armpit, a threshold on the number of vertices in a bin is exceeded. Similarly, the neck and crotch can be detected by reasoning about the average distance to the centroid from slice to slice, and changes in depth. Primary landmarks define sub-search areas on the surface of the body scan in each of which a variety of discriminant functions use shape characteristics such as the maximum local curvature, etc. to detect other landmarks such as: shoulder, elbow, wrist, waist, hip, knee and ankle. This algorithm is part of the system developed automatically to process the Hamamatsu body scans [BDDV00]. In our system we are using the software supplied with the TC^2 scanning system for automatic landmark and size extraction. Fortunately, the location of principal landmarks is quite well standardised from the definitions of the body measurements used in the clothing industry [Ald99]. It would therefore be easy to adapt our system to work with other scanning and body modelling systems.

4.4.2.2 Pre-Positioning of Garments

For each garment type we defined where it should be dressed on the body. For example, a shirt's front panel will be positioned in front of the body. Sleeve panels are positioned so that the seams can easily be joined around the arms. At the moment we use five types of garments described in Section 4.1.1 which were sufficient for our current simulations.

We have defined rules to position the garments by using the following landmarks: crotch point, left shoulder, right shoulder, left waist, right waist, left hand, right hand, left elbow, right elbow, neck point, left knee, right knee, left ankle, right ankle, left hip, right hip.

Examples of a shirt and trousers automatically pre-positioned around the body are depicted in Figure 4.7. For the shirt the flat 2D panels of the sleeves are pre-bent to reduce the time required for the seaming process.

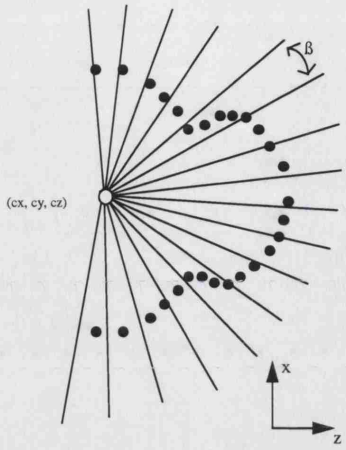

Figure 4.6: Underarm segmentation using re-entrant point tolerance criteria. Black points illustrate the right part of a horizontal body slice at a height around the armpit.

Figure 4.7: Pre-positioned garment panels; Left: A shirt; Right: A pair of trousers. Landmark description as also indicated in the text.

In addition the Y-offset in the garment description can be used to adjust the pre-positioning of the garment in the vertical direction.

4.4.3 Garment Seaming

In order to join the individual panels, elastic seaming forces are applied along the seaming lines. Unlike spring forces that are dependent on the extension of a spring, the seaming forces are constant. Seaming simulation is also described in chapter 4 of Volino and Thalmann's book [VMT00a] and in Fuhrmann et al [FGLW03]. Both approaches use triangular meshes which make it possible always to apply forces between points of the mass spring model. If one side of a seam does not contain as many seaming points as the other new triangles can easily be inserted in the mesh. However, this is not the case in our model which is always described

by quadrangles. Inserting new quadrangles to create the same number of points on each edge or face of a seam pair is not always possible. This is why we had to develop special edge-edge seams and edge-face seams. Darts, fastenings and pressings are described by simple point seams. Darts and pressings are guaranteed by the meshing to have an equal number of points on both seam sides. An illustration of the different seams is given in Figure 4.8. Seams are shown as bold lines. To show which mass points of the garment panel mesh are defined to be joined the panels are rendered in wire-frame mode. The dart seams are illustrated on a pair of trousers. Point-seams are shown on a shirt, where they are used to simulate the effect of shirt-buttons. Edge-face seams are used on the same shirt to simulate a pocket. Two types of edge-edge seams (described below) are shown in the illustration. They are used to seam sleeves on the front and back panel of the shirt as well as to seam front and back panels on the sides.

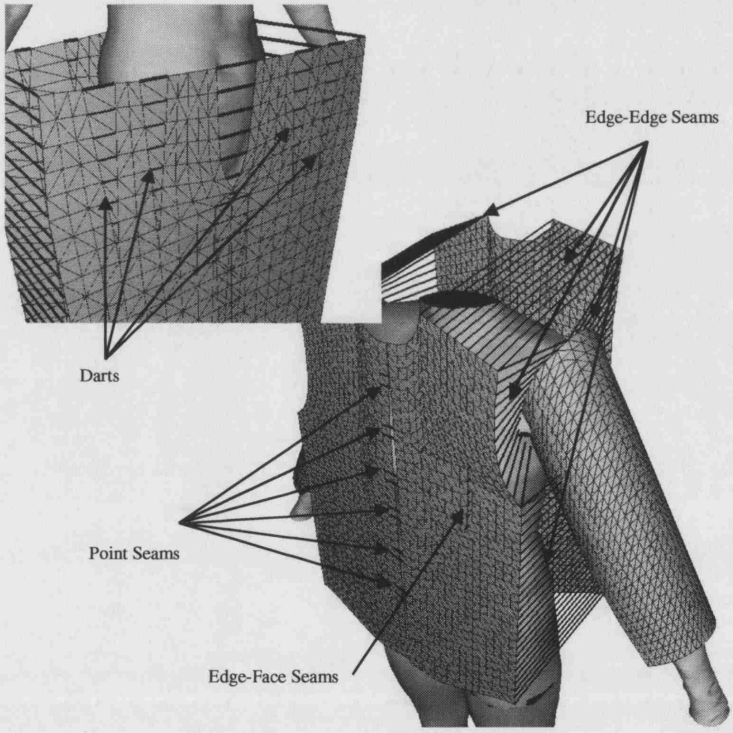

Figure 4.8: Different seaming types.

4.4.3.1 Edge-Edge Seams

Edge-edge seams are the most common seams used for garments. If the number of points is the same on both sides elastic seaming forces can simply be applied between the corresponding points of the sides as illustrated on the left in Figure 4.9. However, often the number of points on one side may be different to the number of points on the other side. This is illustrated on the right of Figure 4.9. In this case the elastic seaming force is applied between a point on one side

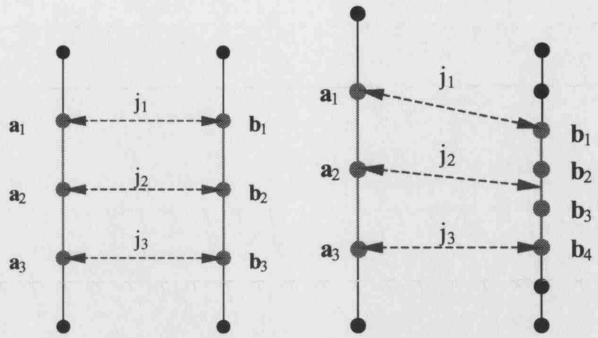

Figure 4.9: Left: point-point seams; Right: point-edge seams.

and an edge on the other side.

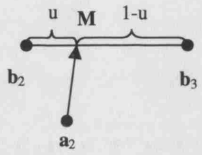

Figure 4.10: Edge-edge seam position interpolation.

Figure 4.10 illustrates how the position of the point on the edge is computed. Given a u value on the edge between point $\mathbf{b}_2$ and $\mathbf{b}_3$, the position $\mathbf{M}$ on the edge is given by the linear interpolation $M = (u)\mathbf{b}_2 + (1-u)\mathbf{b}_3$. The elastic force is interpolated in the same way. In our implementation the points on the side of the seam with the lower number of points are treated as points to which the seaming force is applied and the u values for positions on the edges are computed for the other side. The individual u values for each seam are computed as follows. First the length l_1 and l_2 are defined by the Euclidian distances between all successive points on each side of the seam respectively. Then we iterate through the points of the side with the smaller number of points while we sum the Euclidean distances to the previous points. For each point we compute the u between the corresponding points on the second side by taking the length ratio l_1/l_2 into account. The first and the last point of both sides of the seam are always joined to the corresponding points on the opposite side. The length ratio l_1/l_2 should be close to 1.0 in order to obtain good results for edge-edge seaming.

4.4.3.2 Edge-Face Seams

In some cases it is necessary to seam a garment panel somewhere in the middle of another garment panel. This is the case, for example, for pockets as depicted in Figure 4.8. In order to describe such seams we implemented edge-face seams. Edge-face seams are defined by a starting point and an end point for the edge side of the seam, and a uv coordinate for the

starting point on the panel, and an angle relative to the vertical axis. This is illustrated in Figure 4.11 with edge starting point $\mathbf{a}_1$, end point $\mathbf{a}_3$, coordinates u and v on the face side of the seam, and an angle α. We find the quadrangle on the garment mesh that contains the uv

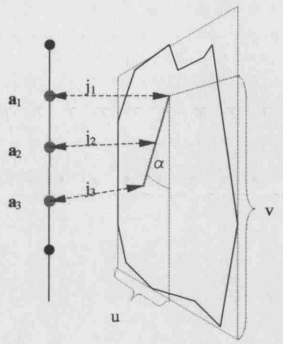

Figure 4.11: Edge-face seams.

coordinates. The corresponding positions of the points on the quadrangle are then approximated as illustrated in Figure 4.12. If the quadrangle is given by $\mathbf{b}_1$, $\mathbf{b}_2$, $\mathbf{b}_3$ and $\mathbf{b}_4$ we approximate $\mathbf{M} = (u)\mathbf{b}_4 + (1-u)\mathbf{b}_3$, $\mathbf{N} = (u)\mathbf{b}_1 + (1-u)\mathbf{b}_2$, and $\mathbf{Q} = (v)\mathbf{N} + (1-v)\mathbf{M}$. In the same way as for the point positions, the elastic force is interpolated and $\mathbf{a}_1$ is attracted to $\mathbf{Q}$. For

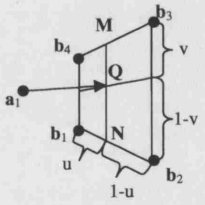

Figure 4.12: Edge-face seam position interpolation.

edge-face seams, the seam line on the side of the face is defined to have the same length as that of the edge.

4.4.3.3 Seaming process

The elastic seaming forces are applied until all seaming points have converged to within a small tolerance. If the garment is too small for the body, seaming may not be possible for some seaming points. For this reason, if it has not converged, we stop the seaming process after a fixed number of iterations. The percentage of seams that cannot be joined within this given number of iterations because of the size of the garment and the person's body shape may be used as a fit feedback measure. We have noticed some problems where a garment does not reach the desired position on the body. For example, the legs of jeans may not always cover the legs of the person but in some cases are sewn outside the person's legs. Fuhrmann et al

[FGLW03] have noticed similar issues and they introduced special seaming particles to make sure that after the seaming process the body is covered by the garment. We addressed this issue by adding a constant force perpendicular to a seam-edge and to the original seam force in order to increase the probability that the seams are joined so that a jean's panels are fitted[6].

4.4.3.4 Pre-Simulated Garments

Pre-simulated garments are used to save computation time if a garment is to be used more than once on the same person. This may be for carrying out different body animations or if several garments are tried-on in different order. The full simulation state containing positions, velocities and forces of each mass point is stored in a file. The pre-simulated garment can be saved at any stage of simulation. If multiple layers of garments are simulated the rest state of the garment is influenced by the interactions between different garment layers. If a garment's simulation state is stored before any interactions with other garment layers happen, the garments can be tried-on in a different order without requiring the computation time needed for the garment to approach the body.

4.5 Summary

Most of the work described in this chapter focuses on system building which is different to research theory and experimentation. Such work is often required to allow researchers to carry out experiments but is not always described in a thesis. However, we have found it important to describe this work here because there are some contributions that may be of interest to the research community and it was a significant element in the creation of the virtual try-on system. We described our garment exchange format along with methods to acquire and simulate garments. We started with the definition of our garment file format. The format allows us to describe fairly complex garments although it would be useful to develop the format further to a standard for garment manufacturing and simulation. A brief description of an extension of a graphics illustration tool commonly used by garment designers to import from a CAD system, mark-up, edit, and export to our garment exchange format followed. We then described a method for reverse engineering of garments that one can buy in a shop. The method may sound obvious but to our knowledge such an approach has not previously been described. In a semi-automatic process, the method allows us to acquire a very realistic garment description from high resolution digital photographs of real garment fabrics. The method could be extended for the acquisition of more reflectance and transparency information. In combination with grading

[6]Jonathan Walters from Bodymetrics had the original idea to tackle the problem which causes a jean's panels sometimes to be sewn incorrectly outside a person's legs by adding a constant perpendicular force to the seam edge.

rules, image morphing and texture synthesis techniques, garment photographs could also be used to describe different sizes of the same type of garment. Following the reverse engineering approach, we discussed methods for garment simulation in more detail. We described non-uniform and uniform meshing techniques to create a rectangular topology, mass-spring system from the bounding contour of a cutting pattern, the fabric properties, and the mesh resolution. The meshing techniques are not without drawbacks. The non-uniform meshing technique limits the description of cutting patterns whilst the uniform meshing technique may lead to instabilities in the simulation. Triangular meshing may offer a better solution but would require a major re-write of the whole dynamical simulation system. We then described the use of body landmark data extracted by scanner software automatically to pre-position garment panels around the body for virtual seaming. Finally, we defined the different types of seams we use to join garment panels. We have noticed that, in some simulations, after the seaming process some garments do not cover the body as intended. A simple modification to the seaming forces to help overcome this was discussed. Other constraints such as manually inserted virtual seaming particles described by Fuhrmann et al [FGLW03] could probably be further developed and automated to ensure the garment always dresses the body correctly. As we noted at the beginning of this section it is important to emphasise the difference between system building work and more theoretical and experimental work.

Chapter 5

Visualisation

This chapter is on the visualisation of garments. The most intuitive way to visualise garments is to create images that look as much as possible like a photograph of a real garment. However, for electronic commerce and design applications there are additional goals for visualisation. It should allow a customer to obtain additional fit feedback and a designer may be interested in the assembling details of a new design. We describe different visualisation modes for garments. Integration with a global illumination system that allows us to generate images with different quality settings for realistic visualisation is discussed. Finally, at the end of this chapter we describe an ActiveX control that provides an Internet interface for garment simulation that is suitable for e-commerce and garment design.

5.1 Surface Representation

As mentioned in Section 2.2.1 different representations for garment surfaces exist: triangular meshes, NURBS surfaces and progressive meshes are the most commonly used. Since our primary goal was that of real-time visualisation on a personal computer equipped with graphics hardware, we chose a triangular mesh representation. Meshes are represented by vertex information and connectivity. On current graphics hardware, vertex information usually consists of position, colour, texture coordinate, vertex normal and material attributes. In the most basic form individual triangles described by three vertices can be passed down the graphics pipeline for rendering by using, for example OpenGL [SAFe02]. However, there are higher level representations for meshes available in OpenInventor [Wer93]. Higher level representations are preferable for three reasons: They are described in the corresponding OpenInventor file format for electronic exchange, they allow us to define meshes in a more structured form, and they enable us to trade-off the rendering performance against the memory requirements. OpenInventor provides five classes to describe triangular meshes. These are summarised in Table 5.1, where "class" describes the OpenInventor class, "performance" describes the rendering performance,

"storage" describes the efficiency of storing the geometry, "versatile" describes whether any surface can be represented, and "VRML" describes if the class is supported by the VRML file standard. In the table, a "+" means that the class has an advantage compared to some of the others and a "-" means that there is a relative disadvantage in that category.

Class	Performance	Storage	Versatile	VRML
FaceSet	-	-	+	-
IndexedFaceSet	-	+	+	+
QuadMesh	+	+	-	-
TriangleStripSet	+	-	-	-
IndexedTriangleStripSet	+	+	-	-

Table 5.1: Inventor's mesh representations.

The representations differ in compactness for storage and efficiency for rendering. Basically, types that have a prefix "Indexed" in their class-name describe connectivity by indexing the vertex information and are therefore more compact because vertex information does not have to be repeated as may be necessary for FaceSets. TriangleStripSets and IndexedTriangleStripSets are the most efficient triangular representation in terms of rendering, since their connectivity information is implicitly given by the vertex order. In these representations, after two vertices have been transferred to the graphics hardware, every additional vertex transferred describes a new triangle. Owing to our rectangular meshing strategy (see Section 4.4.1) the most natural way to represent a cloth surface would be a QuadMesh. QuadMeshes are described by an array that contains vertex information, and the number of vertices per column and row. QuadMeshes can also be rendered efficiently since internally they can easily be described as triangle strips or may even be directly taken as quads by the graphics hardware. However, IndexedFaceSet is the only representation that was taken into the VRML standard [BCM96]. With IndexedFaceSets all meshes describable by the other representations can be defined. They are fairly compact and VRML browsers do not have to implement all the other representations. This also makes life easier for developers. Because we are interested in storing the representation in a standard format and since conversion from QuadMeshes to IndexedFaceSets is trivial, we decided to also use IndexedFaceSets for our garment visualisation.

5.1.1 Quadrilateral and Triangular Meshes

In the conversion from QuadMesh to IndexedFaceSet it is possible to alleviate a disadvantage of QuadMeshes. The automatic QuadMesh triangulation of OpenInventor does not take the surface

normals into consideration, which may cause artefacts in the visualisation. Let us consider a single quadrilateral $\mathbf{v}_0, \mathbf{v}_1, \mathbf{v}_2, \mathbf{v}_3$ on the surface (see Figure 5.1) and let $\mathbf{n}_0$, $\mathbf{n}_1$, $\mathbf{n}_2$, $\mathbf{n}_3$ be the corresponding vertex normals. There are two possible ways of splitting the quadrilateral into

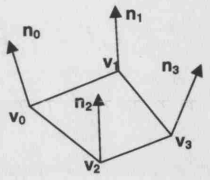

Figure 5.1: Using vertex normals to triangulate a QuadMesh.

two triangles: One is to use the diagonal $\mathbf{v}_0, \mathbf{v}_3$ and the second is to use $\mathbf{v}_1, \mathbf{v}_2$. In order to render a smooth surface, it is best to compare the surface curvatures in the two directions ($\mathbf{v}_0$, $\mathbf{v}_3$ and $\mathbf{v}_1$, $\mathbf{v}_2$) and to split the quadrilateral by using the diagonal corresponding to the smaller curvature. An approximation of the curvature is the angle between the surface normals which can be computed by use of the dot product. Therefore, for smooth rendering we split along diagonal

$$\begin{array}{ll} \mathbf{v}_1, \mathbf{v}_2 & if\ \mathbf{n}_0 \cdot \mathbf{n}_3 \leq \mathbf{n}_1 \cdot \mathbf{n}_2\ and, \\ \mathbf{v}_0, \mathbf{v}_3 & Otherwise. \end{array} \tag{5.1}$$

While this approach produces a smoother surface[1], it takes longer to render than standard QuadMeshes do because it does not use triangle strips. A comparison between the two triangulations is depicted in Figure 5.2. On the left, a tablecloth with the standard triangulation is depicted. Some artefacts are visible on some folds on the left. The right image depicts the same table cloth with curvature dependent diagonal split. The cloth appears smooth everywhere.

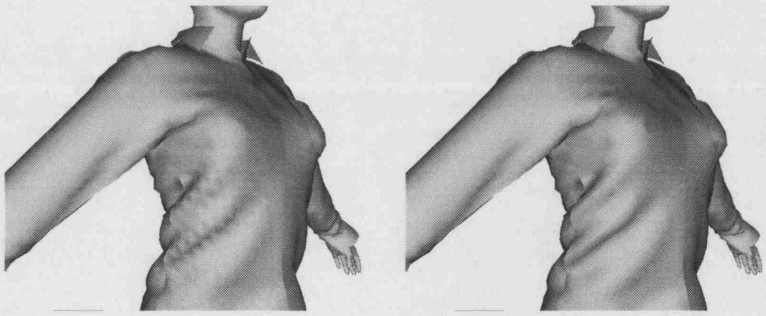

Figure 5.2: Rendering comparison between standard QuadMesh triangulation, left, and QuadMesh triangulation that takes the surface normal into consideration, right.

[1]It was Tzvetomir Ivanov Vassilev's idea to split the quadrangles into triangles according to vertex normals in order to overcome smoothing artefacts.

5.1.2 Fabric Thickness

We visualise fabric thickness by adding an extra polygon layer displaced along the garment's surface normals. The displacement distance is defined per panel. The resulting extra layer is joined with extra triangles on the borders. Texture coordinates for the extra triangles are set so that the graphics hardware interpolates between the texture of the surface border.

5.2 Texture and Transparency Mapping

In general, it is necessary to specify texture coordinates for all the vertices in a mesh explicitly. As described in Section 4.1 our garment exchange format uses only two UV coordinates for texture description. This is possible because the individual garment panel meshes are initially flat and the texture coordinates can be easily computed from the x, y components of the vertex positions relative to a garment panel's bounding rectangle. This is illustrated in Figure 5.3. For

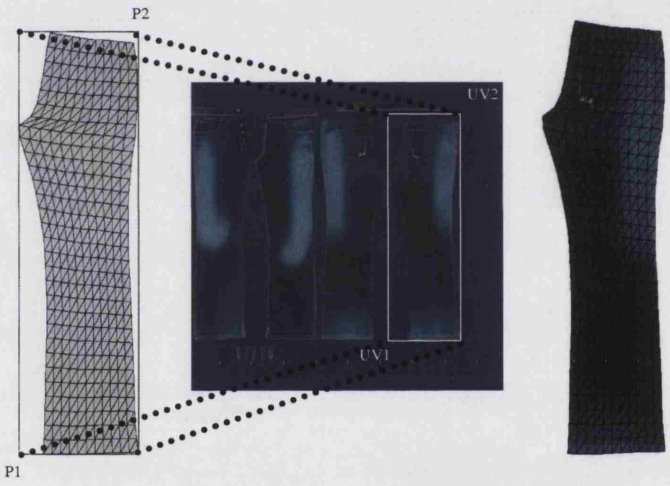

Figure 5.3: Garment panel texture information is given by two UV coordinates.

reasons of graphics hardware implementation, the resolution of the texture images has to be a power of two in both dimensions. UV texture coordinates are defined by values in the unit square and therefore are independent of the image resolution.

Some image file formats exist that can store, in addition to red, green and blue channels, an alpha channel to describe colour and transparency in RGBA form [2]. While the JPEG image format can represent images in a very compact form it does not provide the possibility to describe transparency information. Instead, we use an extra grey-scale JPEG image to store transparency information and merge the RGB and grey-scale JPEG images to form an RGBA tex-

[2]The Portable Network Graphics (PNG) and SGI's RGB image file format support an alpha channel to describe per-pixel transparency.

ture. In order to avoid incorrect transparency rendering we use the SORTED_OBJECT_BLEND mode of OpenInventor's SoGLRenderAction class. Efficiency improvements for correct transparency rendering could be achieved by means of the depth peeling approach described in [Eve01, Mam89].

5.3 Modes of Real-Time Visualisation

The default mode of OpenInventor rendering is that of Phong shaded, filled polygons. Surface normals are used to smooth the surface and for local illumination shading. This mode can achieve fairly realistic appearance in real-time. Further quality improvements could probably be achieved by exploiting recent graphics hardware's shadow mapping facilities to approximate the illumination better. Such hardware was not available for development and thus we did not focus on work in this direction. Instead, we experimented with modes of visualisation that could give feedback about the assembly of a garment and about the garment fit. From our collaboration with a designer and from our own experience in virtual garment construction we found that simple wire-frame and hidden line modes can be helpful in obtaining visual feedback about garment assembly details. An example of a woman's top is given in Figure 5.4. On the left, the default mode is shown. The next image to the right shows the same garment with the wire-frame mesh visualisation in addition to the default rendering. We found this useful in order to debug problems in the meshing. Our designer found pure wire-frame rendering of the garment with smooth polygon rendering of the client's body-scan important for gathering garment assembly information and for examining the space between the garment and the body in certain areas. Finally, on the right the garment is shown with wire-frame mesh visualisation in addition to the default rendering but without the client's body-scan. This mode enables us to view the inside of the garment that would not be visible if the body-scan were shown. Visualisation of seaming lines, as depicted in Figure 4.8, was also found to be useful in order to debug the seaming definition of virtual garments that could not be assembled as desired because of incorrectly defined seaming lines.

5.3.1 False Colour Visualisation of Simulation Data

In order to visualise fit-feedback of a garment we experimented with different false colour representations of cloth simulation data on the garment surface. The most obvious data to visualise were the forces of the mass spring particle system. Since in our system the simulation mesh and the visualisation mesh share the same vertices it is trivial to map the force values of the MSPS to colour values by setting OpenInventor's PER_VERTEX colour binding mode.

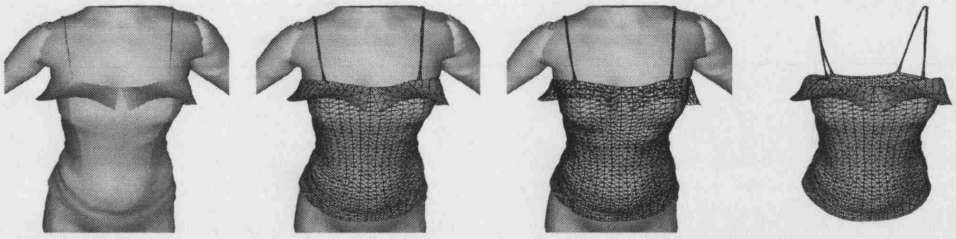

Figure 5.4: A woman's top in different real-time rendering modes from left to right: default, wire-frame on top of default, only wire-frame, and without the client's body-scan.

We chose the hue saturation value (HSV) colour model and mapped the normalised forces[3] to the hue colour component. We separated the internal forces into their stretch, shear and bend components by summing only the corresponding spring forces to create different visualisation modes. In addition, we looked at visualisation of the collision response force. None of these modes produced images that we could interpret as a fit feedback. Mapping the average relative elongations (natural length/current length) of the neighbouring stretch springs of a mass point as the hue component of the HSV colour model to vertex colour produced better results. This mode allowed us to interpret the colours as tightness of the garment on the body-scan. Very tight areas of a garment were mapped to red and loose fitting areas to blue. The elongation values were normalised to the maximum spring extension defined by the description of the fabric used for the garment panels.

This visualisation mode is illustrated in Figure 5.5. A customer scan is dressed in a pair of jeans of different waist sizes 25, 27, 29 and 31. The different sizes are shown in the columns of Figure 5.5. The first row shows the jeans with relative elongations mapped as false colour from the front. The second row shows the same jeans from the same view but uses the standard textured Phong shaded visualisation mode. Rows three and four are the same as rows one and two but viewed from the back of the customer's scan. We can clearly see in the false colour mode where the jeans fit tightly (red) and where they fit loosely (blue). We have also mapped relative elongations of bend and shear springs but could not find an interpretation as to what they might represent in terms of garment fit. We noticed, however, that mapping of the bending spring elongation cannot be interpreted as curvature as might be expected. This is caused by the fact that bend springs are also elongated when the fabric is stretched and therefore their elongations represent a combination of the fabric's resistance to stretching and bending.

[3]Forces are normalised between 0 and 1 according to the minimum and maximum force in the mesh.

Figure 5.5: Jeans with waist size from left to right: 25, 27, 29 and 31. The first row shows a false colour visualisation of the stretch spring elongations of a customer in jeans. The second row shows the same jeans in realistic real-time visualisation mode. Rows three and four show the same data as rows one and two but viewed from the back of the customer's scan.

5.4 Global Illumination and Realistic Augmented Reality

In order to evaluate the quality of our default real-time visualisation, we integrated the clothing system with a global illumination system. The goal of global illumination is to approximate the behaviour of light interactions in a scene. Global illumination is of particular interest for the realistic visualisation of clothing because of the complex light inter-reflections between fabrics, for example, between clothing on the torso and on the arms, or in the ridges, creases and folds of cloth. Such inter-reflection and soft shadow effects cannot be simulated with faster local illumination systems. Radiosity and Monte Carlo path tracing are the most commonly used approaches to find a solution to the rendering equation that take such light interactions into account. RADIANCE [LS98] is one of the systems that approximates the real behaviour of light very well and is freely available in open source. It uses a Monte Carlo path tracer with an oct-tree data structure for efficient ray intersection tests. An irradiance caching strategy uses the gradient of irradiance [WH92] in order to improve the simulation speed of diffuse inter-reflections. RADIANCE has mainly been used for the illumination of architectural designs but is very flexible and we found it can also be harnessed for the illumination of clothes.

5.4.1 Natural Illumination

In [Deb98] Debevec proposed to use RADIANCE with high dynamic range (HDR) panoramic photographs as light sources for global illumination in order seamlessly to insert virtual objects into real scenes. He coined this technique "Natural Illumination". In Debevec's approach the panoramic HDR images are composed of photographs of a chrome ball taken from the same view with different exposure settings[4]. We employ this technique and exploit the panorama transformation and HDR composition features of HDRShop [TD01] to create a so-called light-probe of a target environment in which we want to insert a virtual garment. A light-probe contains the radiance measurements of the scene at a certain point. The light-probe should thus be taken with the chrome ball located near the position at which the virtual garment is going to be inserted in a photograph of the target environment. An example light-probe of our designer's office is depicted in Figure 5.6.

5.4.2 Global Illumination of Virtual Garments

After the real-time garment simulation has converged to a stable state we convert the 3D mesh and reflectance data to a format that can be read by RADIANCE. The appropriate HDR

[4]Different exposures can be generated by varying the shutter speed on the camera. The camera's white balancing mode has to be set constant and not automatic. To ensure alignment of the different exposures the individual images should be taken with a remotely controlled camera that is fixed on a tripod.

Figure 5.6: A HDR light probe of a target location shown at increasing f-stops from left to right. We use this light-probe for natural illumination of virtual garments.

panoramic image or light-probe is loaded into RADIANCE for lighting and an image can be rendered with the camera parameters of the real-time visualisation. In order to render with indirect illumination, such as a light-probe, the number of diffuse inter-reflections of a ray (also called ambient bounces in RADIANCE) simulated has to be greater than zero. We were interested in generating images of clothing with increasing numbers of inter-reflections in order to assess the image quality, under the assumption that the number of simulated inter-reflections would improve the image quality as indicated by McNamaran et al [MCTG00]. More details on our evaluation of image quality and the compositing of images of virtual garments into a photograph are given in Appendix A and in Chapter 7. However, we encountered a problem with the global illumination simulation of diffuse inter-reflections on curved surfaces.

5.4.3 Diffuse Inter-reflections on Curved Surfaces

Diffuse inter-reflections are evaluated by sampling over the whole hemisphere of each surface patch in a scene. For this, both Radiosity and Monte Carlo path tracing rely on the fact that the surfaces are flat. Surfaces that are smoothed by interpolating the normals of the surface vertices generate rendering artefacts when diffuse inter-reflections are simulated in RADIANCE. The problem is illustrated in Figure 5.7[5]. Some of the sample rays of the hemisphere start under the surface and cause problems. To remedy this problem, in general curved surfaces are subdivided into smaller triangles to create a smoother appearance and the resulting triangles are not smoothed by interpolating normals. Subdivision to the required degree, however, often creates large numbers of very small triangles that require a lot of storage space and rendering time. It was beyond the scope of this thesis to try and find a better solution to this problem. The implications of this problem for our augmented reality design scenario will be discussed in more

[5]Thanks to Greg Ward, main author of the RADIANCE rendering system, for explaining these rendering artefacts.

detail in Chapter 7.

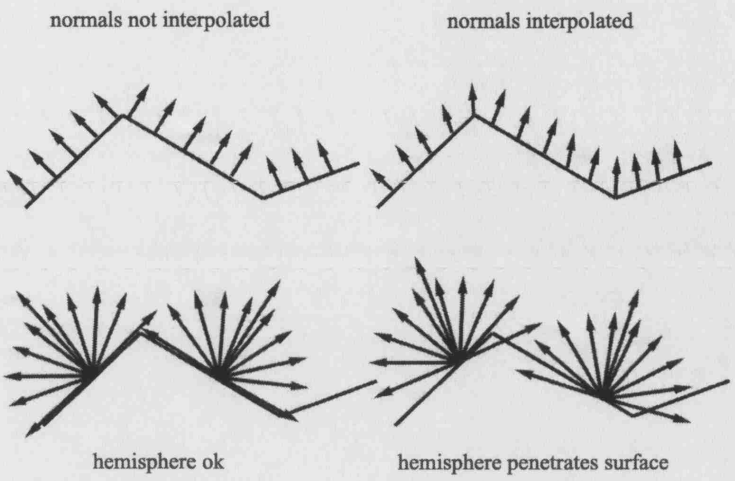

Figure 5.7: Diffuse inter-reflections sample the hemisphere of solid angles above a surface and therefore create rendering artefacts with interpolated normals. On the bottom right, this is illustrated. Sample rays of the hemisphere start below the surface because of the interpolated normal.

5.5 Visualisation on an Internet Interface

In this section, we describe the web interface for Virtual Clothing which was also outlined in [SVB03]. The dynamics and visualisation for real-time garment simulation was integrated into an ActiveX control by using the Active Template Library (ATL) and the Interface Description Language (IDL) [RS99] in combination with C++ and OpenInventor [Wer93]. ActiveX was chosen because it can easily be embedded into HTML Internet pages and controlled via JavaScript, while, at the same time, it gives access to the full processing and graphics acceleration power of the system's hardware. Cordier et al [CSMT03] have also built a garment simulation system based on ActiveX technology. Chittaro et al [CC03] reported a system for Virtual Clothing in Java that extended a standard VRML browser. Protopsaltou et al [PLAMT02] have built a system based on Shout3D [Pol01] technology which is also based on Java. While Java based technology may be platform independent it does not allow us to access the full hardware resources and therefore may be slow. Our ActiveX garment visualisation control is divided into four main processes: Uniform Resource Locator (URL) loader, interface, visualisation and dynamic simulation. Dynamic simulation consists of three parts, the meshing, the numerical simulation (i.e. integration of Newton's law of motion) and collision detection and response.

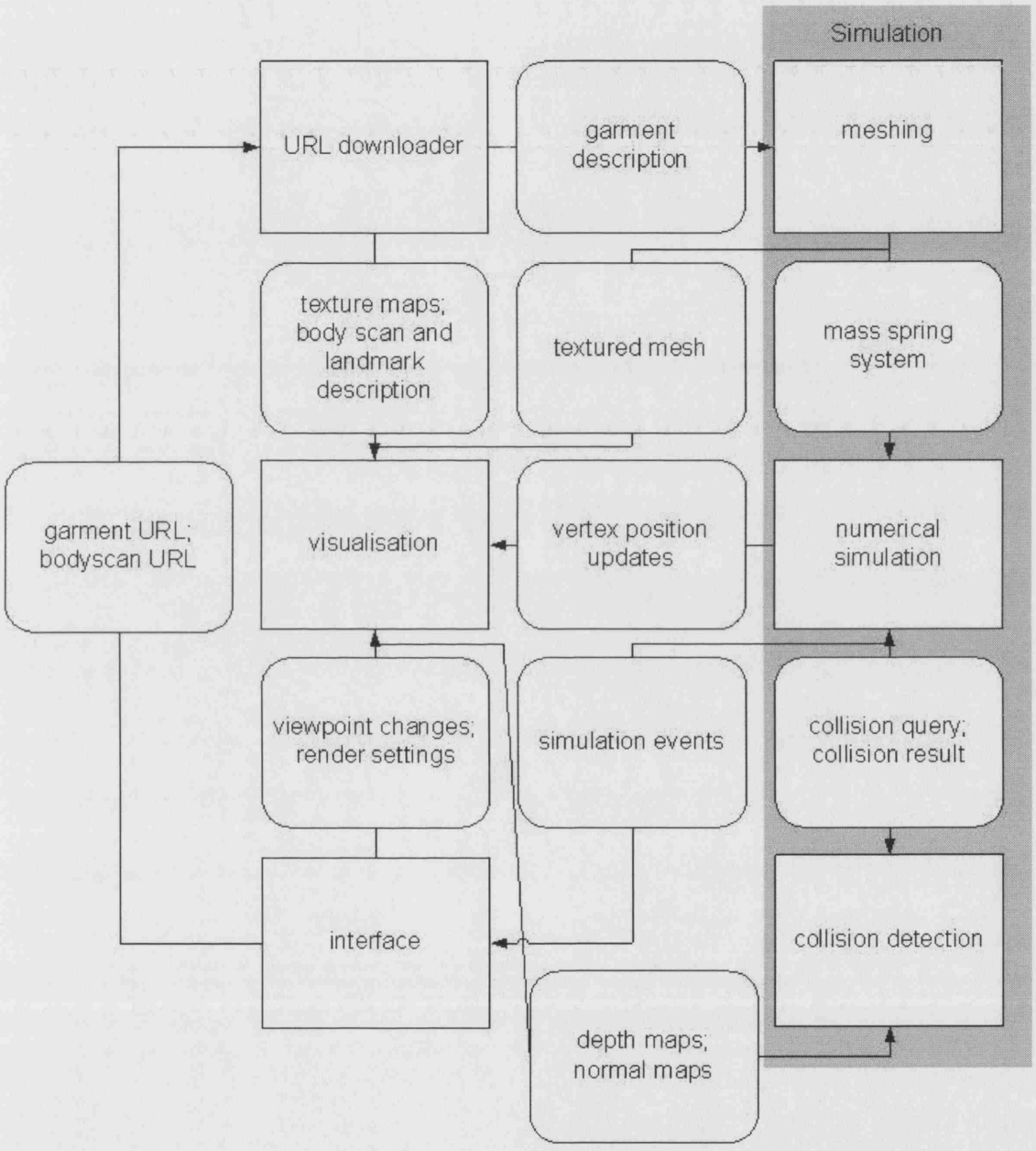

Figure 5.8: Data flow between the internal processes of the ActiveX Internet control for garment visualisation.

5.5.1 Data Flow

A flow chart of the processes and the data in the control is given in Figure 5.8. Data is represented by boxes with round corners while processes are shown as boxes with sharp corners. The control communicates with an HTML page via JavaScript and via direct mouse events to change the camera's view parameters. An example flow for loading and dressing a customer could be as follows: A URL to the customer's body-scan is set via JavaScript, the URL loader retrieves the body-scan data from a web server or a remote database and, after local caching, sends it to the visualiser. The visualiser creates depth and normal maps in an off-screen rendering buffer for body-garment collision detection. If the customer chooses a garment via a web link the corresponding URL is sent to the control. The URL loader reads the garment description again from a remote database and, after caching, sends it to the meshing process. Meshing generates a mass spring system for the numerical simulation and a mesh with texture coordinates for the visualiser. Meanwhile, the URL loader retrieves the required textures from the URLs provided in the garment description. The control would then send a JavaScipt event to the HTML page to notify that it is ready for garment simulation. Usually, a JavaScript event would then be sent back from the HTML page to start the simulation. The numerical simulator integrates mass spring forces, queries for and responds to collisions and updates the visualisation mesh to animate the garment. Once finished, the numerical simulation would send an event to give notice that the control is ready for new actions. One possible action would be to tell the control to convert and save the garment representation to a form suitable for global illumination in RADIANCE.

5.5.2 Exploitation of Parallel Processor Architecture

Since the computations for the simulation mainly involve vector operations, we achieved performance increases by exploiting some of the latest processor architectures which implement parallel data manipulation. Without specifically optimising the code for parallel computation but simply by changing compiler settings to exploit single instruction multiple data (SIMD) and parallel execution a simulation speed-up of 20% could be achieved. For example if the process of seaming a garment took 3 seconds with the original executable it is carried out in 2.4 seconds with the executable that harnesses parallel processor architecture on a 3Ghz Pentium IV.

5.5.3 File Caching

Even though body representation and garment description do not require very much storage space if compressed well, having to download such files again if they have already previously been viewed may be tedious. We address this issue by exploiting the file caching mechanisms of

the Internet Explorer API. Before a file is viewed in the control it is downloaded and stored in the allocated caching space of cached Internet files. The API takes care of consistency checks. Files on the server database that are newer are updated in the cache when viewed. File streaming, to visualise the geometry as a progressive mesh while it is downloaded from the database, is not supported and we did not plan to integrate it. In order to show the user that the download is in progress, a progress status is shown.

5.5.4 Installation and Versioning over the Internet

ActiveX controls are installed automatically when a customer visits a web page with the control embedded in HTML[6]. A software certificate is used to authenticate the control. The user can decide whether to install the control or not. ActiveX has built in mechanisms automatically to update a control if the version identifier of the plug-in on the web server is higher than that of the client machine.

5.5.5 User Interface

User interaction with the 3D graphics is restricted to zoom towards and away from the body, rotation around the body and movement up, down, left or right from the current position. This type of interaction is commonly used in 3D graphics applications.

5.6 Summary

In this chapter we described the methods we used for the visualisation of garments. We started with a description of representations suitable for real-time rendering. For several reasons we chose to use the IndexedFaceSet representation. We discussed different modes of real-time visualisation to gather assembly information and for debugging of virtual garments. Different combinations of wire-frame and polygon rendering modes proved to be useful for such purposes. Visualisation of fit feedback by mapping simulation data as colour values onto the surface was then discussed. We found the mapping of relative spring elongations most useful in order, for example, to visualise how tightly a garment fits. Integration of the garment simulation with a global illumination system that allows us to generate images with different quality settings for evaluation was then discussed. A general problem of simulating diffuse inter-reflections on surfaces, with interpolated normals for smoothing, was encountered and then discussed. Finally, in the last section of this chapter we described an Internet interface for our garment simulation that was used in the retail application detailed in Chapter 7.

[6]Installation can only take place if the security settings of the Web Browser are chosen appropriately, and the user has sufficient permissions on the operating system in order to install the plug-in.

Chapter 6

Body Modelling

In this chapter we describe methods we developed in the context of human body modelling. They do not directly support the main hypothesis but appear to be useful for future developments to improve the virtual try-on system. The chapter is separated into two sections. In the first section we describe a technique that allows us to simulate volume preserving body deformations. This is used for the simulation of interactions between soft tissue and a tight fitting garment.

In the second section we present an automatic approach to create a skeleton from body landmark data and we show how to employ such a skeleton for the animation of a body-scan without manual intervention. An animated body-scan can be loaded into the virtual try-on system to carry out movements after it has been dressed.

6.1 Real-Time Volume Preservation

In this section we present a MSPS for real-time simulation of volume preserving deformable solids [VS02]. A new type of spring that shows collective behaviour was developed called a "support spring". These springs model the "matter" inside an object and help preserve its volume without the need for explicit volume computations during the simulation as done in conventional methods. Comparison of the volume during simulation with the initial volume of the deformable solid demonstrates the accuracy of our approach. Experiments on models of different geometry show the low computational complexity, which is linear in the number of triangles of the deformable solid. Interactions between supportive clothing and a deformable, female upper torso are shown in a simulation at the end of this section.

6.1.1 Background

Methods for volume preservation have been investigated in the fields of geometric modelling [AB97, HML99, lLK84, RSB95, SP86], virtual reality surgery simulations [CHP89,

CZ92, DDBC99, PBP96] and the entertainment industries [AT00, NT98]. Geometric constraints are applied to free form deformations (FFD) as described in [SP86] to make constant volume deformation of objects possible. Rappoport et al [RSB95] applied an iterative Lagrange multiplier method, which they called Uzawa based volume preservation, to constrain deformations so as to preserve the volume of an object modified by FFDs. Aubert and Bechmann [AB97] use a similar approach to that of [RSB95]. Aubert and Bechmann's technique is more flexible because they use an independent deformation function. They compute the exact volume of the triangular surface in a similar way to that proposed in [lLK84]. To permit the handling of curved surface solids, Hirota et al [HML99], who employ FFDs, use a multi-level of detail approach. Chadwick et al [CHP89] applied FFDs to change the appearance of muscles and fatty tissue by changing the FFD control points according to a multi-layered character skeleton. They used Hookean springs automatically to simulate stretch and squash of muscles and tissue, although they did not try to preserve the volume. Chen and Zeltzer [CZ92] implement a FEM to create a complete biomechanical model of muscle action for cartoon character animation. Their approach is very accurate but, because of the computational complexity, it is very slow. Promayon et al [PBP96] approximate surfaces of volumes by mass-points linked to their neighbours. Volume preservation is achieved by constraining the model to its volume calculated using an approach similar to [lLK84]. Nedel and Thalmann [NT98] described a MSPS for modelling real-time muscle deformation. They presented the muscle shape as a surface based model. They fitted the surface to boundaries acquired from medical image data. In order to control the muscle volume during deformation a new type of spring was introduced, which they called "angular springs". The muscle deforms under the impact of external forces, but only if they are applied to a pre-defined line called the "action line", which represents the direction of the forces produced by the muscle on the skeleton segments. Aubel and Thalmann [AT00] extend the work by Nedel and Thalmann [NT98] by introducing a multi-layer model similar to that of Chadwick et al [CHP89]. In the work of Nedel and Thalmann, "action lines" are defined in a more general form by using poly-lines. The main objective of our work was to develop a real-time MSPS for simulating volume preserving deformable objects. A MSPS was chosen because of its simplicity and low computational complexity. We introduce a new type of spring we called a "support spring". Support springs model the "matter" inside an object and approximately preserve its volume.

6.1.2 Support Springs with Explicit Volume Computation

The main feature of the traditional MSPS is that it consists of individual springs, i.e. the response of each spring depends only on its own elongation and not on the elongation of other springs. The idea of this work was to create an ensemble of springs, where the response of each member depends on the state of the whole team. In particular, the algorithm generates a response that will approximately preserve the volume of a deformable solid object.

Let B be a body, the surface of which is triangulated. If all the vertices are connected to the body-centre, then its volume can be computed as the sum of all tetrahedron volumes

$$V = \frac{1}{3}\sum_{i=1}^{ntr} S_i h_i = \frac{1}{3}\sum_{i=1}^{ntr} S_i l_{ik} cos\alpha_i = \frac{1}{6}\sum_{i=1}^{ntr} \mathbf{l}_{ik} \cdot ((\mathbf{p}_{i1} - \mathbf{p}_{i2}) \times (\mathbf{p}_{i1} - \mathbf{p}_{i3})), \qquad (6.1)$$

where: ntr is the number of triangles, S_i is the area of the i th triangle, h_i is the height of the i th tetrahedron, $\mathbf{l}_{ik}$ with $k \in \{1, 2, 3\}$ the vector between the surface vertex and the body-centre[1] with l_{ik} denoting its length, a_i is the angle between the edge k and h_i and $\mathbf{p}_{i1}$, $\mathbf{p}_{i2}$, $\mathbf{p}_{i3}$ are the vertices of the i th triangle. The deformable volume preserving body is constructed as follows. All surface vertices are connected to each other with regular springs. These springs model the elastic membrane of the body and keep the triangulated surface approximately constant. In addition, each vertex is connected with the body-centre by a spring. We call the collection of these springs "support springs". They model the "matter" inside the body. Let l_i^0 denote the natural length of the i th support spring, l_i^t the length of the same spring at time t, and S^t and V^t denote the body surface area and volume at time t respectively, then the following lengths are defined:

$$\Delta l_{tot}^t = (V^t - V^0)/S^t, \quad \Delta l_i^t = l_i^t - l_i^0 \ . \qquad (6.2)$$

The force acting on the surface vertex i at time t due to the i th support spring is computed as

$$\mathbf{f}_i^t = -K(\Delta l_{tot}^t + C\Delta l_i^t)\mathbf{u}_i, \qquad (6.3)$$

where K is the stiffness of the springs, $\mathbf{u}_i = (\mathbf{p}_i - \mathbf{c})/l_i$ is a unit vector with $\mathbf{p}_i$ the i th vertex position of the body, $\mathbf{c}$ denotes the body-centre, and C is a coefficient in [0, 1], which can be varied. As evident from Equation 6.3, the response of a support spring is the result of two different behaviours. The first term in Equation 6.3 is the collective reaction, i.e. each spring opposes any change in volume, trying to preserve a constant volume. The second term in Equation 6.3 gives the individual behaviour of the spring. The coefficient C controls the balance between the collective and individual behaviours. It can be varied, depending on the

[1] We assume that the edge lengths of the tetrahedron that connect the body centre are similar.

type of simulation. The closer C is to one, the stiffer the object, which requires larger forces to deform it.

6.1.3 Support Springs with Implicit Volume Computation

The above-described approach has two major drawbacks. Firstly, it is computationally expensive for objects with a large number of faces. According to Equation 6.1, for each triangle, one vector product and one scalar product have to be computed. Secondly, our tests show that the volume preservation accuracy and the simulation quality depend very much on the spring stiffness K in Equation 6.3. In order to achieve visually pleasing results, this coefficient has to be in a very narrow interval, which unfortunately depends on the magnitude of the applied forces. Otherwise, the volume preservation degrades and for some values of K the simulation may even become unstable . In order to overcome such problems we derived an approximation of Equation 6.1. Let S_{AV} be the average triangle area. By dividing the two sides of Equation 6.1 by S_{AV} and by rearranging the sum on all support springs (tetrahedron edges) instead of all triangles we obtain:

$$V/S_{AV} = \frac{1}{3}\sum_{i=1}^{ntr} S_i/S_{AV}\cos\alpha_i l_{ik} = \frac{1}{3}\sum_{i=1}^{ns} l_i \sum_{j=1}^{ni} S_j/S_{AV}\cos\alpha_j, \tag{6.4}$$

where ns denotes the number of "support springs". The sum $\sum_{j=1}^{ni} S_j/S_{AV}\cos\alpha_j$ indicates that the i th support spring participates in the volume calculation of ni tetrahedrons. There is freedom in selecting one of the three edges for each tetrahedron, but we should make sure that each edge is used at least once, i.e. $n_i > 0$ for all $i = 1,..,ns$, and therefore each support spring contributes to the volume approximation. If we omit the cosines and substitute $c_i = \sum_{j=1}^{ni} S_j/S_{AV}$ we derive the following equations

$$l^t_{tot} = \tfrac{1}{3}\sum_{i=1}^{ns} c_i l^t_i, \quad \Delta l^t_{tot} = l^t_{tot} - l^0_{tot}. \tag{6.5}$$

We consider that the coefficients c_i do not change significantly over time and can be regarded as constants. Only the length of each support spring has to be computed at each time step during simulation. The technique tries to preserve the value l^t_{tot} constant, which is the weighted total length of all support springs. The force acting on the surface vertex i at time t exerted by the i th support spring is thus computed as

$$\mathbf{f}^t_i = -K(c_i\Delta l^t_{tot} + C\Delta l^t_i)\mathbf{u}_i. \tag{6.6}$$

According to Equation 6.6 the reaction force does not depend only on the changes of spring lengths but also on the coefficient c_i. This reflects the difference in the triangles' face areas.

6.1.4 Volume preservation test

The method of support springs with implicit volume computation makes two approximations, so the following volume preservation tests were performed on a deformable ellipsoid and sphere. Forces were applied on the top and bottom areas of the object. The external and internal forces reached their equilibrium and then the forces were released and the solid restored to its original state.

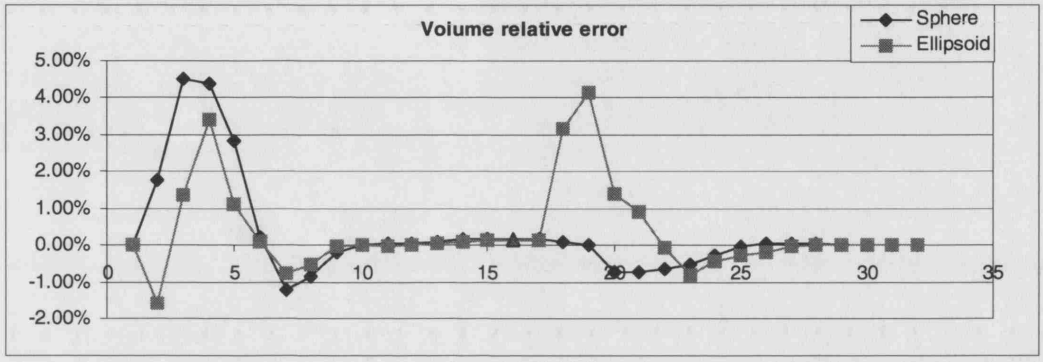

Figure 6.1: Results from the volume preservation test.

The results are shown in Figure 6.1. The relative error $e^t = (V^t - V^0)/V^0$ was computed for 32 evenly distributed time points. The first 16 of them were during the deformation due to the external forces. The simulation reached its equilibrium state at point 16 (marked with a triangle) and then the external forces were removed. The highest errors were measured for the first few points after applying the external forces and the first few points after removing them. A logical explanation for this is that at those stages the speed of deformation is too high and the model cannot completely "catch up" with the fast changes.

6.1.5 Results

The algorithms were implemented on a Pentium III PC, 700 MHz, 128 MB, using Open Inventor for rendering the images. Figure 6.2 shows two examples of a deformed ellipsoid and a hemisphere pressed against a table. The left image was generated for a tessellated sphere, scaled in the direction of the Y-axis, with 578 vertices and 1152 triangles. The entire simulation, including deforming to the equilibrium and then restoring the original shape, took 3.85 seconds, which required the generation of 180 frames. This means that the simulation ran at a speed of 46 frames per second.

The method for volume preserving deformation was implemented in our virtual try-on system in order to simulate deformable human body parts. In order to enhance the realism of the tight clothing such as underwear and swim suits, simulation of body parts such as the breast

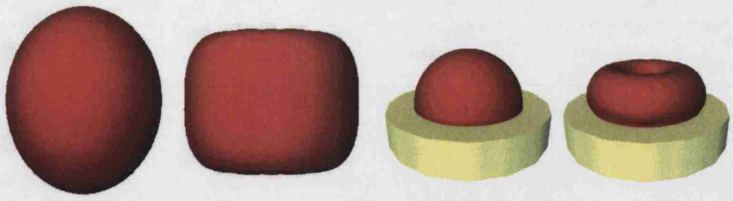

Figure 6.2: Left: Deformed ellipsoid; Right: Hemisphere on a table.

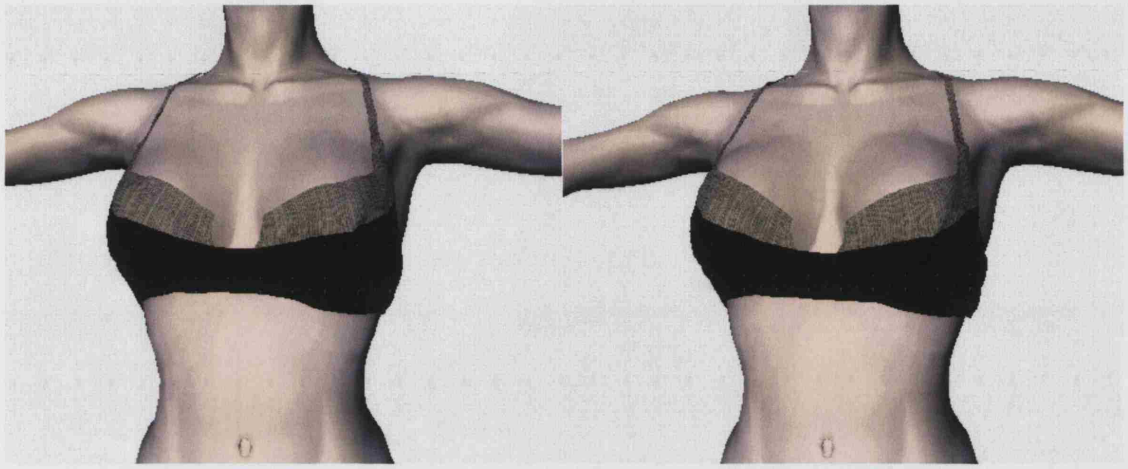

Figure 6.3: Brassiere on a virtual body; Left: No deformation; Right: Breast deformation.

and belly can be defined to deform during simulation under the forces of cloth that touches them. Figure 6.3 shows an example of dressing a virtual female body with a brassiere.

In order to test the efficiency of the algorithm, we measured its speed for different numbers of triangles on the sphere. Results are given in Table 6.1. The times were measured using the profiling feature of Microsoft Visual C++ 6 and they are total times for computing the forces, integration of equations and rendering the image. As shown in the table the simulation still runs in real-time for as many as 6728 triangles.

Number of triangles	time for 100 frames	time per frame (ms)	frames per second
1152	2.13	21.30	46.9
2592	3.30	33.03	30.2
4608	4.99	49.94	20.0
6728	6.68	66.81	14.9

Table 6.1: Performance of the MSPS approach for volume preservation.

6.2 Automatic Animation of Body-Scans

In this section, we describe a system automatically to apply motion capture data to animate a human body-scan [OZSB03]. Preparing body-scans manually for animation is a time consuming task, which may require weeks, if not months, of labour of skilled animators and creative artists. In our method, the surface of the body-scan is mapped automatically to a skeleton. We show how automatic surface landmarks can be used to find an approximate skeleton, which we build from surface landmark data and landmark proximity spheres. We adopt a surface growing technique that does not select other unrelated parts of the model in order to map skeleton segments to the body surface. The mapping is automatically weighted by a blending function in order smoothly to deform the surface if the skeleton is animated. Motion capture data is used to drive the skeleton animation. We have applied our method to a variety of human models, ranging from male and female adults to models of children. This would have been hard to achieve if the techniques required manual intervention at any stage. Our main contribution is the use of automatically or even manually extracted surface landmarks to create a skeleton and to automatically map the body-scan surface to the skeleton for animation.

Next, we briefly review related work on human animation. Following that, we introduce our layered human model and we describe how we build the skeleton. Then we present a novel surface mapping technique. Following that, we briefly describe how we apply motion capture data to the skeleton and we show how we achieve smooth deformations by applying a vertex blending technique. Finally, we show snapshots of different animation sequences on different body scans and we discuss the performance of our technique. Animation sequences were exported from the system to be used in the virtual try-on system.

6.2.1 Background

Animation of realistic 3D human models, typically involves three main tasks: a) modelling of the character: skeleton creation, skin and muscle representation; b) deformation: rigid deformation of the skeleton, soft deformation of the skin and possibly muscles; c) motion control: motion capture, key-frame interpolation, behaviour interpolation, control point guidance, and animation parameters or scripts. Several human animation systems have followed a layered approach to represent skeleton, muscle, skin and control [CHP89, KMTM$^+$98]. For deformation of muscles, and skin, techniques derived from free-form deformations (FFD) methods have been used. Thalmann et al [ST95, TSC96]] tried to personalise avatars with a few thousand polygons by using meta-balls and by scaling the model with five or six parameters. For higher fidelity it would seem natural to use scanned body models. Nebel [Neb00] constructs volumet-

ric meshes of soft tissue above the muscle from photo realistic surface scans. They replicated the surface skin mesh three times to form epidermis, dermis and subcutaneous tissue. They used a finite element method (FEM) to model the different physical properties of the layers, and external forces were applied to simulate skin deformation. Chen et al [CZ92] also used an FEM to model muscle deformation. Scheepers et al [SPCM97] went one step further and modelled anatomy based muscles that deform the skin. Mapping the skin vertices to the underlying skeleton, often relies on a skilled animator [Lan97]. The task of surface mapping can also be quite cumbersome for animators, owing to the global nature of separation planes, as described in section 6.2.4. Sloan et al [SIC00] combine shape blending with simple transform blending for soft deformation of the animated surface. In their system, muscles can contract via target shape position interpolation and at the same time move with the skeleton.

6.2.2 Layered Human Model

The body-scans we use are represented by a triangular mesh. They were constructed from a point cloud, which was obtained from a Hamamatsu Body Line Scanner [Hor95]. The surface was created from the point cloud by a surface reconstruction technique described by Dekker et al in [DKW+98] and simplified by a technique described by Oliveira and Buxton in [OB01]. We use fully automatic techniques to segment the body-scan and to locate key landmarks as described in Section 4.4.2.1. Subjects are typically scanned in a pose that is close to the initial pose of the skeleton defined in the motion capture data. Each skeleton segment is described by a local reference system used to define its local position and orientation. We selected surface landmarks close to the joint locations of the skeleton that we use for animation as shown in Figure 6.4. The skeleton hierarchy matches that of the motion capture data we used for animation. The following subsections describe how we build the skeleton .

6.2.3 Building the Skeleton

We use the surface landmarks, together with proximity spheres (see Figure 6.4) to find the animation skeleton. A few of the surface landmarks can be used to compute the skeleton joint landmarks geometrically. For example the mid-point between armpit and shoulder-point can be used as the shoulder joint. Hip joints are found by moving the surface hip points inward along the line between left and right hip point, and they are levelled with the crotch point. Other joints e.g.: elbow, knee, ankle etc. can be found by averaging the positions of all vertices within a proximity sphere of the corresponding surface landmark as depicted on the left of Figure 6.4. At the moment the radius of the proximity spheres is chosen fixed for each of the relevant landmarks, which works fine for the body-scans we tested, including some scans of

children. Should the method fail (for example if the proximity sphere was too small or too large to capture an appropriate number of nearby vertices to find a good joint position) the radius of the proximity spheres could be set as a percentage of the distance between relevant landmarks. The resulting joint positions may not be anatomically correct but proved to be sufficient for our animations. Another method to find the joint positions that uses an approximate medial axis (AMA) was described in [OZSB03] by Oliveira et al[2]. In [OZSB03] we defined the AMA as the centroids of horizontal slices of the originally segmented body-scan (head, torso, arms, legs)[3]. Joint landmarks were then identified as the closest point on the AMA to the relevant surface landmark. The method finds the exact centre position for joints with a few hundred proximity tests but requires that the body-scan is available in a segmented and sliced form at some stage of the processing. If not optimised for speed, the approach which uses proximity spheres to reconstruct the skeleton, requires far more proximity tests (the number of vertices times the number of proximity spheres) but does not require a segmented and sliced representation of the body-scan. However, all proximity sphere tests are carried out during pre-processing and they are performed in a fraction of a second on the equipment specified in the results section.

The three body-scans on the right in Figure 6.4, show the skeleton generated automatically, based on key landmarks and proximity spheres.

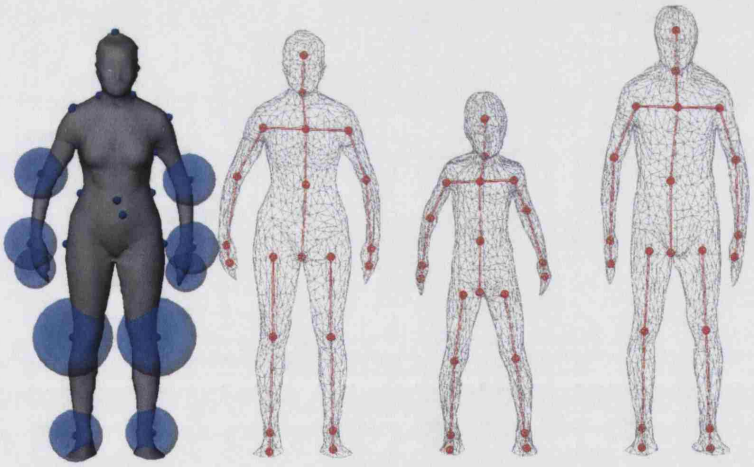

Figure 6.4: From left to right: Surface landmarks and proximity spheres; Extracted skeleton; Two additional body-scans with extracted skeleton which illustrate the method is generic.

[2]It was João Fradinho Oliveira's original idea to use an approximate medial axis to reconstruct the skeleton for the automatic animation of a body-scan.

[3]The point cloud from the Hamamatsu system at UCL is segmented in six body-parts and the parts are sliced horizontally with a constant number of points per slice.

6.2.4 Mapping

Following the building of the skeleton, we divide the surface mesh into segments based on the skeleton, and then map the vertices of the surface segments to their corresponding skeleton segments. In this process, each surface vertex (of the decimated model) is labelled as belonging to a particular segment. This is done by using bi-sector planes that are perpendicular to the plane formed by pairs of skeleton segments. Each vertex position is tested as to whether it is in front or behind a bi-sector plane as shown in Figure 6.5. This is done in a surface growing procedure. We start with a seed vertex at the tip of the left hand. All vertices connected to the tip of the hand, that do not cross the wrist bi-sector plane belong to the hand. A similar procedure is then applied to the lower left arm, etc., until every vertex in the scan is assigned to a region. Two additional planes are created perpendicular to the shoulder bone (Figure 6.5), approximately 3/5 of the distance from the chest joint to the shoulder joint in order to allow for complicated motions in the shoulder region. The separation planes at the shoulders are adjusted to make sure that no vertex that is part of the torso is registered as an arm vertex. This is achieved by using the armpit landmark to orient the plane appropriately as shown by the white landmarks on the left of Figure 6.5.

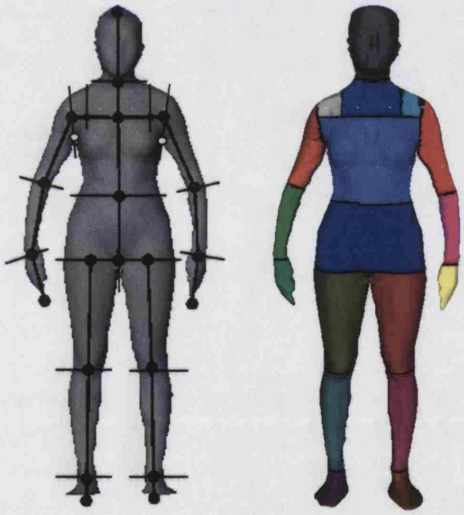

Figure 6.5: Left: Surface separation planes; Right: Grown surface regions.

Typically, an animator would be required to carefully select the individual vertices by tweaking the parameters of bounding volumes or separating planes and it may be required to create additional constraining planes, which may be difficult to control. Our method is automatic and avoids such problems. The mapping between the surface and skeleton sets joint and bone proximity parameters for each vertex that will be used in the blending deformation process described in the next section.

6.2.5 Vertex Blending

In order to ensure that the body surface deforms smoothly and not abruptly near the skeleton joints we apply a vertex blending technique. Vertex blending is available in recent graphics hardware [Die01] and therefore can be performed very efficiently. The idea of vertex blending is quite simple. Instead of applying a single matrix transformation to a surface vertex near a joint, in order to make it move with the skeleton, the vertex is transformed by a linear interpolation of the two transformation matrices of the two nearest skeleton segments. For each vertex the transformation matrices are weighted by a factor w between 0 and 1 which determines the influence of the matrices on the vertex. Vertices belonging only to one skeleton segment are transformed along with that segment and have $w = 1$ for the transformation matrix of the skeleton segment. The new vertex position $\mathbf{x}$ of a vertex near a skeleton joint is calculated as

$$\mathbf{x} = \mathbf{T}_0\mathbf{x}_0 w + \mathbf{T}_1\mathbf{x}_0(1-w), \tag{6.7}$$

where $\mathbf{T}_0$ and $\mathbf{T}_1$ denote the matrices of the skeleton segments and $\mathbf{x}_0$ is the original vertex position. The vertex normal is calculated in the same way. We use the distance from the vertex to the skeleton segments of the nearest joint to compute w for each vertex. Vertices which have a distance greater than a predefined threshold are assigned $w = 1$ in order to be influenced only by the transformation matrix of one skeleton segment.

6.2.6 Motion Capture Data

We apply motion capture data described in the BioVision Hierarchy (BVH) format [Bio01]. The format is split into two blocks, the description of the skeleton, and the positions and angles of each animation frame. In the skeleton part, the hierarchy and an initial pose of the skeleton is defined. The second block describes a sequence of animation frames. Typically, each frame is described by a translation of the whole skeleton and a sequence of Euler angles to rotate the individual skeleton joints. The sequence of parameters is applied to each of our skeleton segment's transformation matrices. We adjust the local matrices in the beginning to reflect the initial pose of the motion capture data and then refresh the angle deformation to produce the different animation frames. Angular interpolation is applied if the motion capture data available is not smooth enough.

6.2.7 Results

Our method was tested on a PC with a 650 MHz Pentium III CPU, 128MB of RAM and a GeForce2 graphics card. Visualisation was carried out with OpenInventor[Wer93]. We applied

different motion sequences[4] to a body scan with 2531 vertices and 5000 triangles. We could achieve about 100 frames per second. Figure 6.6 shows some snapshots of such animations. Figure 6.7 shows results that we generated in a couple of seconds without manual intervention when we applied our method to a variety of body scans. To apply motion sequences to a variety of body scans in traditional animation systems would require a lot of manual editing by skilled animators. However, we have noticed that the skin deformation does not always give realistic results as can be seen in the hip area of the second scan from the left in Figure 6.6. This could probably be improved by using more specific mapping functions for the different joints that can represent the skeleton-skin interaction in a more realistic way.

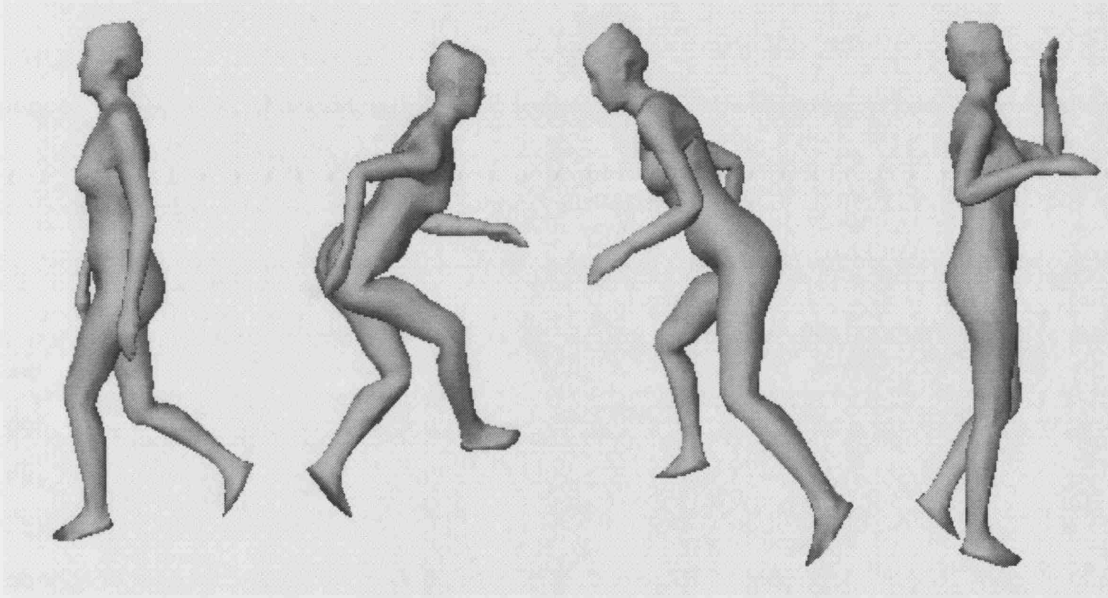

Figure 6.6: Several motions applied to a model (walking, sneaking, running and drinking).

The automatic animation system was not directly integrated into the virtual try-on system because collaborators not related to the sponsoring company were involved in the development. However, we developed an export function that enables us to save the vertex position changes of an animation sequence created by this system. Such an animated character file can be loaded into the virtual try-on system to simulate a garment on an animated body. An example of an animated body-scan dressed in a pair of trousers and a shirt is illustrated in Figure 6.8.

6.3 Summary

In this chapter we described two techniques in the field of body modelling and animation. They do not directly support our main hypothesis but the development of the techniques may be

[4]Motion sequences from the Poser 4 contents CD were used.

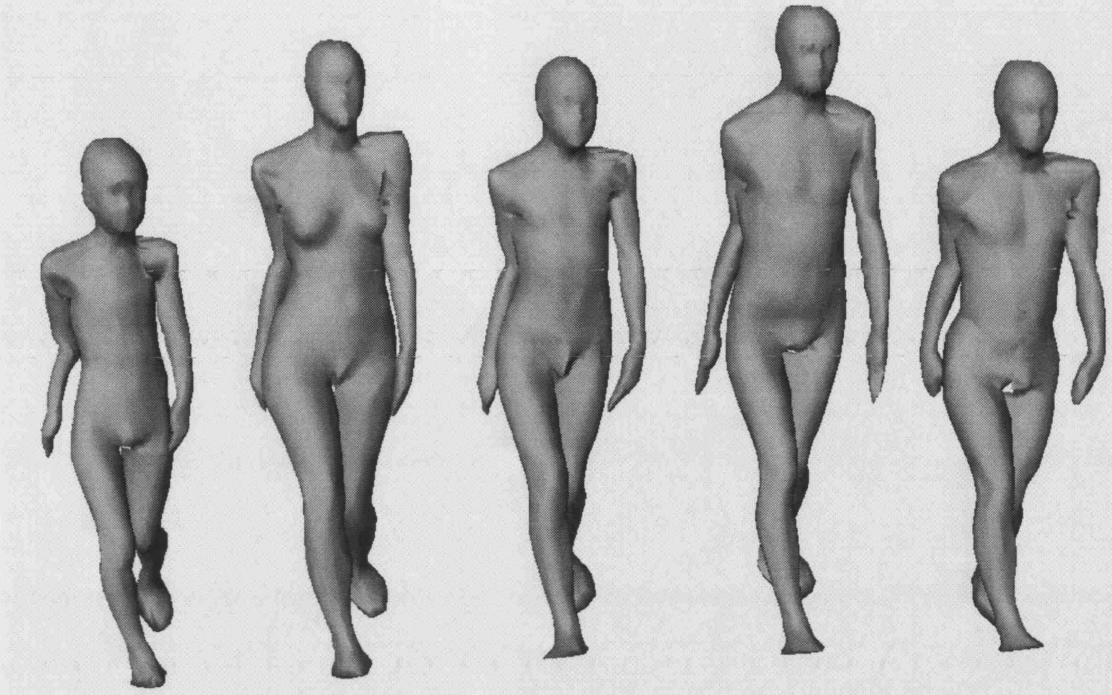

Figure 6.7: The same motion data applied to different models.

useful for future improvements of a virtual try-on system. In order to approximate volume preservation of bodies in real-time we developed techniques that use a MSPS specialised for this purpose. The techniques are applicable for objects represented by triangulated surfaces. They use so-called "support springs", which act as an ensemble with their response depending on the change in the object's volume as well as on each individual spring. Two methods were implemented. The first is based on explicit volume computations. Its volume preservation properties are better than those of the second method, but it is computationally expensive and is not always stable for real-life problems. The second method assumes some approximations and in fact preserves the weighted total length of the support springs. As a result it is faster and more robust. The technique has a very good speed and it runs at near real-time for objects with as many as 7000 triangles. We assume that the technique will not work well for non-convex bodies owing to the way the "support springs" which model the body's internal matter are constructed. A more general approach may be useful, but for our purposes (such as simulation of the influence of a bra on a female breast) the developed techniques proved to be sufficient.

Our second technique allows us automatically to create a skeleton for a body-scan to smoothly deform the body-scan surface when the skeleton is animated. The skeleton is built automatically from body landmark data. The system, however, is sufficiently flexible also to cope with manually selected landmarks. Our surface to skeleton mapping technique has proven

Figure 6.8: Snap-shots from an automatic animation of a body-scan dressed in trousers and shirt.

to be very robust. The vertex blending method we used can generate smooth deformation and is very efficient. However, in some cases vertex blending may generate undesired artefacts. If we can improve the weighting function of the vertices by considering the influence of mapped muscle deformation, the results will probably be more realistic. A variety of body-scans have been automatically animated with our system and we can animate dressed body-scans in our virtual try-on system. In other approaches, such animations would require large amounts of manual editing by skilled animators. It would be interesting to combine the volume preservation technique with the animation system to simulate more realistic muscle deformations. In combination with image based rendering, impostors of automatically animated body scans could be used to populated virtual cities similar to Tecchia et al [TLC02] or more generally to create virtual crowds of avatars with many different body shapes dressed in different clothing.

Chapter 7

Evaluation

In this chapter, we describe tests we carried out in order to evaluate our system. The chapter consists of three main parts. First we evaluate the performance of our cloth model by comparing it to traditional methods and by benchmarking simulations with different settings. Following that we describe an installation of our system at Selfridges, a well known department store in London. This installation demonstrates the commercial potential of virtual clothing as well as showing the robustness and flexibility of the methods developed. Finally at the end of this chapter we describe the results of a collaboration with a fashion designer in which the virtual clothing system was used in an augmented-reality context.

7.1 Cloth Model

In this section, we describe the tests we carried out in order to evaluate our cloth model described in Chapter 3. The initial algorithms of our cloth model were tested on an SGI O2 workstation (R12000 processor) and on a Desktop PC (Pentium III, 1 GHz, 1GB, NVIDIA Geforce2 graphics accelerator) and on a Laptop (1.3 Ghz, Pentium III, 256 MB, NVIDIA Geforce2Go graphics accelerator). Directional Velocity Modification (DVM) was compared to a traditional mass spring particle system (MSPS) and various tests were performed on the image based collision detection (IBCD).

7.1.1 Directional Velocity Modification

The directional velocity modification (DVM) described in Section 3.1 was tested by comparing the visual results of the simulation to those of the traditional MSPS. Figure 7.1 shows the results of a tablecloth draped over a moving sphere. The left image depicts the original MSPS with no correction for super-elasticity. The cloth is too elastic and the model cannot respond fast enough to the moving sphere. In Chapter 3 Figure 3.2 we show another image in which the moving sphere even penetrates the cloth material. The right image in Figure 7.1 was obtained

after we applied the elasticity restriction approach with DVM. The elasticity threshold of the tablecloth fabric was 5%. We can see that the cloth simulated with DVM reacts naturally to the moving sphere. In addition, the DVM was used in tests on static and dynamic body-scans, as described below, and it generated visually pleasing results in all tests.

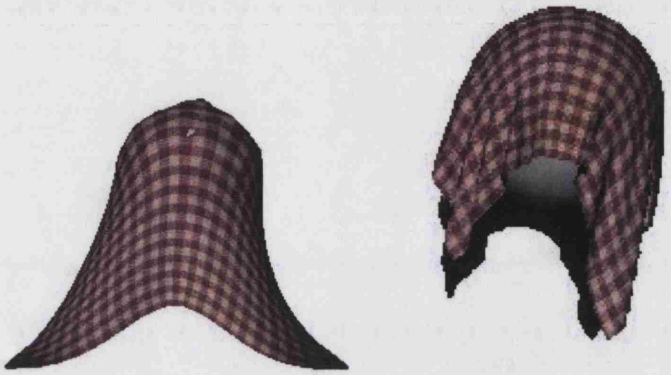

Figure 7.1: Tablecloth draping over a moving sphere; Left: No super-elasticity correction; Right: Super-elasticity corrected by directional velocity modification.

7.1.2 Fabric Property Mapping

As we have described in Section 3.4, we map fabric properties from the Kawabata Evaluation System (KES) to our cloth model. Table 7.1 shows a comparison between six real and simulated fabric types draped over a round table.

Fabric Type	Photograph	Simulation
Black&White Check		

Fabric Type	Photograph	Simulation
Brown Wool		
Denim		
Navy White Gingham		
Pale Mauve Polyester		
Mauve Polyester		

Table 7.1: Comparison of different fabric types mapped onto our cloth model. From left to right: Description of the fabric type; Photograph of the real fabric draped over a round table; Simulated counterpart draped over a virtual round table.

As noted in Section 3.4, the mapping of the KES coefficients onto our cloth model is a very rough approximation. However, the images in Table 7.1 indicate that the simulated fabrics behave similarly to their real counterparts. There is a difference in colour because the images of the virtual garments were created by using a simple local illumination model and no natural global illumination calculations were carried out. A possible methodology to evaluate as to how well the simulation approximates the real fabric is given in Appendix A.

7.1.3 The Influence of Cloth-Mesh Resolution on Performance

A higher garment mesh resolution results in a more flexible garment whilst at low resolution, garments appear to crease too easily. Figure 7.2 depicts a simple, sleeve-less shirt simulated at different mesh resolutions. The images were visualised with the wire-frame mode enabled in order to show the mesh underlying the surface. It is also notable that, at higher resolution, garments appear to be more stretchy, as shown in Figure 7.2, left to right, by the elongation of the shirt. This appears to be owing to the rough mapping of fabric properties from the KES as described in Section 3.4.

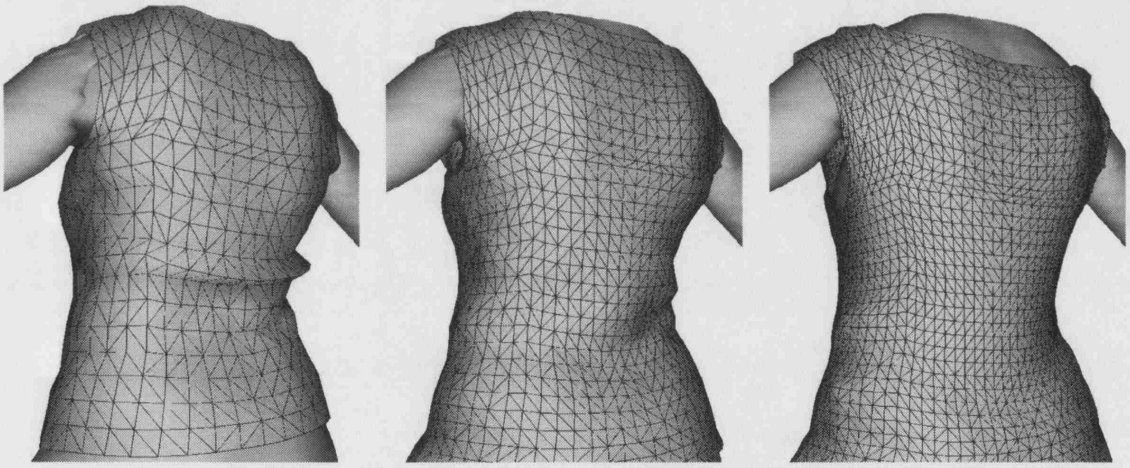

Figure 7.2: From left to right: Shirt simulated with 20×20, 30×30 and 50×50 vertices.

As mentioned in Chapter 4 the garment mesh is created from the cutting pattern contours before each simulation and therefore can easily be changed. We carried out tests to evaluate the influence of the mesh resolution on the performance of the simulation. Figure 7.3 shows the average time spent per frame on the simulation of a shirt, with increasing mesh resolution. We can see that the simulation time increases linearly with the number of simulated vertices.

7.1.4 IBCD versus Traditional Collision Detection

In order to compare the efficiency of our IBCD algorithm to a traditional method, we implemented a classic bounding volume hierarchy approach which tests interference in object space

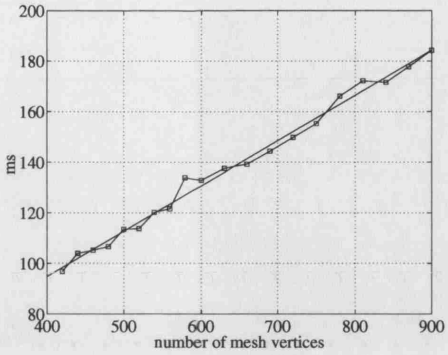

Figure 7.3: The simulation time increases linearly with the number of garment vertices simulated.

(OBCD). For this purpose a tree structure of bounding boxes (BB) was constructed in which the leaves contained the faces on the body geometry with their normal vectors. The algorithm checks for collisions between a vertex of the cloth and a face on the body and computes the response by using the technique described in Section 3.3. Tables 7.2 and 7.3 give the measurements we obtained when we tested the IBCD against the traditional object based collision detection (OBCD) technique in a simulation of a shirt and a dress on the above specified SGI workstation. The times given neither include the creation of the depth and normal maps for the IBCD method nor the generation of the BB tree for the OBCD method. In the table CD&R stands for "collision detection and response", and CS means "cloth simulation". The IBCD approach improves the speed of the collision detection and response by a factor of two to three. CD&R time % gives the percentage of time spent on collision detection and response and CS time % gives the percentage spent on cloth simulation. The table compares the results only for a static body since our OBCD algorithm was implemented only for that case. This means that, in the dynamic case, additional time would be spent computing the velocity of each body point. In our IBCD algorithm this is done by rendering the velocity map and the graphics hardware interpolates the velocities for the intermediate points. For the OBCD algorithm, however, these velocities need to be computed at each frame and interpolated when a collision occurs, so we expect that the advantages of IBCD will be even more obvious in the dynamic case.

7.1.5 Dynamic Body IBCD

Next, we tested the performance of the IBCD with an animated body. Initially, we exported a body mesh for each frame of an animation sequence from the Poser character animation system. The meshes were then loaded frame by frame into our garment simulation system and the velocities of the body surface were approximated for each vertex by computing the difference in position to the previous frame. For each animation frame, depth, normal and velocity buffers

Category	IBCD	OBCD
Time/iteration(ms)	15.8	30.8
CD&R time (ms)	7.6	22.5
CS time (ms)	8.2	8.3
CD&R time (%)	48.1	73
CS time (%)	51.9	27.0

Table 7.2: Performance comparison between IBCD and OBCD for a shirt with 1800 vertices.

	IBCD	OBCD
Time/iteration(ms)	33.0	52.0
CD&R time (ms)	15.1	34.2
CS time (ms)	17.9	17.8
CD&R time (%)	45.7	65.7
CS time (%)	54.3	34.3

Table 7.3: Performance comparison between IBCD and OBCD with a dress for 3840 vertices.

were created by the graphics hardware and finally the cloth simulation was performed. In Figure 7.4 two different frames of a walking body are shown from two different viewpoints. The resolution of the collision detection buffers was set to 160 × 160 pixels. For performance reasons the resolution was chosen lower than that estimated as optimal in Section 3.2.5. This test was carried out on the Desktop PC, specified in the beginning of this section. Table 7.4 gives the timings we obtained when we simulated a simple skirt and a dress with sleeves. The simulation ran at a speed of three to four frames per second (250 to 300 ms per frame), depending on the complexity of the garment. The animation was created carefully to make sure that no overlaps between body parts occur and thus that the problems discussed in Section 3.2.6 were avoided.

In order to test our layered depth map collision detection, described in Section 3.2.6, we created a walking animation of a mannequin. In this animation the arms occasionally overlap with the body if viewed from the orthogonal cameras used for collision detection. Figure 7.5 left depicts the mannequin dressed in a shirt in the initial pose of the animation. The middle

	Skirt	Dress
vertices	672	2300
Frame/sec	4.1	3.4
Sec/Frame	0.244	0.294

Table 7.4: Frames per second in an animation.

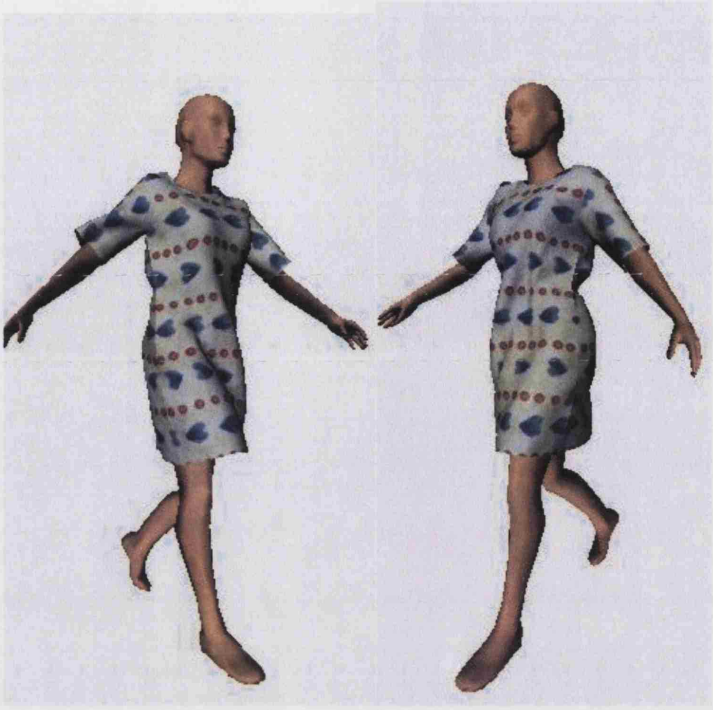

Figure 7.4: Two frames of a walking female model in a dress with sleeves.

of Figure 7.5 depicts the mannequin dressed in the shirt when an overlap between arms and body occurs. Incorrectly detected collisions between the garment and the mannequin cause unwanted simulation behaviour. This is a problem of the original IBCD which happens if overlaps between body and limbs occur. On the right of Figure 7.5 we show how our layered depth map approach can overcome the problem. No false collisions are detected and the simulation behaves correctly. However, the simulation performance decreases with the number of depth layers because for each layer additional depth normal and velocity buffers have to be created and transferred to main memory. The influence of the resolution of the collision buffers on the performance of the simulation is detailed next.

7.1.6 Influence of Collision-Buffer Resolution on Performance

In order to evaluate the influence of the resolution of the collision-maps on the performance, in the dynamic case we carried out another test in which we performed the same walking animation sequence of a body-scan with collision-buffers of different resolution. As a garment we chose a simple, sleeve-less shirt with 840 vertices. This test was performed on the Laptop. The diagram in Figure 7.6 shows how many frames per second could be achieved with buffer resolutions from 100×100 pixels to 500×500 pixels at increments of 100×100 pixels. We could achieve frame rates of over six frames per second on a 100×100 collision-map. Almost two seconds were spent on a collision-map of 500×500. Visually, the results between a low resolution

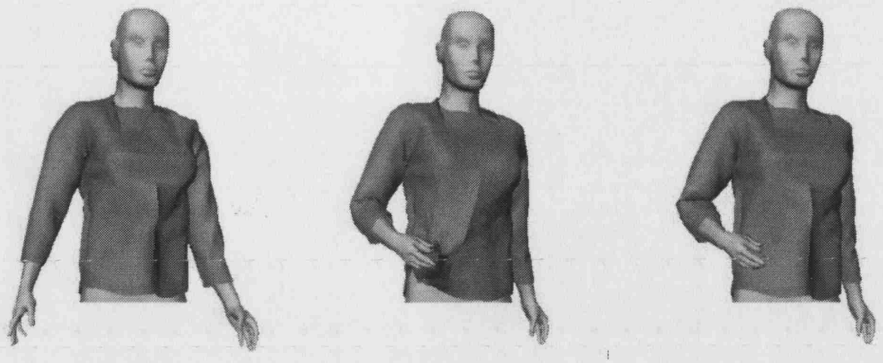

Figure 7.5: Multi-layer collision buffers. From left to right: Initial pose; Collision problems with the right arm; Problem fixed by using multiple collision layers.

collision-map and a high resolution map did not differ much.

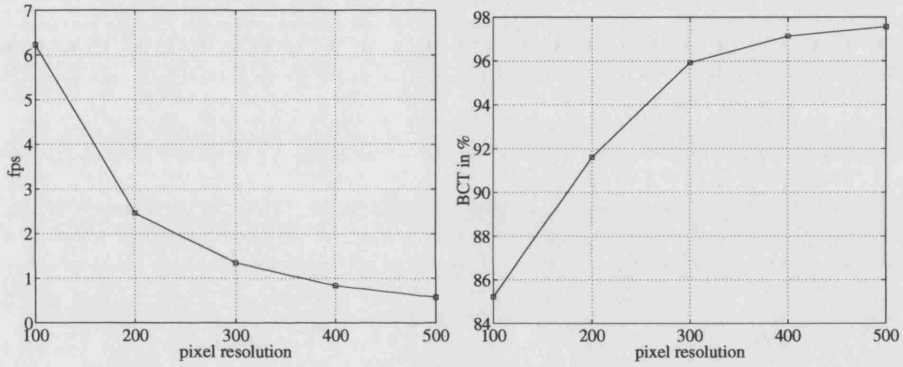

Figure 7.6: Left: By reducing the resolution of the collision buffer we can achieve higher frame rates in an animation sequence; Right: The percentage of time spent on creating the collision buffers. The remaining time is spent on character animation and cloth simulation.

However, collision-maps with a size lower than 100×100 created instabilities in the simulation and produced "bumpy" surface results, such as the one depicted on the left of Figure 7.7. A quantitative analysis of the difference in drape caused by buffer resolution was beyond the scope of the thesis. The right diagram in Figure 7.6 shows the percentage of time spent on the creation of collision-buffers (Buffer Creation Time, BCT). The remaining time was spent on character animation[1] and cloth simulation[2]. We can see that a large amount of the time is spent on creating the collision-buffers. This is because of the time required to transfer the frame buffer from graphics hardware to main memory and the time spent on converting the buffers to

[1] Since the animation frames were pre-computed, character animation only required an interpolation between the frames and could be done very efficiently in about 2 ms at a frame rate of 500 fps.

[2] Cloth simulation involved Euler integration, collision detection and response, and directional velocity modification.

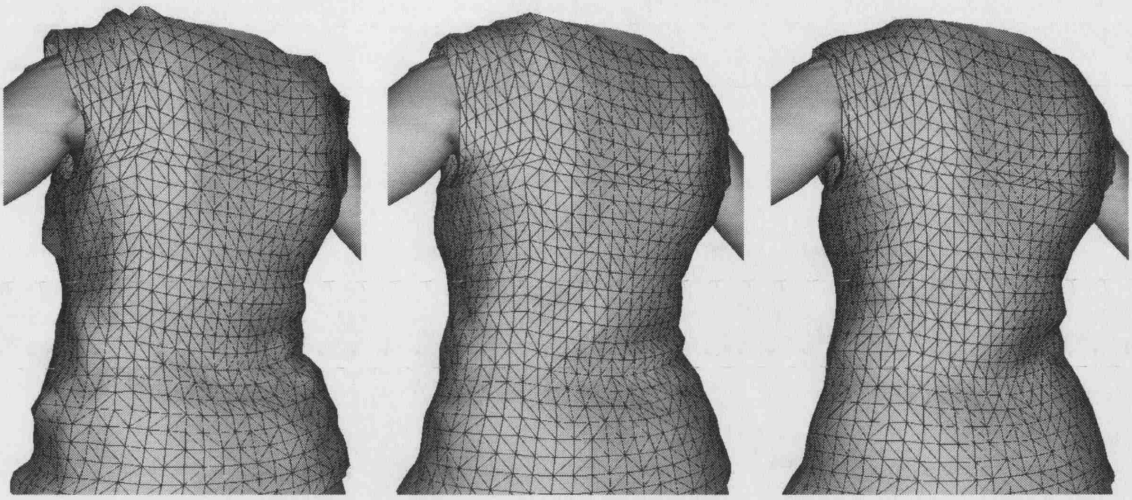

Figure 7.7: Shirt simulated at different collision buffer resolutions. From left to right: 50×50; 100×100; 400×400.

be suitable for collision detection and response as described in Section 3.2. The code could be improved to transfer only the rectangular area of the collision-maps and not the square area as is currently done. Further improvements could be achieved by exploiting OpenGL extensions that allow us to carry out the required buffer conversions (see Section 3.2.4) on the graphics board by using the *glPixelTransfer* function. In general, the performance of the approach will be even better on cards that can achieve higher frame and depth buffer download rates. Since, in character animation, motion sequences are often pre-defined much use could be made of this fact drastically to improve the performance of our cloth animation. In particular, the buffers for collision detection could be pre-computed. In this way, we believe that garment animations at rates of 30 fps and more on state of the art PCs with not too complex garments[3] could be achieved. This would, however, require large amounts of memory. Memory requirements could probably be handled by using a video compression format to store the collision buffers. However, we did not investigate further in this direction.

7.1.7 Influence of Body-Mesh Resolution on Performance

Since IBCD does not use the original geometry of the body-scan but depth, normal and velocity images, it is expected that the simulation time is independent of the mesh resolution of the body-scan. We tested our cloth simulation with a pair of trousers with 2344 polygons on a body scan represented at different levels of detail[4]. The diagram in Figure 7.8 shows the average

[3]Garments with a few thousand vertices and few layers of potentially self intersecting cloth.

[4]Thanks to João Fradinho Oliveira for creating the body-scans at different levels of detail with the software he developed during his PhD studies.

time per frame (TPF) spent in the sewing simulation[5], which is constant. Obviously, buffer creation time (BCT) is dependent on the mesh resolution since the graphics hardware requires more time to render a mesh with higher resolution. However, in the static case, the buffer has to be created only once and therefore does not influence the simulation time. As discussed above, the buffers could also be pre-computed to avoid, also in a dynamic simulation, a performance decrease caused by the mesh resolution of a body-scan.

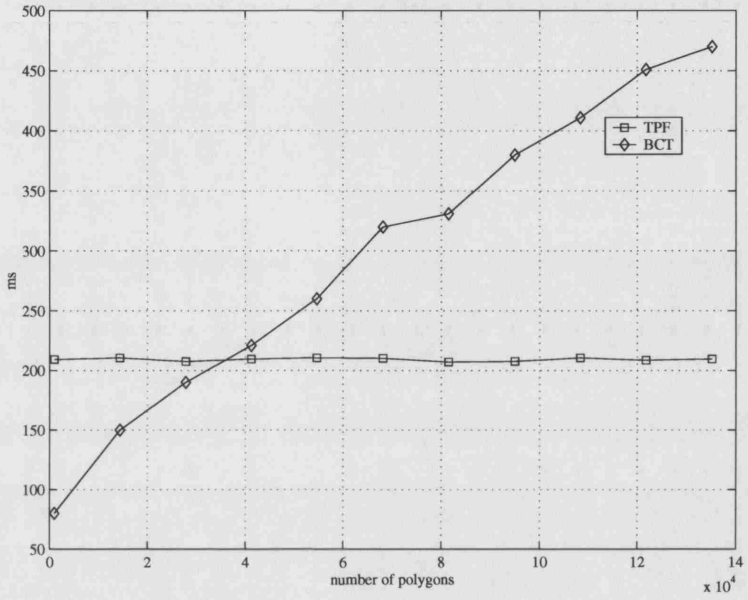

Figure 7.8: The performance of the collision detection is independent of the mesh resolution of a body-scan. The average time per frame (TPF) in a simulation of a pair of trousers with 2355 polygons is constant. Buffer creation time (BCT) which has to be performed only once in the static case, however, increases linearly with the number of polygons.

7.2 Virtual Try-On Installation at Selfridges

In this section, we describe an installation of our virtual try-on system at Selfridges, a well known department store in London. The aim was to build a system for virtual try-on of existing designer jeans in a department store[SVB03, SVWB05]. This was a great opportunity for us to test the robustness of our methods and to evaluate customer acceptance. The initial installation was carried out for the BodyCraze event at Selfridges in May 2003. The system was planned to be installed only for a month for demonstration purposes and women, if interested, could try it for free. Owing to the high customer demand the system was kept in the store and, at the time of writing has been there for over one and a half years, with customers willing to

[5]The sewing simulation is required in order to join the individual garment panels around a body-scan.

pay for the services provided. To our knowledge this is a world first installation of a fully automatic virtual try-on system. The system allows customers to browse and try-on designer jeans on their 3D scan and gives them sufficient visual feedback to decide whether to buy or not. In the process, important body landmarks and a large number of size measurements are automatically extracted from customers' body scans, as described in Section 4.4.2.1. The system uses the DVM and IBCD to simulate the garments on the body-scans. By these means, we are able to virtually dress a customer with a chosen garment within one to two seconds. By using photographs of the real garment as texture maps, acquired in the process described in Section 4.3, we are able to produce very realistic images of the clothes on the customers' body-scans. Kawabata Evaluation System (KES) measurements of the fabric's properties are mapped onto our cloth model, as described in Section 3.4, to ensure appropriate virtual drape behaviour. The system has advantages over a conventional changing room and mirror in that customers can view themselves from any distance and angle and try-on different garments within seconds. The system is built on Internet-based technology, as described in Section 5.5, and customers may view their body from their home PC over a secure link and try-on new garments added to the system's central database.

7.2.1 Implementation

Since Bodymetrics Ltd. already had experience with the scanning system from the Textile/Clothing Technology Corporation ($[TC]^2$) [TC2] from the UK national sizing survey [Siz01] it was employed again here. The $[TC]^2$ system uses a technique called "white light phase measurement profilometry" in which images of a structured light grid projected onto the front and the back of the body are taken and, from distortions of the light grid, the body shape is acquired. This approach is well suited for body measurement because of the short acquisition time (less than ten seconds), safety, accuracy and relatively low cost. The direct output of the scanner is a 3D point cloud. The body surface is reconstructed by $[TC]^2$ software and important body landmarks are extracted automatically. A rule-based language allows users to customise the extraction of body measurements. 3D models are stored in the virtual reality modelling language (VRML) format [BCM96]. For visualisation we remove parts of the geometry that are not essential for the virtual try-on and parts that may not be scanned well such as the head, hands and feet. To leave enough space for dressing we lift the arms of the scan by rotating them around the shoulders. The $[TC]^2$ surface reconstruction leaves holes in areas that are partially obscured during the acquisition process. Such holes in the armpits, crotch and hip areas are identified and patched in our process. Body-scans after the different stages of pre-processing

are shown in Figure 7.9. Our software merges landmarks and geometry in a compact binary Inventor file [Wer93]. The file is further compressed using the purely information theoretic methods of zlib [DlG96]. The resulting file of the body scan which, on average consists of 80000 triangles, including all required information for visualisation, is approximately 150KB in size. Small file size is important for fast loading into main and graphics memory for visualisation and also for use on the Internet.

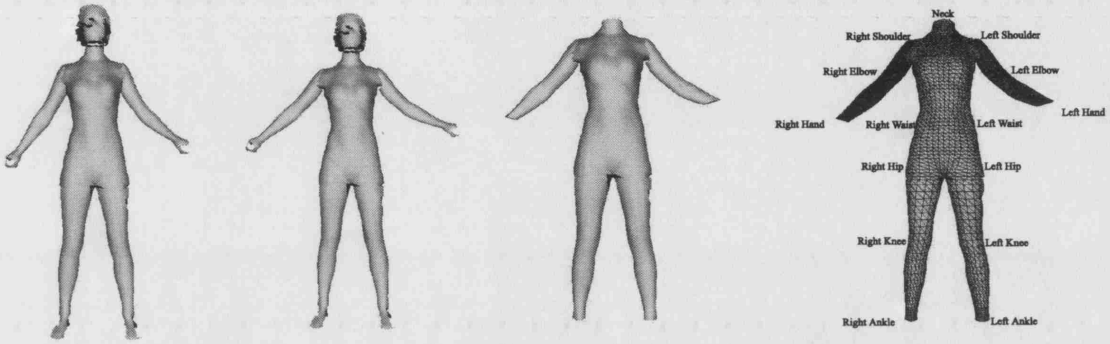

Figure 7.9: From left to right: original body-scan surface reconstructed from a point cloud by $[TC]^2$ software; arms were lifted and most holes patched; head, hands and feet removed; extracted landmarks which are used for pre-positioning of garments are shown.

7.2.2 User Interface and Customer Discretion

The user-interface was designed to be very simple for use by customers and to protect their privacy. Interaction with the dressed 3D body is restricted to garment and viewpoint changes. The user can zoom in and out, pan, and rotate around the 3D model by dragging the mouse. For the try-on of garments we followed a simple point and click paradigm. Once a garment has been chosen it is immediately loaded into the visualisation and the virtual customer is dressed. Not surprisingly, a research study on body-scanning has revealed issues about customers' embarrassment when viewing their bodies [IL99]. We assumed that this would be particularly critical in a public place[6] and took measures to address such issues for the garment retail set-up. Firstly, we designed clothing to make sure the customer is always dressed properly. We call such clothing "default wear". An example is shown in Figure 7.10. The visualisation only shows the customer when she is dressed. Secondly, when a different garment is chosen, we keep on displaying the previous garment and wait until the simulation has converged to a certain degree (for example 90% of the seaming points have found their destination) before we swap to visualise the simulation of the new choice. The customer thus gets important visual feedback

[6]Our Web interface, described in Chapter 5, is also used in the department store installation.

from the seaming simulation animation but, at the same time, we make sure she always appears dressed.

7.2.3 Results

In this section we briefly report on the virtual try-on service based in part on informal interviews with some of the operators that run it. These operators were normally female students from the London College of Fashion (LCF). Their education provides a very good background for them to give recommendations on the fit of jeans. Also, they know how to work with computers though they are not expert computer users. A brief training of less than an hour is sufficient for them to run the service.

7.2.3.1 System Reliability

About one in every fifty customers is scanned a second time owing to size and landmark extraction problems of the $[TC]^2$ software. No problems have been reported with the visualisation and simulation system.

7.2.3.2 Customer Feedback

At the moment the system is for women only. This limitation is because of the type of garments available for simulation. New customers are added to the system every day. They read about the service in the news, have heard about it on TV or are informed by word of mouth. They are coming mainly alone or with a male friend. Customers normally come in to buy jeans anyway and they are willing to pay for the service. In general, they are finding the system useful. Customers find the jeans visualisation sufficiently realistic. A few customers completely trust the simulation and would buy the jeans without trying them on in person. Operators recommend trying on the real jeans before buying, however. Used in this manner, the system helps customers find the best fitting size and style of jeans that they like. Customers are very interested to try out new virtual garment items added to the database.

We found that most of our customers are very confident with their body and embarrassment about viewing their body as suggested by [IL99] only occurs rarely. Some of the customers would like to enter the scanner with high heels to alter their appearance. We find it worth noting that quite a few female customers seem to be encouraged by their male friends to try-out the system. It is also mainly the males who are interested in the data format of the scan and whether they could access it from the Internet.

7.2.3.3 Other Visitors

There are many people visiting the installation just because of interest in the technology. These are mainly people from the film and games industries but also university students who want to find out what the system does and how it works.

7.2.3.4 Internet Access

Once scanned, customers can access the system over a secure link on the Internet. At the time of writing there are several thousand scans stored in Bodymetrics' central database.

7.2.3.5 Visual Quality

Images that illustrate the visual quality of the simulation are given below. Figure 7.10 shows one of our customers in "default wear". Two views of the customer in a pair of jeans that fit well are given in Figure 7.11, on the left a front view and on the right a back view.

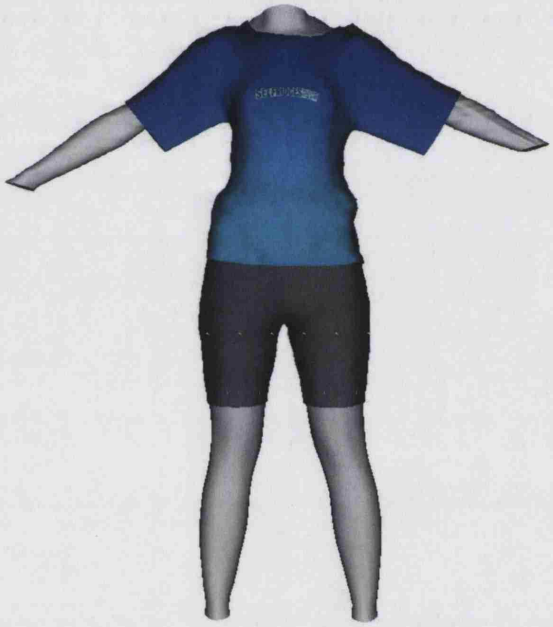

Figure 7.10: Customer in "default wear".

Not all defined seaming lines can be joined on the left of Figure 7.12 because the virtual jeans are too small for that customer. On the right of Figure 7.12 a screenshot of the simulation of jeans that appear very baggy is depicted. Six customers with fairly different body-shapes dressed in the same pair of jeans and a default shirt are depicted in Figure 7.13.

Figure 7.11: Left: Front view of a customer in jeans that fit well; Right: Back view of the same customer in the same pair of jeans.

7.3 Augmented Reality For Garment Design

In this section we describe a scenario in which we used the Virtual Try-On system in combination with natural global illumination in collaboration with a garment designer[7]. A client may approach a garment designer with a specific occasion in mind at which she wants to wear the new design. For the designer it would then be beneficial to experiment with the new design in the target environment and to be able to show photo-realistic images of the client wearing the new clothes at the specified location. Such a system will save time and cost in the process of clothing design [SVB04, SVWB05]. We collaborated with a designer to test our system in a real world setting[8]. As a simple garment, our designer was asked to make a jacket. In order to verify our simulation the designer created the jacket not only in a CAD system for simulation but also made a real toile of the garment. The designer's client was scanned with the $[TC]^2$ system and we took photographs of the client in the real jacket for comparison. A light probe was taken in our designer's office as depicted in Figure 5.6.

[7]Thanks to Anki Lindblom from Anki.biz (www.anki.biz) for her collaboration.

[8]The work described in this section was carried out at the request of Bodymetrics Ltd.

Figure 7.12: Jeans that do not fit well; Left: a customer with jeans too tight; Right: a customer with very baggy jeans.

7.3.1 Merging the Real and Virtual

In order to make the virtual garment appear on the client's photograph, as if the client were dressed in the virtual garment, the photograph of the client must be aligned with an image of the 3D scan of the client. This can be achieved by extracting camera position and direction by using a camera calibration technique such as the one described by Zhang in [Zha00] and by rendering the 3D scan and garment with the camera settings of the photograph. However, for camera calibration multiple photographs of a calibration pattern in the target scene are required which may not be available. Automatic alignment of the model with the image can also be found with image registration techniques. See Lester and Arridge [LA99] for a survey. If the pose of the client in the image is significantly different to the pose of the client's 3D scan, the scan has to be animated with the garment to approach the pose in the photograph as closely as possible. An automatic character animation system (see Section 6.2) combined with an image registration method is required to find the right pose automatically. In the experiment described we did not concentrate on automatic model alignment. Instead, we superimposed the virtual model over the photograph and adjusted the virtual camera to visually match photograph and scan. In addition, rather than attempting to register the limbs, in particular the client's arms, in the scan to match the photograph, we chose to replicate appropriate background texture over the original position of the arms in the photograph. Part of the client's left arm is shown in

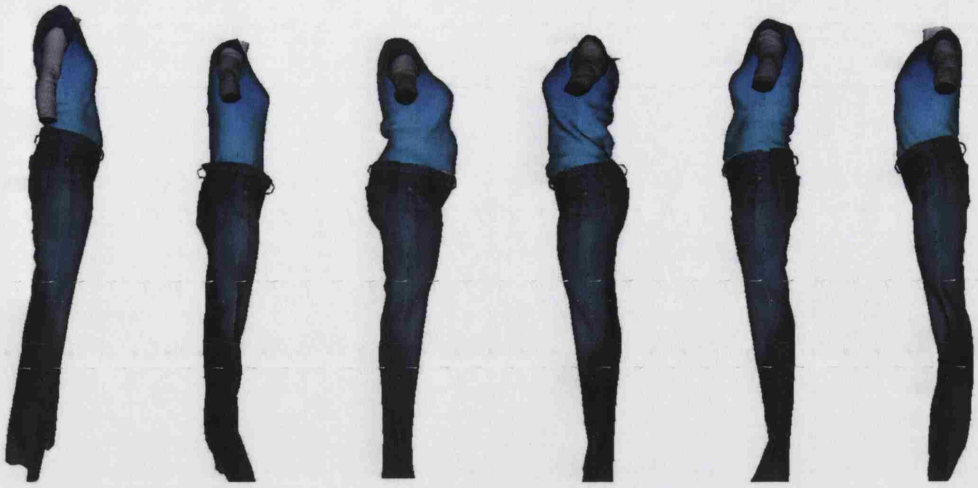

Figure 7.13: Side-view of six customers dressed in a default shirt and the same pair of jeans.

Figure 7.14 to illustrate this process.

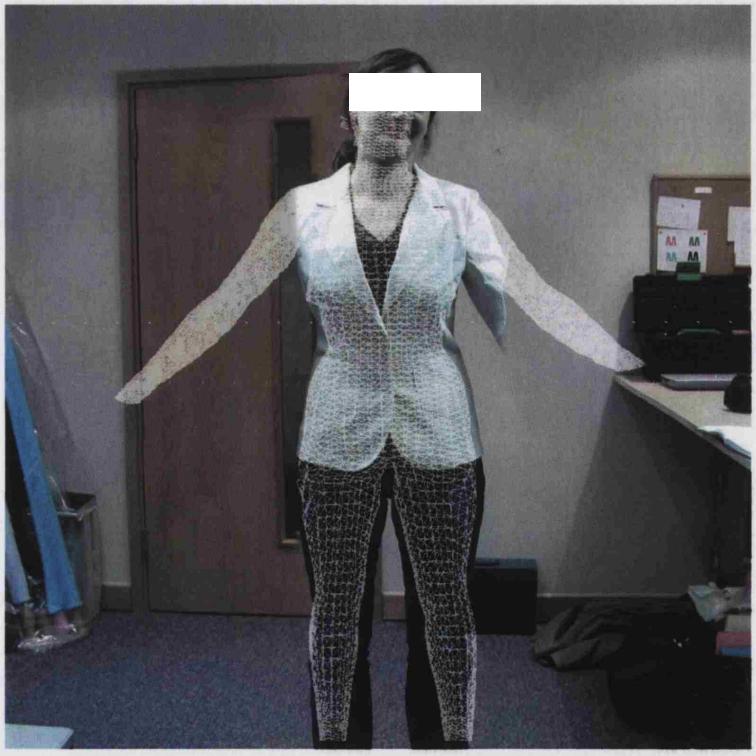

Figure 7.14: 3D scan superimposed on the photograph to approximate camera.

7.3.2 Masking the Rendering for Photo Composition

In order to subtract the garment from the background of the synthetic image it is necessary to create a mask image. The problem is that client-scan and garment interact and it would be difficult manually to generate a good mask to sufficient accuracy. Instead, we use a depth buffer approach. We create a depth buffer image for the 3D scan and background (the light probe)

without the jacket and another depth buffer image of scan with the simulated jacket. A simple filter function can then be used to generate a mask file. The filter function returns 1 if the depth value of the jacket is greater than the depth value of the client-scan and 0 otherwise. An example mask is depicted in centre of Figure 7.15. The right of Figure 7.15 depicts our rendered jacket subtracted from the background.

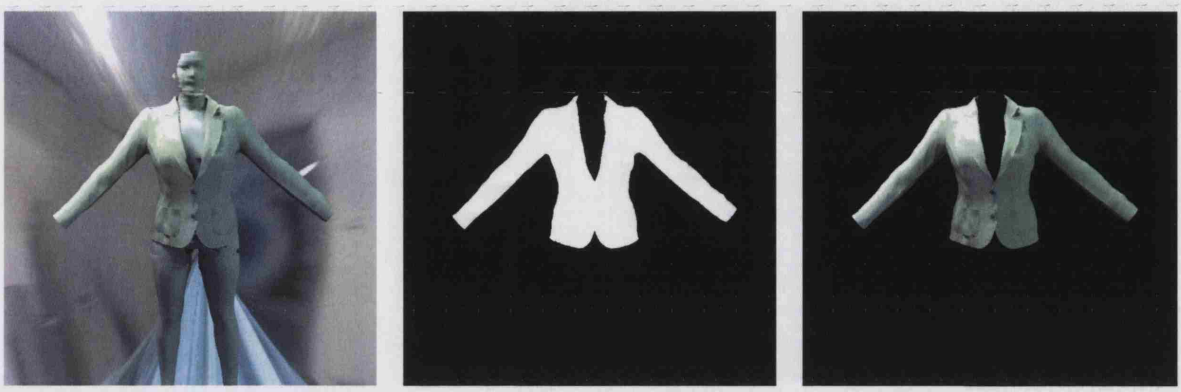

Figure 7.15: From left to right: Scan in jacket the appearance of which has been produced by use of a background light-probe; Automatically generated mask image of the jacket; Extracted illuminated jacket.

7.3.3 Synthesis of Occluded Background

When merging images, the background where the new image is inserted is usually lost. Sometimes it is also required to recreate parts of the background texture occluded by a real garment. For example, parts of our client's real garments may not be sufficiently covered by the synthetic garment and therefore need to be replaced by the background expected in the image as indicated in Figure 7.14. Ideally, an image of the background without the client would be available, but if this were not the case, the background could be approximated by use of texture synthesis techniques. Generally texture synthesis takes as input an area of the image that is similar to what should be regenerated. The area that should be recovered is marked and synthesised with a texture that most likely would have covered that area according to a probability distribution of the specified sample region. We employed a technique described by Harrison [Har01] for this, but the results, though promising, were not as good as those we could obtain by using parts of a background image to replace areas in the foreground layer of Figure 7.16.

7.3.4 Results

Figure 7.16 depicts a client in a real jacket toile on the left and on the right the client dressed in a virtual jacket. We note that, owing to natural illumination, the simulated garment fits

realistically into the photograph. The experiment was done under real-life conditions, with the office otherwise in near-normal use, as can be seen from the fact that the door is slightly open in Figure 7.14 (and therefore also in Figure 7.16, right but closed in Figure 7.16, left). Since the client's hands were removed from the 3D scan they are not present in the image with the virtual garment either. There are creases in the real jacket toile as may be seen on the left of Figure 7.16 which do not appear in the right image of the client composited with a simulated garment. In general, the simulation appears much smoother than the real garment. This may be for two reasons. Firstly, our garment simulation does not account for memory effects of the fabric, while secondly the resolution of the mass-spring mesh could be increased to generate more detailed creases. Also, some shadows, for example, under the arms, appear stronger and sharper in the simulation than in real-life. Finally, we note that parts of the simulated garment, such as on the pockets, right sleeve and left lapel, appear less smooth on the simulation than in real-life. This appears to be caused by limitations on the interpolation of normals in the RADIANCE system when they are used for calculating inter-reflection effects as discussed in Section 5.4.3. Such artefacts could also be reduced by using higher resolution meshes. In spite of these deficiencies, both the designer and client have found the system very useful and interesting. Our designer commented on possible improvements mainly on the garment design and simulation interfaces.

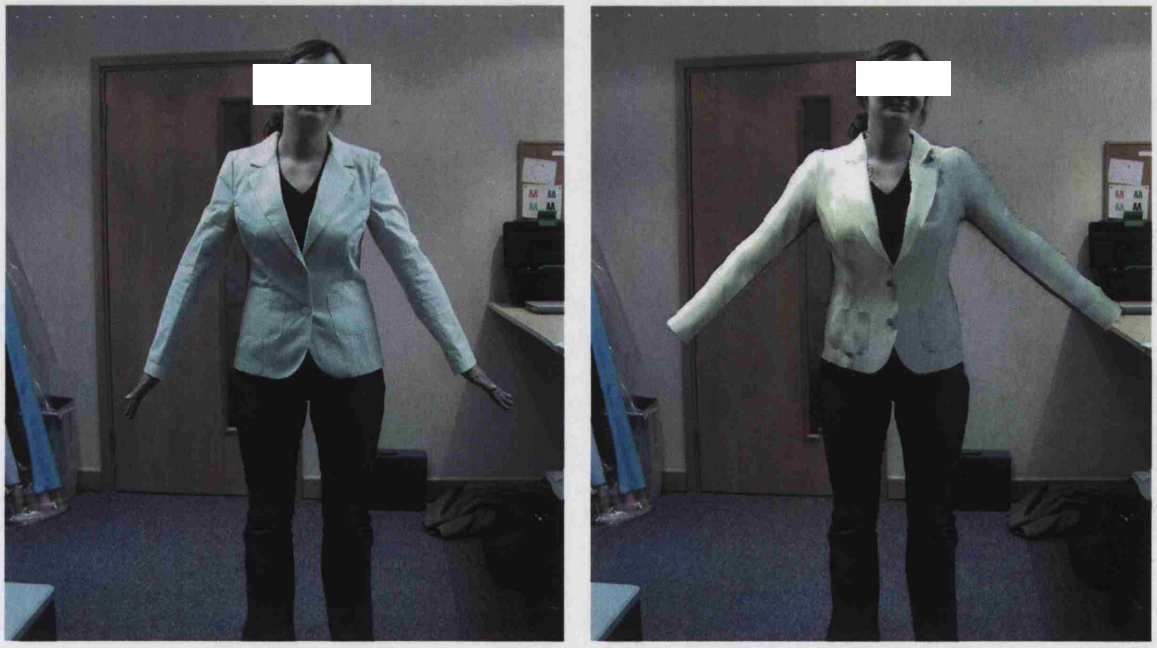

Figure 7.16: Left: Client in the real jacket toile; Right: The illuminated and simulated jacket composited with a photograph of the client.

7.3.5 Future Work

As mentioned earlier, registration between 3D scan and client photograph could be automated by using existing registration or calibration techniques. Automatic pose registration is a particularly challenging and interesting problem. At the moment we do not take into account interaction of light reflected from the client's other real garments with the virtual garment or vice-versa. This would probably require reflectance and geometry measurements of the garments the client wears in the photograph which would be hard to acquire. If naturally illuminated images from different views were required in real-time, a light-mapping technique similar to the one described in [Spa02] will be of particular interest because texture coordinate parameterisation is inherently given by the flat cloth panels with which the garment simulation starts, as discussed in Section 5.2. In order to assess the visual quality of our system we have prepared a user study on the web, described in Appendix A. Preliminary results from ten respondents indicate, however, that many more responses are required before a useful analysis can be carried out.

7.4 Summary

We demonstrated the simulation quality of directional velocity modification (DVM) by showing images of garments simulated with that method. Super-elasticity problems of the original model are overcome. Further experiments on image quality are described in Appendix A. Measurements on the influence of the cloth mesh resolution on the simulation performance show that the simulation time of our method grows linearly with the number of vertices simulated. The performance of IBCD in the static case was shown in a comparison to a traditional collision detection method. We then showed that in the dynamic case, by using the IBCD, we could achieve frame rates of more then four frames per second. We demonstrated the problem of overlapping body-parts in the original IBCD and a solution in which layers of depth maps are used. We show that further performance improvements in the dynamic body case can be achieved by reducing the resolution of the collision buffers. However, too low a buffer resolution may cause problems in the visual quality of the simulation as discussed in Section 3.2.5. Further performance improvements may also be achieved by exploiting improved buffer access functionality of recent graphics hardware. If interactive body animation is not required the collision buffers could be pre-computed and we estimate that cloth simulation frame rates of over twenty frames per second could be achieved on current desktop machines. The fact that the performance of IBCD is independent of the mesh resolution of a body was then shown in an experiment where different body mesh resolutions were used. This scalability property of IBCD is particularly important for the use of human whole body-scan data which often contains a large number of

polygons.

A system for virtual clothing was installed successfully in a department store. At the time of writing the system has run for over eighteen months. There is high customer demand for the system and to meet this we need to add more and different virtual garments to the database. A next step will be a market research study to identify the main customer requirements to improve the system. A possible system improvement may be to allow the virtual customer to change poses or even to carry out animation sequences from motion capture (as described in Section 6.2) in order to get a better idea as to how the garment will interact with the body. The visualisation quality can be improved by adding fabric reflectance properties and by simulating fabric light interactions in more detail (as described in Section 5.4).

In addition we have presented a system that enables designers to generate photo realistic images of a client dressed in a garment that is at the design stage. In a collaboration with a designer we tested our system with a client. Both client and designer found our system interesting and useful. Many system improvements are possible as listed in the section 7.3.5. A methodology to evaluate the quality of the images that can be generated by the system is given in Appendix A.

Chapter 8

Commercial Potential of Virtual Clothing

In this chapter, we evaluate the commercial potential of Virtual Clothing[1]. Virtual Clothing is a paradigm-busting[2] technology that has the potential to revolutionise many aspects of the entire apparel industry, from garment design to manufacturing, marketing and retailing. Our aim is to identify the most attractive target market for an introduction of Virtual Clothing and to find a strategy to enter that market. We act as BodyMetrics Ltd., a University College London (UCL) spin-off founded in 2001 by Prof. Philip Colin Treleaven and Dr. Suran Asitha Goonatilake. BodyMetrics provides anthropometric analysis tools and virtual fashion technologies. Its key area of competitive differentiation is that it hosts the data of the UK national sizing survey, a database of around 11,000 3D body-scans. BodyMetrics has installed the world's first fully automatic virtual try-on system at Selfridges[3]. Consumers are cautious of buying apparel online largely because of size, touch and feel problems. A high return rate is a direct result, and reduces the profitability of online sales. Virtual Clothing solves the size issue and brings the purchasers the beneficial psychological effect of seeing the product placed on a virtual representation of their own bodies. We have examined the strength, weaknesses, and possible applications of the technology, alongside different market entry scenarios. Taking into account market timing, complementary technologies, anticipated resistance and commercial value, we find the best entry position to introduce the technology to a wider market. We identify a major retailer with a presence in both traditional stores and online as an ideal partner for rolling out the technology. Such a partnership will help popularise Virtual Clothing and build a critical mass of users, paving the way for a wider application of the technology in the future. With a successful roll-out, we can capture first mover advantage and build a leadership position in Virtual Clothing

[1]Most of this work was carried out during a scholarship from the Centre of Scientific Enterprise London (CSEL) in the New Technology Ventures (NTV) course at London Business School (LBS) in collaboration with Brian Allbriton, Anthony Sibthorpe, Steven Seget and Annie Ting Ngai Lai.

[2]Adapted from the Harvard Business School "Documentum Inc", case [LL02].

[3]See Section 7.2 of this Thesis.

technology. In order to cover all relevant perspectives in assessing the feasibility of Virtual Clothing a three-stage approach was applied. As with all technology-related ventures, the opportunity must be assessed from the technology, commercial and business levels. Our project approach is outlined in Figure 8.1. The feasibility of the technology has been shown with the

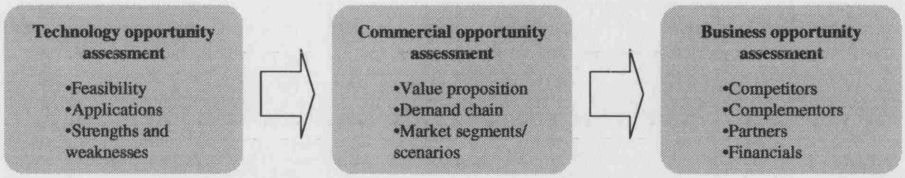

Figure 8.1: Outline of the commercial evaluation.

installation described in Section 7.2. A detailed description of applications for Virtual Clothing was already given in Chapter 1 of this thesis. These are: Internet Clothes Shopping, Fashion Design, Games Industry, Film Industry, Virtual Environments, and Textile Engineering. The technological background was presented in the Chapters 2 to 7.

8.1 Strengths, Weaknesses

In this section, we list the advantages, disadvantages and uncertainties of the virtual clothing technology.

8.1.1 Advantages

- A completely automatic method to dress a body-scan with clothes of choice in near real-time.
- Lower return rates for online retailers.
- Rare goods to be brought to a distant customer (no location limitation as for brick and mortar retailers).
- Increased online shopping.
- Customers could inspect their dressed virtual selves from any distance and angle.
- Design lead-times could be reduced and manufacturing processes streamlined.

8.1.2 Disadvantages

- Requires high processing power on customer's PC (CPU, Graphics Hardware).
- Requires broadband connection to the Internet.

- Some hold the idea that people spend too much time in front of their computer and should go to shops to get their clothes and meet other people.

8.1.3 Uncertainties

- It is unclear how closely the simulation can represent the real garment. The simulation is a model and therefore always an approximation to the real garment.
- Very complex garments (garments consisting of many layers and over twenty pieces of fabric) may be difficult to construct (significantly impacting on design applications).
- The interface that enables the user (usually designer or a CAD engineer at the garment manufacturer) to define seaming information (locations where garment panels are sewn together) and fabric property information (fabric drape behaviour such as weight, resistance to stretch, shear and bend, and properties such as diffuse and specular light reflectance) is not well established. Different interfaces exist[4] but will have to be adapted to designers' requirements.
- There is no standard file format to exchange garments electronically for virtual try-on.
- Software that creates body-surfaces from scanned point clouds may result in bumps that require manual editing to achieve high quality body-scans.
- Display devices may not be able to faithfully re-produce a garment's colours.

8.2 Choosing a Target Market

At this stage of our research, we determined that the greatest opportunity for BodyMetrics' Virtual Clothing technology was to be found in online apparel retailing. This application was considered to be sufficiently mature in its development and would provide the initial roll-out opportunity for Virtual Clothing. Other applications, including computer-based entertainment and animation and fashion design, were considered possible future applications of the technology, but are not feasible for the initial development and market entry of Virtual Clothing.

8.3 Commercial Value

An obvious question to ask is: "Is Virtual Clothing an innovation in search of a problem, or can it address a real need in the market?". To answer this question we assess whether there is a significant customer base beginning to demand the Virtual Clothing technology solution.

[4] Our design interface was discussed in Section 4.2.

As previously mentioned in Chapter 1, we may quote [Bec00]: *"Online apparel sales exceeded $1 billion in 1999 and are expected to skyrocket to over $22 billion by 2004. This growth will result from the combination of an increasingly large number of online consumers and the growing number of online retailers. Bear Stearns apparel analysts project that 10% of Internet apparel sales will be new sales - or sales that would not have occurred through other channels. Sales have picked up over the past year as companies (i.e. retailers) begin to substitute experiences that help consumers simulate the sight, touch, and feel experience they get in the brick-and-mortar store. "*

A survey of forty executives from the apparel, beauty and home decor markets revealed the following statistic: "Success stories are drowned-out by industry-wide grumbling: 38% cite lack of touch and feel as the number one obstacle to better sales" [DDJ99]. A major result of this problem is the current return rate for online apparel sales. It is estimated to be up to 30% of all items, a rate markedly higher than that for corresponding sales in brick and mortar stores, but equivalent to that of mail-order companies [Fra00]. This return rate is the prime indicator of what is wrong with the current method of online apparel sales - shoppers are not getting what they want from the experience, which is simply clothes that look good and fit well. Accenture has identified three important metrics of retail performance: average order value, return rate and conversion rate[5] [Acc]. Online sales of apparel have lagged behind other categories on these metrics primarily owing to the "touch and feel" factor [Min01]. Whereas items such as books and CDs are known commodities and do not differ in appearance in the virtual world as compared to the physical world, shoppers are much more cautious about purchasing clothing online owing to the problems of size, fit and feel. Additionally, many shoppers prefer to "see" what the clothing looks like on themselves in order to gauge how an item matches their personal style. This is, of course, where Virtual Clothing comes into the picture, solving a major part of the sight, touch and feel problem by giving the customer the opportunity to see what they will look like dressed in the specific item of clothing. While online shoppers will not get to physically feel a product before purchasing, the psychological effect of seeing the product placed on a virtual representation of their own bodies will go a long way to alleviating these problems. By reducing the cost of returns alone, Virtual Clothing stands to save the industry some 21% of gross sales that are currently lost in areas such as customer service, shipping, and customer loyalty [Bec00]. Also to be considered are the costs of re-handling, re-stocking, refurbishing (if needed), re-inspecting, and re-adjusting inventory [Lan04]. Accenture estimates that improved

[5]The conversion rate describes the number of website visits that are "converted" into purchases. It is an important measure in eCommerce.

fit alone can reduce return rates by up to 50%, increase purchase rates by over 25% and amplify average order sizes by nearly 15% [Acc]. Moreover, Forrester reports that any leverage in competition is highly valuable as most online retailers *"have already come a long way in developing their customer experience and marketing programs, leaving little differentiation among sites"* [Joh04]. Taking these factors into consideration, the current operations of online apparel retailers stand to gain a tremendous amount by providing a better experience to their shoppers. Most sites today offer customers no more than colour photographs of the goods and an often out-dated and inaccurate sizing chart. With the advent of body scans, virtual fabrics, powerful computers and broadband, it is easy to see the potential market for Virtual Clothing.

8.4 The Virtual Clothing Value Chain

Still to be answered is where this innovation fits into the value chain of clothing sales. There are numerous steps between initial design and the consumer, including those shown in Figure 8.2 below.

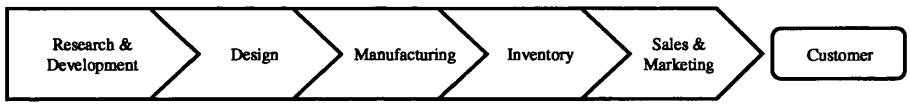

Figure 8.2: Value Chain of Virtual Clothing.

Virtual Clothing can help to bring competitive advantage to these areas as follows:

- Research and development – From the point of view of textile engineering, the modelling of the fabric itself allows for new concepts of stretch, shear and bend to be examined in R&D. While the current state of the technology is to measure the characteristics of different fabrics then model them later, it is not hard to imagine this process working in reverse, allowing a new fabric to be modelled even before manufacture.

- Design and manufacture – The design and manufacturing phases could also be greatly simplified. Today the process is quite labour intensive, but with Virtual Clothing, as soon as the concept drawing is rendered and the requisite clothing seams identified, a pattern could be automatically generated and sent to the CAM equipment for execution.

- Inventory – In terms of inventory, the savings from Virtual Clothing technologies have the potential to be significant. Already, companies such as H&M and Zara practice the concept of Just-in-Time manufacturing. They store no inventory in warehouses, but rather take a design from fashion catwalk directly to retail outlet in only a matter of days. With

	Brick & Mortar	Catalogue	Current Online	Virtual Clothing Online	Tailor
Pricing	2	8	9	9	1
Staff Advice	10	3	6	8	10
Customised Product	1	1	3	10	10
Sight and Touch	10	1	1	8	10
Choice / Variety	4	6	10	10	10
Convenience	1	8	10	10	1
Fit	5	1	1	10	10

Table 8.1: Tabular representation of the estimated value curve for Virtual Clothing in eCommerce.

a fully executed Virtual Clothing business model, this practice would gain even greater efficiency, as no clothing would ever have to be produced until it was actually sold. Theoretically, a 100% efficiency goal could be reached with regards to never producing an item that did not sell[6].

- Sales and marketing – Finally, in terms of sales and marketing, the economic picture has already been drawn. Online apparel sales are rapidly growing, but so are returns and associated costs. Virtual Clothing offers the ability not only to augment these sales, but also to reduce the high costs of returns. Furthermore, from a marketing perspective, always getting a perfect fit would serve to increase customer loyalty and drive repeat sales.

8.5 Value Curves in Apparel Retailing

In terms of relative advantage, the value curve is often a useful tool for analysing strengths and weaknesses. In our report [SAS+04] we presented the value curve in the traditional from often used by business minded people. This representation did not appear to be satisfactory for scientists and we therefore replaced it by a table of values which may be more accessible. Table 8.1 gives the estimated strengths and weaknesses (values between 1, indicating a weakness, and 10, a strength) of the chosen categories for the different forms of supply.

In this case, the characteristics of Price, Staff Advice, Customised Products, Sight and Touch, Choice / Variety, Convenience and Fit are the key attributes in play. In terms of price,

[6]We say theoretical because we assume that customers are satisfied with their purchase, which they could try-on virtually, and would not return it.

Online and Catalogue sales have long been known for their deep discounts. Without the additional fixed overheads of their bricks & mortar and tailoring competitors, they can offer lower prices. Not having to inventory items in multiple locations adds to their advantage on this attribute. No entity in this grouping can rival a bespoke tailor on either knowledge or customised products, as the attention they pay a customer is unrivalled. However, with a database of information at hand, online players are rapidly making advances on brick and mortar outlets. Context sensitive searches and instant chat are very effective tools for communicating information to customers that mail order can never offer. Sight and touch is, of course, the major issue affecting both online and mail order. However, as mentioned earlier, this is one of the main areas addressed by Virtual Clothing. Web sites using this technology therefore have a clear advantage over both their current online counterparts and traditional catalogues. Choice and Variety rate fairly high for all groups, but Convenience is another key differentiator. Ordering from a catalogue over the phone is adequate, but One-Click Shopping is incredibly convenient; there is no need to leave the couch or reach for a credit card. Virtual Clothing takes this one step further, as the customer does not even have to try on the clothing to know that it will fit. Conventional online and catalogue retailers perform poorly on this measure, while Brick and Mortar stores do not rate much higher with their standard size ranges.

8.6 Demand Chain Analysis

Another interesting tool for the analysis of Virtual Clothing is the Demand Chain, which shows the progression from Need for a product to the Repetition of purchase. At each step in any purchase cycle, there tends to be some level of fall-off. For each product, there are different factors that drive this progression, but with regards to the online purchase of clothing, it can be modelled as described below and illustrated in Figure 8.3.

- Need - Every person has a fundamental need for clothing; it is one of only a few categories that a person cannot live without.

- Awareness - With regards to online purchase availability, it is nearly ubiquitous in all developed countries, and people are well aware of the concept.

- Consideration - With the rapid increase of Internet usage, the volume of online shopping has grown in value year-on-year. On a daily basis, more people are doing more of their shopping online, across every category. The consideration of whether or not to purchase apparel online is where Virtual Clothing first enters the Demand Chain. By reducing the anxiety and associated hesitation of purchasing apparel online, Virtual Clothing increases

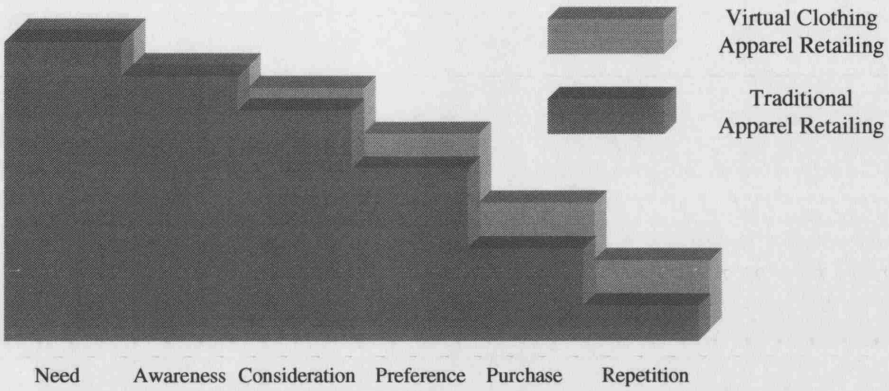

Figure 8.3: Generic demand chain analysis of Virtual Clothing. There is a fall-off from one stage to the next.

the number of shoppers who would even consider going online for their clothing, thereby keeping more of the target segment in the Demand Chain.

- Preference - By offering a superior fit over other purchase channels, more customers will come to prefer the Virtual Clothing method of apparel purchase.

- Purchase - Through the personalisation of the virtual model and the presentation of clothes on that model, it can be assumed that the sales response itself will increase by some degree. By allowing the shopper to interact with the clothing, more sales will be made and returns will be limited.

- Repetition - Once a customer has gone through the Virtual Clothing purchase cycle, the entire concept actually runs more smoothly the second time than the first. Because the "work" of creating a virtual mannequin has already been completed, follow-on purchases become even easier and thus more frequent.

8.7 Competing Innovations/Major Players

Currently, there are only a few clothing simulators on the market and these compete without any significant innovation. Some of these companies (Browzwear, OptiTex) use adjustable mannequins for which the designer or customer can enter size data and the 3D model is deformed accordingly. Such methods, however, will not allow the reproduction of a customer's exact body-shape. Furthermore, customers have to know many size measurements of their body. These could be taken by tape measure, but that solution is time consuming and quite unreliable. Other competitors currently in the market include online catalogues. A number of online retailers have simply put the catalogues they once sent via post on the Internet. Two-

	Industry	Focus	Advantage
My Virtual Model	Apparel	Online retail	Early start
Browzwear	Apparel	Online retail	Partnered w/ mfrs
OptiTex	Apparel	CAD/CAM	Currently selling
Digital Fashion	Apparel	Virtual Try-on	Location - close to mfrs
Havok	Entertainment	E-Commerce	Relies on installed tech
SyFlex	Entertainment	Cloth simulation	Software is in use
Pad System	Apparel	Design	Products in use
GerberTechnology	Apparel	CAD/CAM	Products in use
Lectra	Apparel	CAD/CAM	Products in use

Table 8.2: Comparison of the major players in the Virtual Clothing markets.

dimensional mix and match (such as that provided by "My Virtual Model" [MyV90]) is also available. This technology, however, lacks the total customisation of Virtual Clothing. Finally, there are firms in the film industry conducting their own research into Virtual Clothing such as Pixar [Pix] , SyFlex [Syf], etc. These companies are currently mainly interested in more realistic rendering of clothing in digital films, but the technology is quite similar to that required for a consumer application and could be competitive in the future. Only a few companies concentrate on the development of physical garment simulation for electronic commerce. These are Browzwear [Bro00], OptiTex [Opt87], Digital Fashion Ltd [Dig01], and SyFlex [Syf] together with Pad Systems Inc. [Sys]. Havok [Hav98] is a company that potentially has the technology to create Virtual Clothing systems but is currently concentrating on the computer games and entertainment market. "My Virtual Model" provides image mix and match techniques for electronic garment shopping and are making customers aware of the technology with their web presence. However, they do not provide 3D garment simulation. Finally, there are the two major companies that provide software and hardware for garment manufacturing, GerberTechnology [Ger] and Lectra [Lec]. Table 8.2 summarises the key competitors in clothing simulation and Virtual Clothing. A more detailed presentation of each company is given in Appendix C.

8.8 Challenges on the Route to Commercialisation

Exploiting the Virtual Clothing technology will involve a number of key challenges. These are discussed below.

8.8.1 Coordinating Access to Complementary Technologies

The parallel development of a number of different technologies is vital to the effective exploitation of Virtual Clothing technology. The specific technologies are summarised in the following list

Digital Imaging – This equipment is important because it is used to acquire reflectance and assembly information from real garments through reverse engineering. Developments in digital imaging also benefit 3D scanners.

3D Scanners – 3D scanners acquire full human body shapes in millimetre precision within seconds. They are based on laser measurements or digital imaging in combination with a light projection system to acquire shape and skin colour information. Software automatically to extract size and landmark data from the measurements has been developed and is often supplied with the scanner. Such software will be vital for made-to-measure clothing systems but also for fully automatic virtual try-on systems. With advances in digital imaging and computer vision software, we can expect that 3D scanners will drastically reduce in price and may become ubiquitous.

Fast Processors – Virtual Clothing is computationally very expensive and requires a lot of processing power for real-time performance. Recent developments in parallel processing architectures on PC CPUs have improved the performance and thus the availability of Virtual Clothing software. In addition, according to Moore's law, processor performance doubles approximately every eighteen months. The performance of state of the art PCs is, as we have shown, already sufficient to dress a body-scan within seconds. In the near future it will be possible to simulate much more complex garments.

Graphics Hardware – Game console requirements have pushed the development of graphics hardware. Developments in Virtual Clothing have shown that such hardware can markedly improve its performance and realism. According to [Rob02] graphics hardware performance doubles every six month, three times as fast as Moore's law implies for general purpose processors. We expect further developments of dynamic simulations on graphics hardware as suggested in [KW03] which may improve the speed of virtual clothing by a factor of ten or more.

Broadband – Broadband is a key technology for making Virtual Clothing viable for virtual try-on over the Internet [DCBY99]. Body-scans and garment descriptions are too large to be transferred in reasonable times with dial-up. It is predicted that more than half of online

households will have broadband by the end of 2005 [Joh04]. In Europe more than half of the 100 million Internet surfers already use digital subscriber lines (DSL) or TV cable connection for broadband access [Reu04]. The growth of broadband is also reinforced by governments because it offers small and medium sized enterprises the chance to boost both innovation and productivity [EUB04].

Computer Controlled Garment Manufacturing – Advances in automatic cutting and knitting machines will be important for automating the production of clothes. Such technology is required to increase the accessibility of made-to-measure clothing. However, it is currently not possible to manufacture sewn garments in a completely automatic way because automatic sewing machines do not yet exist.

Electronic Garment Exchange Standard – While there are some standards for CAD systems, they are neither sufficient for the assembly of Virtual Clothing nor for the automatic production of real garments. Proprietary formats are currently in use that enable manufacturers automatically to create a garment piece directly from a CAD file. However, no standard has evolved yet. Additionally, in the times of peer-to-peer file sharing, such a standard would be feared by garment designers who would find it difficult to protect their intellectual property.

All of these complementary technologies will be required to ensure the success of Virtual Clothing technology. Access to some of this technology will be easy to gain; access to other areas will be harder to negotiate. Access to body-scanning technology would not involve any potential conflicts of interest, with both technologies highly complementary and mutually reinforcing. However, major risks are involved in body scanning technology companies developing their own Virtual Clothing solutions, contracting exclusively with an alternative source of Virtual Clothing technology, or failing to successfully distribute the body-scanning technology widely across the potential consumer base. Access to clothing and fabric design modelling technology is necessary in order to input the clothing data into the Virtual Clothing software. Currently, clothing designers and manufacturers tend to maintain their own design templates, so therefore all inputs for the Virtual Clothing technology would need to be standardised. Additionally, fabric data such as wear and drape would need additional modelling and inputs. Major risks involve resistance from clothing designers and manufacturers to make public their design templates and the difficulty in standardising Virtual Clothing inputs from multiple, proprietary clothing designs. Access to visual 3D graphical software/hardware is not considered to involve any potential problems. The technology is widely available and is continually becoming faster

at processing Virtual Clothing simulations.

8.8.2 Communicating the Value of Virtual Clothing to Resistant Customers

Targeting corporate customers (those that will implement the system) for Virtual Clothing technology must be handled carefully. Effectively communicating the value of this new technology to potential customers could also prove to be difficult. The introduction of a technology that may redefine a number of the traditional customer relationships and value chain activities must develop acceptance across as wide a customer group as possible. The value to a clothing purchaser is more tangible and less conflicting than the value to a clothing designer, manufacturer or retailer. Certainly, some clothing retailers may prove resistant to the technology given that it overlaps with services such as try-on, fit and promotion that are currently provided in physical shop space. Online retailers and those physical shop retailers with extensive design and manufacturing models may see value from the technology in allowing for both highly efficient and highly effective clothing promotion. Some designers may see the technology as a way of bypassing the big clothing merchandisers, but may also feel the technology encroaches on their creative space.

8.9 Capturing Value through IPR Protection and Licensing

Exploiting the technology will require careful protection of the associated intellectual property rights (IPR) and know-how. It is likely that a licensing model similar to that of other complementary technologies would prove appropriate. Using the technology to sell directly to clothing consumers goes far beyond the established competencies.

8.9.1 Licensing Contracts

Possible licensing arrangements could be formed with online retailers, whereby fees are paid to access the technology (on a web-site for example) and then some level of variable fee paid based on the number of clothing line items added to the technology or number of customer details. Alternatively, the technology could be licensed directly to clothing consumers, with customers paying fees each time they use the Virtual Clothing visualisation. However this would be more difficult to coordinate. Possible future licensing arrangements might include large clothing designers, manufacturers and retailers paying significant fees to access to large chunks of the technology to integrate into their own value chain.

8.10 How to Exploit the Technology?

Of the potential marketplace, it seems natural to adopt a modular strategy that incorporates not only the Virtual Clothing technology, but also body-scanning. Each phase of development is not necessarily affected by, nor is dependent upon, prior phases, and thus mitigates the risk of all future development being derailed by a failure to place one link in the chain correctly. The modular scheme is outlined below:

1. Provide anonymous body size information to national agencies allowing better standardisation of clothes sizing through body-scan data.

2. A revolution in cheap and easy body-scanning means that Virtual Clothing can be used to inform customers which stores currently offer the clothes that will fit them best. This allows them to see the exact nature of the fit through web based interactive visualisation of garments on their personal body shape. Customers can also then mix and match garments (from different retailers) to achieve the look they are seeking.

3. Garments custom manufactured to fit individuals.

4. Clothing design.

While it is only items 2 & 4 which require Virtual Clothing technology, item 1 has already begun to be introduced, and forms the backbone of "Size UK", the first UK national sizing survey since 1952, and the first anywhere to use 3D body-scanners as the principal means of data capture. Item 2 addresses the need to reproduce the sight, touch and feel experiences of brick-and-mortar stores for online apparel consumers. The clothing design sector (item 4) appears to offer a laterally dependent area of growth. Allowing designers to visualise how certain types of fabric might look when cut in a particular way removes the need for the preparation of costly prototypes and the sourcing of fit models of particular sizes on which the prototypes must be tested, as all of this can be done virtually. In order to assess which module it is best to exploit initially, we need to better understand the potential markets.

8.10.1 Is the Timing Right?

Although the time may not be right for a wholesale introduction of Virtual Clothing technology now, it seems likely that the pace of change is such that it is the right time to enter into negotiation with clothing manufacturers and retailers to discover what they would require from such a service. There also appears to be a requirement for dealing with the fact that body-scan data may have an unintended effect: it will force consumers to face up to their own body shapes, "warts

and all" [DCBY99]. While this may make some customers want to upgrade their wardrobes, others may give up on this type of shopping altogether. It seems clear that there is both enormous revenue potential in this marketplace and a demand for Virtual Clothing technology from the consumer; this is supported by the continued increase in adoption of broadband services in domestic residences. Customers no longer need take time out from their working day to conduct online purchasing at the office (these generally possess high-speed Internet connections, making the download of animated images much faster), but can now do so from the comfort of their own home. Convincing retailers to pro-actively respond to the growth in demand for broadband by providing content rich solutions for online apparel retail may prove the biggest stumbling block. While online catalogue companies such as Lands' End already have a business model that can support such a strategy, brick-and-mortar retailers may have to see further and more compelling evidence that this technology heralds a bright new future [DCBY99].

8.10.2 Market Entry Scenario

Detailed below are a number of market entry scenarios in which Virtual Clothing technology could be used. Graphs that describe the different stake-holders and their relationships are given. Figure 8.4 illustrates a time-line of the potential introduction and development of the different key technologies:

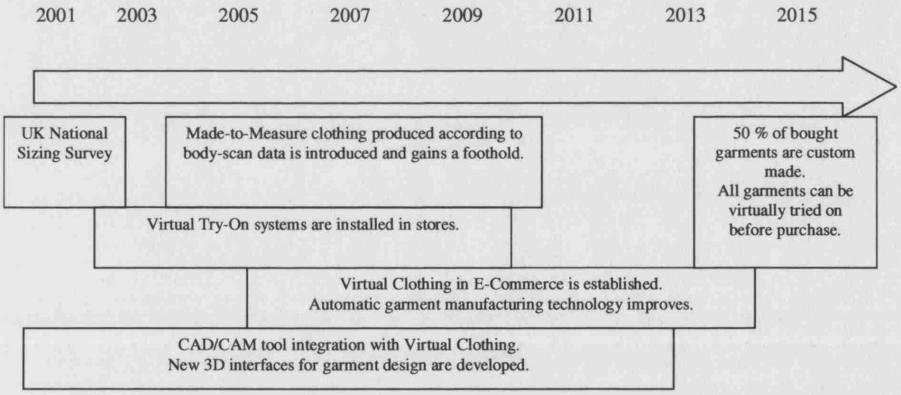

Figure 8.4: Timeline of known and predicted introduction of key technologies that are related to Virtual Clothing.

8.10.2.1 Virtual Clothing in a Department Store

The customer enters a department store as usual, but before trying on items in a changing room Virtual Clothing could help them to find the right item. The customer has a 3D scan taken and then uses a computer to browse through items in the virtual shelves before physically trying on the narrowed-down choice. This scenario will be mainly utilised to introduce the technology to

customers and most importantly create shop space availability for 3D scanners. A diagram of the stakeholder relationships is given in Figure 8.5.

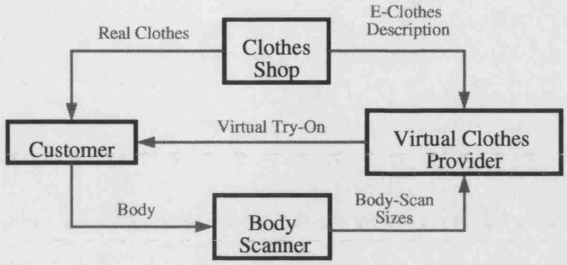

Figure 8.5: Virtual Clothing in a Department Store.

We identified the *E-Clothes Description* as the most critical relationship in this diagram. Clothes shops may provide real garments to the Virtual Clothes Provider for reverse engineering as described in Section 4.3. However, an *E-Clothes Description* standard is essential to make the technology accessible on a wider scale.

8.10.2.2 Virtual Clothing in CAD/CAM Systems

Virtual Clothing software is integrated into existing CAD/CAM tools so that garment designers can examine their designed cutting patterns directly in 3D on a mannequin or body-scan. As detailed in Section 8.7 this integration process is already in progress.

8.10.2.3 E-Commerce via Garment Retailers

The customer can access her/his body-scan from a central database after being scanned in a 3D scanner, e.g. in one of the retailer's nearby shops. The customer can browse Virtual Clothing realistically draped on their body-scan over the Internet and buy if satisfied. The retailer sends the ordered clothes to the customer by post. A diagram of the stakeholder relationships is given in Figure 8.6.

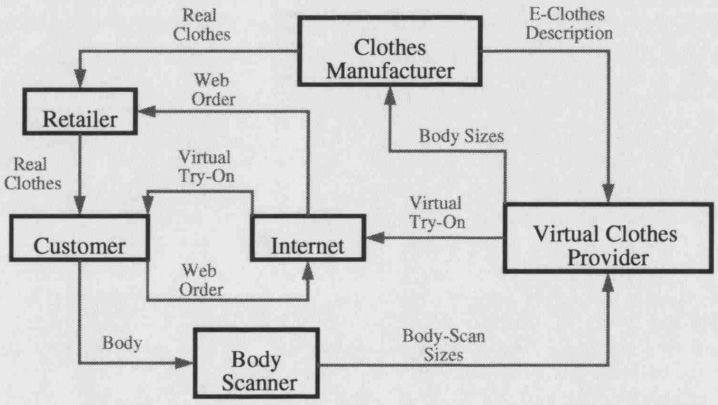

Figure 8.6: Virtual Clothing for E-Commerce.

In this diagram a new critical path can be identified, the *Virtual Try-On* over the Internet. While the developed system described in Section 5.5 was designed to be used on the Internet, it has not been tested thoroughly for such a scenario.

8.10.2.4 E-Commerce the Made-to-Measure Way

Garments are manufactured according to the customer's precise size. Before manufacturing, the customer can try-on the desired garment virtually over the Internet. Mall kiosks or garment shops could be used by customers to obtain body-scans. A diagram of the stakeholder relationships is given in Figure 8.7.

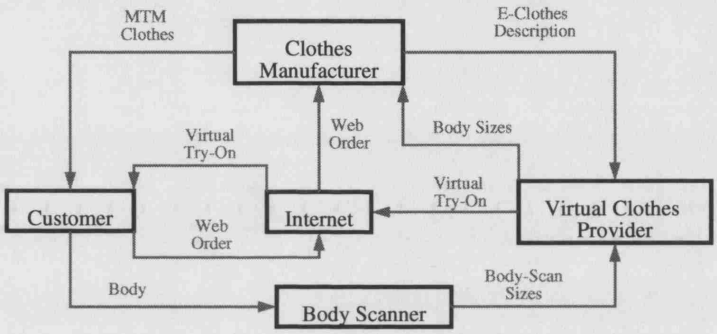

Figure 8.7: Virtual Clothing for Made-to-Measure inspection.

We identified *MTM Clothes* as the new critical relationship in this diagram. While manufacture of MTM clothes from scanned size data should not pose any problems, it requires technology that has been introduced only recently and therefore may cause initial problems.

8.10.2.5 From the Garment Designer Directly to the Customer

In this scenario, the garment designer directly communicates with the customer in order to offer different designs (which do not yet exist). The customers can then try-on these designs over the Internet using their body-scan. Once satisfied, the design is sent to the manufacturer and the mainly automatically produced garment is sent to the customer by post. A diagram of the stakeholder relationships is given in Figure 8.8. In this diagram we identified the *Desired Design Modifications* as a new critical relationship. Suggestions for design modifications by the customer may be purely text based but a Virtual Clothing system has the potential to offer more advanced 3D interactions between customer and fashion designer over the Internet.

8.10.3 Positioning of Virtual Clothing

The positioning of the Virtual Clothing technology venture is the final step in a 3-step process. Figure 8.9 breaks down this chapter's key findings at the levels of technology, commercial and business opportunity assessment.

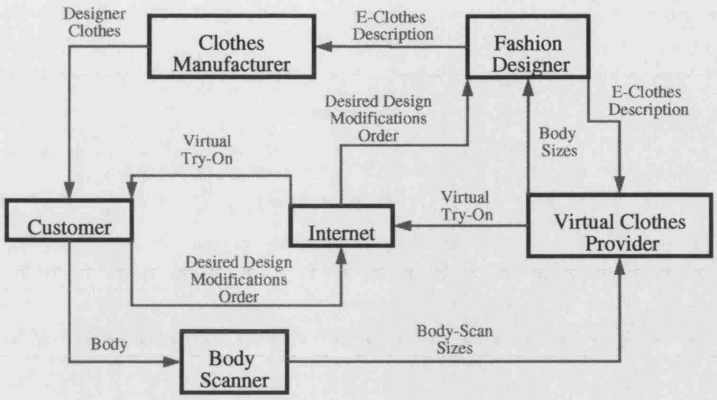

Figure 8.8: Virtual Clothing to Inspect e-Commerce Designer Clothing.

While the technological and commercial opportunities are now clear, the exact business case must balance three key features:

- The need to access customers and create availability of body scanning equipment.
- The need for partnerships with manufacturers to ensure availability of clothing/garment data.
- The need for commercial relationships to validate technology and create opportunities for future financing and scale-up.

These required key features are also illustrated in Figure 8.10. Determining who is in the best position to exploit the technology is difficult. It is clear that in the early stages of technology and market testing, the technology should be driven by the developer/entrepreneur. However, whether Virtual Clothing becomes a stand-alone platform in the long run is not clear. Unless the technology becomes an industry standard the likelihood is that a major online/high street retailer might be in the best position to fully exploit the technology, using it as a key source of competitive advantage.

Of the examined scenarios and applications, the most viable roll-out strategy for Virtual Clothing might involve a major retailing partner. A mass retailer with significant online presence, such as Gap or J.C. Penney, would be an ideal first customer for Virtual Clothing technology.

To illustrate the potential of such a strategy, the following case study is based upon a hypothetical partnership between BodyMetrics and Gap.

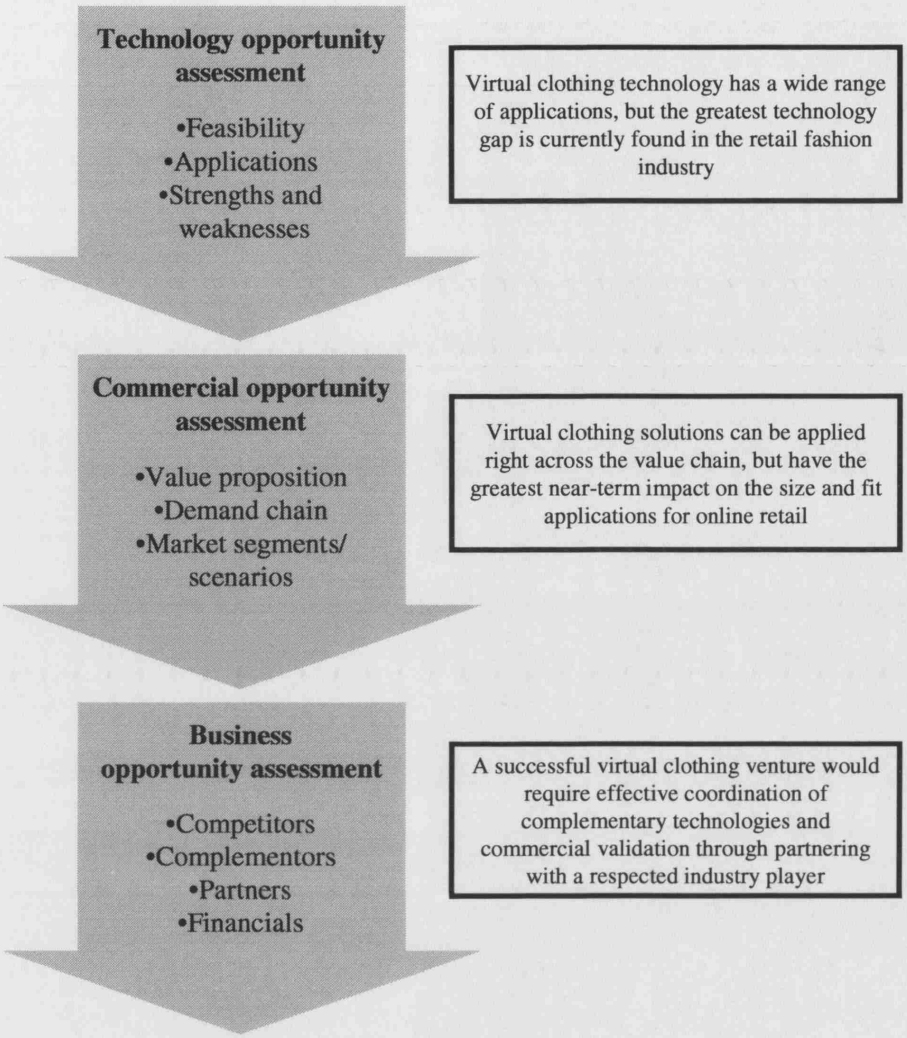

Figure 8.9: Key findings in the commercial evaluation.

8.10.4 Bridging the Gap

As a fully integrated clothing concern, Gap is involved in every step of the Virtual Clothing value chain and would stand to benefit tremendously from the technology. The sell into Gap would be staged, starting with the introduction of scanners and scanned merchandise in order to exploit the online benefits of Virtual Clothing. Although this is the endpoint of the value chain it is the easiest step to implement, and the potential gains are significant. Once the benefits of Virtual Clothing are established in this area, the other applications can then be pulled backwards, into the domains of Manufacturing and Inventory, as customised made-to-measure clothing would be the next step. Finally, moving back to R&D and Design would be the final step in pulling the full value from Virtual Clothing technology.

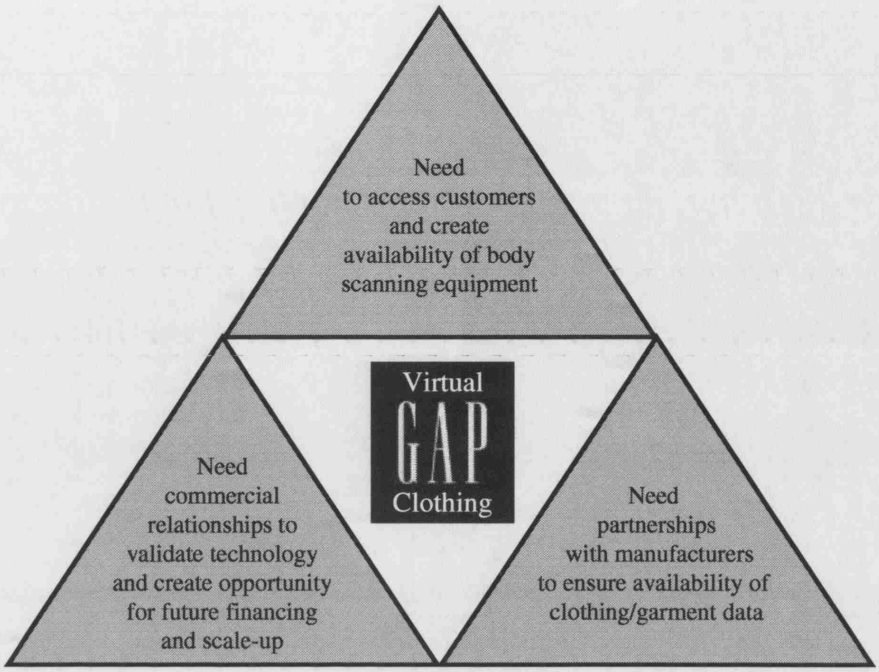

Figure 8.10: Partnership with a major online retailer.

8.10.5 Scaling

Having highlighted an effective market positioning for Virtual Clothing, a number of different business models can be considered. Each model describes different levels of scope and relative trade-offs in the risks and responsibilities of the two partners. While any number of models can be used, Figure 8.11 describes three viable product/service offerings for Virtual Clothing.

8.11 Financing and Partners

In this section we identify a potential partner, a major retailer, to introduce virtual clothing to a wider audience and we give financial projections for such a partnership.

8.11.1 GAP Inc.

A detailed profile of Gap can be found in Appendix D. The double presence of Gap in traditional stores and online cyberspace makes it an ideal partner for rolling out the Virtual Clothing technology. With over 3000 stores, Gap is in a good position to provide a large network of body-scanners without much additional investment in terms of rent and staffing costs. The fact that online customers will be able to return online purchases to neighbourhood stores will help to reduce customers' resistance to try the Virtual Clothing technology. The shopping windows of numerous physical stores offer good advertising space for "Gap's Virtual Clothing technology, powered by BodyMetrics" without much cost. This will allow Virtual Clothing technology

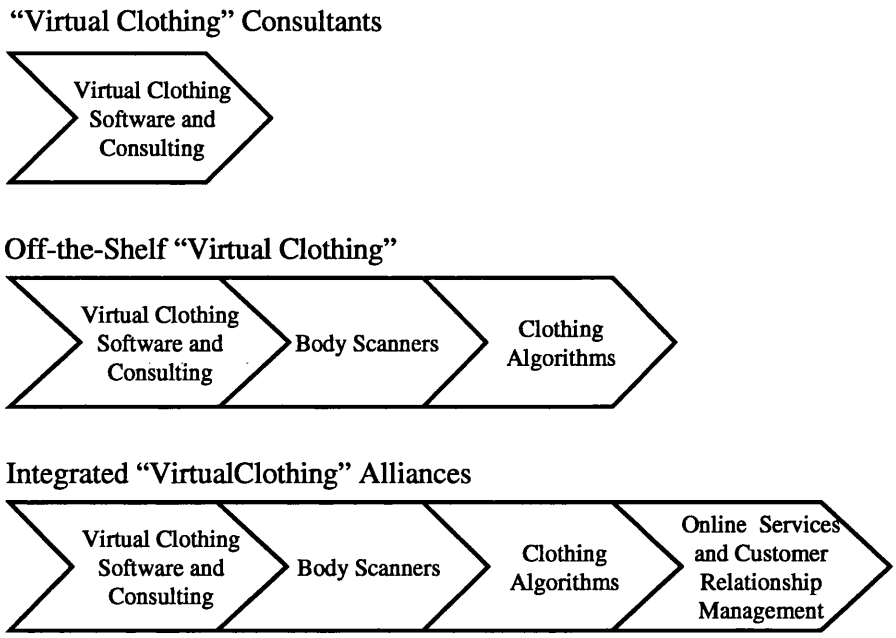

Figure 8.11: Business Models for Virtual Clothing.

to build the much needed critical mass to move on to the next phase. At the same time, Gap is ready to capture the expected increase in online apparel sales (42% expected growth in 2004 according to eMarketer Inc.) and becomes a leader in Virtual Clothing technology. Ultimately, success in this approach will help Gap reduce the number of traditional stores in the long term and improves profit margins. Further up the value chain, Gap will be able to improve its clothing designs based on updated body-size information collected during this exercise.

8.11.2 A Potential Financing Scenario

With these expected advantages, Virtual Clothing technology could be licensed to Gap at a fixed plus incremental licence fee for two years exclusively in the USA. A fixed licence fee of US$300,000 would provide initial cash required to employ technical support staff, develop a database for Virtual Clothing and body-scans and Internet servers to support the Virtual Clothing technology for Gap. The ongoing running cost will be financed by negotiating a 15% share of Gap's incremental profit on a monthly basis on additional online sales after the implementation of the technology. On the assumption that this arrangement is acceptable to Gap, BodyMetrics avoids selling cheap equity to venture capitalists at the early stage of development. The body-scanning data will belong to both Gap and BodyMetrics, and this should be stated in the licence agreement. To facilitate the technical support required by Gap during the initial implementation, technical support staff employed by BodyMetrics should be located in San Francisco to work closely with Gap's IT personnel. Since it will take time for body-scanners

to be ordered and installed in Gap's stores, we expect the first lot of fifteen body-scanners to be ready in July 2005 if a licence agreement with Gap can be reached before March 2005[7]. Gap and BodyMetrics together will decide the locations of stores to be the first to roll-out the body-scanning technology. One of the main factors to be taken into consideration is the existence of complementary technologies, as mentioned earlier. Another fifteen body-scanners will be added in October 2005. Depending on the utilisation of these scanners, the number of body-scanners to be installed in 2006 and early 2007 can be increased to thirty per quarter. By June 2007, the number of body-scanners in a single town can be increased to over 200. Once saturation levels of scanner installations are reached in a given location, new installation rates would fall with subsequent efforts limited to broadening the geographical coverage of scanning equipment. Gap, being the designer and manufacturer of the clothing, has ready access to cutting data and fabric property information of apparel sold over their web-sites. We believe that a minimum of five clothing scanners[8] will be required initially to make the Virtual Clothing data available online. In the second year, to push the use of our technology up the design and manufacturing chain, five clothing scanners will be added. To drive the popularity of the technology, the body-scanning services can be provided to Gap's customers free of charge. Since the data is stored on BodyMetrics' database and linked only to Gap's web-sites, the problem of free riders should not be a concern. With this arrangement, cash-flow projections for Gap specific to the adoption of Virtual Clothing technology are estimated as in Table 8.3.

[7]Thanks to David Bruner at $[TC]^2$ for giving us an estimate on the manufacturing and installation time of 3D scanners.

[8]Clothing Scanners are used to obtain garment information for GAP products in order to enable realistic assembly, simulation and visualisation of virtual garments (as described in Section 4.3). Ideally, clothing scanners are installed near the garment manufacturers to reduce logistics (instead of sending the real garments to the scanners from the manufacturers).

Year (US$'million)	2H2005	2006	1H2007
Cash Inflows			
Increase in online sales revenue in Gap (vs. 2004) (Note 1)	5.61	24.30	33.64
Gross Profit Margin in Gap Inc. (based on annual report)	38%	38%	38%
Increase in Gross Profit Margin in Gap Inc.	2.11	9.14	12.65
Incremental Fulfilment Cost (assume 15% of sales)	0.84	3.64	5.05
Incremental Marketing Cost	0.20	0.50	0.1
Incremental Operating Cost	1.04	4.14	5.15
Incremental Profit (before interest, depreciation, taxation)	1.07	4.99	7.50
Less: Taxation (assume 39%)	0.42	1.95	2.93
Incremental Profit (after taxation)	0.65	3.04	4.58
BodyMetrics' share of Incremental Profit (%)	15%	15%	15%
BodyMetrics' share of Incremental Profit (US$'million)	0.10	0.46	0.69
Gap Inc's Retained Incremental Profit (US$'million)	0.55	2.59	3.89
Cash Outflows			
Less: Initial Licence Fee for Technology	0.30	-	-
Less: Increase in Capital Expenditure in Gap (Note 2)	0.93	3.63	1.80
Total Cash Outflow	1.23	3.63	1.80
Net Cash-flows	(0.67)	(1.04)	2.09
Cumulative Net Cash-flows	(0.67)	(1.71)	0.38

Table 8.3: Cash-flow projections for GAP Inc.

(Note 1) We assume: (1) Gap's online sales is US$445 million in 2004, (2) lost sales owing to uncertain size and returns is 42% according to market research by E-BuyersGuide.com, (3) 3% of the lost sales mentioned in (2) are captured in the second half of 2005, an additional 10% in 2006 and then 5% in the first half of 2007, respectively.

(Note 2) We assume fifteen and then thirty (in the second half of 2005, 2006, and the first half of 2007 respectively) body-scanning machines are introduced each quarter at the cost of US$25,000 each and US$5,000 incurred in store renovation. Five Virtual Clothing scanners are introduced in 2005 and 2006 respectively at the cost of US$5,000 each. Although the cumulative net cash-flows generated to Gap through e-commerce in the two years is not very significant, the body-scanners are assets not fully depreciated at the end of the licence period. The value Gap obtains through mastering updated body size data and in the design process has not yet been quantified and is therefore not included in Table 8.3. Nevertheless, the culmulative cash flow for GAP is positive at the end of the three-year period. Cash-flow projections for BodyMetrics specific to the licensing arrangement with Gap are estimated as in Table 8.4.

Year (US$'million)	2H2005	2006	1H2007
Cash Inflows			
BodyMetrics' share of Gap's Incremental Profit (US$'million)	0.10	0.46	0.69
Initial Licence Fee from Gap Inc.	0.30	-	-
Total Cash Inflow	0.40	0.46	0.69
Cash Outflows			
Less: Royalty fee to UCL (assume 3% of Revenue)	0.01	0.01	0.02
Less: Database Server Initial Set Up Cost	0.10	-	-
Less: Server Hiring Costs (assume $1000pm)	0.01	0.01	0.06
Less: Technology Support Cost	0.20	0.25	0.15
Less: Continual R&D Expense (assume 10% of Revenue)	0.04	0.05	0.07
Total Cash Outflow	0.36	0.32	0.30
Net Cash-flows	0.04	0.14	0.39
Cumulative Net Cash-flows	0.04	0.17	0.56

Table 8.4: Cash-flow projections for BodyMetrics Ltd.

With the above projections, significant value for Bodymetrics can be built out of Virtual Clothing technology at the end of the two year licence period. If we assume a Price / Free Cash-flow ratio of 20, the value of this venture at the end of the two year licence period in mid 2007 will be in the region of US$7-8 million. Gap has been chosen for the reasons stated above but, it is not the only possible partner. Other major retailers, with significant double presence in physical stores and cyberspace, who target mass markets in technologically advanced countries are also possible candidates. It is most important to make the technology popular and to build critical mass. Only after that has been achieved can we expect "viral effects" [9] and significant increases in application and revenues. With an established technology and sizeable body size database, BodyMetrics will have more financing options to further develop this venture in mid 2007. Depending on market sentiment, the actual valuation recognised and the expected growth rate at that stage, BodyMetrics will be in a position to consider either:

- to continue the licensing arrangement with Gap and extend the relationship to other major retailers, or
- to raise funds from venture capitalists to speed up the introduction of Virtual Clothing

[9]The term "viral effect" was used in the Havard Business School Case "Zaplet, Inc.(A)" [LD01] to describe the rapid growth of HOTMAIL which spread to 11 million users in 18 months. This growth rate is believed to be mainly owing to the automatically attached message on the bottom of each sent email "GET YOUR FREE E-MAIL AT HOTMAIL.COM".

technology.

To motivate Gap to share its Virtual Clothing experience with future retailing partners, BodyMetrics could offer up to 2% equity in this venture to Gap Network externality. Following a good valuation, money raised from venture capitalists will help finance the recruitment of a quality management team to market the technology to a much wider range of apparel retailers, and will bring the technology to more countries that are technologically advanced.

8.12 Conclusions

While Virtual Clothing can improve the believability of computer games and can help to create amazing effects in movies, the main potential for the commercial application of the system we have developed is in online apparel retailing and garment design. In combination with 3D scanning technology, Virtual Clothing can help garment shoppers to find the best fitting clothes. This will increase online apparel sales and reduce the number of items returned. 3D scanning technology can also be used to create made-to-measure clothing that can be inspected in virtual reality before manufacturing. Such technology will improve streamlining from CAD to possibly automatic garment manufacturing. The learning curve to produce Virtual Clothing technology is high but, on the other hand, it will be difficult for Virtual Clothing companies to sell their own CAD tools because garment designers will probably need a good reason to change from tools they know best. This is why some companies that create CAD/CAM tools team up with specialised Virtual Clothing companies. The complementary technology required for Virtual Clothing (CPU power, Internet speed, graphics hardware) is only just becoming powerful enough for online retailing. Companies that build a body-scan database of customers and implement the full Virtual Clothing solution will have a competitive advantage over those that do not. BodyMetrics' successful pilot test at Selfridges already bears out the feasibility of this technology. With several thousand scans already in this consumer system, the technology is ready to be rolled out to a larger audience. The business case outlined in this report will, however, meet with a number of key challenges over the coming 2-3 years. BodyMetrics could face problems in inter-nationalising its operations. With a research and development effort based at UCL and a likely key partner and customer-base located in the US the management and coordination of technology and commercialisation will be challenging. Either senior managers spend an excessive amount of time on aeroplanes or the integral relationship between development and marketing is compromised[10]. Creating the right relationship with a leading retailer such as Gap will be difficult. Both parties will require incentives, but BodyMetrics must be careful

[10] As was in evidence in the Harvard Business School case "Spotfire" [KE00].

not to surrender too much control in order to remain free to scale-up operations for an industry-wide service launch once the exclusive license with Gap is concluded. Getting the right partner without giving away too much of the value is critical for BodyMetrics' future success[11].

[11] As was in evidence in the Harvard Business School case "Elliot Lebovitz" [GT98].

Chapter 9

Conclusions and Future Work

In this chapter we state again our hypothesis and we summarise the extent to which the sub-clauses are met and to which we have failed to falsify the hypothesis. We summarise our main contributions and briefly comment on their significance. We recapitulate the technological opportunities, the commercial possibilities and barriers. Finally we discuss potential future work.

9.1 Our Hypothesis

Our Hypothesis was:

"*existing cloth modelling and visualisation techniques can be extended and developed in order to enable us to build an apparatus for fully automatic virtual try-on that creates realistic images of clothes on scanned people in an on-line manner*"

Our commercial installation of an apparatus for fully automatic virtual try-on of garments that demonstrates the feasibility of the technology indicates that our main hypothesis, cannot be falsified. In the following sub-sections we summarise to what extent our sub-clauses are met.

9.1.1 Existing Cloth Modelling and Simulation Techniques

In Chapter 2, we identified the drawbacks of existing cloth modelling and simulation techniques. In particular, we identified the main issues of numerical integration, stability of stiff cloth and realistic drape behaviour. In our Directional Velocity Modification method, described in Chapter 3, these issues are to some extent overcome. A mathematical evaluation of the stability of the method remains to be carried out, however.

Collision detection proves to be a bottleneck for dynamic simulation. Hierarchical and uniform spatial subdivision strategies are commonly used to improve speed. However, these techniques can still be slow and memory intensive. With Image Based Collision Detection, described in Chapter 3, we propose a solution to the problem of cloth-body collision detection

which is fast and does not require much memory. A comparison to a traditional object space based approach showed that our method is two to three times faster. It only requires two RGB and two depth images with a resolution of about 350 × 350 pixels for an accuracy better than 0.5 cm as detailed in Section 3.2.5.

9.1.2 Existing Visualisation Techniques

In the second part of Chapter 2 we summarised visualisation and reflectance modelling techniques that have been used to create fairly realistic images of clothing. Such techniques can generate amazing images but they are slow and, owing to memory requirements for storage of reflectance data, they cannot realistically render a whole garment without distracting texture repetitions. In Chapter 4, along with a garment exchange format, we introduce a reverse engineering technique that enables us to acquire realistic texture information from real garments. In addition, this technique allows us to extract cutting patterns and assembly information for our virtual garments in a semi-automatic way. Since the garment description can be prepared off-line, manual intervention at this stage still permits a fully automatic virtual try-on system. Visualisation that portrays a garment as closely as possible to that of a photograph is only one aspect of customers' and designers' requirements of such a system.

9.1.3 Enable us to Build

In our installation, we utilised a scanning system from the $[TC]^2$ company in order to build the virtual try-on apparatus. The scanning system provides functionality for the construction of the body surface and important body landmarks are automatically extracted. Our garment visualisation system uses this information automatically to pre-position garments around the body before virtual sewing. Details are given in Section 4.4.2. We process the body-scans to be suitable for virtual try-on of clothes as described in Section 7.2.1.

9.1.4 Fully Automatic

For our systems there is no manual intervention required to place the garments around the virtual body, as is the case for garment modelling tools [FGLW03]. Our system is thus fully automatic. This is possible because we are using landmark data which is automatically extracted from the body-scan data. However, our system is run by an operator who is available to give additional advice on the style and fit of the garments.

9.1.5 Apparatus for Virtual Try-On

Our apparatus for Virtual Try-On is the combination of a body scanner with our dynamic simulation and visualisation of Virtual Clothing into one system. In addition, the apparatus is built

on Internet technology, as described in Section 5.5, which enables customers to access their body information also from their home PC virtually to try-on clothing.

9.1.6 Realistic Images of Clothes

The commercial success of the installation described in Section 7.2, with several thousand customers who have used the system, indicates that the degree of realism achieved by the system is sufficient. A large scale experiment to evaluate the realism of the images remains work for the future although we have carried out a pilot study, described in Appendix A.

9.1.7 On Scanned People

As mentioned in Section 7.2, owing to the type of garments in the database, the virtual try-on apparatus has only been extensively used for female customers with a fairly normal body-shape. We cannot identify any reasons as to why the system might not work with children or male customers. In fact, we have carried out such simulations as shown in Chapter 6.2. However, the system has not been tested as extensively for such subjects as it has been for women.

9.1.8 In an On-Line Manner

Obviously the time required to construct the body surface and to extract body landmarks depends on the computational power of the machine and the software that carries out this task. In our virtual try-on apparatus a low end PC supplied with the $[TC]^2$ scanner is employed for this purpose and the time for processing the body-scan takes less than 30 seconds. Fitting a virtual garment onto a body-scan is achieved in one to two seconds on a high end 3GHz PC. A customer may therefore try-on garments virtually as soon as she is dressed again. Because of the fast speed of the simulation it is possible to try-on far more garments virtually than would be the case were real garments physically tried-on and taken-off.

9.2 Contributions

In this section we summarise our main contributions and we briefly comment on their significance.

9.2.1 Image-Based Collision Detection for Cloth Simulation

We have introduced a novel image based technique for collision detection. The technique uses state of the art graphics hardware for cloth-body collision detection and also for collision response. The approach is described in detail in Chapter 3. Our detailed evaluation in Section 7.1 shows that the performance of a traditional collision detection method can be improved by at least a factor of two by using the IBCD technique. The number of publications that have

cited our approach indicate the significance of it is high. In particular, owing to the fact that the computational complexity of the technique is independent of the number of triangles on the body-model used in the garment simulation, the approach is very well suited for use with body-scan data.

9.2.2 Method to Compensate for Super-Elasticity Effects

We have shown that our directional velocity modification approach, described in Section 3.1, efficiently overcomes the super-elasticity phenomenon of a traditional mass spring system. The efficiency of the approach was demonstrated in Section 7.1 and we presented images of clothing simulated with this technique which show that it generates visually pleasing images for local, global, static and dynamic deformations. However, a full mathematical evaluation of the stability properties of this technique remains to be carried out. It is clear that implicit integration can provide more stable simulations for very stiff materials but at the cost of fabric that behaves as unrealistically damped [VMT01] for simulations with large time steps.

9.2.3 Reverse Engineering Approach for a Realistic Garment Description

We have developed a technique that enables us to obtain data from real garments to simulate Virtual Clothing that appears fairly realistic. The degree of realism is hard to quantify but it proved to be satisfying to thousands of clothes shoppers who used the system. We use high resolution digital photographs of the real garments in order semi-automatically to extract virtual pattern, assembly and texture information. Since such information is often not available for garments one can buy in a shop, this technique represents a key part of the virtual try-on system. In this reverse engineering approach the data is obtained in a pre-processing step and therefore the fact that this step is semi-automatic still permits a virtual try-on system that is fully automatic.

9.2.4 Installation of a Fully Automatic Virtual Try-On System

The exploitation of the developed techniques in the fully automatic virtual try-on system, which was installed at Selfridges, was a brilliant opportunity for us not only to demonstrate the robustness of the developed methods, but also to test the feasibility of the technology in a commercial set-up. Several thousand customers have used the system and they are willing to pay for the service. In Chapter 8 we evaluate the commercial potential of Virtual Clothing by identifying the main competitors, by investigating the complementary technologies and by proposing a market entry strategy. We conclude that a partnership with a major garment retailer could lead to a multi-million dollar business.

9.2.5 Commercialisation

Virtual Clothing is a paradigm-busting technology that has the potential to revolutionise many aspects of the entire apparel industry, from garment design to manufacturing, marketing and retailing. We believe that a partnership with a major garment retailer will be a key market entry strategy to make Virtual Clothing a technology easily accessible to the general public. Key complementary technologies such as digital imaging, body-scanners, performance of CPUs and graphics cards, and broadband Internet access are now maturing and improving at a rapid pace. One major barrier still to overcome will be a standardisation that will enable designers, manufacturers and retailers to exchange garment descriptions electronically. Such a standard will have to be sufficiently detailed for Virtual Clothing simulation. Our garment exchange format described in Section 4.1 could present a first step towards such a standard. A study based on the customers that have used the virtual try-on installation at Selfridges will be useful to identify the main requirements for improvements. Such improvements may be necessary for a wide customer acceptance of this new technology.

9.3 Future Work

In this section we give an outlook on possible future developments of the techniques described in this thesis.

9.3.1 Dynamic Simulation and Garment Fit Feedback

For dynamic scenes with known animation sequences the performance of IBCD could be improved significantly by pre-computing the required collision buffers as discussed in Section 7.1.

Improvement of stability and performance of a dynamic simulation may still be possible. In particular, fast finite element methods [EKS03] for continuous models and hybrid implicit-explicit integration methods [BA04] for mass spring particle systems are still active research areas that aim to improve stability and performance of cloth simulation.

According to "The Technology Network" [Rob02], Moore's law is currently outpaced three times by the development of graphics hardware resulting in a doubling of the performance of such systems every six months. Researchers [BFGS03, KW03] have started to exploit the increased parallel processing power of graphics processor architectures also for dynamic simulations. They have introduced a method to implement a conjugate gradient solver, often used for implicit integration, on graphics hardware. Krueger et al [KW03] claim that matrix and vector operations can be executed twelve to fifteen times faster on a graphics processing unit (GPU) than they are on the central processing unit (CPU). However, they simulate fluids,

rather than clothing. We believe, however, that in the near future, it will be possible to perform garment simulations entirely on graphics hardware. Other visibility tests, similar to the depth buffer approach presented in this thesis, such as the visibility pre-processing for self-shadowing described in [SSK03] may also be used for cloth-cloth collision detection on future graphics hardware. A step in this direction was made by Baciu and Wong [BW02].

9.3.2 Visualisation

In our augmented reality scenario we used the RADIANCE rendering system to generate realistic looking images. Since the images were created off-line, rendering performance was not an issue. Recent implementations on graphics hardware [SAFe02] of applications such as shadow buffers and shader programs will enable researchers to develop more realistic garment visualisations in real-time in the near future.

9.3.3 Evaluation of Realism

A major challenge for future research in Virtual Clothing will be to quantify as to how closely the garments simulated behave in comparison to their real counterparts. One step towards such a comparison was made in Section 7.3 of this thesis where we described methods to generate images of virtual garments in the context of a real scene.

Experiments similar to the one described in Appendix A towards quantitatively evaluating the quality of a simulated garment will help us to identify in which direction it would be best to focus research to improve simulation and visualisation quality.

9.3.4 User Interface

There are many possibilities to improve the interface between customer and garment simulation. One step will be animation, which will allow a user to obtain a better idea of the way the garment behaves when he or she moves. This could be achieved by applying motion capture data to the body scan in the manner described in Section 6.2.

Simulation data, such as the percentage of sewn points as mentioned in Section 4.4.3, or that obtained by using a false colour visualisation as described in Section 5.3.1, could be used to provide customers with additional fit-feedback.

Observation of the developments in tactile and force feedback devices [Bur96], suggests that customers will not be able to touch or feel virtual garments in the foreseeable future. However, first steps in the direction of generating tactile feedback for fabrics with a state of the art device, a PHANToM with a pen like probe, were recently reported by Metaxas et al [HMG03, GGHM03].

9.4 Summary

In this thesis we have shown that it is possible to develop techniques that allow a person to try-on clothes virtually. The integration of the developed techniques with a 3D whole body scanner has resulted in the world's first fully automatic virtual try-on system, which is commercially available in a department store in London. In particular, we have developed techniques that harness state of the art graphics hardware for the dynamic simulation of garments. Researchers have already started to develop some of the presented techniques further. We believe that future work will concentrate on methods that will allow us to realistically simulate and visualise whole garments entirely on graphics hardware. Evaluation of the realism of such simulations remains a challenging area of future research. From our observation on the commercial potential of Virtual Clothing we conclude that the technology will be available to a wide customer audience in the near future. Electronic commerce, however, only presents one market segment of the value chain of the apparel industry. We believe that Virtual Clothing will have an impact on all segments of that value chain and will revolutionise the way garments are designed, manufactured and sold.

Appendix A

Pilot User Study

In order to move towards quantifying the quality of the garment images generated, we prepared a pilot user study. Our goal was to investigate how we might identify the factors that contribute most to the perception of realism of images of garments. The garments used for the pilot were the designer jeans that we modelled for the commercial set-up at Selfridges, described in Section 7.2. We created images that would allow us to investigate how to test the factors: light simulation quality, dynamic simulation quality, and texture image quality. The different garment images were presented to subjects for different periods of time on a web-based interface. While the pilot experiment was carried out primarily in order to test the viability of the set-up we also carried out statistical tests on the gathered data. However, whilst the methodology of the pilot seems sound, given the number of responses obtained, no statistically significant results could be found.

A.1 Background

Our pilot user study is most similar to the research carried out by Rademacher et al [RLCW01]. They described an experimental technique designed to enable them to measure which visual factors are most important in order to make people believe that a computer generated image was real. Rademacher et al carried out a series of controlled human subject experiments. The experiments were set up to cover the visual factors: shadow softness, surface smoothness, number of objects, variety of object shapes and number of light sources. In their set-up, subjects were asked whether the presented image was computer generated or a photograph[1]. What the subjects did not know was that all images shown were photographs of a real scene which was carefully set up to allow them to vary the factors in the different images. They gathered statistically significant results, in particular that people tend to believe that images with sharp shadows

[1]They chose a binary response variable so that subjects only needed to maintain a single internal differentiation threshold.

and images with very smooth surfaces are computer generated. In their experiment no significant results could be inferred from the tests with images in which the following factors were varied: number of objects, variety of shapes, and number of light sources. They claim they obtained similar results when they carried out the experiment with exclusively computer generated images [RLCW01].

A.2 Factors

We chose the following image generation factors to be tested in our pilot experiment:

1. *Light simulation quality*: Varying this factor changes the fidelity of light simulations. Changing the quality influences the settings of the light simulation system. One quality factor varies the sampling resolution of the light rays. A low sampling resolution can create artefacts in the image generated but simulation time is low. Another light simulation quality also influences the accuracy of light interactions between materials. This interaction quality is controlled by the number of diffuse inter-reflections simulated. It also has an effect on the quality of shadows between objects and between folds of the cloth. Both lighting parameters were summarised to three levels (low, medium and high) in an appropriate way[2] .

2. *Dynamic simulation quality*: We assumed that an increase in the resolution of the mass spring mesh of a garment improves the quality of the dynamic simulation. A low resolution permits very fast simulation but the realism of the appearance of a garment suffers. Low resolution does not allow the simulation of accurate wrinkles and some areas of a garment may appear flat. Dynamic simulation quality was also summarised in three levels (low, medium and high) where each level corresponds to a particular mesh resolution.

3. *Texture quality*: The accuracy of fabric texture highly influences the realism of the final garment image. If garments are simulated on a customer's home PC the size of the garment texture images significantly contributes to the download time required to retrieve the whole garment description. Typically, fabric textures are encoded as JPEG images. JPEG encoding allows lossy compression which influences the file size and image quality. Texture quality was similarly summarised in three levels (low, medium and high) by varying the quality setting of the JPEG compression.

[2]The level's quality is defined by the low, med and high setting of the RADIANCE "rad" command which adjusts the direct and indirect sampling parameters of the RADIANCE light simulation system.

A.3 Image Generation

From the installation at Selfridges, described in Section 7.2, we had highly realistic models of four brands of designer jeans which we also used for this experimental set-up. The jeans models in the size that fit best were virtually tried-on a randomly chosen body-scan. Light sources were extracted from a natural indoor light probe image (see Section 5.6). The images were generated of all four brands in all possible combinations of quality levels from a single view. In order to add view variety without changing the contents of an image we flipped each image horizontally as well. Since we were only interested in the perception of realism of the appearance of the garment, background and scan were removed from the image and filled black. Altogether the four brands, three levels of light simulation quality, three levels of mechanical quality and three levels of texture quality from two views (horizontally flipped images) led to the collecting of 216 images. An example image of a jeans brand in the three levels of cloth simulation quality is depicted in Figure A.1.

Figure A.1: Cloth simulation factor levels varied by changing the mesh resolution of the mass spring particle system from left to right: Low, Medium and High.

A.4 Experimental Design

As in [RLCW01] we also chose a binary response variable. Subjects could choose between "photograph" or "computer generated". Experimental design strategies were used to generate the necessary permutations of brand, view and image quality levels[3]. The aim in permutating the images is to get a good mix of variety while at the same time covering all the main factors with as few subjects required as possible. In addition, since we assumed that subjects could always, after carefully studying it for some time, identify that an image was computer generated we added as another factor to our design, image presentation time. Image presentation time has been used in psychology vision experiments for a long time [Wat86]. Because of the instrument

[3]Thanks to Mel Slater for discussions about the experimental design and analysis.

typically used for such experiments, these are called tachistoscopic experiments. With the above proposed factors the experiment would have to be performed by over 200 subjects[4] to find statistical significance between the factors.

Since we were mainly interested in the influence of the dynamic simulation on the realism of appearance we decided only to test the mechanical accuracy factor with two levels, low and high in our pilot study.

A.4.1 Experimental Process

The pilot experiment was, as mentioned above, web-based. The initial web-page contained a welcome text to introduce the subject to the experiment. This page is shown in Figure A.2. Then, in a short pre-questionnaire we asked questions to gather information about the subject's gender, age, computer knowhow, amount of computer game playing, knowhow about computer generated images, and knowhow in garment design. Our pre-questionnaire page is shown in Figure A.3. Following the pre-questionnaire the subject was given instructions to continue with the experiment. These instructions are depicted in Figure A.4. Then, once the subject had chosen to start the experiment a randomly chosen[5] image was presented for a short period of time. The start page is depicted in Figure A.5. Before each image stimulus a countdown from three to one was shown to allow the subject to be prepared for the image. Figure A.6 depicts the last digit of the countdown.

In the Tachistoscope, four images were shown for a very short period of time (between half a second and a second) and four images for a longer period of time (between two and three seconds). A pair of jeans in our Web tachistoscope is depicted in Figure A.7. We assumed, owing to the very similar appearance of the images, that as the experiment proceeded we would obtain an increasingly random response because subjects may quickly become bored. Thus, we chose a small number of image stimuli for each subject. After the images were presented subjects were asked to write their comments about the experiment.

A.4.2 Data Collection and Analysis

The experiment was carried out with Internet technology for questionnaires, image stimuli and for data collection of the subject's responses. Common Gateway Interface (CGI) Perl scripts

[4]We assume that each subject is presented about eight images. A rule of thumb estimate in experimental design is to obtain responses of between five to ten times the number of stimuli available. The number of subjects could be reduced by presenting more images to one subject. However, owing to the similarity of the images we expect subjects to become bored quite quickly by the task and hence that they may start to respond randomly.

[5]Dependent on the sequence number of the subject the images were loaded from a pre-computed permutation to make sure all combinations of factors affecting the images were tested.

were used for the generation of stimuli permutations, to alter the required web-pages, to collect subject responses and to prepare the collected data for analysis. The resulting data was prepared ready to be loaded into the statistics tool GLIM [FGP93]. Logistic regression analysis was used to evaluate dependencies between quality levels and the subjects' responses.

A.5 Results

The experiment was only a pilot to test the feasibility of the approach. Thus, the experiment was carried out with ten subjects from the Virtual Environment and Computer Graphics group of the Department of Computer Science at UCL. This was mainly to test the experimental set-up and to eliminate possible error sources in the presentation and data-collection systems. Subjects used their work PC to do the experiment. Individual PCs had some differences in graphics settings (screen resolution and colour depth). This information was collected from the client PCs to allow us to analyse their influence on the subject's responses. Ideally, the experiment would be carried out on systems with identical display settings for all subjects but this clearly cannot be guaranteed for a web-based experiment. The number of subjects was not sufficient to allow us to find statistical significance in the data. Simple frequency counts showed that 30% of the images were perceived as photographs. This number is not representative of what might be obtained in a full web-based experiment not only because we did not obtain any statistically significant results but also because all subjects were computer graphics experts. From the comments we obtained from the feedback we were not encouraged to continue with this experiment on a larger scale in a more controlled environment. This was because some subjects could identify rendering artefacts in all the images and correctly judged all images as computer generated. In addition, some subjects commented that all images were at least edited on a computer because the background was removed.

A.6 Conclusions

We set-up a pilot experiment in order to investigate how we might try to identify the factors that influence the perception of realistic images of garments. We identified three factors we were interested to test: light simulation quality, cloth simulation quality, and surface texture quality.

Since testing all three of these factors, each at three levels, at a number of different presentation times on each of the four different brands of clothing, seen from two views would require a very large number of images to be presented to many subjects, the pilot study was restricted to just two levels of mesh quality in order to test the feasibility of the approach. A single brand of jeans was used, as illustrated in figure A.1. But since eight stimuli were presented to each sub-

ject (the two mesh resolutions, were each presented two times at each of two different durations of display to each subject), both views were utilised in order to retain the subjects' interest. Ten computer graphics researchers volunteered as subjects which we had expected to be sufficient to generate statistically useful results in this restricted trial. Unfortunately, this turned out not to be so, with the statistical analysis using GLIM yielding no results of sufficient statistical significance. From inspection of the data and study of feedback from the subjects, it would seem that variation in the display monitors used even within our laboratory was a problem. Moreover, it would seem that some subjects could always tell that the images were synthesised, or they treated any signs of editing, such as background removal as indication of computer generated imagery.

Our conclusion therefore is that if the experiment is to be carried out to test all the factors of interest, a very large study will be required, with very careful presentation of the images and definition of the response categories. In order to carry out a study of the required size, the experiment could be carried out on the Internet, if we could make sure that all subjects use similar computer and display equipment or if sufficient responses were collected to allow us to treat monitor variation as a separate factor or factors.

Since we have been unable to overcome these problems and set-up a valid user study of this kind, we note that alternative quantitative approaches should perhaps be considered. Ideally, such an approach would be developed in conjunction with a valid user study in order to provide a firm baseline for interpretation of the quantitative image quality measures to be used. Unfortunately, establishing what quantitative quality measures are appropriate seems itself to be a difficult problem.

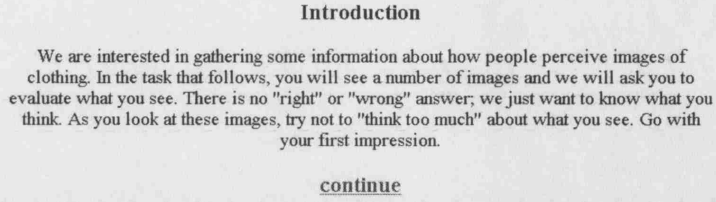

Figure A.2: Introduction to our Web-based user-study.

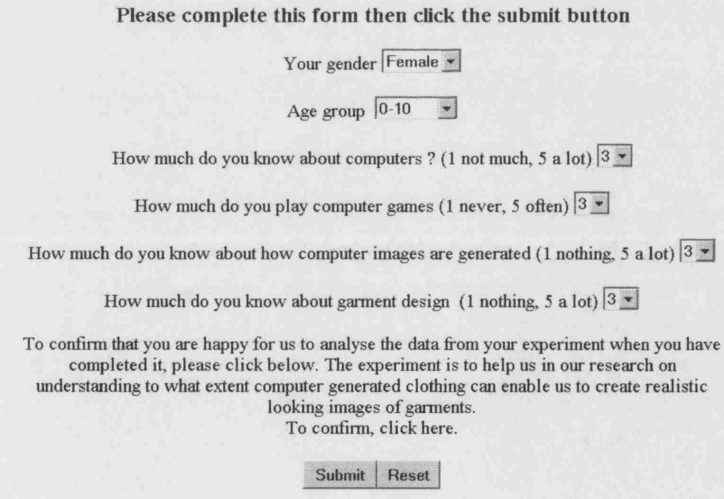

Figure A.3: Pre-Questionnaire of our Web-based user-study.

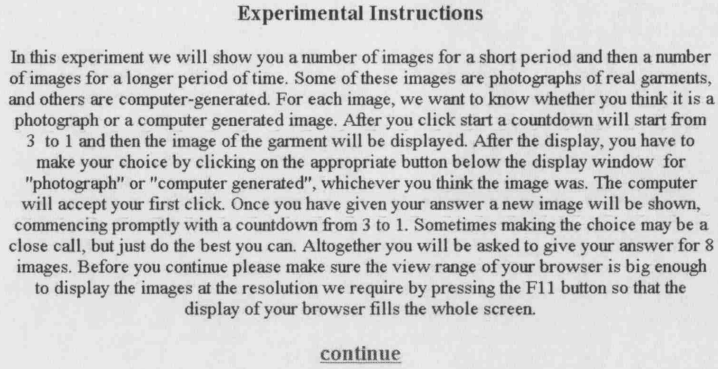

Figure A.4: Instructions for our Web based user-study.

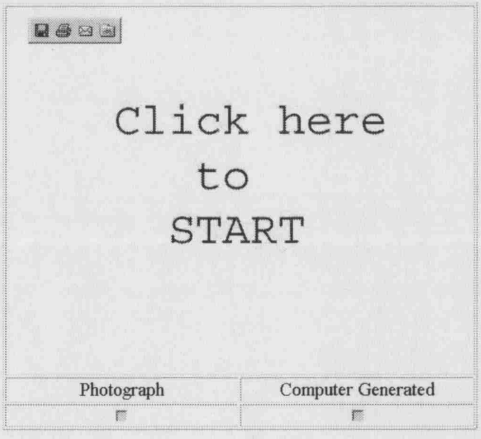

Figure A.5: Start-page of our Web-based user study.

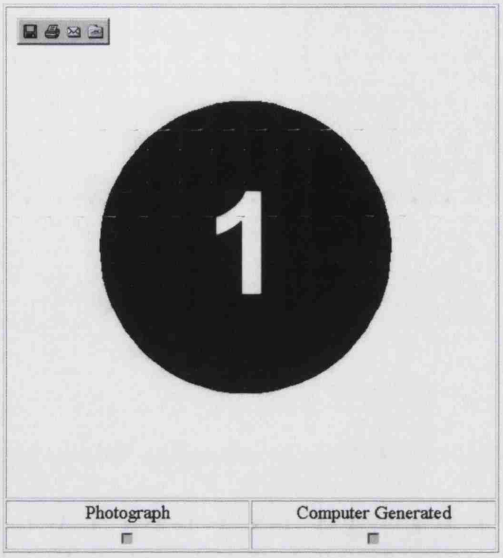

Figure A.6: Last countdown digit (from three to one) of our Web-based user study.

Figure A.7: A pair of jeans in our Web-tachistoscope.

Appendix B

Newspaper and Magazine Articles

In this appendix we list newspaper articles that were published to describe the virtual try-on installation at Selfridges, detailed in Section 7.2.

Figure B.1: The Evening Standard 14th May 2003.

Figure B.2: Elle May 2003.

Figure B.3: Sunday Times Style May 2003.

Figure B.4: Glamour October 2004.

Appendix C

The Major Players

In this appendix we enumerate the major players in the Virtual Clothing market and we give an indication of their individual competitive advantage.

C.1 My Virtual Model

My Virtual Model Inc., previously Public Technologies Multimedia Inc. (PTM), was co-founded by Louise Guay, and Jean-Francois St-Arnaud in 1990. They provide image mix and match technology for online retailers. Recently they have teamed up with OptiTex also to target the 3D Virtual Clothing market. Their main advantage is that they have started early and already have links with online retailers.

C.2 Browzwear

Browzwear was founded in 2000 in Tel Aviv. Initially the company began developing a product called C-Me - a virtual fitting room for people wishing to buy clothes online. Browzwear has built alliances with GerberTechnology in May 2003 and is in a partnership with Koppermann Computersysteme, a German company that provides garment design and editing tools for images of textiles. Benetton is a client of both companies. Their competitive advantage is that they have started partnering with manufacturers. However, according to internal gossip in the Virtual Clothing community their initial technology was based on OptiTex and they cannot continue the development of their core technology any further.

C.3 OptiTex

Formerly known as Scanvec Garment Systems (SGS), OptiTex was founded in Israel in 1987. OptiTex provide a virtual drape system that integrates with their pattern design system. They employ a parameterisable mannequin for virtual dressing. Their 2D CAD pattern design system is called OptiTex PDS and can import Lectra and Gerber pattern formats. OptiTex also offers

digitizers and plotters for pattern production together with their CAD software. Their competitive advantage is that they are already selling products complementary to Virtual Clothing.

C.4 Digital Fashion

Digital Fashion Ltd is based in Osaka and was founded in 2001 by the Japanese corporation, Toyobo. The company produces products in the field of 3D photography, simulation of cosmetics and 3D simulation of clothing. One of their main shareholders is the 3D scanner company Hamamatsu. Digital Fashion's pattern making plug-ins were used for garment simulation by Alias Wavefront's Maya, which was also used for major movies. Digital Fashion has also created a standalone application called DressingSim. In a BBC news article [New04] it was reported that Digital Fashion have partnered with Toshiba Inc. in order to develop Virtual Try-On technology. They are planning to launch a product in the beginning of 2006. Their advantage is their location, Japan, which is close to major Asian garment manufacturers and the partnership between equipment and software providers.

C.5 Havok

Havok was founded in 1998 by Dr Steven Collins and Hugh Reynolds in Dublin, Ireland [Hav98]. They provide software development kits (SDKs) for physical simulation. Havok's SDK is used in computer game consoles such as Playstation and XBox. Havok also provides a physics engine for 3D Studio Max called Reactor and physical simulation for Macromedia Flash. Since Macromedia Flash is often already installed on computer systems, it would seem that Havok may have a competitive advantage in the electronic commerce market of Virtual Clothing.

C.6 SyFlex

Syflex LLC was founded in early 2002 by computer graphic veterans in Kailua, Hawaii. Syflex LLC provides efficient cloth simulation software that has been used in recent movies such as "Troy" and "Hellboy". Since May 2003 Syflex LLC is working together with PAD System Inc. to create Virtual Clothing technology for garment designers. Their competitive advantage is that their software is being used by modellers for film production, and therefore they can generate very realistic visual images of garments. They are also in partnership with PAD System Inc (see below).

C.7 PAD System

PAD System Inc. was founded in 1988, in Montreal, by creative personnel from the apparel industry. They provide CAD/CAM integrated solutions, dedicated to the apparel, textile and leather industry. The software is distributed in more than fifty countries and available in more than fifteen languages. Their competitive advantage is that their products are used already by garment designers and manufacturers.

C.8 Gerber Technology

Gerber Technology [Ger68] was founded in Connecticut USA in 1968 by H. Joseph Gerber, the inventor of the GerberCutter, a computer controlled knife for cutting material. Gerber Technology provides hardware and software for manufacturing garments and is listed on the New York Stock Exchange under the symbol "GRB". Gerber Technology has alliances with Browzwear Inc. (see above) to create Virtual Clothing. Gerber Technology's competitive advantage is that their products are used by many garment manufacturers.

C.9 Lectra

Lectra, at the moment the market leader in CAD/CAM software and hardware, was founded in 1973 in France. Lectra has developed clothes simulation tools in-house that are integrated with their CAD tools. Lectra shares are listed on the Second March of the Euronext Paris Stock Exchange. Lectra's competitive advantage is that their products are used by many garment manufacturers and designers.

Appendix D

Gap Inc.

In this appendix we give details about Gap Inc. a potential partner for the commercial exploitation of the technology described in this thesis. Gap Inc. sells casual apparel, accessories and personal care products for men, women and children under a variety of brand names, including Gap, Banana Republic and Old Navy. The Company operates in the United States, Canada, Europe and Japan, selling both online (Gap.com [early web presence since 1997], BananaRepublic.com and oldnavy.com) and through traditional retail stores utilising an approach they have dubbed 'Clicks and Mortar'. As of November 2004, the company operated a total of 3,051 store locations, see Figure D.1 and Table D.1.

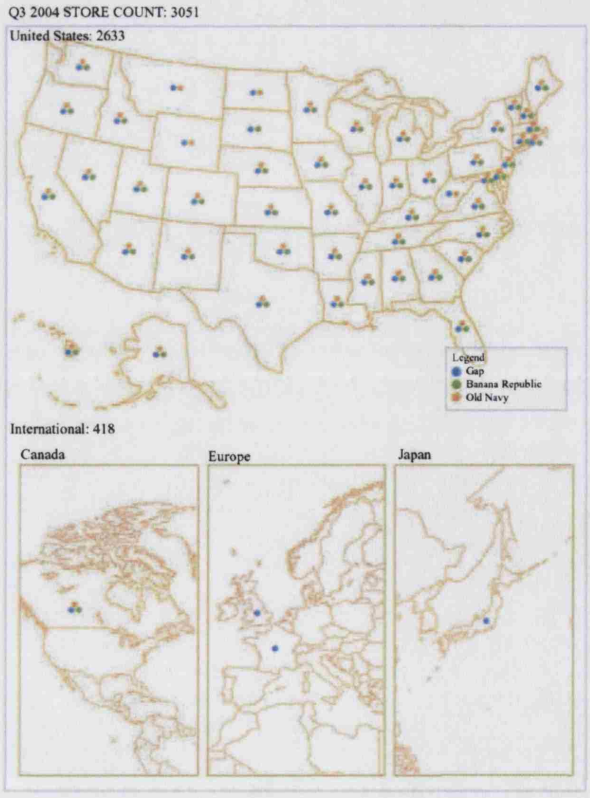

Figure D.1: Locations of stores of GAP Inc., a possible partner to introduce virtual clothing.

TOTAL STORES	
GAP (USA)	1,355
GAP (INTERNATIONAL)	
Canada	103
United Kingdom	135
France	35
Japan	77
Banana Republic United States	441
Canada	18
Old Navy	
United States	837
Canada	50
	Total 3,051

Table D.1: Number of stores of Gap Inc.

For the 39 weeks ended 30/10/04, revenues rose 4% to US$11.37 billion. Net income rose 14% to US$771 million . Gap Inc. has a market capitalisation [1] of: US$20.5bn.

Gap Inc's 2002 annual report [GAP02] claims that their provision of an online shopping capacity has generated additional revenue, rather than just redistributing sales away from 'brick and mortar' outlets:

"We also found that customers who shop both online and in our stores spend significantly more than customers who shop only in store. We'll continue to use our profitable online channels as a testing ground for new product lines and categories".

Opening online shops in Amazon.com's new Apparel Accessories Store in November 2002 [Bus04] gives the company even more online distribution and branding options. The success of their online retail strategy has resulted in an easy-to-use site with strong logistics and a pleasant user experience. Individuals can personalise their Gap website, and clicking on catalogue items allows shoppers to choose colours, sizes, and multiple addresses to which orders can be shipped. In an attempt at providing realistic clothes visualisation for the online shopper, Gap's system shows entire garments in different colours, rather than just displaying a small swatch tile. The integrated 'Clicks and Mortar' approach has been used to great effect, and any neighbourhood Gap store will accept online purchase returns.

[1] The number of outstanding shares (i.e. those currently owned by investors) X current market price.

Appendix E

Publications, Marketing, Presentations and Patents

In this appendix the publications of the work described in this thesis are given. Most of the presented work was published in papers as listed below. Some, in particular on cloth modelling, relate to work carried out during the "Centre for 3D electronic commerce project". In addition, much of the work was presented at a commercial conference where American, Asian and European representatives of companies that develop products in related fields were present. The work was also presented at an exhibition to attract the attention of the film industry. Some of the work, in particular, the methods that describe the core contributions, has also been patented as noted below.

E.1 Papers

A Virtual Clothing System for Retail and Design

Authors: Spanlang Bernhard, Vassilev Tzvetomir I., Walters Jonathan and Buxton Bernard F.

Journal: accepted in the Research Journal of Textile and Apparel

Date: 2005.

Compositing Photographs With Virtual Clothes for Design

Authors: Spanlang Bernhard, Vassilev Tzvetomir I. and Buxton Bernard F.

Place: Rousse, Bulgaria

Book: Proceedings of CompSysTech 04

Date: Jun. 2004.

Image-space Based Collision Detection in Cloth Simulation on Walking Humans

Authors: Dochev Vladimir, Vassilev Tzvetomir I. and Spanlang Bernhard

Place: Rousse, Bulgaria

Book: Proceedings of CompSysTech 04

Date: Jun. 2004.

Bodymetrics Virtual Try-On in a Department Store

Authors: Spanlang Bernhard, Vassilev Tzvetomir I. and Buxton Bernard F.

Place: Athens, Greece

Book: Proceedings of Eurasia Tex

Date: Nov. 2003.

Animating Scanned Human Models

Authors: Oliveira João F., Zhang Dongliang, Spanlang Bernhard and Buxton Bernard F.

Place: Prague, Czech Republic

Book: Proceedings of WSCG03

Date: Jan. 2003.

A Mass-spring Model for Real Time Deformable Solids

Authors: Vassilev Tzvetomir I. and Spanlang Bernhard

Place: Graz, Austria

Book: Proceedings of East-West-Vision 02

Date: Sep. 2002.

Fast Cloth Animation on Walking Avatars

Authors: Vassilev Tzvetomir I., Spanlang Bernhard and Chrysanthou Yiorgos L..

Place: Manchester, UK

Book: Proceedings of Eurographics 01

Date: Sep. 2001.

Efficient Cloth Model and Collision Detection for Dressing Virtual People

Authors: Vassilev Tzvetomir I., Spanlang Bernhard and Chrysanthou Yiorgos L.

Place: Hong Kong, China

Book: CD-Proceedings of Game Technology Conference

Date: Jan. 2001.

Efficient Cloth Model for Dressing Animated Virtual People

Authors: Vassilev Tzvetomir I. and Spanlang Bernhard

Place: Enschede, Netherlands

Book: Proceeding of the Learning to Behave Workshop

Date: Oct. 2000.

E.2 Patents

Some of the work was patented by the authors, University College London and Bodymetrics Ltd: METHOD FOR DRESSING AND ANIMATING DRESSED CHARACTERS

Patent Number:WO03017205

Publication Date: 2003-02-27

Inventor: Vassilev Tzvetomir I., Chrysanthou Yiorgos L. and Spanlang Bernhard.

Applicant: Vassilev Tzvetomir I., Chrysanthou Yiorgos L., Spanlang Bernhard and University College London.

SYSTEM AND METHOD FOR VISUALIZING PERSONAL APPEARANCE

Patent Number: EP1240623

Publication Date: 2002-09-18

Inventor: Buxton Bernard F., Chrysanthou Yiorgos L., Lawrence Kelvin D., Spanlang Bernhard, Vassilev Tzvetomir I., Thompson Giles, Gootanilake Suran A., Treleaven Philip C., Walters Jonathan.

Applicant: Bodymetrics Ltd. and University College London.

E.3 Talks and Marketing

A list of conferences and shows where the work was presented is given below. This includes presentation of several of the mentioned papers, but also includes shows and presentations to representatives of companies that manufacture products in related areas.

CompSysTech04

Compositing Photographs With Virtual Clothes for Design

Rousse, Bulgaria,

Jun. 2004.

MipTV03 Show

One Week Presentation of the Clothing and Animation system at the London First Stand

Cannes, France,

Mar. 2003.

An exhibition where representatives of most major broadcasting and film companies were present.

Eurasia Tex

Bodymetrics Virtual Try-On in a Department Store

Athens, Greece,

Nov. 2003.

Representatives of companies potentially interested in the technology such as Optitex, $[TC^2]$, Alias Wavefront were present.

London College of Fashion

From an Interactive Cloth Model to Virtual Try-On of Garments

Oct. 2003.

London, UK, Representatives of London College of Fashion, and Santoni, the world leading manufacturer of automatic knitting machines were present.

Eurographics

Fast Cloth Animation on Walking Avatars

Manchester, UK,

Sep. 2001.

Game Technology Conference

Efficient Cloth Model and Collision Detection for Dressing Virtual People,

Hong Kong, China,

Jan. 2001.

Learning to Behave Workshop

Efficient Cloth Model for Dressing Animated Virtual People

Enschede, Netherlands,

Oct. 2000.

Bibliography

[AB97] Fabrice Aubert and Dominique Bechmann. Volume-preserving space deformation. *Computers and Graphics*, 21(5):625–639, September–October 1997.

[Acc] Accenture. Innovations in online retailing. `http://www.accenture.com/xdoc/en/services/technology/myvirtualmodel_final.pdf`. URL accessed 18.11.2004.

[AFMT03] Neeharika Adabala, Guangzheng Fei, and Nadia Magnenat-Thalmann. Visualization of woven cloth. In *Eurographics Symposium on Rendering*, pages 178–185. Eurographics Association, 2003.

[AK90] Aono and Hyeong-Seok Ko. A wrinkle propagation model for cloth. In *Proc. CG International*, pages 95–115. Springer Verlag, 1990.

[Ald99] Winfred Aldrich. *Metric Pattern Cutting*. Blackwell Science, 1999. ISBN 0-63203-612-5.

[AMT03] Neeharika Adabala and Nadia Magnenat-Thalmann. Real time rendering of woven clothes. In *Proceedings of VRST*, pages 41–47. Eurographics Association, October 2003.

[APS00] Michael Ashikhmin, Simon Premoze, and Peter S. Shirley. A microfacet-based brdf generator. In *Proceedings of ACM SIGGRAPH 2000*, Computer Graphics Proceedings, Annual Conference Series, pages 65–74. ACM Press / ACM SIGGRAPH / Addison Wesley Longman, July 2000. ISBN 1-58113-208-5.

[Ass92] American Apparel Manufacturing Association. Aama/ansi 292 american national standard for pattern data interchange, 1992.

[AT00] Amaury Aubel and Daniel Thalmann. Realistic deformation of human body shapes. In Nadia Thalmann-Magnenat, Daniel Thalman, and Bruno Arnaldi,

editors, *Proceedings of the Eurographics Workshop on Computer Animation and Simulation (EGCAS-00)*, pages 125–136. Springer, 2000.

[BA04] Eddy Boxerman and Uri Ascher. Decomposing cloth. In *SCA '04: Proceedings of the 2004 ACM SIGGRAPH/Eurographics symposium on Computer animation*, pages 153–161. ACM Press, 2004.

[BCM96] Garvin Bell, Rick Carey, and Chris Marrin. The virtual reality modeling language (vrml) version 2.0 moving worlds specification, 1996.

[BDDV00] Bernard Francis Buxton, Laura Dekker, Ioannis Douros, and Tzvetomir Ivanov Vassilev. Reconstruction and interpretation of 3d whole body surface images. In *Scanning 2000*, Paris, France, May 2000.

[BE00] Robert Bigliani and J.W. Eischen. Collision detection in cloth modeling. In Donald .H. House and David. E. Breen, editors, *Cloth Modeling and Animation*, pages 197–217. A K Peters, 2000.

[Bec00] Brian Beck. Key strategic issues in online apparel retailing. `http://www.techexchange.com/thelibrary/online_fit.html`, 2000. URL accessed 18.11.2004.

[BFA02] Robert Bridson, Ronald Fedkiw, and John Anderson. Robust treatment of collisions, contact and friction for cloth animation. *ACM Transactions on Graphics (ACM SIGGRAPH 2002)*, 21(3):594–603, July 2002.

[BFGS03] Jeffrey Bolz, Ian Farmer, Eitan Grinspun, and Peter Schröder. Sparse matrix solvers on the gpu: conjugate gradients and multigrid. *ACM Trans. Graph.*, 22(3):917–924, 2003.

[BHW94] David E. Breen, Donald H. House, and Michael J. Wozny. Predicting the drape of woven cloth using interacting particles. In *Computer Graphics Proceedings, Annual Conference Series*, volume 94, pages 365–372, 1994.

[Bio01] BioVision. Biovision hierarchical motion capture fromat. `http://www.biovision.com/bvh.html`, 2001. URL accessed 5.6.2001.

[Bli77] James F. Blinn. Models of light reflection for computer synthesized pictures. In James George, editor, *Computer Graphics (SIGGRAPH '77 Proceedings)*, volume 11, pages 192–198, July 1977.

[Bli78a] James. F. Blinn. *Computer display of curved surfaces.* Ph.d. thesis, University of Utah, 1978.

[Bli78b] James F. Blinn. Simulation of wrinkled surfaces. In *Computer Graphics (SIGGRAPH '78 Proceedings)*, volume 12, pages 286–292, August 1978.

[Bou04] Jennifer Bougourd. Automatic cutting and sewing of garments. private communications, November 2004.

[Bro00] Browzwear. Home-page of browzwear. `http://www.browzwear.com/`, 2000. company founded in 2000, URL accessed 28.11.2004.

[BT75] Phong Bui-Tuong. Illumination for computer generated pictures. *Communications of the ACM*, 18(6):311–317, June 1975.

[BTH+03] Kiran S. Bhat, Christopher D. Twigg, Jessica K. Hodgins, Pradeep K. Khosla, Zoran Popović, and Steven M. Seitz. Estimating cloth simulation parameters from video. In *Proceedings of ACM SIGGRAPH/Eurographics Symposium on Computer Animation (SCA 2003)*, pages 37–51. ACM Press, 2003.

[Bur96] Grigore C. Burdea. *Force and Touch Feedback for Virtual Reality.* Wiley-Interscience, 1996. ISBN 0-47102-141-5.

[Bus04] BusinessWire. Gap inc. announces strategic alliance with amazon.com. `http://www.businesswire.com/webbox/bw.110702/223110228.htm`, 2004. URL accessed 23.11.2004.

[BW98] David Baraff and Andrew Witkin. Large steps in cloth simulation. In *SIGGRAPH '98: Proceedings of the 25th annual conference on Computer graphics and interactive techniques*, pages 43–54. ACM Press, 1998.

[BW02] George Baciu and Wingo Sai-Keung Wong. Hardware assisted self-collision for deformable surfaces. In *Proceedings of the ACM Symposium on Virtual Reality Software and Technology (VRST 2002)*, pages 129–136, 2002.

[BWK03] David Baraff, Andrew Witkin, and Michael Kass. Untangling cloth. *ACM Transactions on Graphics (ACM SIGGRAPH 2003)*, 22(3):862–870, July 2003.

[BWS99] George Baciu, Wingo Sai-Keung Wong, and Hanqiu Sun. Recode: an image-based collision detection algorithm. *The Journal of Visualization and Computer Animation*, 10(4):181–192, October - December 1999. ISSN 1049-8907.

[CC03] Luca Chittaro and Demis Corvaglia. 3d virtual clothing: from garment design to web3d visualization and simulation. In *Proceeding of the eighth international conference on 3D Web technology*, pages 73–ff. ACM Press, 2003.

[CCOS91] J.R. Collier, B.J. Collier, G. O'Toole, and S.M. Sargand. Drape prediction by means of finite-element analysis. *Journal of the textile institute*, 82(1):96–107, 1991.

[CHP89] John E. Chadwick, David R. Haumann, and Richard E. Parent. Layered construction for deformable animated characters. In Jeffrey Lane, editor, *Computer Graphics (SIGGRAPH '89 Proceedings)*, volume 23, pages 243–252, July 1989.

[CK02] Kwang-Jin Choi and Hyeong-Seok Ko. Stable but responsive cloth. In *Computer Graphics (ACM SIGGRAPH '02 Proceedings)*, 2002.

[CMT02] Frederic Cordier and Nadia Magnenat-Thalmann. Real time animation of dressed virtual humans. In *Computer Graphics Forum*, volume 21, pages 327–335, April - June 2002.

[CSMT03] Frederic Cordier, Hyewon Seo, and Nadia Magnenat-Thalmann. Made-to-measure technologies for an online clothing store. *IEEE Computer Graphics and Applications*, 23(1):38–48, January/February 2003.

[CT81] Robert. L. Cook and Kenneth. E. Torrance. A reflectance model for computer graphics. In *Computer Graphics (SIGGRAPH '81 Proceedings)*, volume 15, pages 307–316, August 1981.

[Cyb82] Cyberware. Home-page of cyberware inc. `http://www.cyberware.com/`, 1982. company founded in 1982, URL accessed 28.11.2004.

[CYTT92] Michel Carignan, Ying Yang, Nadia Magnenat Thalmann, and Daniel Thalmann. Dressing animated synthetic actors with complex deformable clothes. In *Computer Graphics Proceedings, Annual Conference Series*, volume 92, pages 99–104, 1992.

[CZ92] David T. Chen and David Zeltzer. Pump it up: Computer animation of a biomechanically based model of muscle using the finite element method. In Edwin E. Catmull, editor, *Computer Graphics (SIGGRAPH '92 Proceedings)*, volume 26, pages 89–98, July 1992.

[DCBY99] Evie Black Dykema, David M. Cooperstein, Josh Bernoff, and Donnie Young. Fashion: The online frontier. *Forrester Research*, (1), May 1999.

[DDBC99] Gilles Debunne, Mathieu Desbrun, Alan H. Barr, and Marie-Paule Cani. Interactive multiresolution animation of deformable models. In Nadia Magnenat-Thalmann and Daniel Thalmann, editors, *Computer Animation and Simulation '99*, SpringerComputerScience, pages 133–144. Springer-Verlag Wien New York, 1999. Proceedings of the Eurographics Workshop in Milano, Italy, September 7–8, 1999.

[DDBT98] Laura Dekker, Ioannis Douros, Bernard Francis Buxton, and Philip Treleaven. Building symbolic information for 3d human body modelling from range data. In *Proceedings of the Second International Conference on 3-D Digital Imaging and Modeling*, pages 388–397, 1998.

[DDJ99] Evie Black Dykema, Kate Delhagen, and Carrie A. Johnson. Apparel's on-line makeover. *Forrester Research*, May 1999.

[Deb98] Paul E. Debevec. Rendering synthetic objects into real scenes: Bridging traditional and image-based graphics with global illumination and high dynamic range photography. *Computer Graphics*, 32(Annual Conference Series):189–198, August 1998.

[Die01] Sim Dietrich. Vertex blending under directx 7 for the geforce 256. *nVidia Developer*, 2001.

[Dig01] DigitalFashion. Home-page of digitalfashion inc. `http://www.dressingsim.com/`, 2001. company founded in 2001, URL accessed 28.11.2004.

[DKW+98] Laura Dekker, S. Khan, E. West, Bernard Francis Buxton, and Philip Treleaven. Models for understanding the 3d human body form. In *IEEE International Workshop on Model Based 3D Image Analysis*, pages 65–74, May 1998.

[DlG96] Peter L. Deutsch and Jean loup Gailly. Zlib compressed data format specification version 3.3. `http://www.ietf.org/rfc/rfc1950.txt`, May 1996.

[DLHS01] Katja Daubert, Hendrik P. A. Lensch, Wolfgang Heidrich, and Hans-Peter Seidel. Efficient cloth modeling and rendering. In *Proceedings of the Eurographics Workshop on Rendering*, pages 63–70. Springer-Verlag, 25–27 June 2001.

[DV03] Vlado Dochev and Tzvetomir Ivanov Vassilev. Efficient super-elasticity handling in mass-spring systems. In *Proceedings of Computer Systems and Technology (CompSysTech03)*, Sofia, Bulgaria, June 2003.

[DvGNK99] Kristin J. Dana, Bram van Ginneken, Shree K. Nayar, and Jan J. Koenderink. Reflectance and texture of real-world surfaces. *ACM Transactions on Graphics*, 18(1):1–34, 1999.

[DVS04] Vlado Dochev, Tzvetomir Ivanov Vassilev, and Bernhard Spanlang. Image-space based collision detection in cloth simulation on walking humans. In *Proceedings of Computer Systems and Technology (CompSysTech04)*, Rousse, Bulgaria, June 2004. ISBN 954-9641-38-4.

[EDC96] Jeffrey W. Eischen, Shigan Deng, and Timothy G. Clapp. Finite-element modeling and control of flexible fabric parts. *IEEE Computer Graphics and Applications*, 16(5):71–80, September 1996 1996. ISSN 0272-1716.

[EEH00] Olaf Etzmuß, Bernhard Eberhardt, and Michael Hauth. Implicit-explicit schemes for fast animation with particle systems. In *Computer Animation and Simulation 2000*, pages 138–151. Eurographics, August 2000. ISBN 3-211-83392-7.

[EEHS00] Olaf Etzmuß, Bernhard Eberhardt, Michael Hauth, and Wolfgang Straßer. Collision adaptive particle systems. *8th Pacific Conference on Computer Graphics and Applications*, pages 338–347, October 2000. ISBN 0-7695-0868-5.

[EKS03] Olaf Etzmuß, Michael Keckeisen, and Wolfgang Straßer. A Fast Finite Element Solution for Cloth Modelling. *Proceedings of Pacific Graphics*, 2003.

[EUB04] EUBusiness. Take-up of broadband in europe accelerates. `http://www.eubusiness.com/topics/Rd/EUNews.2004-05-13.4257`, 2004. URL accessed 15.12.2004.

[Eve01] Cass Everitt. Interactive order independent transparency. *nVidia Developer*, May 2001.

[EWS96] Bernhard Eberhardt, Andreas Weber, and Wolfgang Straßer. A fast, flexible, particle-system model for cloth draping. *j-IEEE-CGA*, 16(5):52–59, September 1996.

[FGL03] Arnulph Fuhrmann, Clemens Groß, and Volker Luckas. Interactive animation of cloth including self collision detection. In *Proceedings of Winter School of Computer Graphics (WSCG 2003)*, pages 203–208, 2003.

[FGLW03] Arnulph Fuhrmann, Clemens Groß, Volker Luckas, and A. Weber. Interaction free dressing of virtual humans. *Computers & Graphics*, 27(1):71–82, 2003.

[FGP93] Brian Francis, Mick Green, and Clive Payne, editors. *The GLIM system: The Statistical System for Generalized Linear Interactive Modelling*. Oxford University Press, 1993. Release 4 manual. Correct reprint in 1994. ISBN 0-19-852231-2.

[FHI+00] Matt Foster, Joe Holt, George Ishii, Paul Ferguson, and Thomas Ruark. Adobe illustrator 9.0 plug-in software development kit programmer's guide for macintosh and windows. `http://www.adobe.com/`, 2000. URL accessed 1.8.2002.

[Fra00] Mark Del Franco. Return rates: Good news about returns. *Catalogue Age Magazin (Strategies for Profitable Multichanel Marketing*, March 2000.

[FSG03] Arnulph Fuhrmann, Gerrit Sobottka, and Clemens Groß. Distance fields for rapid collision detection in physically based modelling. In *Proceedings of GraphiCon*, pages 58–65, 2003.

[fTM01] American Society for Testing and Materials. D6673-01 standard practice for sewn products pattern data interchange-data format, 2001.

[GAP02] GAPInc. Annual report. `http://www.gapinc.com/financmedia/AR_proxy.htm`, 2002. URL accessed 23.11.2004.

[GBC04] Marco Gillies, Daniel Ballin, and Balzs Csand Csji. Efficient clothing fitting from data. In *Proceedings of Winter School of Computer Graphics (WSCG 2004)*, University of West Bohemia,Czech Replublic, February 2004.

[Ger] GerberTechnology. Home-page of gerbertechnology. `http://www.gerbertechnology.com/`. company founded in 1968, URL accessed 28.11.2004.

[GFL03] Clemens Groß;, Arnulph Fuhrmann, and Volker Luckas. Automatic prepositioning of virtual clothing. In *Proceedings of the 18th spring conference on Computer graphics*, pages 99–108. ACM Press, 2003.

[GGHM03] Muthu Govindaraj, Ashis Garg, Gang Huang, and Dimitris Metaxas. Haptic simulation of fabric hand. In *EuroHaptics 2003 Conference - Incorporating the PHANTOM users Research Symposium*. EuroHaptics, 2003.

[Gla03] Andrew Glassner. Digital weaving, part 3. *IEEE Comput. Graph. Appl.*, 23(2):80–89, 2003.

[GLS95] L. Gan, N.G. Ly, and G.P. Stevens. A study of fabric deformations using non linear finite elements. *Textile Research Journal*, 65(11):660–668, 1995.

[GMN94] Jay S. Gondek, Gary W. Meyer, and Jonathan G. Newman. Wavelength dependent reflectance functions. In Andrew Glassner, editor, *Proceedings of SIGGRAPH '94 (Orlando, Florida, July 24–29, 1994)*, Computer Graphics Proceedings, Annual Conference Series, pages 213–220. ACM SIGGRAPH, ACM Press, July 1994. ISBN 0-89791-667-0.

[Gou71] Henri Gouraud. Continuous shading of curved surfaces. *IEEE Transactions on Computers*, C-20(6):623–629, June 1971.

[GRLM03] Nada Govindaraju, Stephane Redon, Ming C. Lin, and Dinesh Manocha. Cullide: interactive collision detection between complex models in large environments using graphics hardware. In *Proceedings of the ACM SIGGRAPH/EUROGRAPHICS conference on Graphics hardware*, pages 25–32. ACM Press, Feb 2003.

[GRS95] Eduard Gröller, René T. Rau, and Wolfgang Straßer. Modeling and visualization of knitwear. *IEEE Transactions on Visualization and Computer Graphics*, 1(4):302–310, December 1995. ISSN 1077-2626.

[GT98] Paul A. Gompers and Alexander C. Tsai. Elliot lebowitz, November 1998. Harvard Business School, case number 9-297-094.

[Ham53] Hamamatsu. Home-page of hamamatsu photonics. `http://www.hamamatsu.com/`, 1953. company founded in 1953, URL accessed 28.11.04.

[Har01] Paul Harrison. Non-hierarchical procedure for re-synthesis of complex textures. In *Proceedings of Winter School of Computer Graphics (WSCG 2001)*, 2001.

[Hav98] Havok. Home-page of havok. `http://www.havok.com`, 1998. company founded in 1998, URL accessed 28.11.04.

[HB00] Donald H. House and David E. Breen, editors. *Cloth Modeling and Animation.* A.K. Peters, 2000.

[Hec86] Paul S. Heckbert. Survey of texture mapping. *IEEE Computer Graphics and Applications*, 6(11):56–67, November 1986.

[HM90] Brendan K. Hinds and Jim McCartney. Interactive garment design. *The Visual Computer*, 6(2):53–61, March 1990.

[HMG03] Gang Huang, Dimitris Metaxas, and Muthu Govindaraj. Feel the "fabric": an audio-haptic interface. In *SCA '03: Proceedings of the 2003 ACM SIGGRAPH/Eurographics Symposium on Computer animation*, pages 52–61. Eurographics Association, 2003.

[HML99] Gentaro Hirota, Renee Maheshwari, and Ming C. Lin. Fast volume-preserving free form deformation using multi-level optimization. In *Proceedings of the fifth ACM symposium on Solid modeling and applications*, pages 234–245. ACM Press, 1999.

[Hor95] C. Horiguchi. Sensors that detect shape. *Advanced Automation Technology*, 7(3):210–216, 1995.

[HPH96] Dave Hutchinson, Martin Preston, and Terry Hewitt. Adaptive refinement for mass/spring simulations. In *Proceedings of the Eurographics Workshop on Computer Animation and Simulation (CAS 1996)*, pages 31–45. Springer-Verlag, 1996.

[HTG04] Bruno Heidelberger, Matthias Teschner, and Markus Groß. Detection of collision and self-collision using image-space techniques. In *Proceedings of Winter School of Computer Graphics (WSCG 2004)*, University of West Bohemia,Czech Replublic, Feb 2004.

[HTSG91] Xiao D. He, Kenneth E. Torrance, Francois X. Sillion, and Donald P. Greenberg. A comprehensive physical model for light reflection. In Thomas W. Sederberg, editor, *Computer Graphics (SIGGRAPH '91 Proceedings)*, volume 25, pages 175–186, July 1991.

[IL99] Cynthia L. ISTOOK and L.McKinnon. Psychological issues concerning body scanning. In *Annual International Textile and Apparel Association Meeting*, Santa Fe, November 1999.

[Ima99] Imaginarix. Home-page of imaginarix. `http://www.imaginarix.com`, 1999. company founded in 1999, URL accessed 28.11.04.

[Jak01] Thomas Jakobsen. Advanced character physics. In *Game Developer Conference*, 2001.

[Jam01] Doug James. Fast simulation of elastostatic deformable models. In *Game Developer Conference*, 2001.

[JF03] Doug L. James and Kayvon Fatahalian. Precomputing interactive dynamic deformable scenes. *ACM Trans. Graph.*, 22(3):879–887, 2003.

[JH97] Nebojsa Jojic and Thomas S. Huang. Estimating cloth draping parameters from range data. In *International Workshop on Synthetic Natural Hybrid Coding and 3D Imaging*, pages 73–76, Rhodes, Greece, 1997.

[Joh04] Carrie A. Johnson. Trends 2005: Online retail. *Forrester Research*, Nov 2004.

[Kas95] Michael Kass. An introduction to continuum mechanics for computer graphics. *SIGGRAPH Course Notes*, 1995.

[Kaw80] S. Kawabata. The standardization and analysis of hand evaluation. *The Textile Machinery Society of Japan*, 1980.

[KCP+00] Young-Min Kang, Jeong-Hyeon Choi, Chan-Jong Park, Hwan-Gue Cho, and Do-Hoon Lee. Real-time animation technique for flexible and thin objects. In *Proceedings of Winter School of Computer Graphics (WSCG 2000)*, pages 322–329, February 2000.

[KE00] Walter Kuemmerle and Chad Ellis. Spotfire: Managing a multinational start-up, June 2000. Harvard Business School, case number 9-899-078.

[KM99] Jan Kautz and Michael D. McCool. Interactive rendering with arbitrary BRDFs using separable approximations. In Dani Lischinski and Greg Ward Larson, editors, *Rendering Techniques '99*, Eurographics, pages 247–260. Springer-Verlag Wien New York, 1999. Proc. 10th Eurographics Rendering Workshop, Granada, Spain, June 21–23, 1999.

[KMG96] Konrad F. Karner, Heinz Mayer, and Michael Gervautz. An image based measurement system for anisotropic reflection. *Computer Graphics Forum*, 15(3):119–128, August 1996. ISSN 1067-7055.

[KMTM+98] Prem Kalra, Nadia Magnenat-Thalmann, Laurent Moccozet, Gael Sannier, Amaury Aubel, and Daniel Thalmann. Real-time animation of realistic virtual humans. *IEEE Computer Graphics and Applications*, 18(5):42–57, September/ October 1998.

[Kno03] David Knott. Cinder collision and interference detection in real time using graphics hardware. Master's thesis, University of British Columbia, 2003.

[KW03] Jens Krüger and Rüdiger Westermann. Linear algebra operators for gpu implementation of numerical algorithms. *ACM Transactions on Graphics (TOG)*, 22(3):908–916, 2003.

[LA99] Hava Lester and Simon R. Arridge. A survey of hierarchical non-linear medical image registration. In *Pattern Recognition*, volume 32, pages 129 – 149, 1999.

[Lan97] Jeff Lander. Skin them bones: Game programming for the web generation. In *Game Developer Magazine*, May 1997.

[Lan04] Walt Langer. Poor size, fit drain profits for catalogs, web retailers. `http://www.bobbin.com/bobbin/headlines/viewpoints_display.jsp?vnu_content_id=1000475612`, 2004. URL accessed 18.11.2004.

[LD01] Dorothy Leonard and Brian DeLacey. Zaplet, inc. (a), July 2001. Harvard Business School, case number 9-601-165.

[Lec] Lectra. Home-page of lectra. `http://www.lectra.com`. company founded in 1973, URL accessed 18.11.2004.

[Lew93] Robert Lewis. Making shaders more physically plausible. In Michael F. Cohen, Claude Puech, and Francois Sillion, editors, *Fourth Eurographics Workshop on Rendering*, pages 47–62. Eurographics, June 1993. held in Paris, France, 14–16 June 1993.

[LFTG97] Eric P. F. Lafortune, Sing-Choong Foo, Kenneth E. Torrance, and Donald P. Greenberg. Non-linear approximation of reflectance functions. *Computer Graphics*, 31(Annual Conference Series):117–126, August 1997.

[LG98] Ming C. Lin and Stefan Gottschalk. Collision detection between geometric models: A survey, 1998.

[LKC96] J. D. Liu, M. T. Ko, and R. C. Chang. Collision avoidance in cloth animation. *The Visual Computer*, 12(5):234–243, 1996. ISSN 0178-2789.

[LKG+01] Hendrik P. A. Lensch, Jan Kautz, Michael Goesele, Wolfgang Heidrich, and Hans-Peter Seidel. Image-based reconstruction of spatially varying materials. In *Rendering Techniques 2001: 12th Eurographics Workshop on Rendering*, pages 103–114. Eurographics, June 2001. ISBN 3-211-83709-4.

[LL02] Rajiv Lal and Sean Lanagan. Documentum inc., April 2002. Harvard Business School, case number 9-502-026.

[lLK84] Sheue ling Lien and James T. Kajiya. Symbolic method for calculating the integral properties of arbitrary nonconvex polyhedra. *IEEE Computer Graphics and Applications*, 4(10):35–41, October 1984.

[LMTT91] Benoit Lafleur, Nadia Magnenat-Thalmann, and Daniel Thalmann. Cloth animation with self collision detection. In *Conference on Modeling in Computer Graphics*. Springer-Verlag, 1991.

[LS98] Greg Ward Larson and Rob Shakespeare. *Rendering with Radiance: The Art and Science of Lighting Visualization.* Morgan Kaufmann Publishers Inc., 1998.

[LYS01] Xinguo Liu, Yizhou Yu, and Heung-Yeung Shum. Synthesizing bidirectional texture functions for real-world surfaces. In ACM, editor, *SIGGRAPH 2001 Conference Proceedings, August 12–17, 2001, Los Angeles, CA*, pages 97–106, New York, NY 10036, USA, 2001. ACM Press.

[Mac00] Dean P. Macri. Real-time cloth. In *Proceedings of the Game Developers Conference (GDC 2000)*, 2000.

[Mam89] Abraham Mammen. Transparency and antialiasing algorithms implemented with the virtual pixel maps technique. *IEEE Computer Graphics and Applications*, 9(4):43–55, July 1989.

[MCS90] James F. Murray-Coleman and A. M. Smith. The automated measurement of brdfs and their application to luminaire modelling. *The Illuminating Engineering Society*, 1990.

[MCTG00] Ann McNamara, Alan Chalmers, Tom Troscianko, and Iain Gilchrist. Comparing real and synthetic scenes using human judgements of lightness. In Bernard

Piroche and Holly Rushmeier, editors, *Proceedings of the Eurographics Workshop in Brno*. Eurographics, June 2000. ISBN 3-211-83535-0.

[MDDB00] Mark Meyer, Gilles Debunne, Mathieu Desbrun, and Alan H. Barr. Interactive animation of cloth-like objects in virtual reality. *Journal of Vizualisation and Computer Animation*, 2000.

[Mel02] Paul E. C. Melis. Real-time cloth simulation in a 3d virtual environment. Master's thesis, University of Twente, 2002.

[Men02] Sergei Menchenin. Cam2com. `http://www.sabsik.com/Cam2Com/`, 2002. URL accessed 1.3.2004.

[MH93] W.W. Morton and J.W.S. Hearle. *Physical properties of textile fibres*. The Textile Institute, 1993. ISBN 1-87081-241-7.

[Min01] Mintel. Uk vs us online shopping, June 2001.

[MKE03] Johannes Mezger, Stefan Kimmerle, and Olaf Etzmuß. Hierarchical techniques in collision detection for cloth animation. In *Proceedings of Winter School of Computer Graphics (WSCG 2003)*, pages 322–329, January 2003.

[MOK95] Karol Myszkowski, O. G. Okunev, and T. L. Kunii. Fast collision detection between complex solids using rasterizing graphics hardware. *The Visual Computer*, 11(9):497–512, 1995. ISSN 0178-2789.

[MW88] Matthew Moore and Jane Wilhelms. Collision detection and response for computer animation. *Computer Graphics (Proceedings of SIGGRAPH 88)*, 22(4):289–298, August 1988. Held in Atlanta, Georgia.

[MWL+99] Stephen R. Marschner, Stephen H. Westin, Eric P. F. Lafortune, Kenneth E. Torrance, and Donald P. Greenberg. Image-based brdf measurement including human skin. In *Eurographics Rendering Workshop 1999*, Granada, Spain, June 1999. Springer Wein / Eurographics.

[MyV90] MyVirtualModel. Home-page of my virtual model. `http://www.mvm.com`, 1990. company founded in 1990; URL accessed 29.11.2004.

[Neb00] Jean-Christophe Nebel. Soft tissue modelling from 3d scanned data. In *Deform 2000*, Geneva, Switzerland, November 2000.

[New04] BBC News. Virtual dummy to try on clothes. *BBC World Edition*, January 2004. `http://news.bbc.co.uk/2/hi/technology/3430131.stm`, URL accessed 2.2.2004.

[NG96] Hing N. Ng and Richard L. Grimsdale. Computer graphics techniques for modeling cloth. *IEEE Computer Graphics and Applications*, 16(5):28–41, September 1996 1996. ISSN 0272-1716.

[NKB+] Ravi Nielsen, Bob Keates, Sally Breckenridge, Dana Cartwright, Jane Eisenstein, Mark Kloosterman, and Bjorn Myhre. Weaving information file. `http://www.mhsoft.com/wif/wif.html`.

[NRH+77] Fred E. Nicodemus, J. C. Richmond, J. J. Hsia, I. W. Ginsberg, and T. Limperis. Geometric considerations and nomenclature for reflectance. Monograph 161, National Bureau of Standards (US), October 1977.

[NSI99] Ko Nishino, Yoichi Sato, and Katsushi Ikeuchi. Eigen-texture method: appearance compression based on 3d model. In *Proceedings of IEEE Conference on Computer Vision and Pattern Recognition (CVPR'99)*, volume 1, pages 618 – 624, June 1999.

[NT98] Luciana Porcher Nedel and Daniel Thalmann. Real time muscle deformations using mass-spring systems. In Franz-Erich Wolter and Nicholas M. Patrikalakis, editors, *Proceedings of the Conference on Computer Graphics International 1998 (CGI-98)*, pages 156–165. IEEE Computer Society, 1998. ISBN 0-8186-8445-3.

[OB01] João Fradinho Oliveira and Bernard Francis Buxton. Light weight virtual humans. In *Proceedings of Eurographics-UK*, May 2001.

[Opt87] OptiTex. Home-page of optitex. `http://www.optitex.com`, 1987. company founded in 1987, URL accessed 28.11.04.

[OZSB03] João Fradinho Oliveira, Dongliang Zhang, Bernhard Spanlang, and Bernard Francis Buxton. Animating scanned human models. In *Proceedings of Winter School of Computer Graphics (WSCG 2003)*, University of West Bohemia, Czech Replublic, January 2003.

[PBP96] Emmanuel Promayon, Pierre Baconnier, and Claude Puech. Physically-based deformations constrained in displacements and volume. *Computer Graphics Forum*, 15(3):C155–C164, September 1996.

[Pix] Pixar. Home-page of pixar animation studios. `http://www.pixar.com`. company founded in 1986, URL accessed 29.11.04.

[PLAMT02] Dimitris Protopsaltou, C. Luible, M. Arevalo, and Nadia Magnenat-Thalmann. A body and garment creation method for an Internet based virtual fitting room. In *Proceedings of Computer Graphics International 2002 (CGI 2002)*, pages 105–122. Springer-Verlag, 2002.

[Pol01] Rob Polevoi. *Interactive Web Graphics with Shout3D*. SYBEX Inc., 2001.

[Pro95] Xavier Provot. Deformation constraints in a mass-spring model to describe rigid cloth behaviour. In *Proceedings of Graphics Interface*, pages 141–155, 1995.

[Pro97] Xavier Provot. Collision and self-collision handling in cloth model dedicated to design. *Computer Animation and Simulation '97*, pages 177–190, September 1997. ISBN 3-211-83048-0. Held in Budapest, Hungary.

[PTVF92] William H. Press, Saul A. Teukolsky, William T. Vetterling, and Brian P. Flannery. *Numerical Recipes in C, 2nd. edition.* Cambridge University Press, 1992.

[PW03] Junyoung Park and Carl .R. Wassgren. Modeling the dynamics of fabric in a rotating horizontal drum using the discrete element method. In *Particulate Science and Technology*, volume 92, pages 157–175, April - June 2003.

[Reu04] Reuters. Broadband pushes europe web users to 100 million. `http://news.zdnet.com/2110-1035_22-5475326.html`, 2004. URL accessed 12.12.2004.

[RLCW01] Paul Rademacher, Jed Lengyel, Ed Cutrell, and Turner Whitted. Measuring the perception of visual realism in images. In *Rendering Techniques 2001: 12th Eurographics Workshop on Rendering*, pages 235–248. Eurographics, June 2001. ISBN 3-211-83709-4.

[RMS92] Jarek Rossignac, Abe Megahed, and Bengt-Olaf Schneider. Interactive inspection of solids: Cross-sections and interferences. *Computer Graphics (Proceed-*

ings of SIGGRAPH 92), 26(2):353–360, July 1992. ISBN 0-201-51585-7. Held in Chicago, Illinois.

[Rob02] Jack Robertson. Graphics chips outpacing moore's law. `http://www.my-esm.com/printableArticle.jhtml?articleID=2916132`, 2002. URL accessed 10.12.2004.

[RS99] Brent E. Rector and Chris Sells. *ATL Internals*. Pearson Education, 1999. ISBN 0-20169-589-8.

[RSB95] Ari Rappoport, Alla Sheffer, and Michel Bercovier. Volume-preserving free-form solid. In *SMA '95: Proceedings of the Third Symposium on Solid Modeling and Applications*, pages 361–372. ACM, May 1995.

[SAFe02] Mark Segal, Kurt Akeley, Chris Frazier(ed), and Jon Leach (ed). *The OpenGL Graphics System: A Specification (Version 1.4)*. Silicon Graphics Inc., 2002.

[SAS+04] Bernhard Spanlang, Brian Allbriton, Anthony Sibthorpe, Steven Seget, and Annie Ting Ngai Lai. The commercial potential of virtual clothing. Report, London Business School, 2004.

[Sch94] Christophe Schlick. An inexpensive BRDF model for physically-based rendering. In *Computer Graphics Forum*, volume 13, pages 233–246. Eurographics, Basil Blackwell Ltd, 1994. Eurographics '94 Conference issue.

[Sch04] Steven H. Schwartz. *Visual Perception*. McGraw-Hill Medical, 2004. ISBN 0-07141-187-9.

[SF91] Mikio Shinya and M.-C. Forgue. Interference detection through rasterization. *The Journal of Visualization and Computer Animation*, 2(4):132–134, October–December 1991.

[SGHS98] Jonathan W. Shade, Steven J. Gortler, Li-Wei He, and Richard Szeliski. Layered depth images. *Computer Graphics*, 32(Annual Conference Series):231–242, August 1998.

[She94] Jonathan Richard Shewchuk. An introduction to the conjugate gradient method without the agonizing pain. Computer Science Tech. Report 94-125, Carnegie Mellon University, Pittsburgh, PA, 1994.

[SIC00] Peter-Pike Sloan, Charles F. Rose III, and Michael F. Cohen. Shape and animation by example. Technical Report MSR-TR-2000-79, Microsoft Research, 2000.

[Siz01] SizeUK. Home-page of the national sizing suvey. `http://www.sizeuk.org`, 2001. URL accessed 10.10.04.

[SP86] Thomas W. Sederberg and Scott R. Parry. Free-form deformation of solid geometric models. In David C. Evans and Russell J. Athay, editors, *Computer Graphics (SIGGRAPH '86 Proceedings)*, volume 20, pages 151–160, August 1986.

[Spa02] Bernhard Spanlang. Lightmaps from hdr light probes. In *CD Proceedings of the First International Radiance Workshop*, October 2002.

[SPCM97] Ferdi Scheepers, Richard E. Parent, Wayne E. Carlson, and Stephen F. May. Anatomy-based modeling of the human musculature. In Turner Whitted, editor, *SIGGRAPH 97 Conference Proceedings*, Annual Conference Series, pages 163–172. ACM SIGGRAPH, Addison Wesley, August 1997. ISBN 0-89791-896-7.

[SSK03] Mirko Sattler, R. Sarlette, and R. Klein. Efficient and realistic visualization of cloth. In *Eurographics Symposium on Rendering 2003*, June 2003.

[ST95] Jianhua Shen and Daniel Thalmann. Interactive shape design using metaballs and splines. In *Implicit Surfaces '95*, April 1995.

[Str90] Paul S. Strauss. A realistic lighting model for computer animators. *IEEE Computer Graphics and Applications*, 10(6):56–64, November 1990.

[SVB03] Bernhard Spanlang, Tzvetomir Ivanov Vassilev, and Bernard Francis Buxton. Bodymetrics virtual try-on in a department store. In *Eurasia Tex*, Athens, Greece, November 2003.

[SVB04] Bernhard Spanlang, Tzvetomir Ivanov Vassilev, and Bernard Francis Buxton. Compositing photographs with virtual clothes for design. In *Proceedings of Computer Systems and Technology (CompSysTech04)*, Rousse, Bulgaria, June 2004. ISBN 954-9641-38-4.

[SVWB05] Bernhard Spanlang, Tzvetomir Ivanov Vassilev, Jonathan Walters, and Bernard Francis Buxton. A virtual clothing system for retail and design. *Research Journal of Textile and Apparel*, 2005. to appear.

[SW91] Martin M. Shoben and Janet P. Ward. *Pattern Cutting and Making-Up The professional approach.* Butterworth-Heinemann, 1991. ISBN 0-75060-364-X.

[Syf] Syflex. Home-page of syflex llc. `http://www.syflex.biz`. company founded in 2002, URL accessed 29.11.2004.

[Sys] PAD System. Pad system technologies inc. `http://www.padsystem.com`. company founded in 1988, URL accessed 10.10.2004.

[TC2] TC2. Home-page of the tailored clothing technology corporation. `http://www.tc2.com/`. company founded in 1979, URL accessed 27.11.2004.

[TD01] Chris Tchou and Paul E. Debevec. Hdrshop. `http://www.ict.usc.edu/graphics/HDRShop/`, 2001. URL accessed 5.8.2004.

[TF88] Demetri Terzopoulos and Kurt Fleischer. Deformable models. *The Visual Computer*, 4(6):306–331, 1988.

[TKZ+04] Matthias Teschner, Stefan Kimmerle, Gabriel Zachmann, Bruno Heidelberger, Laks Raghupathi, Arnulph Fuhrmann, Marie-Paule Cani, François Faure, Nadia Magnetat-Thalmann, and Wolfgang Straßer. Collision detection for deformable objects. In *Proc. Eurographics State-of-the-Art Report.* EG Association, September 2004.

[TLC02] Franco Tecchia, Céline Loscos, and Yiorgos Chrysanthou. Image-based crowd rendering. *IEEE Computer Graphics and Applications*, 22(2):36–43, 2002.

[TPBF87] Demetri Terzopoulos, John Platt, Alan H. Barr, and Kurt Fleischer. Elastically deformable models. *Computer Graphics*, 21(4):205–214, July 1987.

[TS67] Kenneth E. Torrance and Ephraim M. Sparrow. Theory for off-specular reflection from roughened surfaces. *Journal of Optical Society of America*, 57(9), 1967.

[TSC96] Daniel Thalmann, Jianhua Shen, and Eric Chauvineau. Fast realistic human body deformations for animation and vr applications. In *Computer Graphics International IEEE Computer Society Press*, pages 166–174, 1996.

[Vas01] Tzvetomir Ivanov Vassilev. Mass-spring cloth model for simulating different fabric types. In *Proceedings of Computer Systems and Technology (CompSysTech01)*, Sofia, Bulgaria, June 2001.

[Vas04] Tzvetomir Ivanov Vassilev. Kes mapping. private communications, July 2004.

[VCT95] Pascal Volino, Martin Courchesne, and Nadia Magnenat Thalmann. Versatile and efficient techniques for simulating cloth and other deformable objects. *Computer Graphics*, 29(Annual Conference Series):137–144, November 1995.

[Ver67] Lennard-Jones Verlet. Computer experiments on classical fluids the thermodynamical properties of lennard-jones molecules. In *Physical Review*, pages 98–103. Springer Verlag, 1967.

[Vit97] Vitronic. Home-page of vitronic inc. `http://www.vitronic.com/`, 1997. company founded in 1997, URL accessed 28.11.2004.

[VMT94] Pascal Volino and Nadia Magnenat-Thalmann. Efficient self-collision detection on smoothly discretised surface animations using geometrical shape regularity. *Computer Graphics Forum*, 13:155–166, 1994.

[VMT95] Pascal Volino and Nadia Magnenat-Thalmann. Collision and self-collision detection: efficient and robust solution for highly deformable surfaces. *Sixth Eurographics Workshop on Animation and Simulation*, pages 55–65, 1995.

[VMT00a] Pascal Volino and Nadia Magnenat-Thalman. *Virtual Clothing*. McCraw-Hill, 2000. ISBN 3-54067-600-7.

[VMT00b] Pascal Volino and Nadia Magnenat-Thalmann. Implementing fast cloth simulation with collision response. In *Computer Graphics International 2000*, pages 257–268, June 2000. ISBN 0-7695-0643-7.

[VMT01] Pascal Volino and Nadia Magnenat-Thalmann. Comparing efficiency of integration methods for cloth simulation. In *Computer Graphics International 2001*, pages 265–272, July 2001. ISBN 0-7695-1007-8.

[VS02] Tzvetomir Ivanov Vassilev and Bernhard Spanlang. A mass-spring model for real-time deformable solids. In *East-West Vision*, pages 73–76, Graz, Austria, September 2002.

[VSC01] Tzvetomir Ivanov Vassilev, Bernhard Spanlang, and Yiorgos Chrysanthou. Fast cloth animation on walking avatars. *Computer Graphics Forum*, 20(3):260–267, 2001. ISSN 1067-7055.

[War92] Gregory J. Ward. Measuring and modeling anisotropic reflection. In Edwin E. Catmull, editor, *Computer Graphics (SIGGRAPH '92 Proceedings)*, volume 26, pages 265–272, July 1992.

[War94] Gregory J. Ward. The RADIANCE lighting simulation and rendering system. In Andrew Glassner, editor, *Proceedings of SIGGRAPH '94 (Orlando, Florida, July 24–29, 1994)*, Computer Graphics Proceedings, Annual Conference Series, pages 459–472. ACM SIGGRAPH, ACM Press, July 1994. ISBN 0-89791-667-0.

[Wat86] Andrew B. Watson. *Temporal Sensitivity in Handbook of Perception and Human Performance*. Wiley, 1986. ISBN 0-47188-544-4.

[WAT92] Stephen H. Westin, James R. Arvo, and Kenneth E. Torrance. Predicting reflectance functions from complex surfaces. In Edwin E. Catmull, editor, *Computer Graphics (SIGGRAPH '92 Proceedings)*, volume 26, pages 255–264, July 1992.

[Wei86] Jerry Weil. The synthesis of cloth objects. In David C. Evans and Russell J. Athay, editors, *Computer Graphics (SIGGRAPH '86 Proceedings)*, volume 20, pages 49–54, August 1986.

[Wer93] Josie Wernecke. *The Inventor Mentor: Programming Object-Oriented 3d Graphics with Open Inventor Release 2*. Addison-Wesley Longman Publishing Co. Inc., 1993.

[WH92] George J. Ward and Paul S. Heckbert. Irradiance gradients. In Derek Paddon Alan Chalmers and François Sillion, editors, *Rendering Techniques '92*, Eurographics, pages 85–98. Consolidation Express Bristol, 1992. Proc. 3rd Eurographics Rendering Workshop, Bristol, England, May 17–20, 1992.

[Wic73] WicksAndWilson. Home-page of wicks and wilson ltd. `http://www.wwl.co.uk/`, 1973. company founded in 1973, URL accessed 28.11.2004.

[WWY03] Charlie C.L. Wang, Yu Wang, and Matthew M.F. Yuen. Feature based 3d garment design through 2d sketches. *Computer Aided Design*, 35(7):659–672, June 2003.

[XCL+01] Ying-Qing Xu, Yanyun Chen, Stephen Lin, Hua Zhong, Enhua Wu, Baining Guo, and Heung-Yeung Shum. Photo-realistic rendering of knitwear using the lumislice. In *Proceedings of ACM SIGGRAPH 2001*, Computer Graphics Proceedings, Annual Conference Series, pages 391–398. ACM Press / ACM SIGGRAPH, August 2001. ISBN 1-58113-292-1.

[YMT93] Ying Yang and Nadia Magnenat-Thalmann. An improved algorithm for collision detection in cloth animation with human body. *First Pacific Conference on Computer Graphics and Applications*, August 1993.

[YYiT92] Takami Yasuda, Shigeki Yokoi, and Jun ichiro Toriwaki. A shading model for cloth objects. *IEEE Computer Graphics & Applications*, 12(6):15–24, November 1992.

[Zha00] Zhengyou Zhang. A flexible new technique for camera calibration. *IEEE Transactions on Pattern Analysis and Machine Intelligence*, 22(11):1330–1334, 2000.

[ZT91] Olgierd C. Zienkiewicz and R.L. Taylor. *The Finite Element Method.* McCraw-Hill, 1991.

[ZY00] Dongliang Zhang and Matthew M. F. Yuen. Collision detection for clothed human animation. *8th Pacific Conference on Computer Graphics and Applications*, pages 328–337, October 2000. ISBN 0-7695-0868-5.